# Investigating the role of changes to the mammary gland immune microenvironment in pregnancy-induced oncoprotection

*A dissertation presented by*

Amritha Varshini Hanasoge Somasundara

*to the*

School of Biological Sciences

*in partial fulfillment of the requirements for the degree of*

Doctor of Philosophy

*in*

Biological Sciences

*at*

Cold Spring Harbor Laboratory

November 2022

*"…it's fine to fake it till you make it*

*'til you do, 'til it's true"*

*Taylor Swift*

## Summary

Pregnancy is the physiological stimulus that induces complete mammary gland development. Epidemiological, clinical, and experimental data have shown that one factor that affects the risk of developing breast cancer is pregnancy. More specifically, an early age of first pregnancy has been associated with a long-term protective effect against breast cancer development. Subsequent pregnancies can extend this protection even further. This protective effect seems to have an evolutionary root, given that even in a variety of rodent models, parity has been reported to reduce the frequency of mammary tumor development. While many hypotheses have been developed to address why post-pregnancy epithelial cells are less likely to be engaged in cancer initiation, the contribution of mammary resident immune cells in post-pregnancy cancer protection remains mostly unknown.

Mammary-resident cells of the adaptive and innate immune system play a critical role during mammary gland development. Changes to the immune microenvironment have been described to influence, and in some cases, guide pregnancy-induced mammary development. In this study, we set out to define the link between pregnancy, immune microenvironment, and oncogenesis to better understand the effect of pregnancy on breast cancer development.

We used single cell RNA-sequencing to define the diversity of epithelial and non-epithelial cells in mammary tissues from nulliparous and parous female mice. Our analysis supports the conclusion that pregnancy epigenetically reprograms mammary epithelial cells (MECs) - marked by an upregulation of immune communication signaling pathways. We identified a population of Natural Killer T-cells (NKT) that are expanded in healthy, post-involuted mammary glands, and a corresponding elevation in the expression of CD1d, an antigen presenting molecule, on the surface of MECs that has the potential to induce NKT maturation. Loss of CD1d expression or an overall lack of activated NKT cells in various mouse strains leads to increased tissue hyperplasia in response to cMyc overexpression or Brca1 loss, in a pregnancy-independent manner, pointing to a role for this immune sub-population in restricting oncogenic transformation in the post-pregnancy mammary gland.

Natural killer T-cells (NKT) are a rare subset of T cells that exhibit characteristics of both innate and adaptive immune cells. Like adaptive immune cells, they express antigen specific T-cell receptors (TCR) generated by VDJ recombination, but like innate cells, they do not develop immunological memory and react rapidly to antigen exposure. This makes NKT cells uniquely capable of mounting a rapid response in response to activation by specific antigens. We used flow cytometry to assess any changes to the TCR repertoire of NKT cells and found that post-pregnancy NKT cells predominantly expressed γδ-TCRs on their surface, unlike typical NKTs that express αβ-TCRs, indicating a role in specialized antigen recognition.

While a loss of CD1d and activated NKT cells promotes oncogenesis in our mouse models, we observe that in post-pregnancy mice that do not develop signs of hyperplasia, the tumor-free mammary glands are enriched in NKT cells that express γδ-TCRs, and the MECs have elevated CD1d on their surface. We found that by culturing healthy, pre-pregnancy mammary gland organoids with pregnancy hormones *in vitro*, we are able to increase the expression of CD1d on the MECs. By implanting these high-CD1d MECs into pregnancy naïve recipient female mice, we found that NKT cell abundance is transiently increased in the glands injected with pregnancy hormone treated organoids, compared to those injected with untreated control organoids. This points us to the potential of reprogramming MECs to exhibit post-pregnancy properties and to explore opportunities to extend pregnancy-induced protection to never-pregnant recipients in future rodent studies.

Collectively, our findings illustrate how pregnancy-induced changes modulate the communication between MECs and the immune microenvironment, and establish a causal link between pregnancy, the immune microenvironment, and mammary oncogenesis. Given the emerging role of immunotherapy in blocking cancer progression, this study sets the ground for understanding pregnancy-induced changes in the context of oncoprotection.

## Acknowledgements

They say it takes a village. My village has been closer to the scale of a small metropolitan city. It would take an entire thesis to express my gratitude to everyone who has been by my side through this crazy journey, but I will give it my best shot.

First and foremost, I thank my parents, Lalitha and Somasundara Hanasoge. Even though you never understood why I wanted to spend so many years of my life in school, you continued to support me and believe in me. I cannot imagine how hard it must have been for you to let your only child move across the world to pursue her dreams. You sent me off with smiles on your faces, I cannot express in words how much that helped me in my first few months of learning to be an adult in a foreign country. Thank you for being so excited about my curiosity and indulging me since childhood. For instilling in me the core values of being a good human being and the value of hard work and dedication. For being so proud of all my little achievements and making sure I knew it. I could not have done this without you.

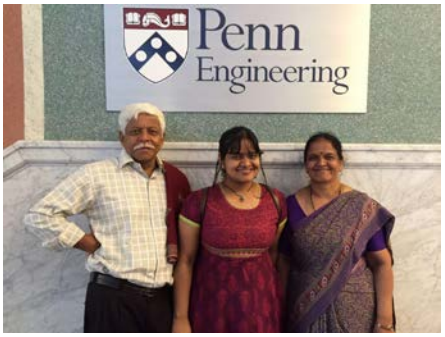


I am incredibly lucky to have been mentored by my research advisor, Camila dos Santos. I have made many good choices in my life, but joining Camila's lab is undoubtedly the best choice I have ever made. Not only is Camila an incredibly smart and driven scientist from whom I have learned innumerable scientific skills, she is one of the kindest and most genuine human beings I have ever known. Camila, I knew that doing a PhD would be hard, but I was definitely unprepared for the kinds of hardship I would face during these four years. I can honestly say that I may have quit if it weren't for your unwavering support and understanding. You made sure that I knew you were there during the darkest times, and

continued to believe in me when I did not. Your faith in me made me want to push myself to be better, to work harder, to not let you down. You have made me not only a better scientist, but a better person. Thank you for everything, I'm really proud to have been your first grad student and I will always treasure that! Thank you also for trusting me to take care of Xuxa every now and then, it has been an absolute joy to be one of her favorite people in lab. Nothing brightens up my day more than hearing her dog collar jingling as she runs through the halls!


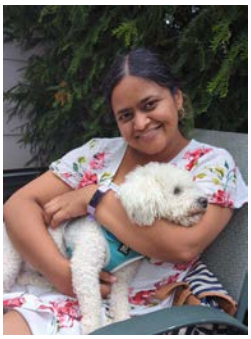


I am grateful to my academic mentor, Leemor Joshua-Tor, and my thesis committee members, David Spector, Lloyd Trotman, and Semir Beyaz, for their guidance, support, and critical feedback during and outside my committee meetings. I also thank my external committee member, Jose Silva, for being such a dedicated judge of this thesis.

I would not be here today without the support of the staff of the CSHL School of Biological Sciences. I am forever grateful to Alex Gann for taking a chance on me, despite my not stellar grades. I will always remember interviewing with him during recruitment. Even though he asked me about my grades, he said "…we understand that grades aren't reflective of your ability to be a good scientist. Besides, you have great recommendation letters". I want to thank Alyson, Monn, Kim, and Kim for all of the behind-the-scenes work they do every day to make sure that we can focus on research and not get lost in the details of things like planning and scheduling thesis committee meetings and completing academic requirements. I have felt very spoiled and cared for during my grad school years, and that is a very special feeling that I will carry with me for the rest of my life.

Being a member of the dos Santos lab is an unforgettable experience. I have looked forward to going to lab every day because of the extremely special group of people that I have had the privilege to work with over the last 4 years. When I joined the lab in 2019, we were a much smaller group in a smaller lab space. But even as the lab has grown and expanded over the years, the friendships and experiences I have shared in the lab have really shaped me as a person. From group Halloween costumes, ugly holiday sweaters, to karaoke nights out in the city, everything about the lab makes everyone feel included in a tight-knit and highly supportive community. Mary, Sam, Chen, City, and Mike – thank you for welcoming me into the fold from day one! Even though the school insists that the students should not make decisions about which lab we join until the end of all 3 rotations, I told Sam on the second day of my rotation that I had made up my mind to join the lab (I will never live this one down). Marygrace, Sam Henry, James, Steven, Mackenzie, Deep, Dhivyaa, Lucia – all of you bring so much joy to my life, in and out of the lab! And of course, our honorary dos Santos lab members and a natural extension of the friend group over the years – Kaarina, Nim, Tania, Dennis, Percy, and Francesca, thank you for making my time in grad school memorable and so much fun! I thank Sabrina Boettcher and Nancy Bolanos for all the administrative and technical support. I am grateful beyond words for all the love and support, and much needed confidence you have all placed in me through all these years!

I thank Akshitha Sriraman, my biggest inspiration and fiercest friend. Akshitha, thank you for always being there, for never once doubting that I could do this, for always bringing out the best in me, for being the big sister I never had, and for everything that you are, exactly as you are.



I thank Janhavi Pandurangi for being my constant support system and biggest cheerleader. Janu, CSHL was your dream first. Thank you for sharing it with me, I would not be here without you. I can't wait for the day when you finally make it to this side of the pond so that I can show you around!


A big shout-out to my friend Karen Wei – you remind me to take care of myself first and help me fight my imposter syndrome. I'm excited to be able to see you more often once I'm back in the city!


One of the many special things about the CSHL-SBS is that it comes with a built-in support system in the form of classmates that you live with for at least one year. I consider myself the luckiest person alive to have found a family. Marie, Alexa, Jonathan, and Mo (Team Roxy, as we fondly call ourselves), thank you all for always being there, for your steadfast love, friendship, and loyalty, for taking care of me when I couldn't do it myself. From being trapped in the house during a blackout, and then a pandemic, nobody else will know the joy and (sometimes literal) pain of our time together. Pickles, the cutest, most clumsy little kitty in all the world, thank you for giving me a reason to take hundreds of photos that we can all look back on. I also thank my classmates and friends for all the fun times and fond memories.

Moving across the world was hard, but it would have been infinitely harder without my family on this side of the world. Shekhar chikkappa, Shalini akka, Shreya, and Leelu ajji – thank you for always making sure I knew I wasn't alone and sending me off with more home-cooked food than I could carry after every visit! Rajanna, who is now in California, for checking in, keeping me grounded, and all the love and support. I thank my family and friends back home for always wanting the best for me, and for being there for my parents. For being more excited about the things I do than I am, and for being so proud of me.

This work was completed with financial support from the CSHL School of Biological Sciences and the Bristol-Myers Squibb Fellowship.

## Table of Contents

**Summary** ..... **1**

**Acknowledgements** ..... **3**

**Table of Contents** ..... **8**

**List of Abbreviations** ..... **10**

**List of Figures** ..... **14**

**List of Tables** ..... **15**

**1. Introduction** ..... **16**

***1.1 An overview of mammary gland development*** ..... *17*
1.1.1 The hierarchy of Mammary Epithelial Cell development ..... 17
1.1.2 The stages of mammary gland development ..... 19
1.1.3 Mammary glands retain a memory of pregnancy ..... 24
1.1.4 The role of the tissue microenvironment in mammary gland development and oncogenesis ..... 25

***1.2 Breast cancer*** ..... *30*
1.2.1 Molecular subtypes of breast cancer ..... 32
1.2.2 Breast cancer cell of origin and tumor heterogeneity ..... 34
1.2.3 Pregnancy and breast cancer ..... 36
1.3.1 In vivo models ..... 39
1.3.2 In vitro models – 3D organoid cultures to study mammary gland development ..... 41

***1.4 Exploiting immune cells for breast cancer therapies*** ..... *44*
1.4.1 Unconventional T cells as potential ACT agents ..... 45

***1.5 Research hypotheses*** ..... *50*

**2. Parity induced changes to the mammary epithelial and immune composition** ..... **52**

***2.1 Author contributions*** ..... *52*

***2.2 Results*** ..... *52*
2.2.1 Single cell analysis identifies changes to the transcriptional programs and immune composition of the post-pregnancy mammary gland ..... 53
2.2.2 Pregnancy induces the expansion of a specific population of NKT cells in the mammary gland ..... 64
2.2.3 NKT expansion requires CD1d expression on post-pregnancy MECs ..... 72

**3. Pregnancy and oncoprotection in genetic models of mammary cancer** ..... **77**

***3.1 Author contributions*** ..... *77*

***3.2 A brief introduction to the GEMMs used in this section*** ..... *77*
3.2.1 The CAGMYC mouse model ..... 77
3.2.2 The K5-CreERT2 Brca1$^{fl/fl}$ p53$^{-/+}$ (Brca1 KO) mouse model ..... 78

***3.3 Results*** ..... *80*

3.3.1 Lack of mammary oncogenesis is marked by NKT expansion and CD1d+ MECs in CAGMYC and Brca1 KO parous mice ..... 80
3.3.2 Functionally active NKT cells are required to block malignant progression of post-pregnancy MECs ..... 88

**4. Establishing an *in vitro* system to reprogram and assay pregnancy naïve MECs ..... 96**

***4.1 Author contributions*** ..... *96*

***4.2 Introduction*** ..... *96*

***4.3 Results*** ..... *97*
4.3.1 Pregnancy hormones are the most effective inducers of CD1d expression on MECs and may increase NKT abundance *in vivo* ..... 97
4.3.2 Post-pregnancy immune cells exhibit an enhanced ability to induce cell death in Brca1 KO tumor organoids ..... 100

**5. Conclusions and Perspectives ..... 104**

***5.1 Highlights*** ..... *107*

***5.2 Future directions*** ..... *108*

**6. Experimental Procedures ..... 111**

***6.1 Data and Code Availability*** ..... *111*

***6.2 Experimental Model and Subject Details*** ..... *111*

***6.3 Method Details*** ..... *112*

**7. References ..... 128**

**8. Appendix 1 – Supplementary tables ..... 146**

**9. Appendix 2 – List of publications ..... 158**

## List of Abbreviations

| | |
|---|---|
| ACT | Adoptive Cell Therapy |
| AR | Androgen Receptor |
| ATAC-seq | Assay for Transposase-Accessible Chromatin with high throughput sequencing |
| ATM | Ataxia Telangiectasia Mutated |
| BC | Breast Cancer |
| BCL11B | BAF Chromatin Remodeling Complex Subunit BCL11B |
| BLG | Beta Lactoglobulin |
| BM | Basement Membrane |
| BRCA1 | BRCA1 DNA Repair Associated |
| BRCA2 | BRCA2 DNA Repair Associated |
| CAF | Cancer Associated Fibroblast |
| CAR | Chimeric Antigen Receptor |
| CBX3 | Chromobox 3 |
| CCL2 | C-C Motif Chemokine Ligand 2 |
| CCL5 | C-C Motif Chemokine Ligand 5 |
| CCR5 | C-C Motif Chemokine Receptor 5 |
| CD | Cluster of Differentiation |
| CDX | Cell line-Derived Xenograft |
| CHEK2 | Checkpoint Kinase 2 |
| cMYC | MYC proto-oncogene |
| CNV | Copy Number Variation |
| CSC | Cancer Stem Cell |
| CTLA-4 | Cytotoxic T-Lymphocyte Associated Protein 4 |
| CXCR6 | C-X-C Motif Chemokine Receptor 6 |
| DEG | Differentially Expressed Gene |
| DMBA | 7,12-Dimethylbenz(a)anthracene |
| DNA | Deoxyribonucleic Acid |
| DOX | Doxycycline |
| E2 | Estrogen |
| ECM | Extracellular Matrix |
| EGFR | Epidermal Growth Factor Receptor |
| EGR2 | Early Growth Response 2 |
| EMT | Epithelial to Mesenchymal Transition |
| EPCAM | Epithelial Cell Adhesion Molecule |
| EPP | Estrogen, Progesterone, Prolactin |
| ER | Estrogen Receptor |

| | |
|---|---|
| ERK1/2 | Extracellular signal Regulated Kinase 1/2 |
| EZH2 | Enhancer Of Zeste 2 Polycomb Repressive Complex 2 Subunit |
| FACS | Fluorescence Activated Cell Sorting |
| FAS | Fas Cell Surface Death Receptor |
| FOXP3 | Forkhead Box P3 |
| GATA3 | Globin Transcription Factor binding protein 3 |
| GEMM | Genetically Engineered Mouse Model |
| GFP | Green Fluorescent Protein |
| GH | Growth Hormone |
| GLI2/3 | GLI Family Zinc Finger 2/3 |
| GO | Gene Ontology |
| GSEA | Gene Set Enrichment Analysis |
| GVHD | Graft Versus Host Disease |
| GZMA | Granzyme A |
| GZMB | Granzyme B |
| H&E | Hematoxylin and eosin stain |
| HER2 | Human Epidermal growth factor Receptor 2 |
| Hh | Hedgehog pathway |
| HOX | Homeobox family |
| ICI | Immune checkpoint inhibition |
| IF | Immunofluorescence |
| IFN-γ | Interferon Gamma |
| IHC | Immunohistochemistry |
| IL-1β | Interleukin 1 Beta |
| IL-6 | Interleukin 6 |
| ITGAX | Integrin Subunit Alpha X |
| JAK2 | Janus Kinase 2 |
| K14/KRT14 | Cytokeratin 14 |
| K5/KRT5 | Cytokeratin 5 |
| K8/KRT8 | Cytokeratin 8 |
| KI | Knock In |
| KLRK1 | Killer Cell Lectin Like Receptor K1 |
| KO | Knock Out |
| LYPLA1 | Lysophospholipase 1 |
| MACS | Magnetic-Activated Cell Sorting |
| MAF | Avian Musculoaponeurotic Fibrosarcoma (MAF) Protooncogene |
| MAGED1 | MAGE Family Member D1 |
| MAIT | Mucosal Associated Invariant T-cells |
| MDSC | Myeloid Derived Suppressor Cell |

| | |
|---|---|
| MEC | Mammary Epithelial Cells |
| MET | Mesenchymal to Epithelial Transition |
| MHC | Major Histocompatibility Complex |
| MMPs | Matrix Metalloproteinases |
| MMTV | Mouse Mammary Tumor Virus |
| MR1 | Major Histocompatibility Complex, Class I-Related |
| mTOR | Mechanistic Target Of Rapamycin Kinase |
| NK | Natural Killer cell |
| NKG7 | Natural Killer Cell Granule Protein 7 |
| NKT | Natural Killer T cell |
| OXT | Oxytocin |
| P4 | Progesterone |
| p53 | Tumor Protein P53 |
| PABC | Pregnancy Associated Breast Cancer |
| PALB2 | Partner And Localizer Of BRCA2 |
| PARP | Poly(ADP-Ribose) Polymerase |
| PD-1 | Programmed death-1 |
| PD-L1 | Programmed death-ligand 1 |
| PDK4 | Pyruvate Dehydrogenase Kinase 4 |
| PDX | Patient-Derived Xenograft |
| PIK3CA | Phosphatidylinositol-4,5-Bisphosphate 3-Kinase Catalytic Subunit Alpha |
| PR | Progesterone Receptor |
| Prl | Prolactin |
| PTEN | Phosphatase And Tensin Homolog |
| RAG1 | Recombination Activating Gene 1 |
| RAS | Rat Sarcoma oncogene |
| RNA | Ribonucleic acid |
| RORγT | Retinoic acid receptor-related Orphan Receptor gamma 2 |
| RSG5 | Regulator of G-protein Signaling 5 |
| scRNA-seq | Single Cell RNA Sequencing |
| SLUG | Snail Family Transcriptional Repressor 2 |
| STK11 | Serine/Threonine Kinase 11 |
| TAA | Tumor Associated Antigen |
| TAM | Tamoxifen |
| TAMs | Tumor Associated Macrophages |
| Tbet/TBX21 | T-Box Transcription Factor 21 |
| TCR | T Cell Receptor |
| TEB | Terminal End Bud |
| TF | Transcription Factor |

| | |
|---|---|
| TGF-β | Transforming Growth Factor Beta |
| Th17 | T helper 17 cell |
| TIL | Tumor Infiltrating Lymphocytes |
| TNBC | Triple Negative Breast Cancer |
| TNF-α | Tumor Necrosis Factor Alpha |
| TRAIL | TNF-related apoptosis-inducing ligand |
| T-reg | Regulatory T cell |
| TWIST | Twist Family Base-Helix-Loop-Helix Transcription Factor |
| UMAP | Uniform Manifold Approximation and Projection for Dimension Reduction |
| UTX | Ubiquitously transcribed tetratricopeptide repeat, X chromosome |
| VEGF | Vascular Endothelial Growth Factor |
| WAP | Whey Acidic Protein |
| WNT | Wingless-Type |
| WT | Wild-Type |
| ZBTB16/PLZF | Zinc Finger And BTB Domain Containing 16 |
| ZEB1 | Zinc Finger E-Box Binding Homeobox 1 |
| α-GalCer | alpha-Galactosylceramide |
| α-SMA | Alpha Smooth Muscle Actin |

## List of Figures

Figure 1-1 Simplistic model of mammary epithelial cell differentiation hierarchy. 18
Figure 1-2 The stages of mammary gland development. 20
Figure 1-3 Molecular mutations in breast cancer. 31
Figure 1-4 Effect of pregnancy and age at first birth on breast cancer risk in humans. 36
Figure 2-1 Single cell level classification of pre- and post-pregnancy MECs. 54
Figure 2-2 Single cell analysis identifies post-pregnancy biased epithelial cells in mammary tissue from parous female mice. 56
Figure 2-3 Pathway analysis of post-pregnancy biased epithelial cells indicates changes to immune communication signatures 57
Figure 2-4 Single cell analysis identifies transcriptional programs and immune cellular heterogeneity in mammary tissue from parous female mice. 59
Figure 2-5 Characterization of pre- and post-pregnancy mammary resident immune cells. 60
Figure 2-6 Single cell analysis identifies post-pregnancy biased immune cell identity as NKT cells. 61
Figure 2-7 scRNA-seq identification of post-pregnancy NKT cells. 63
Figure 2-8 Pregnancy induces expansion of specific populations of NKT cells. 65
Figure 2-9 Cellular characterization of post-pregnancy mammary immune microenvironment. 66
Figure 2-10 Cellular characterization of post-pregnancy NKT cells shows altered TCR expression. 68
Figure 2-11 The molecular signature of post-pregnancy NKT cells. 70
Figure 2-12 The epigenetic signature of post-pregnancy NKT cells. 71
Figure 2-13 Pregnancy alters CD1d transcription and expression on the surface of MECs. 73
Figure 2-14 The effects of pregnancy in controlling CD1d expression. 74
Figure 2-15 NKT expansion depends on CD1d expression on post-pregnancy MECs. 76
Figure 3-1 Characterization of $Krt5^{CRE\text{-}ERT2}Brca1^{ko}p53^{het}$ (Brca1 KO) mouse model. 79
Figure 3-2 The effects of cMYC-overexpression on pregnancy-induced immune changes and CD1d+ post-pregnancy MECs. 81
Figure 3-3 Lack of mammary oncogenesis is marked by NKT expansion and CD1d+ MECs in CAGMYC parous female mice. 83
Figure 3-4 Pregnancy decreases the frequency of Brca1 KO mammary tumor development. 84
Figure 3-5 Lack of mammary oncogenesis is marked by increased CD1d expression on MECs in Brca1 KO parous mammary tissue. 86
Figure 3-6 Lack of mammary oncogenesis is marked by NKT expansion in Brca1 KO parous mammary tissue. 87
Figure 3-7 cMYC-overexpression induces oncogenesis of post-pregnancy MECs transplanted into NOD/SCID mammary fatpads. 90
Figure 3-8 Functionally active NKT cells are required to block malignant progression of post-pregnancy MECs. 92
Figure 3-9 Loss of CD1d expression supports the malignant transformation and oncogenesis of post-pregnancy CAGMYC MECs. 95
Figure 4-1 Pregnancy hormones induce an increased CD1d expression on the surface of MECs in mammary organoid cultures derived from healthy Balb/C mice. 99
Figure 4-2 2D co-culture of primary tumor organoids with primary NKT cells is not an informative system to assess changes in NKT cytotoxicity 101
Figure 4-3 3D co-culture of primary tumor organoids with primary immune cells shows increased cell death caused by post-pregnancy immune cells 103

## List of Tables

Table 4-1 CD1d inducing compounds used in the screen, related to Figure 4-1 ..... 98
Table 8-1 Differential gene-expression analysis (avg_log2FC) comparing selected pre- and post-pregnancy mammary epithelial scRNA-seq clusters, related to Figure 2-3. ..... 146
Table 8-2 Differential gene-expression analysis (avg_log2FC) comparing FACS-isolated pre- and post-pregnancy luminal mammary epithelial cells, related to Figure 2-3. ..... 156
Table 8-3 Differential gene-expression analysis (log2FoldChange) comparing FACS-isolated pre- and post-pregnancy mammary resident NKT cells, related to Figure 2-11. ..... 157

# 1. Introduction

Breast cancer is the most commonly diagnosed cancer in women, with one in eight women being affected during their lifetime. Breast cancer is not a single disease, given its distinct histopathology, genomic variations, and clinical outcomes. Although a lot has been understood about the biology of breast cancer, and effective therapies exist for specific subtypes of the disease, we still lack a clear picture for when or whether an individual will develop breast cancer. Moreover, targeted therapies for the more aggressive subtypes such as luminal B and triple negative breast cancer (TNBC) have not yet been developed (Collins et al. 2015). Therefore, there must be an increase in efforts to define better risk prediction models and additional and effective therapies for the disease.

There are several factors that may influence breast cancer risk. These include genetic predisposition, age, race, ethnicity, age of menarche and menopause, reproductive history, alcohol consumption, weight and physical activity, hormone therapy, and exposure to radiation (CDCBreastCancer 2022).

This thesis focused on pregnancy as a mediator of sustained changes to the cells of the mammary gland, particularly the immune compartment, and their association with cancer inhibition. In the introduction, I will outline the normal developmental process that the mammary gland goes through and the signals that cause it to reach its fully differentiated state, and how changes to normal processes can promote tumorigenesis. I will briefly describe the work that has been done to understand the stromal components of the mammary gland during various developmental stages. Next, I will go over the commonly used *in vivo* and *in vitro* models to study normal and cancerous mammary gland development. Finally, I will describe the limited ways in which immunotherapy and engineered immune cells have been used to treat breast cancer in the clinic and challenges that remain in order to make this treatment more widely available.

## 1.1 An overview of mammary gland development

The mammary gland is composed of a variety of cell types – epithelial cells, immune cells, fibroblasts, and adipocytes. We will briefly discuss the role of each of these cell types in mammary gland development.

### 1.1.1 The hierarchy of Mammary Epithelial Cell development

The epithelial cells of the mammary gland can be subdivided into cell types that have different functions but make up the mammary tree together (**Fig. 1-1**). Broadly, the two main epithelial cell compartments in the mammary gland are the luminal compartment (the inner layer) and the basal compartment (the outer layer) that is in direct contact with the basement membrane.

Recent studies that use lineage tracing and scRNA-seq approaches have demonstrated that the luminal and basal compartments are not solely maintained by one common pool of bipotential mammary stem cells (MaSC), but also have lineage-restricted stem and progenitor cells from embryonic development through puberty (Pal et al. 2017; Bach et al. 2017; Cristea and Polyak 2018).

Luminal cells can be further subdivided into progenitor, alveolar, and ductal cells. Luminal progenitor cells have the ability to give rise to differentiated cells. Alveolar cells are predominantly responsible for the production of milk during lactation. Ductal cells form the milk ducts that carry milk to the nipples in response to the suckling stimulus from offspring. There is also a lineage of hormone receptor (ER) positive cells in the luminal compartment that is distinct from ER negative alveolar and ductal cells (Fu et al. 2020; Tiede and Kang 2011).

The basal progenitor gives rise to highly contractile myoepithelial cells which guide milk from the lumen, and are also involved in deposition and remodeling of the basement membrane (Fu et al. 2020; Tiede and Kang 2011).

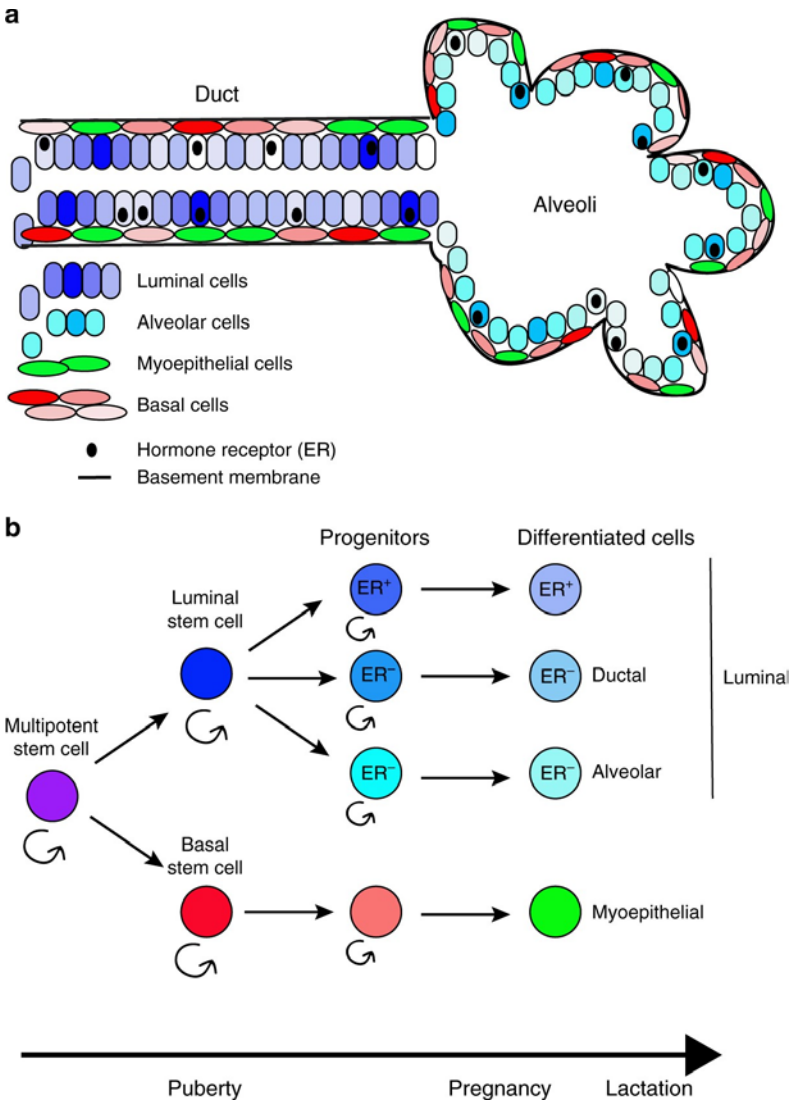


***Figure 1-1 Simplistic model of mammary epithelial cell differentiation hierarchy.***

A. Schematic outline of a ductal-alveolar unit with location of the various cell types indicated.
B. A putative map of mammary epithelial cell differentiation. A multipotent stem cell present during development gives rise to luminal epithelial and basal stem cells, which further divide into luminal and basal progenitors during puberty. Ductal and alveolar hormone-receptor negative progenitors are distinct lineages and there is also a separate hormone receptor positive luminal lineage.
*Figure from: Cristea and Polyak., 2018, Nature Communications. Image used under a Creative Commons 4.0 International License. http://creativecommons.org/licenses/by/4.0/*

### 1.1.2 The stages of mammary gland development

Mammary gland development (**Fig. 1-2**) mainly occurs postnatally, even though it sees its beginnings in the embryonic stages.

*Embryonic development*

Embryonic development of the mammary gland is initiated during mid-gestation. In mice, the primary species that has been used as the model system to study mammary gland development, mammary gland formation begins at embryonic day 10 (E10) (Macias and Hinck 2012; Slepicka et al. 2021). Thick bands of ectodermal cells form bilateral and vertical mammary lines at E11.25 whereupon clumps of ectoderm (placodes) bloom along the mammary line at day E11.75. At day E12.5 the placodes protrude into the mesoderm, forming an early mammary bud surrounded by a basement membrane (BM) and the first traces of a mammary mesenchyme (fat pad). Between E13 and E14, the bud will give rise to mammary bulbs with an ectodermal stalk that will elongate into a sprout surrounded by the mesenchyme at E15.5. Lumen formation commences at day E17-18, involving the programmed death of ectodermal cells localized at the center of the mammary branches.

Members of the fibroblast growth factor (FGF) and the wingless-related integration site (WNT) protein families govern signaling in mammary embryonic tissues, and they regulate transcription factors (TFs) from the Homeobox gene family (HOX), GATA3 (GATA binding protein 3), and the T-box family (TBX), which are intermittently expressed either in the endoderm or mesoderm (Carroll and Capecchi 2015; Asselin-Labat et al. 2007; Davenport et al. 2003).

Other regulators of mammary embryogenesis include TFs that are part of the Hedgehog (Hh) pathway. Through a signaling cascade with members of the Hh network, Gli3 activates gene-specific transcription that controls bud formation (Lee et al. 2013a; Tickle and Jung 2016; Robinson 2007). Gli2 functions in ductal branching through its localization in the tissue surrounding mammary branches (stroma) from embryogenesis to adulthood, but it becomes stromal and epithelial during pregnancy and lactation (Hatsell and Cowin 2006).

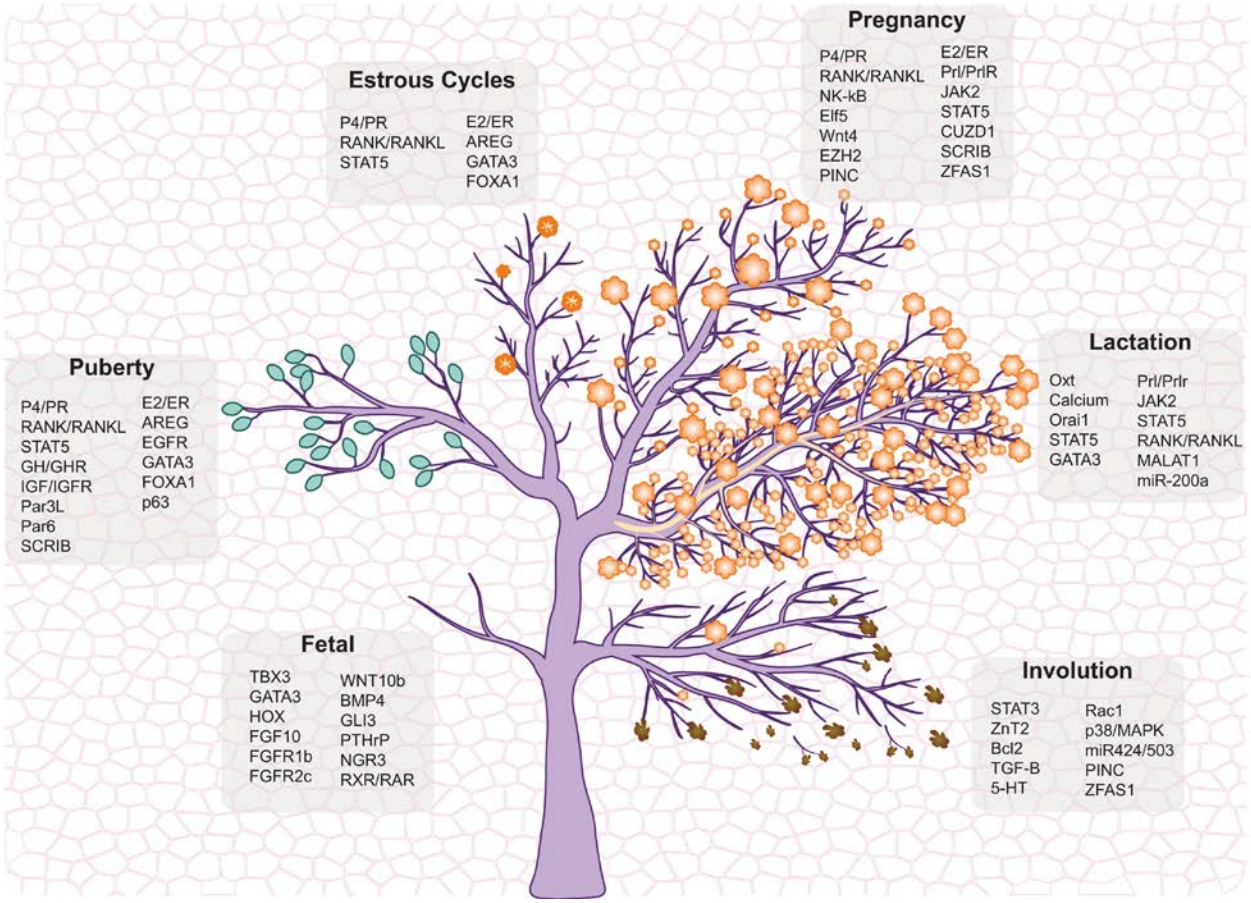


***Figure 1-2 The stages of mammary gland development.***

Schematic illustration of mammary gland developmental stages, showing fetal, puberty, estrous cycles, pregnancy, lactation and involution (from left to right). In puberty, green buds represent TEBs. Mammary alveoli are shown as orange flowers in estrous cycles, pregnancy and lactation. In lactation, the milk is represented as yellow sap flowing from the alveoli (flowers) to the ducts (branches). During involution, the regression of the mammary tissue is depicted with falling dead flowers and branches into the background, which portrays the fat pad. The main molecular regulators of each developmental stage are highlighted in the grey squares.
*Figure from: Slepicka et al., 2021, Seminars in Cell and Developmental Biology*

*Pubertal development*

During embryogenesis, maternal hormones provide the initial stimuli to the rudimentary mammary gland for ductal development. However, after birth, cessation of maternal signaling reduces ductal and branching genesis in the postnatal mammary gland. This activity resumes with the onset of puberty, a stage marked by the production of female sexual hormones, which will complete mammary morphogenesis and prepare the gland for milk production in the event of pregnancy.

Puberty varies widely, from a few weeks to several years post-birth, in different mammalian species (5 weeks in mice and 9-18 years in humans). The onset of puberty is triggered by the increase in gonadotropin levels that lead to the secretion of ovarian hormones, mainly estrogen (E2) and progesterone (P4). Peak levels of E2 production are between the follicular phase and ovulation and, depending on the vertebrate, E2 synthesis occurs every 2-4 days in mice and once every month in humans (Fata et al. 2001).

*Estrous cycles in adulthood*

In the pubertal and adult female, the mammary gland undergoes developmental modifications tightly correlated with ovarian/uterine reproductive cyclical repetitions (4-5 days in mice and 26-32 days in humans). The rapid increase in mammary morphogenesis through branch initiation, invasion of the fat pad, and ductal elongation, transforms a pre-formed, rudimentary mammary epithelium into an extensive ductal network. Hormonal signaling promotes differentiation and proliferation of Mammary epithelial cells (MECs), culminating in an extensively branched mammary morphology (Robinson et al. 1995).

Overall, several molecular pathways and factors act during puberty to promote mammary ductal maturation, and these pathways remain active throughout adulthood. As each reproductive cycle promotes lobulo-alveologenesis and branching, we speculate that the constant promotion of mammary cell differentiation and proliferation may induce tumorigenesis over time or otherwise elicit oncogenic pathways that are dormant in the first years of adulthood.

*Pregnancy and Lactation*

A complete pregnancy cycle involves gestation, lactation, and involution and, collectively represents the second postnatal stage of mammary gland development, which prepares the gland to produce nourishment to support the offspring.

During pregnancy, Progesterone (P4) and prolactin (Prl) orchestrate the differentiation of MECs into specialized alveolar structures, which are capable of synthesizing and secreting milk during lactation. Like its function during puberty, the main role of P4 during pregnancy is to promote extensive ductal branching but, in pregnancy, P4 signals substantially increase the number of alveolar structures to promote a lactation-competent gland. During the early stages of pregnancy, markedly increased Prl levels play a role in maintaining the *corpus luteum* (a hormone secreting structure in the ovary, responsible for the production of P4), expression of E2 and P4, and in inducing mammary morphogenesis (Ormandy et al. 1997a, 1997b).

The release of oxytocin (peptide and neuropeptide hormone secreted by the hypothalamus, OXT) is one of the factors that control parturition (the act of giving birth) and lactation. OXT controls calcium uptake and contractibility of myoepithelial cells and induces mechanical constriction of luminal alveolar cells to eject milk droplets into the lumen of alveoli (Moore et al. 1987).

While the placental hormones regulate Prl function mid-pregnancy, Prl levels increase during lactation. Prl is mainly expressed by lactotrophic cells in the pituitary gland and released into the bloodstream, but it is also expressed locally in several tissues, including by MECs in the mammary glands. Late during gestation and early during lactation, formation of tight junctions during luminal cell specification controls cellular polarity, which is crucial for directional secretion of milk droplets into the lumen (Rodriguez-Boulan and Macara 2014), which is principally coordinated by Prl/Jak2 modulation of Erk1/2 function (Liu et al. 2015).

*Involution*

Offspring weaning removes the suckling stimulus and causes milk stasis, which triggers a series of remodeling processes leading to regression of mammary tissue to a pre-pregnancy state, also known as

involution (**Fig. 1-2**). In humans involution lasts an average of 24 months, while in rodents it lasts for ~10-20 days and encompasses two main phases, the reversible phase (days 0-2 of involution) and the irreversible phase (days 8-18) (Jindal et al. 2014; Sharp et al. 2007).

The reversible phase is characterized by reduced milk production, milk absorption, epithelial cell shedding, alveolar cell death, phagocytosis of apoptotic cells by non-specialized epithelial cells, leukocyte infiltration, and breakdown of tight junctions. As the name implies, resumption of suckling and the suckling stimulus restores lactation through the release of accumulated milk. During lactation, the mammary gland may commence reversible involution after a few hours of milk accumulation, which restores milk-producing cells and avoids over production of milk.

During the irreversible phase (days 2-6), the mammary extracellular matrix (ECM) undergoes substantial remodeling, with the activation of wound healing processes, via increased activity of matrix metalloproteases (MMPs), deposition of collagen and BM, in addition to changes in many signaling pathways (Green and Lund 2005). Macrophages and non-professional phagocytic MECs clear the remainder of the cellular debris, resulting in a second wave of inflammation and immune cell recruitment (Stein et al. 2004; Monks et al. 2005).

The ECM also plays a role in immune cell recruitment and activation, as well as broader immune system functions, as collagen and laminin fragments may also induce an influx of macrophages and neutrophils to the involuting gland (Jena et al. 2019). Accordingly, TGF-β regulates MEC cell death and phagocytosis, and helps in the maintenance of ECM integrity, thus also playing a role during the final stages of involution (Xu et al. 2009; Pang et al. 2016). Signaling pathways and the high cell-turnover modulate mammary involution, and they also promote an increase in self-antigen reactions, creating an immune tolerant environment and a mucosal barrier. Increased numbers of $ROR\gamma T^{+}$ $FoxP3^{+}$ $CD4^{+}$ T regulatory cells, dendritic cells, and memory Th17-Treg cells are observed during involution. The immune environment then reverts to its nulliparous state when involution comes to an end (Betts et al. 2018).

### 1.1.3 Mammary glands retain a memory of pregnancy

Pregnancy brings about many changes in the mammary gland, some transient and some more permanent, and these can influence breast cancer risk. The protective effect of pregnancy on breast cancer has been hypothesized to involve both cell non-autonomous and cell autonomous mechanisms. The cell non-autonomous changes likely involve persistent changes in hormone levels and the stromal composition of the mammary gland post-pregnancy (Thordarson et al. 1995; Schedin et al. 2004). Reduced levels of prolactin (PRL) and growth hormone (GH) are observed post-pregnancy, and in studies investigating the effects of hormone levels, elevated PRL and GH have been associated with an increased incidence of mammary tumorigenesis (Harvey 2012). The stromal composition including in the extracellular matrix (ECM) and collagen organization are altered by pregnancy, which has been hypothesized to reduce tumor growth and invasion (Maller et al. 2013).

Cell autonomous changes brought about by pregnancy that have been implicated in breast cancer protection include changes in the differentiation and alteration in cell fates of populations of mammary epithelial cells (MEC). After involution, even though the physiological state of the mammary gland goes back to its pre-pregnant state, there are several changes that persist. This includes a reduction in the rate of proliferation and an increased ability to repair DNA damage (Barton et al. 2014). It has been hypothesized that pregnancy induced terminal differentiation removes cells prone to become cancerous and hence reduces the risk of developing breast cancer (Meier-Abt and Bentires-Alj 2014). Pregnancy associated hormonal changes have also been hypothesized to change the developmental fate of certain MEC subpopulations by causing persistent changes to signaling pathways and other regulatory molecules that control the “stemness” and proliferation potential of mammary progenitor cells. The Wnt/Notch signaling, TGFβ signaling pathways, and the cell cycle regulator p27 have been implicated in this cell fate alteration to $CD44^{+}/CD24^{-}/CD10^{-}$ breast progenitor cells, leading to a downregulation of pro-tumorigenic pathways (Meier-Abt et al. 2013; Choudhury et al. 2013).

The terminal differentiation of the mammary gland also brings with it changes in gene regulation. Cells in the post-pregnant mammary gland show a higher content of heterochromatin (more condensed) as

compared to cells in the pre-pregnant gland which contain mostly euchromatin. This is thought to be due to the lack of terminal differentiation of the cells in the pre-pregnant gland (Russo et al. 2012). The more differentiated post-pregnant cells are more resistant to transformation into cancer cells. A parity induced genomic signature was described in post-pregnancy MECs which provides clues to the mechanism of pregnancy induced protection against tumorigenesis (Blakely et al. 2006). Post-pregnancy MECs show an upregulation of genes like *EZH2*, *GATA3*, and *CBX3* which are involved in gene silencing by chromatin condensation, a feature seen in the parous mammary gland (Russo et al. 2012).

Pregnancy has been found to permanently alter the epigenetic landscape and induce long term changes in the breast tissue (Choudhury et al. 2013; Blakely et al. 2006). An epigenetic memory of pregnancy has been shown to persist in the mammary gland, allowing the gland to react quicker and more efficiently to subsequent pregnancies (Dos Santos et al. 2015). These changes have been shown to affect cMyc driven oncogenesis – post-pregnancy MECs resist oncogenesis in response to cMyc overexpression. This has been linked to reduced H3K27ac activation marks in cMyc enhancer regions that persist post-pregnancy (Feigman et al. 2020).

### 1.1.4 The role of the tissue microenvironment in mammary gland development and oncogenesis

The microenvironment surrounding mammary tissue plays a pivotal role in the gland development, predominantly via regulation of epithelial-to-mesenchymal transition (EMT), during which epithelial cells lose cell polarity and cell adhesion to become mesenchymal cells with migration and invasion properties. Both EMT and mesenchymal-epithelial transition (MET), the reverse of EMT, are associated with normal mammary development – as with the placodes during embryogenesis, and with cancer - as mammary tumor-initiating cells acquire stem-cell properties through EMT (Creighton et al. 2009; Ye et al. 2015). EMT-inducing transcription factors (i.e. Zeb1, Slug, Twist) have been detected in cells at terminal end buds (TEBs) during puberty, and Wnt and transforming growth factor beta (TGF-β) signaling pathways in TEBs have also been reported as regulators of EMT (Nassour et al. 2012).

The stroma of the mammary gland is made up of several cell types – adipocytes, fibroblasts, vascular and lymphatic cells, and immune cells. The role of each of these in the normal and oncogenic mammary gland development is described in this section.

*Adipocytes*

The mammary stroma is largely composed of fat-filled adipocytes that make up the mammary fat pad, into which the mammary epithelial tree grows in response to previously described signals. In addition to providing structural support for the epithelium, adipocytes also serve an endocrine function in the mammary gland. They secrete vascular endothelial growth factor (VEGF), which points to their role in regulating angiogenesis in the mammary gland. They are thought to be involved in regulating epithelial growth and function, as well as cell to cell communication in the mammary gland (Gregor et al. 2013; Hovey and Aimo 2010).

An increase in adiposity of the mammary gland associated with obesity is considered an independent risk factor for breast cancer. Cancer-associated adipocytes can release inflammatory factors such as CCL2, CCL5, IL-1β, IL-6, TNF-α, VEGF, and leptin, that can promote the progression and metastatic potential of breast cancer (Wu et al. 2019a; Fujisaki et al. 2015; Dirat et al. 2011; D'Esposito et al. 2016). Mature adipocytes have been shown to have elevated expression of PD-L1, which inhibits the anti-tumor function of CD8+ T-cells (Wu et al. 2019a, 2018).

*Fibroblasts*

Fibroblasts communicate with the mammary epithelium either by direct cell-cell contact or by secreting various growth factors and proteases and have been implicated in having a role in regulating the survival and morphogenesis of epithelial cells in the fat pad (Liu et al. 2012; Makarem et al. 2013; Wang and Kaplan 2012; Howard and Lu 2014). They also secrete the components that make up the extracellular matrix (ECM), such as collagens, proteoglycans, and fibronectin. Intralobular fibroblasts regulate the expression of TGF-β1 and α-SMA, which is similar to the expression profile of tumor stroma. It has been

suggested that these act as a “reservoir” of cancer-associated fibroblasts (CAFs) (Avagliano et al. 2020; Morsing et al. 2016).

Fibroblasts have been thus implicated in regulating oncogenesis by altering the composition or density of the ECM (Lühr et al. 2012), which can support cancer cell migration, invasion, and survival in circulation – all key processes in the metastatic cascade (Hill et al. 2020; Ao et al. 2015). The role of CAFs in solid tumors is a widely studied topic, but is beyond the scope of this dissertation and will not be further elaborated upon.

*Vascular and lymphatic networks*

The mammary fat pad has an extensive network of vascular and lymphatic networks that are formed during pubertal development. Lymphangiogenesis is driven by the secretion of VEGF-C and/or VEGF-D by the myoepithelial cells and macrophages (Betterman et al. 2012). While the lymphatic vasculature remains relatively stable in adults, inflammation caused by either immune cells or in the tumor microenvironment can induce excess production of VEGF-C and VEGF-D, which increase lymph flow by dilating the vasculature and allowing infiltration of invading tumor cells. Lymphatic networks have thus been shown to be involved in metastatic spread by numerous studies, and breast cancer metastasis in particular (Schoppmann et al. 2004; Fisher et al. 1983; Pepper et al. 2000; Betterman et al. 2012; Stacker et al. 2001; Skobe et al. 2001; Ran et al. 2010).

*Immune cells*

Immune cells, including macrophages, mast cells, and eosinophils, are involved in various stages of mammary gland development. At puberty, they regulate ductal elongation and branching morphogenesis and mediate the invasion of the branching epithelial tips into the fat pad (Gouon-Evans et al. 2000; Lilla and Werb 2010). CD4+ T-helper cells guide lineage commitment and differentiation of MECs (Plaks et al. 2015). During pregnancy, they are involved in regulating the differentiation of epithelial cells and the development of the alveolar structures required for milk production (Pollard and Hennighausen 1994).

During lactation, secretory immune cells are recruited to the mammary gland and these cells produce immunoglobulins that are passed on to the offspring through the milk (Bourges et al. 2008). Finally, during involution, macrophages provide growth factors and help clear the excess ducts and remaining milk particles to return the mammary gland to its pre-pregnancy architecture (Dawson et al. 2020; Hitchcock et al. 2020; Plaks et al. 2015; Rahat et al. 2016; Stewart et al. 2019; Wang et al. 2020; O'Brien et al. 2010).

IFN-γ is a cytokine that is secreted by and can activate more than one type of cytotoxic immune cell. MECs have been shown to directly respond to interferon-γ (IFN-γ) secreted by CD4+ T cells, leading to changes in luminal cell differentiation (Plaks et al. 2015). This, in addition to several other studies on T-cell effector cytokines (Chan et al. 2014; Khaled et al. 2007), lends support to the idea that immune cells can directly regulate MECs. In addition, there are likely a variety of other cytokines/secreted factors involved in the epithelial-immune communication in normal/cancerous tissue yet to be identified.

Changes that impact immune cell function and abundance can also influence the development and progression of mammary oncogenesis (Bach et al. 2021; Ibrahim et al. 2020). Immune surveillance and communication in the mammary gland are critical to post-pregnancy mammary tissue homeostasis, particularly as part of mammary reconstruction during post-partum involution, and have been suggested to influence mammary tumor progression (Lyons et al. 2011). For example, T-cell activity is suppressed by the infiltration of involution-associated macrophages, an immune reaction that may also induce mammary tumorigenesis (Martinson et al. 2015; Freire-de-Lima et al. 2006; Guo et al. 2017; Fornetti et al. 2012; O'Brien et al. 2010).

Conversely, cell-autonomous processes in MECs contribute to pregnancy-induced breast cancer protection, a lasting effect that decreases the risk of breast cancer by ~30% in rodents and humans (Medina 2009; Britt et al. 2007; Terry et al. 2018). For example, p53 function is critical for blocking mammary tumor development in murine and human MECs, with a complete loss of p53 in post-pregnancy MECs promoting tumor initiation (Sivaraman et al. 2001; Medina and Kittrell 2003). Epigenetic-mediated alterations of post-pregnant MECs have been shown to interfere with the transcriptional output of cMyc,

which suppressed mammary oncogenesis via oncogene-induced senescence (Feigman et al. 2020). Given that oncogene-induced senescence signals influence the immune system, a link between normal pregnancy-induced mammary development, the immune microenvironment, and oncogenesis needs to be addressed to fully understand the effects of pregnancy on breast cancer development.

## 1.2 Breast cancer

Breast cancer (BC) is not a single disease, but a heterogeneous group of diseases with each subtype having its own tumorigenesis pathways and disease presentation. Breast cancer tumors (like all tumors) are made up of many cell types, and there is heterogeneity in the cells of the tumor tissue. Tumors are made up of variable proportions of proliferative malignant cells, stromal cells, and immune cells, and all of these have been hypothesized to play a variety of roles in tumor heterogeneity.

The exact mechanism that initiates breast cancer remains unknown, but there has been extensive effort in the field to characterize the molecular events that cause abnormal development that lead to cancer development and progression over time. The prevailing theory is the clonal evolution model, where mutations accumulate over time and the cells with mutations and epigenetic modifications that provide them with a fitness advantage survive and evolve into cancer initiating cells (or cancer stem cells). Furthermore, molecularly, breast cancer progression has been linked to ER expression which determines tumor grade and proliferation (discussed in detail in section 1.2.1). There are gains, losses, and amplifications of chromosomal regions of genes that are associated with the ER phenotype and the HER2 phenotype (Ellis et al. 2012; Lopez-Garcia et al. 2010; Harbeck et al. 2019).

The most frequent somatically mutated and/or amplified genes in tumor cells are *TP53* (41% of tumors), *PIK3CA* (30%), *MYC* (20%), *PTEN* (16%), *CCND1* (16%), *ERBB2* (13%), *FGFR1* (11%) and *GATA3* (10%) (**Fig. 1-3**) (Nik-Zainal et al. 2016). These genes control processes such as the cell cycle, proliferation, apoptosis, and inhibiting oncogenic pathways. Most breast cancers are caused by dysregulation of more than one of these genes working cooperatively.

Even though hereditary breast cancers are less common (5-10% of all diagnosed cases) than those caused by somatic mutations acquired in the breast tissue, they are a major risk factor because of the high penetrance of the disease in carriers (Godet and Gilkes 2017).

Mutations in the *BRCA1* and *BRCA2* genes have been widely studied and well described as a significant risk factor in carriers. It is estimated that 7 in 10 women with a *BRCA1* or *BRCA2* mutation will develop breast cancer by the age of 80 (Godet and Gilkes 2017; Chen and Parmigiani 2007).

Other, less common, mutations can also increase the risk of breast cancer, including *ATM*, *TP53*, *CHEK2*, *PTEN*, *STK11*, and *PALB2* (Renwick et al. 2006; Zhang et al. 1998; Walsh et al. 2006; Lynch et al. 1997; Boardman et al. 1998; Rahman et al. 2007). Still, not all women with genetic or other predisposition factors will develop breast cancer.

Classification of BC into subtypes is based on the presence or absence of established biomarkers such as estrogen receptor (ER), progesterone receptor (PR), and the overexpression of the HER2 (human epidermal growth factor receptor 2) oncogene. These features, along with histopathology, are used to divide BC into luminal A, B, and B-like, HER2+, and basal (triple negative) subtypes. Molecular classification of BC not only helps inform patient prognosis, but also in predicting therapy response and in developing treatment strategies (Sokolova et al. 2022; Dai et al. 2016).

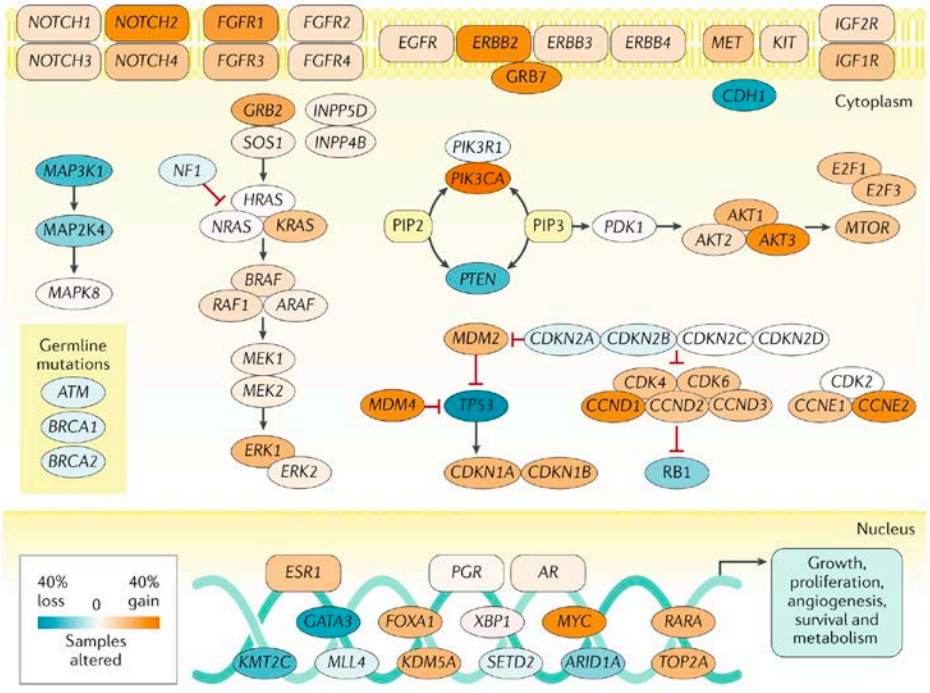


***Figure 1-3 Molecular mutations in breast cancer.***

The Cancer Genome Atlas data on breast tumor DNA copy number and somatic mutations were used to identify the frequency of each genetic alteration across 792 patients with breast cancer (all subtypes). Each gene is shaded according to the overall frequency of alteration. Orange indicates a high level of amplification and/or likely gain-of-function mutations; blue represents homozygous deletions and/or likely loss-of-function mutations.
*Figure from: Harbeck et al., 2019, Nature Reviews Disease Primers. Image used with publisher's permission (License # 5447821165732).*

### 1.2.1 Molecular subtypes of breast cancer

*Hormone receptor positive BC*

Patients with ER+ and/or PR+ cancers (i.e. hormone receptor positive) are responsive to treatment with hormonal therapy (i.e. ER inhibitors such as tamoxifen or aromatase inhibitors). Hormone receptor positive BCs are associated with mutations in *BRCA2, PALB2, ATM,* and *CHEK2* (Breast Cancer Association Consortium et al. 2022; Sokolova et al. 2022; Waddell et al. 2010). Luminal A, B, and B-like are all classified as being hormone receptor positive. Chemotherapy is generally omitted in patients with luminal A tumors, but in all hormone receptor positive BCs, the use of chemotherapy is guided by the assessment of the risk of recurrence based on markers such as Ki-67 expression (Harbeck et al. 2019).

Luminal A breast cancers:

ER+ and PR+, but HER2 negative. Luminal A breast cancers have low levels of Ki67 expression, and tend to be slow-growing, lower grade, and have better patient outcomes. The most frequently mutated genes in luminal A cancers are *PIK3CA, GATA3, MAP3K1,* and *TP53* (Ciriello et al. 2013; Cancer Genome Atlas Network 2012; Banerji et al. 2012).

Luminal B and B-like breast cancers:

Luminal B BCs are ER+ and HER2 negative, and either PR- or have high levels of Ki-67, hence more proliferative than Luminal A.

Luminal B-like BCs are also ER+ and HER2 negative, but can either be PR+ or PR-, and can have any level of Ki67 expression.

Luminal B/B-like cancers grow faster than Luminal A, and have a slightly worse prognosis. The most frequently mutated genes in luminal B and B-like cancers are *PIK3CA, TP53, GATA3, CDH1, MAP3K1, RUNX1,* and *PTEN* (Ciriello et al. 2013; Cancer Genome Atlas Network 2012; Banerji et al. 2012).

*HER2-positive BC*

ER- and PR-, but HER2-positive. These grow faster than luminal cancers, and can have a worse prognosis but are able to be treated with HER2 targeted therapies. HER2+ cancers can be targeted with a small molecule inhibitor (Lapatinib) or monoclonal antibodies (Trastuzumab, Pertuzumab). *TP53* pathogenic variants and *CHEK2* variants have been associated with HER2+ cancers (Breast Cancer Association Consortium et al. 2022; Melhem-Bertrandt et al. 2012; Wilson et al. 2010).

*Triple Negative BC (TNBC)*

A small proportion of breast cancers stain negative for ER, PR, and HER2, and these are classified as triple negative breast cancers (TNBC). A majority of TNBCs present with a more basal phenotype, which is more aggressive than luminal cancers, and therapy options have more limited efficacy (Foulkes et al. 2003; Sønderstrup et al. 2019; Lakhani et al. 2005). Chemotherapy is the standard for TNBC, typically consisting of an anthracycline and a taxane, and a platinum compound may be added for improved overall survival, though it leads to increased hematological toxicity. More recently, the use of PARP inhibitors (olaparib or talazoparib) in combination with other chemotherapy has shown promise in improving the survival and quality of life for people with TNBC (Harbeck et al. 2019).

*BRCA1* associated breast cancers are very commonly linked with TNBC. More than 60% of *BRCA1* mutation associated tumors are triple-negative, and TNBC has been shown to be predictive of *BRCA1* mutation status. Additional genes involved in DNA damage repair have been associated with TNBC, including variants of *BRCA2*, *PALB2*, *RAD51C*, *RAD51D*, and *BARD1* (Heikkinen et al. 2009; Breast Cancer Association Consortium et al. 2022).

### 1.2.2 Breast cancer cell of origin and tumor heterogeneity

Each tumor subtype has been hypothesized to have a different cell of origin which also correlates with clinical outcomes. These subtypes fit into the broader grouping of "basal" or "luminal" types, according to their similarities to the corresponding normal MECs. In other words, basal-type breast cancers express high levels of basal cell markers (Krt5/6, Krt14, Krt17). Luminal-type breast cancers express luminal markers (ERα, Krt8/18, GATA 3-binding protein) (Sørlie et al. 2003; Chaffer and Weinberg 2010). It was thought that each lineage gives rise to its own subtype of breast cancers – basal cancers arise from transformed basal progenitors and luminal cancers arise from transformed luminal progenitors. However, several studies have shown that this is not always the case.

BRCA1 mutations greatly increase the chance of developing a basal-type breast carcinoma. However, in a mouse model of *Brca1* loss driven by the *Blg* promoter (hence MEC restricted), a luminal ER- progenitor has been identified as the cell-of-origin, even though it formed basal-like tumors (Molyneux et al. 2010; Lim et al. 2009; Chaffer and Weinberg 2010). This suggests that the cell-of-origin may have the ability to dedifferentiate into a different progenitor cell type, and thus have the ability to give rise to basal tumors.

The plasticity of tumor cells and their ability to self-renew is another factor that contributes to tumor heterogeneity. Cells with self-renewal capabilities are also called "cancer stem cells" (CSCs). CSCs have the ability to differentiate into cell types of the parental tissue, but differentiated cells in tumors also have the ability to dedifferentiate. Oncogenes may be a driving factor in this process, as shown by studies using *PIK3CA* mutant basal and luminal differentiated cells where they dedifferentiate into multipotent stem-like cells (Koren et al. 2015; Van Keymeulen et al. 2015). Though the mechanism of this plasticity is not yet understood, the process of EMT could be involved, since basal-like cancers express several EMT markers (Skibinski and Kuperwasser 2015; Guo et al. 2012).

Clonal diversity in tumor cells adds another layer of heterogeneity to the tumor tissue. Genetic evolution, where tumor cells that have acquired mutations that provide them with a survival benefit expand into larger sub-clones, has been attributed as a source for tumor heterogeneity for many years (Nowell 1976;

Kreso and Dick 2014; Marusyk and Polyak 2010). Recent studies using single cell RNA-seq have shown that TNBC tumors have multiple cancer and normal cell types. Signatures derived from bulk analyses thus do not accurately represent the properties and behavior of breast cancers and may be the reason why these signatures have not been useful as diagnostic tools for TNBC (Karaayvaz et al. 2018; Samocha et al. 2019). There are also cell-to-cell differences in copy number variation that is distributed across clones within tumors, and this can significantly change gene expression levels since CNVs cause large scale expression differences in multiple genes in the amplified regions (Funnell et al. 2022).

It is clear that tumor heterogeneity is caused by interplay between a variety of processes. It is important to understand the ramifications of heterogeneity on response to therapies over a long term so that we may develop better, long-lasting treatments.

1.2.3 Pregnancy and breast cancer

Epidemiological, clinical, and experimental data have shown that one of the factors that affects the risk of developing breast cancer is pregnancy (Rosner et al. 1994; Schedin 2006). A pregnancy cycle causes alterations in the metabolism, gene expression, epigenome profiles, and proliferation of MECs. These changes have been shown to significantly alter the risk of breast cancer development. The age and duration of the first pregnancy, as well as the number of pregnancies a woman goes through have all been shown to alter the overall risk of breast cancer development (MacMahon et al. 1970; Albrektsen et al. 2005; Wohlfahrt and Melbye 2001). Induced abortions and other pregnancies of short durations have been shown to not affect breast cancer risk (Melbye et al. 1997; Beral et al. 2004).

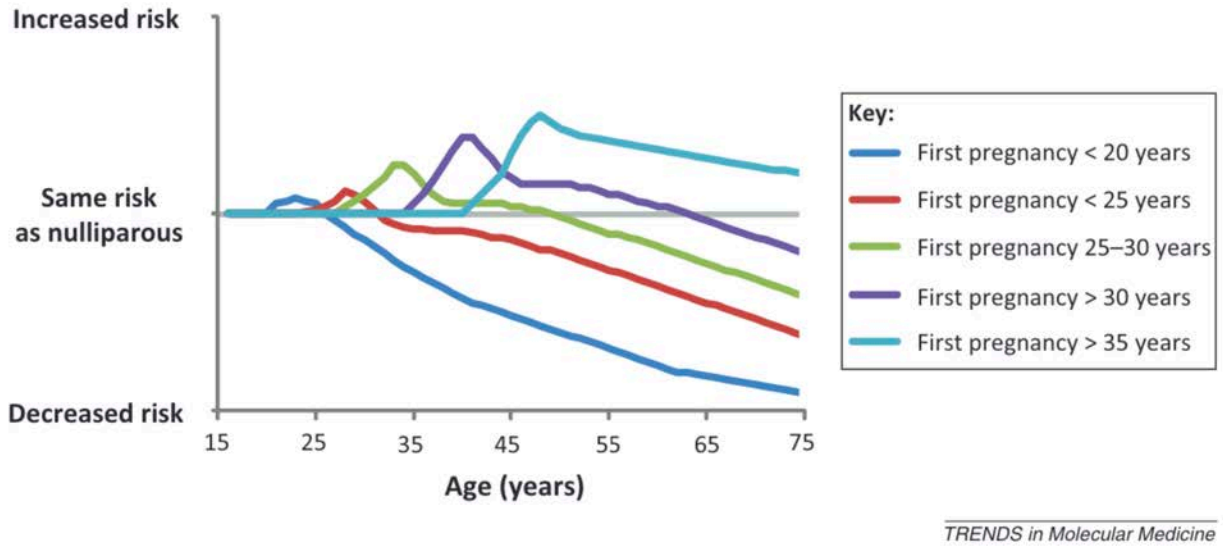


***Figure 1-4 Effect of pregnancy and age at first birth on breast cancer risk in humans.***

Schematic illustration demonstrating that: (i) early pregnancy decreases breast cancer risk in the long term; (ii) the breast cancer protective effect of pregnancy is greater the earlier the pregnancy has occurred; (iii) pregnancy leads to a transient increase in breast cancer risk following parturition; and (iv) pregnancy-associated increase in breast cancer risk becomes more pronounced with increasing age at first pregnancy. The figure represents a qualitative summary adapted from several epidemiological studies and highlights the principal relationship between age at first pregnancy and breast cancer risk.
*Figure from: Meier-Abt and Bentires-Alj., 2014, Trends in Molecular Medicine. Image used with publisher's permission (License # 5438410815739).*

Pregnancy provides a long-term protective effect against breast cancer development in women who complete their first full term pregnancy in their late teens to early twenties (**Fig. 1-4**) (MacMahon et al. 1970; Albrektsen et al. 2005). Subsequent pregnancies can extend this protection even further (Kelsey et al. 1993). However, the protection against breast cancer reaches the same levels as observed in nulliparous women for women whose first full-term pregnancy occurs after the age of 30, increasing further with age (MacMahon et al. 1970; Meier-Abt and Bentires-Alj 2014). This protective effect seems to have an evolutionary root, given that even in rodent models of chemically induced carcinogenesis, parity has been reported to reduce the frequency of mammary tumor development (Russo et al. 2008; Russo and Russo 1996; Sinha et al. 1988; Guzman et al. 1999). A recent retrospective study identified that the minimal length of 34 weeks of gestation is required to confer substantial reduction in breast cancer risk (Husby et al. 2018). They also showed that any subsequent pregnancies at an early maternal age provide additive protection and this is not restricted to the first pregnancy.

Lactation and breastfeeding have been reported to provide a protective effect against breast cancer, especially in the case of hormone receptor negative cancers (Lord et al. 2008; Islami et al. 2015). The number of pregnancies did not affect risk in cases with early age at first birth (< 25 years), whereas in the cases of late age at first birth, multiple pregnancies and breastfeeding cycles incrementally provided protection against breast cancer risk (Stordal 2022). The exact reasons for how and why breastfeeding can provide oncoprotection remain unknown, but it has been theorized that there could be changes in the population of breast cancer stem cells and differentiation properties associated with extended lactation. A slower, more gradual process of involution might also be beneficial in reducing the likelihood of creating a tumor supportive niche due to the inflammatory process of involution (Kobayashi et al. 2012).

While it has been widely accepted that an early full-term pregnancy reduces the long-term risk of developing breast cancer, there is an increase in short-term risk (until 5 years after giving birth) (**Fig. 1-4**). This is known as pregnancy associated breast cancer (PABC), and is independent of factors such as age, race, and number of pregnancies (MacMahon et al. 1970; Albrektsen et al. 2005; Meier-Abt and Bentires-Alj 2014; Shakhar et al. 2007; Slepicka et al. 2019). The tumor subtypes diagnosed in PABC tend to be

more aggressive – luminal B-like and triple negative breast cancers (TNBC) are more frequently diagnosed in women within the first 5 years post-pregnancy (Collins et al. 2015; Zhang et al. 2021; Allouch et al. 2020; Pilewskie et al. 2012). The stromal component of the mammary gland plays a crucial role in driving disease progression. Current data suggests that breast tumors from PABC are indistinguishable from non-PABC tumors (Zhang et al. 2021; Middleton et al. 2003). But this does not explain the differential disease progression and outcome of PABC. Since assessment of tumors generally only involves identifying hormone receptor status, the stromal component is not taken into consideration. We know that pregnancy significantly remodels the mammary stroma – including, but not limited to, ECM architecture and composition, immune cell infiltration, and elevated angiogenesis (Green and Lund 2005; Stein et al. 2004; Monks et al. 2005; Betterman et al. 2012). All of these processes can contribute to cancer progression and metastatic dissemination. Although PABC metastasizes to the same sites as non-PABC, it disseminates earlier and at a higher frequency and presents later in life as late stage invasive disease (Goddard et al. 2019; Callihan et al. 2013). It also exhibits an increased likelihood for disease relapse, and this has been suggested to be related to the earlier age of initial PABC diagnosis (Hartman and Eslick 2016). Given that metastasis and disease relapse are the two main drivers of cancer related deaths, understanding how pregnancy influences these processes will help inform better ways to diagnose and treat PABC.

Pregnancy, thus, plays a dual role in breast cancer risk. Some molecular changes may promote tumorigenesis, while others provide a cancer preventive effect. It is imperative that we gain a better understanding of the molecular mechanisms involved in the dual effect of pregnancy so that we may develop better prophylactic interventions suitable for specific types of breast cancers.

## 1.3 Models to study mammary gland development and tumorigenesis

### 1.3.1 In vivo models

The mammary gland is an extensively studied system in mouse models in the context of both normal development and tumorigenesis. This is due to the easy accessibility of the gland for the purposes of manipulation. Early studies in mouse models of breast cancer were performed on spontaneous tumors that were usually due to oncogenic viruses (such as MMTV). There were also models of chemically induced tumorigenesis using agents such as 7,12-dimethylbenzanthracene (DMBA), and exposure to radiation. However, the cleared fat pad transplantation model paved the way for many further discoveries about mammary gland biology that continue to drive research questions to this day (DeOme 1967; Medina 2010).

*Transplantation models*

As described previously, most of the mammary gland develops postnatally, and is driven by pubertal hormones. There is only a rudimentary ductal tree that has not invaded the fat pad in mice when they are ~3 weeks of age. The cleared fat pad transplantation model takes advantage of this by surgically removing the portion of the fat pad that contains epithelial ducts in these young mice. MECs from a syngeneic mouse (regardless of age), when into the remaining fat pad, are able to repopulate the gland and respond normally to hormonal stimuli at puberty. If tumor cells are injected, hyperplastic lesions form and progress into tumors with the same phenotypic characteristics as the original tumor.

The cleared fat pad model is an “orthotopic” transplantation model, where the external cells are injected into the same site they were collected from. There are also “ectopic” transplantation models, where MECs are typically injected into the subcutaneous stroma. This has been used to determine the potential of cells to proliferate as either normal or malignant growth, and also to evaluate the invasive and metastatic properties (Cardiff and Kenney 2011).

We can also perform xenografts – transplanting cells from a donor of a different species to a recipient mouse. Xenografts can be performed either with immortalized cell lines (CDX), or from primary

tissue derived from human patients (PDX) (Kuperwasser et al. 2004). Recipient mice for xenografts are immunodeficient in order to bypass host-mediated killing of injected cells. Humanized mice are a good alternative and can be used to study the interaction of the immune system with tumor cells or therapies.

Finally, it is also possible to inject cells directly into the primary ducts (intraductal transplantation) as a modification of the cleared fat pad transplant model. The advantage of this is that the recipient mice can be of any age (Behbod et al. 2009), and there is no need to surgically remove the existing fat pad.

*Genetically engineered mouse models*

Like every model system, the transplant models have their drawbacks. Mainly, they bypass the early stages of cancer development, including the development of tumor permissive niches, and immune involvement (in the case of xenograft models). Genetically engineered mouse models (GEMMs) can be used to overcome some of these challenges – by activating oncogenes that cause tumorigenesis in an immune competent environment.

GEMMs are typically designed to have gene alterations that resemble the genetic profiles of human cancers. Oncogenes and/or tumor suppressors are usually altered via an inducible system where a Cre-lox or FLP/FRP system is activated to alter expression under a specific promoter. Tamoxifen inducible Cre-ER and tetracycline inducible Tet-off and Tet-on systems are most commonly used (Couto and Bentires-Alj 2017; Lewandoski 2001).

Historically, studies that focused on the role of pregnancy in inducing or preventing the development of mammary tumors heavily relied on tissue-specific inducible gene knockouts controlled by mammary specific promoters such as MMTV, BLG, and WAP (Webster et al. 1995; Wagner et al. 2001; Wen et al. 1995). These models were pivotal in establishing fundamental aspects mammary tumorigenesis driven by many oncogenes, including neu/ErbB2, cyclin D1, cyclin E, PIK3CA, RAS, and Myc (Couto and Bentires-Alj 2017; Taneja et al. 2009). However, they do not accurately recapitulate the situation of patients with germline mutations, where mutations are not restricted to breast cells. More importantly, MMTV,

BLG, and WAP promoter activity is enhanced by pregnancy hormones, thus clouding our understanding of the effects of pregnancy in inducing or preventing the development of mammary tumors.

Mammary basal or luminal progenitor cells can also be used to drive the expression of genes of interest. This removes the confounding effect of pregnancy hormone driven expression changes. Through lineage tracing studies, cytokeratin 14 (K14) and cytokeratin 5 (K5) have been identified to be expressed in progenitor cells that give rise to basal and luminal lineages of the mammary epithelium, and cytokeratin 8 (K8) which is only active in the luminal compartment (Van Keymeulen et al. 2011; Rios et al. 2014; Van Keymeulen et al. 2015). K14-CreER, K5-CreER, and K8-CreER systems have been used to generate GEMMs to study key breast cancer oncogenes such as *Brca1*, *Brca2*, *Tp53*, and *PIK3CA* (Liu et al. 2007; Hollern et al. 2019; Hanasoge Somasundara et al. 2021; Jonkers et al. 2001; Koren et al. 2015). Cytokeratins are not limited to mammary tissue, and are expressed more widely in epithelial tissues in the body such as the skin, gut, and the reproductive organs. This model better mimics the phenotype exhibited by patients that bear germline mutations in *BRCA* genes, as the loss of *BRCA1* is not restricted to the mammary tissue unlike a majority of existing mouse models.

### 1.3.2 In vitro models – 3D organoid cultures to study mammary gland development

While rodent models have provided crucial insights in understanding mammary gland development, it is difficult to scrutinize the molecular events that take place in whole animal studies. Most tissues and organs have been successfully cultured *ex vivo* in various forms – whole organ, cell lines, primary cells, and tissue organoids. However, 2D cell cultures do not faithfully represent the *in vivo* conditions, and thus exhibit altered morphological and molecular signaling networks. Moreover, as with all cell lines, the immortalization process may have modified the proliferation and differentiation properties of the cells. Even though whole organ (or organ slice) cultures are easily achieved *ex vivo*, there are several limitations to this method. Thick tissues are not suited to long term culture as nutrients and other molecules cannot permeate the tissue to reach all cells, thus limiting tissue viability. Additionally, the roles of individual cell types in complex tissues cannot be delineated by these culture methods.

Over the last few decades, it has been demonstrated that functional differentiation and development of tissues is dependent on three-dimensional architecture. Consequently, there has been a surge in studies that use 3D cultures to model mammary gland development. Numerous protocols have been developed for 3D cultures of tissues and organs, and the resulting structures are collectively referred to as “organoids”. However, the definition of the organoids depends on the source tissue. In the case of mammary glands, organoids are cultures of mammary epithelial ducts in 3D gels whose composition is similar to the ECM (Simian et al. 2001; Shamir and Ewald 2014). By depriving epithelial cells of their natural stroma, the roles of epithelial-stromal interactions versus the innate properties of the epithelium can be delineated.

Mammary organoids can be grown in commercial 3D matrices such as Matrigel (Kleinman and Martin 2005) or collagen I (Wolf et al. 2009), which contain basement membrane (BM) matrix proteins required for epithelial cell growth and differentiation. Culturing mammary organoids in Matrigel gives rise to organized clusters of bi-layered mammary epithelium, which can be stimulated into branching morphogenesis with growth factors, partially resembling normal *in vivo* mammary gland development (Jamieson et al. 2017; Florian et al. 2019). Such organoid systems can also be used as models to study the modifications that pregnancy brings about to the mammary gland. By culturing organoids with pregnancy hormones, organoids can be stimulated to secrete milk proteins (lactation), and removal of such signals can mimic some of the stages seen during involution (Feigman et al. 2020; Sumbal et al. 2020; Ciccone et al. 2020). Additionally, to understand the role of various stromal components during normal mammary gland development, several co-culture assays for MECs or primary mammary organoids with fibroblasts have been developed (Koledova and Lu 2017; Krause et al. 2008). There are also 3D-printing strategies for controlled placement of cells in the hydrogel matrix, which allows for reproducible, high-throughput experiments (Reid et al. 2018). Furthermore, it has been shown by single-cell analysis that normal and pre-malignant organoid cultures can retain the complex system of multiple MEC states (stem/progenitor and differentiated) and protein expression patterns (Rosenbluth et al. 2020).

In addition to gaining a better understanding of normal development, organoids can help advance our knowledge of cancer. Organoid cultures can be established from primary tissue samples obtained from

breast cancer patients. These organoids can also be used in personalized medicine – to test new and existing therapies that could predict the specific patient's response. Although lacking the complex interactions with the microenvironment, human tissue organoids can be used as a model system to characterize cellular and molecular changes during development and to test the susceptibility of an individual to a variety of therapies.

### 1.4 Exploiting immune cells for breast cancer therapies

The therapeutic interventions currently used to treat breast cancer are surgery, radiotherapy, and chemotherapy. Based on the subtype of breast cancer, hormone therapy and HER2-guided therapy are effective against hormone receptor positive (HR+) and HER2-positive breast cancers. But in cases of recurrent, therapy resistant disease, or for triple negative breast cancers (TNBC), there are no targeted therapies readily available for standard use. Although there are FDA approved therapies such as antimetabolites, taxanes, and anthracycline for use in TNBC, these are only somewhat beneficial at early stages of TNBC (Zhang et al. 2022; Slade 2020). Newer treatments like platinum, PARP inhibitors, androgen receptor (AR) inhibitors, immune checkpoint inhibitors, and PI3K/mTOR/AKT inhibitors have been the focus of recent studies on novel therapies.

The immune system plays a very important role in responsiveness to therapy. High levels of tumor-infiltrating lymphocytes (TILs) have been identified as a favorable prognostic marker. Checkpoint inhibitor immunotherapies (ICIs), such as PD-L1/PD-1/CTLA4 targeting antibodies, are currently in clinical trials as monotherapy or in combination with the more classical treatments (Zhang et al. 2022) for TNBC.

In general, breast cancer forms “cold” tumors – there is not much immune infiltration in tumor tissue. This severely reduces the effectiveness of ICI therapies which rely on the host immune system to engage, unlike in other solid tumors such as melanoma and lung cancer that are “hot” (Lesterhuis et al. 2011). Thus, in the case of breast cancers, adoptive cell transfer (ACT) therapies may be more effective.

Adoptive cell transfer (ACT) is a cell-based immunotherapy that involves several steps (Humphries 2013; Maus et al. 2014; Restifo et al. 2012):

1. Isolation of circulating or tumor-infiltrating lymphocytes
2. *In vitro* selection of specific cells, modification and/or activation, and expansion
3. Re-administration into patients in combination with cytokines that are required to keep these cells alive.

One way of modifying the isolated immune cells *in vitro* is to genetically modify them to express a tumor associated antigen-specific (TAA) TCR or a chimeric antigen receptor (CAR). This gives the

modified cells the ability to recognize and kill TAA-expressing cells independently of MHC recognition. TAA-TCR or TAA-CAR T cells have been shown to be beneficial in hematological malignancies (Brentjens et al. 2011; Kalos et al. 2011; Ray et al. 2010; Robbins et al. 2011). There are currently a number of clinical trials that are recruiting breast cancer patients to test CAR-T cells that are specifically targeted towards common BC antigens, as summarized recently (Yang et al. 2022).

Most studies on the therapeutic potential of T cells against various cancers have focused on conventional CD8+ and CD4+ T cells. Conventional T cells recognize peptide antigens presented by major histocompatibility complex (MHC) I and II molecules. Following antigen presentation and activation, CD8+ T cells undergo clonal expansion and differentiate into cytotoxic T lymphocytes (CTL) and can target and kill tumor cells expressing the activating antigen(s). CD4+ T cells can help enhance the CD8+ T cell response against certain types of antigens (Coulie et al. 2014). However, there are several types of unconventional T cells whose anti-tumor potential has not been harnessed yet, even though they have been implicated in anti-tumor immunity.

### 1.4.1 Unconventional T cells as potential ACT agents

Unconventional T cells can be divided into groups based on the molecules they use to recognize antigens. Unlike MHC-restricted T cells, these cells rely on different antigen presentation molecules such as CD1d (natural killer T cells), MR1 (mucosal associated invariant T cells), and γδ T cells to name a few (Godfrey et al. 2018). The advantages of unconventional T cells include their ability to respond much more rapidly by secreting cytotoxic cytokines without needing activation and clonal expansion, and their ability to naturally home to non-lymphoid sites in various tissues making them helpful in targeting solid tumors. They are present in significantly greater numbers in humans (2-4 fold higher) when compared to CD8+ T cells (Godfrey et al. 2015).

*Natural Killer T-cells (NKT)*

Of these unconventional T cells, CD1d-restricted natural killer T cells (NKT cells) are perhaps the most well studied and characterized cell type. The CD1 family of antigen presenting molecules consists of four members: CD1a, CD1b, and CD1c – collectively known as group 1 CD1, and CD1d – group 2. CD1d restricted NKT cells are however the focus of most studies as this molecule is expressed in mice, but none of the group 1 molecules are expressed (Godfrey et al. 2018). Within CD1d restricted NKT cells, there are subgroups based on the types of T cell receptors (TCRs) that are expressed and the types of antigens they can recognize. These are as follows:

- Type I NKT cells: also known as invariant NKT (iNKT) cells. They express semi-invariant TCRs (specific combinations of αβ chains) and react to the glycolipid antigen α-galactosylceramide (α-GalCer) and its analogs (Hong et al. 1999).
- Type II NKT cells: all other CD1d restricted αβ TCR expressing T cells and react to a diverse array of antigens not including α-GalCer (Godfrey et al. 2018).
- Atypical NKT cells: express atypical TCRs including γδ, and hybrid δαβ TCRs which may also recognize α-GalCer, though this is uncommon (Le Nours et al. 2016; Uldrich et al. 2013; Pellicci et al. 2014).

Type I NKT cells (hereafter referred to as iNKT cells) are more common in mice than humans and have been shown to have anti-tumor properties by many studies (Bassiri et al. 2014; Hix et al. 2011). Following antigen presentation by CD1d, iNKT cells are activated and rapidly produce a diverse array of cytokines such as IFN-γ, TNF, IL-4, IL-13, IL-17, IL-21, and IL-22 (Coquet et al. 2008), and cytotoxic factors such as perforin, granzymes, FAS-ligand, and TRAIL to directly lyse tumor cells (Metelitsa et al. 2001; Smyth et al. 2002). The secreted factors can further recruit and activate other immune effector cells including dendritic cells, CD4+ and CD8+ T cells (Shimizu et al. 2007; Hermans et al. 2003). They can also attack cells involved in creating a tumor supporting stromal microenvironment such as tumor associated macrophages (TAMs) and myeloid derived suppressor cells (MDSCs) (Song et al. 2009; Santo

et al. 2008). However, iNKT cells can also have immunosuppressive properties and have been shown to be involved in controlling autoimmune diseases and graft versus host disease (Godfrey and Kronenberg 2004; Hong et al. 2001; Zeng et al. 1999). This is likely due to the immunosuppressive cytokines produced by specific iNKT cell subsets (IL-4 by NKT2, IL-10 by NKT10) (Lee et al. 2013b; Sag et al. 2014). These subsets have not been individually studied for their anti-tumor or tumor suppressive properties so far.

Type II NKT cells have a more diverse repertoire of TCRs and do not have a universal activating antigen like α-GalCer. Though more abundant in humans than iNKT cells, type II NKT cells are not present in mice (Godfrey et al. 2018). This has made them harder to study and there are very few studies being conducted. The data available so far suggests that type II NKT cells have an immunosuppressive role and that their effector functions depend on IL-13 secretion (Terabe et al. 2005).

Transcriptionally, there are various markers that have been used to classify NKT cells based on their intracellular staining patterns. PLZF, EGR2, T-bet, GATA-3, and RORγt expression patterns distinguish NKT cells into subsets – NKT1, NKT2, and NKT17, which produce effector molecules such as IFN-γ, IL-4, and IL-17 respectively (Lee et al. 2013b; Klibi et al. 2020).

A number of clinical trials have been conducted to study the effect of using α-GalCer on iNKT cells to harness their potential as immunotherapeutic agents. Injecting dendritic cells pulsed with α-GalCer or *in vitro* expanded iNKT cells intravenously into patients causes iNKT cell expansion, and have been suggested to lead to tumor regression (Nagato et al. 2012; Richter et al. 2013). Chimeric antigen receptor expressing NKT (CAR-NKT) cells have also been shown to be effective in a mouse model of neuroblastoma (Heczey et al. 2014).

*Mucosal associated invariant T-cells (MAIT)*

Mucosal associated invariant T (MAIT) cells are another type of innate-like unconventional T cells. Their abundance depends on the species – while found in humans, they are much less common in mice. MAIT cells are found in mucosal organs, but also in peripheral blood and liver. MAIT cells can be activated

in response to viruses and bacteria, and rapidly secrete cytokines like IFN-γ and TNF following activation (Salio et al. 2014). MAIT cells rely on the MR1 molecule for antigen presentation, a molecule related to MHC-I but specific to the TCRs expressed on MAIT cells (Treiner et al. 2003). There are no specific antigens for MR1, but in certain cases of viral infections, MAIT cells can be activated without the need for antigen recognition (Ussher et al. 2018).

*Gamma Delta T-cells (γδ)*

Another type of unconventional T cells that have gained a lot of interest over the last decade are γδ T cells. γδ T cells make up ~1-5% of circulating T cells in humans. γδ T cell subsets are defined based on the TCR variable (V) chains used, TCRγ in mice and TCRδ in humans. Mouse and human γδ T cells also differ in their tissue homing ability – mouse γδ T cells are found mostly in peripheral sites like skin, intestine, liver, lungs, and the reproductive tract, whereas human γδ T cells are found in the peripheral blood in addition to skin and large intestine (Godfrey et al. 2015; Ebert et al. 2006).

γδ T cells can be subdivided into two classes based on their function – effector γδ T and regulatory γδ T cells. Activated γδ T cells play an antitumor role by secreting cytokines, antibody dependent cellular cytotoxicity (ADCC), and other effects, and these are the effector γδ T cells. On the other hand, regulatory γδ T cells are responsible for modulating the immune tolerance, and can promote cancer growth by dampening the functions of various effector cells and by inducing immune-senescence of naïve T cells and dendritic cells (Paul and Lal 2016).

The presence of γδ T cells in tumors has been found to be a very favorable prognostic marker (Gentles et al. 2015), and they possess properties that make them promising candidates for immunotherapy. γδ T cells are activated by small phosphorylated metabolite antigens known as phosphoantigens. These are typically produced by foreign pathogens but tumor cells can also produce them (Gober et al. 2003). Of interest, some γδ T cells can also be activated by α-GalCer presented by CD1d (Uldrich et al. 2013). Once activated by antigens *in vivo* or *in vitro*, γδ T cells expand readily. This makes them suitable for adoptive transfer therapies. γδ T cells also have more favorable homing properties to epithelial tissues and solid

tumors compared to αβ T cells. Since they are not MHC restricted, they do not cause Graft versus Host disease (GVHD) even when transferred to an MHC mismatched host (Godder et al. 2007).

Unconventional T cells can thus be a valuable tool to be harnessed for immunotherapy against solid tumors, and more research is required to understand how we can use them effectively against breast cancers. It is, however, important to note that all of these unconventional T cells play a dual role in cancer development. Some of their subtypes or effector functions may promote cancer progression. NKT17 and γδ T17 cells are major sources of IL-17, which can have an immunosuppressive role in cancer. Vγ1 γδ T cells have been reported to secrete TGF-β which can induce epithelial-to-mesenchymal transition and aid in cancer cell dissemination and metastasis (Klibi et al. 2020; Yang and Weinberg 2008).

### 1.5 Research hypotheses

Previous studies have established that both a full pregnancy cycle (gestation, lactation, and involution), and an induced pseudo-pregnancy (exogenous delivery of pregnancy hormones) decreased the frequency of mammary tumors in several epidemiological studies and mouse models. Yet, pregnancy does not fully prevent the development of breast cancer, thus suggesting that cellular and biological alterations taking place right before pregnancy, or throughout a woman's life span could bypass the preventive effects of pregnancy. It is also possible that pregnancy-induced changes to mammary gland stroma and to the mammary immune microenvironment could alter signals that block cancer development. Our previous work has shown that MECs exhibit a state of semi-senescence in response to cMyc overexpression as an oncogenic stressor, and this could be engaging the immune system. *We hypothesized that pregnancy alters the overall immune composition of the mammary gland after the completion of a full pregnancy cycle.*

We undertook an unbiased approach to define the cellular heterogeneity of the mammary glands from pre- and post-pregnancy female mice by single cell RNA-sequencing (scRNA-seq). We illustrated that the fully involuted, post-pregnancy mammary gland is populated with an expanded population of resident NKT cells, suggesting a prolonged role for these cells in tissue homeostasis post- involution. We showed that post-pregnancy NKT cells express mostly γδTCRs, as opposed to pre-pregnancy NKT cells which express αβTCRs. γδTCR expressing immune cells are known to possess a high antitumor capability. *We hypothesized that post-pregnancy mammary NKT cells play a role in pregnancy associated protection against oncogenesis.*

We set out to investigate this hypothesis in various mouse models of mammary hyperplasia. Our previous results indicate that pregnancy brings cell autonomous (epithelial cell epigenome) and non-autonomous (immune microenvironment) changes to mammary glands that block *cMyc*-induced mammary oncogenesis (Feigman et al. 2020). *We hypothesized that pregnancy will also influence the development of Brca1-deficient mammary tumors.* To address this hypothesis, we developed a new transgenic model of inducible *Brca1*-loss that drives mammary oncogenesis to define whether Brca1 deficiency interferes with

the pregnancy-induced epigenome of epithelial cells and pregnancy-induced mammary immune microenvironment. These analyses were performed both in asymptomatic tissue (without malignant lesions) and in mammary tumor tissue to elucidate the establishment of pregnancy-induced modifications, and how they are sustained in the event of tumor development, in a Brca1 deficient background. Given that *BRCA1* mutations in humans increase the risk of development of breast cancer by over 50%, our work could elucidate strategies to prevent tumorigenesis in high risk populations.

# 2. Parity induced changes to the mammary epithelial and immune composition

## 2.1 Author contributions

I acknowledge the following people who assisted with this project. Mary Feigman and Camila dos Santos conceptualized and performed the initial experiments and prepared cells for single cell RNA-seq libraries. The Single Cell Sequencing core at CSHL provided the sequencing files. Matt Moss and Marygrace Trousdell analyzed the scRNA-seq data and generated the data plots. Marygrace Trousdell assisted with ATAC-seq analysis. Mary Feigman provided the preliminary flow data for CD1d KO mice and CD1d expression on MECs. Samantha Cyrill performed the pregnancy hormone pellet implantation experiments and corresponding flow cytometry. Michael Ciccone performed the organoid culture experiment for CD1d expression changes. J. Erby Wilkinson performed the histopathological analyses. Semir Beyaz generously provided the UTX KO mice and provided critical feedback. Camila dos Santos oversaw the project, and participated in experimental design and data analyses.

## 2.2 Results

The use of single cell strategies has elucidated the dynamics of epithelial cell lineage specification and differentiation across major mammary developmental stages (Gray et al. 2022; Twigger et al. 2022; Henry et al. 2021; Bach et al. 2017; Chung et al. 2019; Li et al. 2020a; Pal et al. 2017, 2021). Previous studies have indicated that post-pregnancy epithelial cells bear an altered transcriptome and epigenome, thus suggesting that pregnancy stably alters the molecular state of MECs (Blakely et al. 2006; Feigman et al. 2020; Huh et al. 2015; Dos Santos et al. 2015). However, it is unclear whether pregnancy leads to disproportionate changes in the transcriptome of specific mammary cell populations, which we investigated in this study.

2.2.1 Single cell analysis identifies changes to the transcriptional programs and immune composition of the post-pregnancy mammary gland

In order to characterize the effects of parity on the cellular composition and heterogeneity of mammary glands, we used single cell RNA-sequencing (scRNA-seq) to compare the abundance, identity and gene expression of mammary gland epithelial and non-epithelial cells from nulliparous (virgin, never pregnant, n=2) and parous female mice (20 days gestation, 21 days lactation, 40 days post-weaning, n=2). scRNA-seq clustering defined 20 cell clusters (TCs), which were further classified into 3 main cell types; epithelial cells (Krt8+ and Krt5+), B-lymphocytes (CD20+), and T-lymphocytes (CD3e+), and 2 smaller clusters, encompassing fibroblast-like cells (Rgs5+) and myeloid-like cells (Itgax+) **(Fig. 2-1 A-B).**

**Figure 2-1**

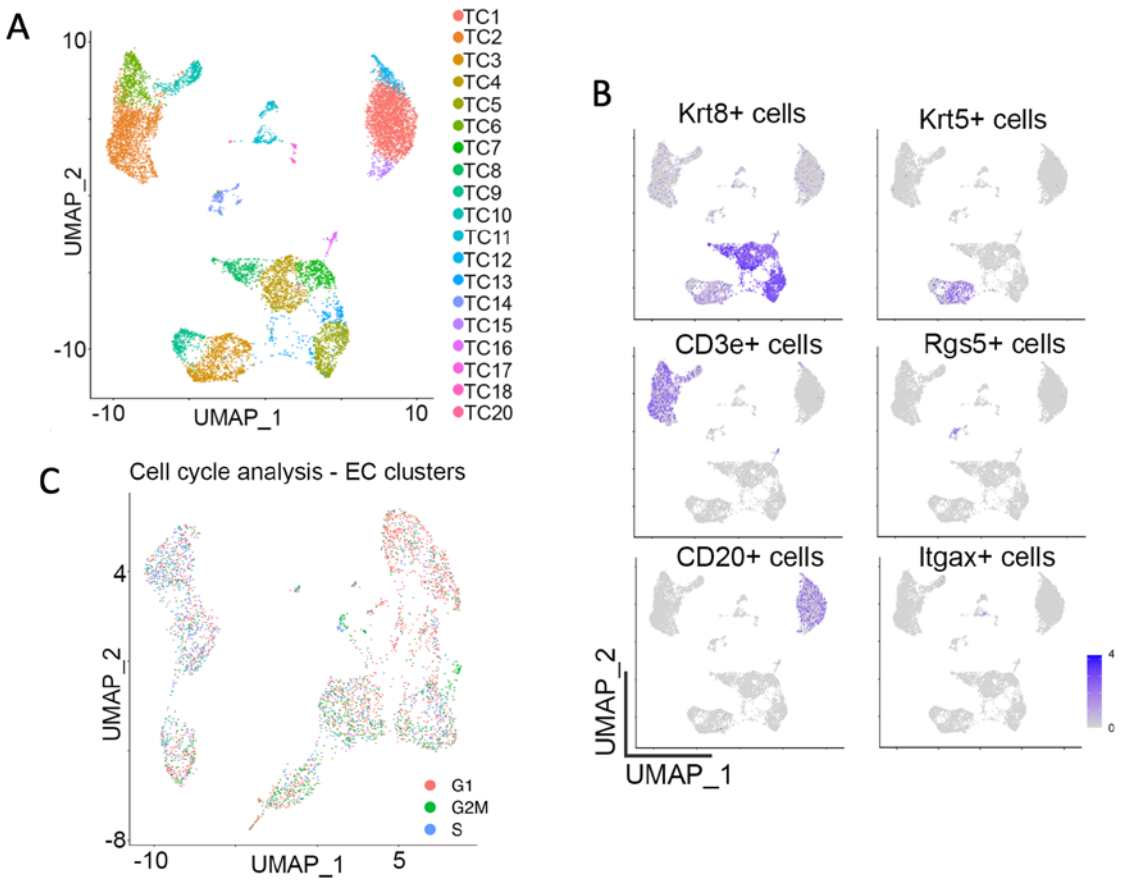

***Figure 2-1 Single cell level classification of pre- and post-pregnancy MECs.***

**(A)** UMAP showing the distribution of total, pre- and post-pregnancy mammary resident cells.
**(B)** Classification of mammary resident lineages based on the expression of *Krt8* and *Krt5* (epithelial cells), *Cd20* (B-cells), *Cd3e* (T-cells), *Rags5* (Fibroblasts), and *Itgax* (myeloid cells).
**(C)** UMAP showing the distribution of mammary epithelial clusters according different stages of cell cycle.

*Changes to the mammary epithelial compartment*

To characterize the cellular heterogeneity across pre- and post-pregnancy MECs, we used a re-clustering approach, which selected for cells expressing the epithelial markers *Epcam*, *Krt8*, *Krt18*, *Krt14 and Krt5*, and resolved 11 clusters of mammary epithelial cells (ECs) with similar cell cycle states (Henry et al. 2021) (**Fig. 2-2 A, 2-1 C**). Analysis of cellular abundance and lineage identity revealed that clusters EC7 (mature myoepithelial MEC), EC9 (luminal common progenitor-like MEC), EC10 and EC11 (bi-potential-like MECs), were evenly represented in pre- and post-pregnancy mammary tissue, thus demonstrating populations of cells that are mostly unchanged by a pregnancy cycle. We also identified clusters predominantly represented within pre-pregnancy MECs (EC2, EC4, and EC8), and those biased towards a post-pregnancy state (EC1, EC3, EC5, and EC6), classified as luminal alveolar-like clusters (EC1, EC2 and EC6), myoepithelial progenitor-like clusters (EC3 and EC4), and luminal ductal-like clusters (EC5 and EC8) (**Fig. 2-2 B-D**).

**Figure 2-2**

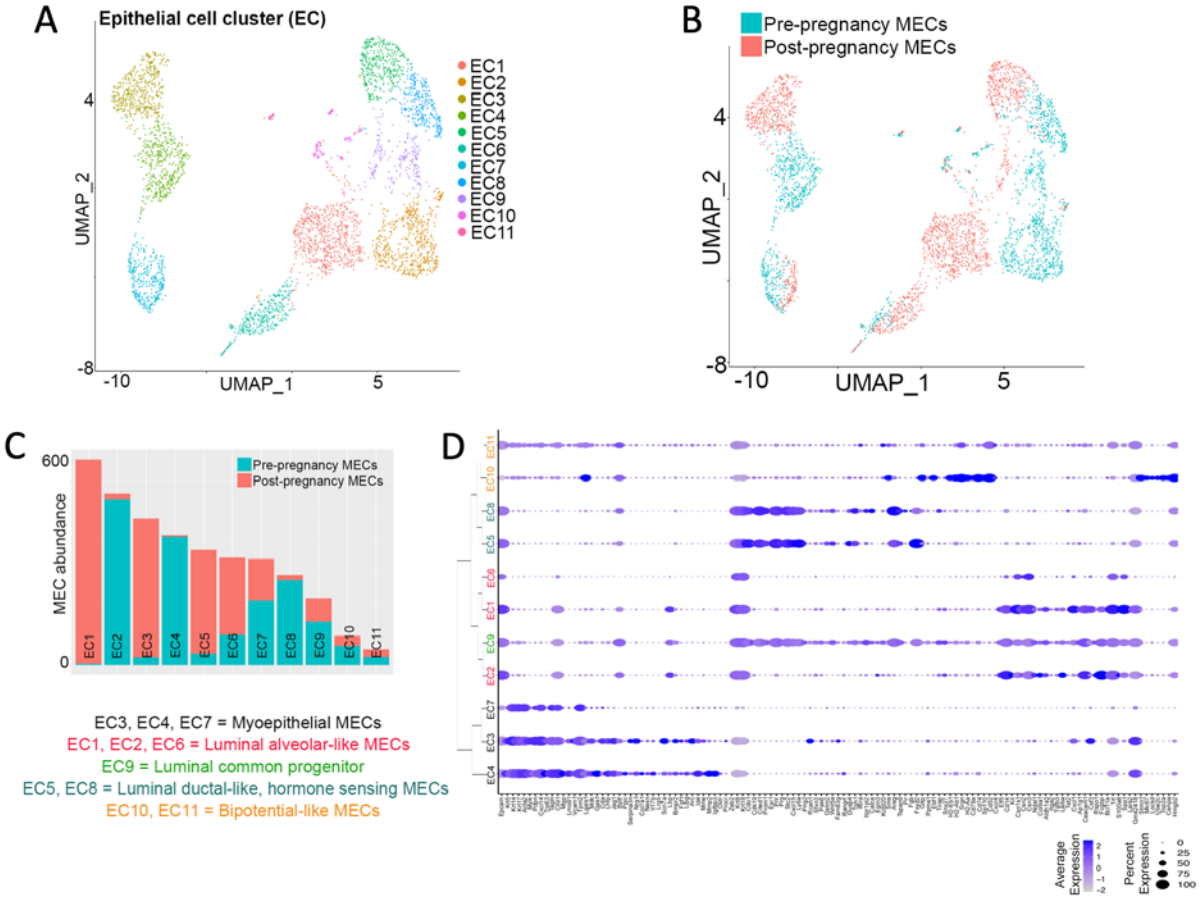


***Figure 2-2 Single cell analysis identifies post-pregnancy biased epithelial cells in mammary tissue from parous female mice.***

**(A)** UMAP showing epithelial-focused re-clustering (Epcam+, Krt8+, Krt18+, and Krt5+ cells) of pre- and post-pregnancy MECs.
**(B)** UMAP showing epithelial-focused re-clustering (Epcam+, Krt8+, Krt18+, and Krt5+ cells) of pre-pregnancy (blue) and post-pregnancy (pink) MECs.
**(C)** Cell abundancy of pre- and post-pregnancy epithelial cells across all 11 epithelial clusters.
**(D)** Dot plot analysis of molecular signatures and lineage identity of pre- and post-pregnancy MECs.

Comparative gene expression analysis indicated that processes associated with immune cell communication, such as *Complement* and *Inflammatory Response*, were markedly enriched in luminal and myoepithelial cell clusters biased towards the post-pregnancy state (**Fig. 2-3 A-C and Table 8-1**). This observation was supported by analysis of previously published pre- and post-pregnancy bulk RNA-seq data, which suggested an overall enrichment for immune communication signatures in epithelial cells after a full pregnancy cycle (Feigman et al. 2020) (**Fig. 2-3 D and Table 8-2**).

**Figure 2-3**

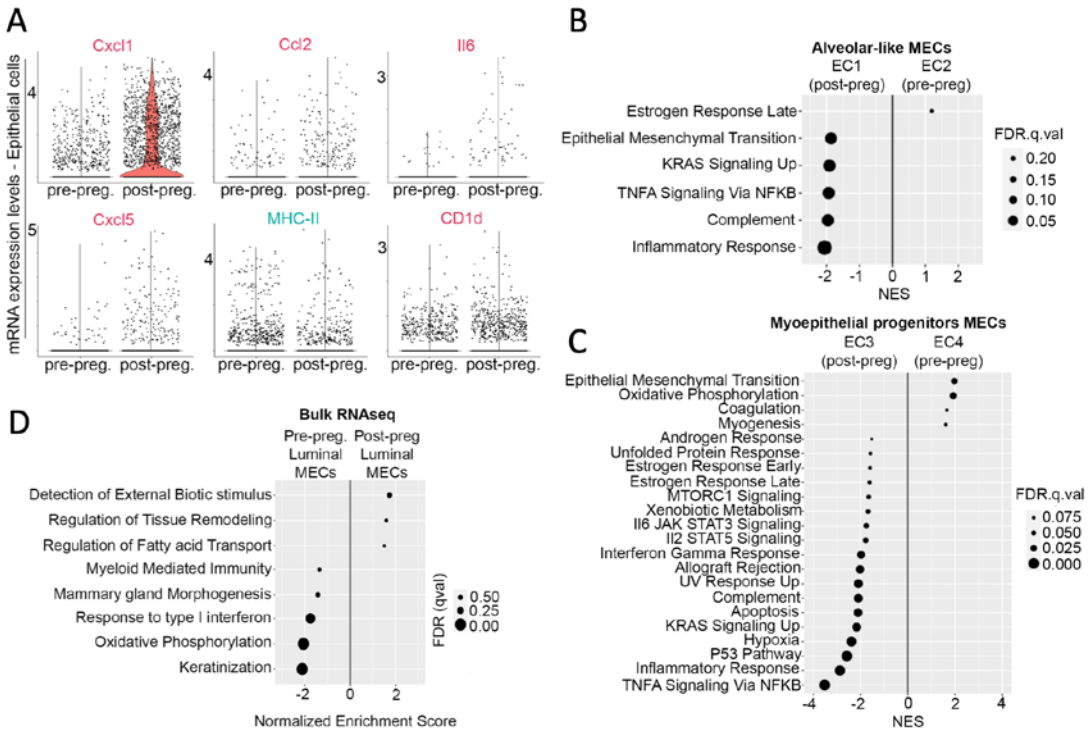


***Figure 2-3 Pathway analysis of post-pregnancy biased epithelial cells indicates changes to immune communication signatures***

**(A)** mRNA levels of senescence-associated, immune communication genes *Cxcl1*, *Ccl2*, *Il6*, *Cxcl5*, *Mhc-II* and *Cd1d* in pre- and post-pregnancy MECs.
**(B, C)** Gene set enrichment analysis (GSEA) of pathways differentially enriched in **(B)** alveolar-like MECs, and **(C)** myoepithelial progenitor-like MECs.
**(D)** Gene set enrichment analysis (GSEA) of pathways differentially enriched in FACS-isolated, pre- and post-pregnancy luminal MECs.

*Changes to the mammary immune compartment*

Changes in the immune microenvironment are known to contribute to pregnancy-induced mammary development (Coussens and Pollard 2011). A series of single cell strategies have identified alterations to mammary immune composition across several stages of mammary gland and cancer development (Bach et al. 2021; Dawson et al. 2020; Saeki et al. 2021). However, it is still unclear whether the immune composition of fully involuted, post-pregnancy mammary tissue resembles its pre-pregnancy state, or if a combination of epithelial and non-epithelial signals collectively influences the normal and malignant development of mammary tissue. In light of the potentially altered epithelial-immune cell communication identified in post-pregnancy MECs suggested above, we set out to understand the effects of pregnancy on the mammary resident immune compartment using scRNA-seq.

Transcriptional analysis of clusters representing B-lymphocytes (CD20+) did not identify major differences in gene expression between cells from pre- and post-pregnancy mammary glands, even though there were non-significant cell abundance differences, suggesting that B-cells may not be significantly altered in fully involuted mammary tissue (**Fig. 2-4 A**). Re-clustering of CD3e+ T-lymphocytes identified 9 distinct immune cell clusters (IC) marked by the expression of immune lineage genes such as *Cd4, Cd8, Klrk1*, and *Gzma* (**Fig. 2-4 B-C**). Classification according to cell abundance and lineage identity of pre- and post-pregnancy mammary resident lymphocytes, revealed 2 cell clusters, IC1 (CD4+ memory-like T-cells), and IC2 (CD8+ T-cells), which were evenly represented across pre- and post-pregnancy mammary tissue (**Fig. 2-5 A-B**). Differential gene expression analysis of clusters IC1 and IC2 identified minimal expression changes, suggesting that the transcriptional output of CD8+ T-cells (IC2), and certain populations of CD4+ T-cells (IC1) were not substantially altered by parity (**Fig. 2-5 C-D**).

**Figure 2-4**

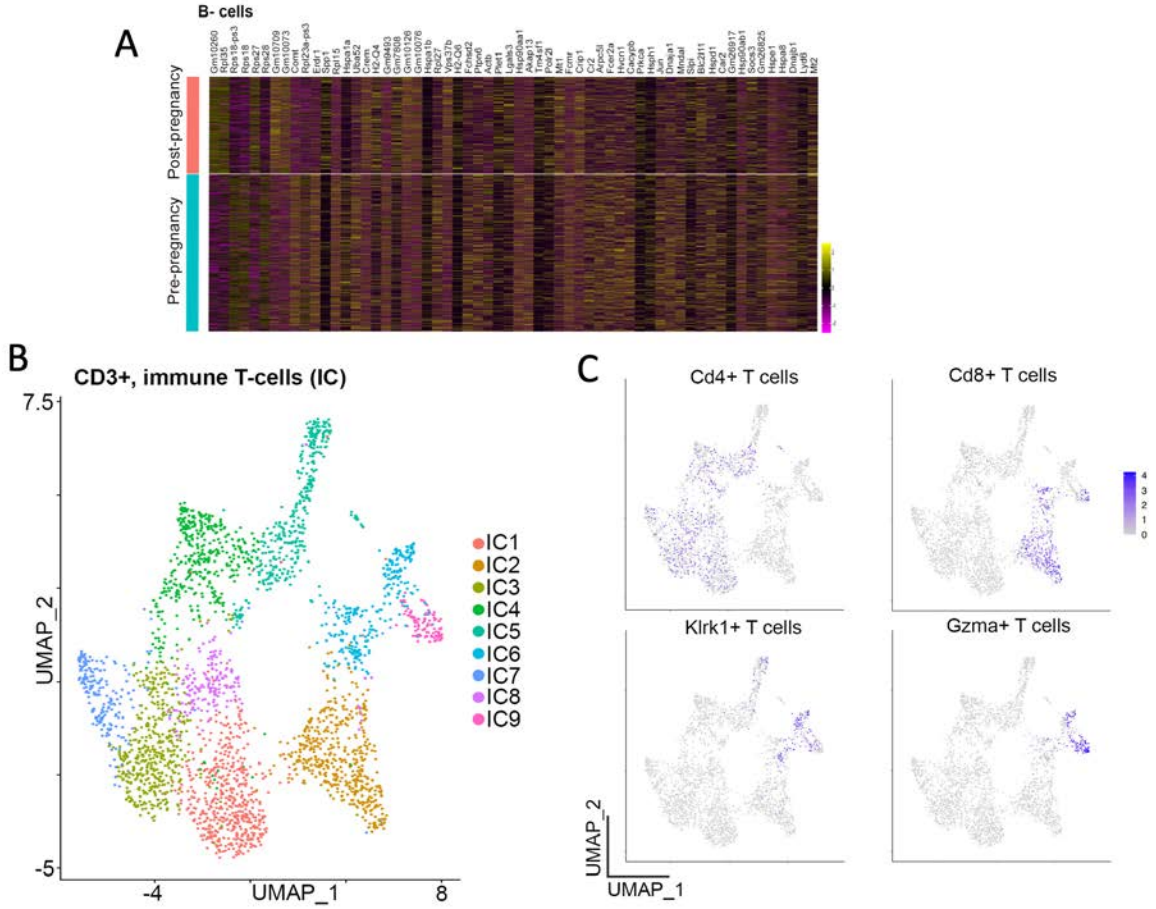


***Figure 2-4 Single cell analysis identifies transcriptional programs and immune cellular heterogeneity in mammary tissue from parous female mice.***

(**A**) Heatmap showing top DEGs across pre- and post-pregnancy B-cell clusters.
**(B)** UMAP showing T-cell focused re-clustering (CD3e+ cells) of pre- and post-pregnancy mammary resident immune cells.
**(C)** Feature plots showing the expression of T cell markers *Cd4*, *Cd8*, *Klrk1* and *Gzma*.

**Figure 2-5**

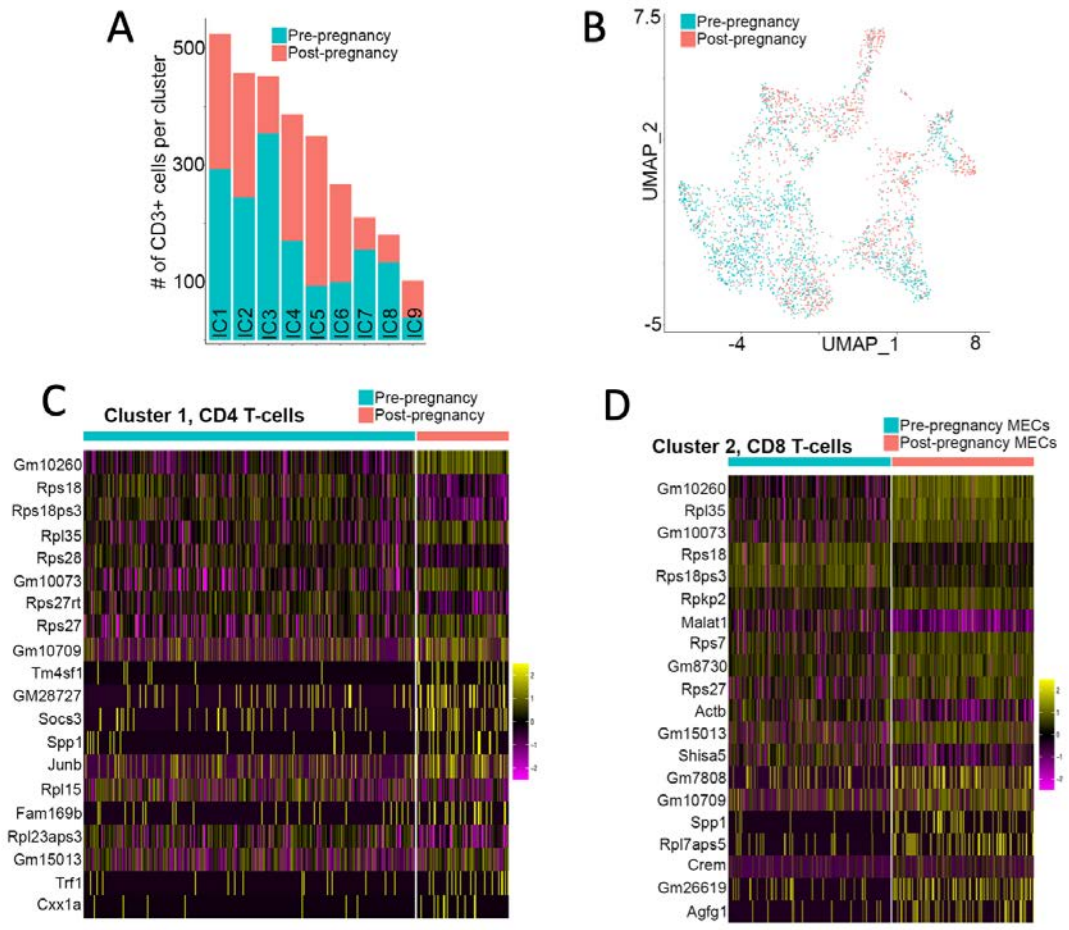


***Figure 2-5 Characterization of pre- and post-pregnancy mammary resident immune cells.***

(**A**) Cell abundancy of pre- and post-pregnancy CD3+ immune cells.
(**B**) UMAP showing CD3+ focused re-clustering of pre-pregnancy (blue) and post-pregnancy (pink) immune resident cells.
(**C-D**) Heatmap showing top 20 DEGs across CD4+ T-cells (**C**, cluster 1) and CD8+ T-cells (**D**, cluster 2) harvested from pre and post-pregnancy mammary tissue.

Analysis of clusters biased towards pre-pregnancy mammary tissue identified several populations of CD4+ T-lymphocytes, with gene identifiers supporting their identity as CD4+ Tregs (IC3), CD4+ naïve T-cells (IC7 and IC8), and CD4+ helper T-cells (IC4), suggesting that pre-pregnancy mammary tissues are enriched for populations of CD4+ T-cells (**Fig. 2-6 A**). Conversely, clusters enriched with post-pregnancy mammary immune cells (IC5, IC6, and IC9) were classified as NKT cells, a specialized population of T-cells involved in immune recruitment and cytotoxic activity (Godfrey et al. 2004) (**Fig. 2-6 A**). These clusters expressed master regulators of NKT cell fate, including transcription factors (TFs) *Tbx21* (*Tbet*), and *Zbtb16* (*Plzf*) (Townsend et al. 2004; Savage et al. 2008).

**Figure 2-6**

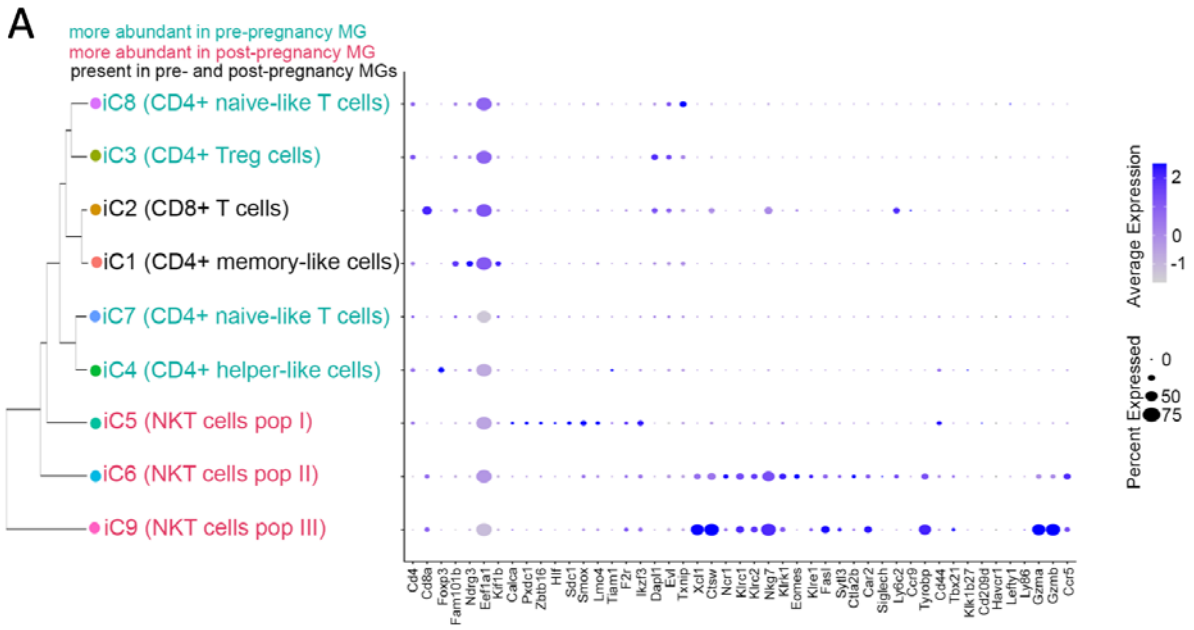


***Figure 2-6 Single cell analysis identifies post-pregnancy biased immune cell identity as NKT cells.***

**(A)** Dendrogram clustering and dot plot showing molecular signature and lineage identity of pre- and post-pregnancy mammary resident CD3+ immune cells. NKT cells are specifically enriched in post-pregnancy mammary glands.

While Natural Killer (NK) cells are known to play a role in mammary gland involution and parity-associated mammary tumorigenesis (Fornetti et al. 2012; Martinson et al. 2015), the role of NKT cells in this process has yet to be determined. Therefore, we analyzed clusters of immune cells expressing the common NK/NKT marker *Nkg7* to further define the influence of pregnancy on the abundance and identity of NK and NKT cells. Deep-clustering analysis of Nkg7+ immune cells revealed 6 distinct cell clusters (NC1-6). Cells classified under cluster NC5, which includes cells from both the pre- and post-pregnancy mammary tissue, lacked expression of CD3e, and therefore was the only cluster with an NK cell identity in our dataset (**Fig. 2-7 A-C**). Further gene expression analysis confirmed that post-pregnancy mammary glands are enriched with a variety of NKT cells, including those expressing markers of cell activation (*Gzmb* and *Ccr5*) and of a resting state (*Bcl11b*) (**Fig. 2-7 C**). In agreement, each of the post-pregnancy-biased NKT cell clusters were enriched with an array of immune activation signatures, suggesting an altered state for these cell populations after pregnancy (**Fig. 2-7 D**).

Collectively, our scRNA-seq analysis of fully involuted mammary tissue confirmed that pregnancy leads to a stable alteration of the transcriptional output of post-pregnancy MECs, including gene expression signatures that suggest enhanced communication with the mammary immune microenvironment. Our study further indicates that mammary resident NKT cells are present at higher levels in post-pregnancy glands, suggesting that pregnancy plays a role in inducing changes to the mammary immune microenvironment.

**Figure 2-7**

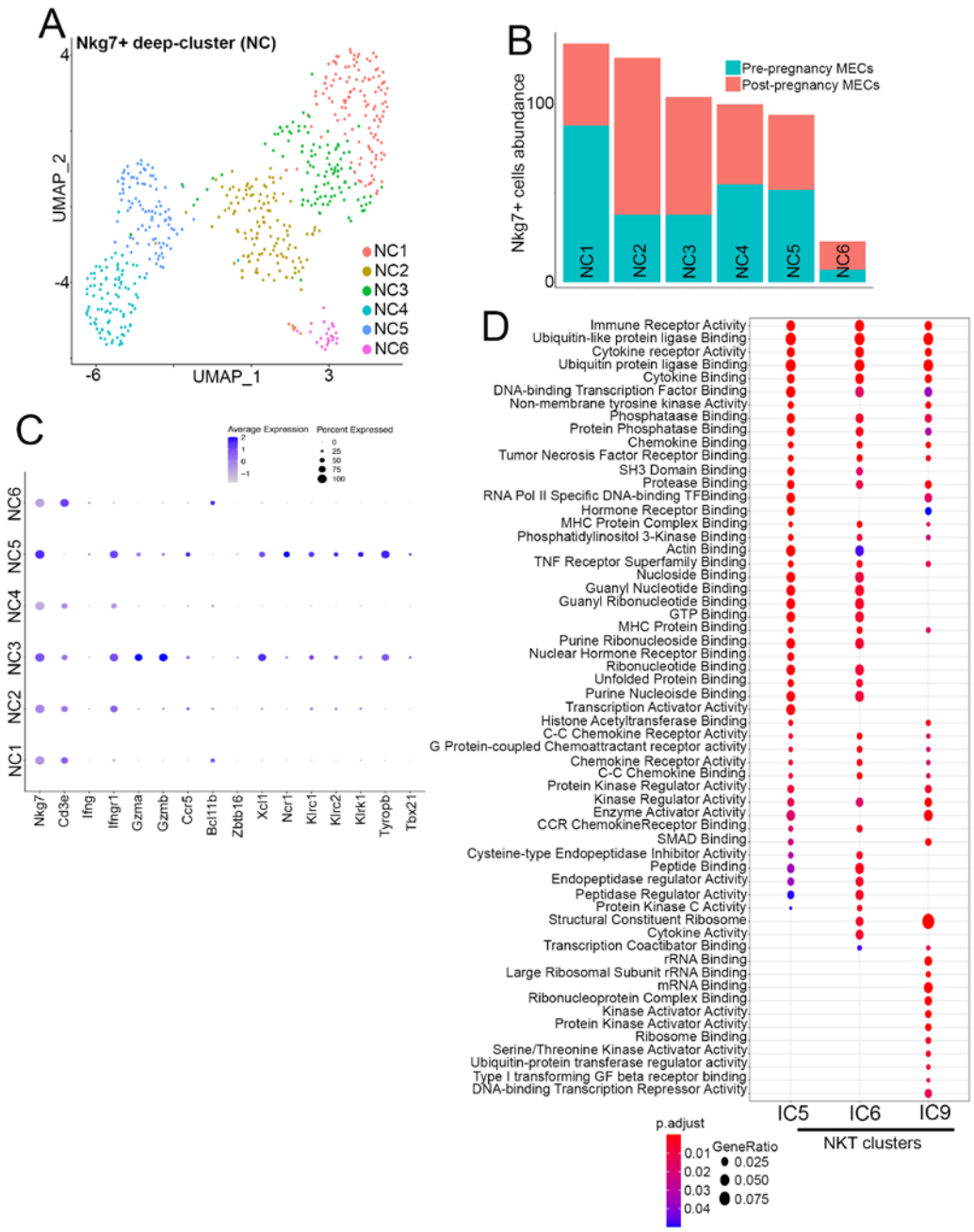


***Figure 2-7 scRNA-seq identification of post-pregnancy NKT cells.***

**(A)** UMAP showing Nkg7+ expressing cells focused re-clustering (NKT/NK cells) of pre- and post-pregnancy mammary tissue.
**(B)** Cell abundancy of pre- and post-pregnancy Nkg7+ immune cells.
**(C)** Dot plot showing the expression of NKT/NK associated genes across Nkg7+ cell clusters.
**(D)** Dotplot of pathway analysis across populations of CD3+ NKT cells (IC5, IC6 and IC9).

2.2.2 Pregnancy induces the expansion of a specific population of NKT cells in the mammary gland

During post-partum mammary gland involution, there is an influx of infiltrating mast cells, macrophages, neutrophils, dendritic cells and natural killer cells, which remove apoptotic epithelial cells and support the remodeling of the gland (Guo et al. 2017; Kordon et al. 2017; O'Brien et al. 2010; Schwertfeger et al. 2001). Since our scRNA-seq analyses suggested that fully involuted, post-pregnancy mammary glands are enriched for populations of NKT cells, we next utilized a series of flow cytometry analyses to validate this observation.

Analysis using antibodies against the markers NK1.1 and CD3, which defines NKT cells (NK1.1+CD3+), identified a 12-fold increase in the abundance of NKT cells in post-pregnancy mammary tissue, consistent with the results of our scRNA-seq data (**Fig. 2-8 A**). Further analysis indicated a 2.3-fold higher abundance of NKT cells in recently involuted mammary tissue (15 days post offspring weaning), compared to mammary glands from nulliparous mice, or those exposed to pregnancy hormones for 12 days (mid-pregnancy), suggesting that the expansion of NKT cells is likely to initiate at the final stages of post-pregnancy mammary involution (**Fig. 2-8 B**). The selective expansion of NKT cells was further supported by the analysis of markers that define mammary resident neutrophils (Ly6G+) and macrophages (CD206+), which were largely unchanged between pre- and post-pregnancy mammary tissue (**Fig. 2-8 C-D**).

Immunofluorescence analysis of Cxcr6-GFP-KI mammary tissue, previously described to selectively label NKT cells (Germanov et al. 2008), demonstrated several GFP+ cells surrounding ductal structures from pre-pregnancy mammary tissue, an observation that supports the presence of NKT cells in mammary tissue (**Fig. 2-9 A**). Moreover, analysis of bone marrow and spleen from nulliparous and parous mice showed no difference in the abundance of NK1.1+CD3+ cells, suggesting that pregnancy-induced expansion of NKT cells is mammary-specific (**Fig. 2-9 B-C**).

**Figure 2-8**

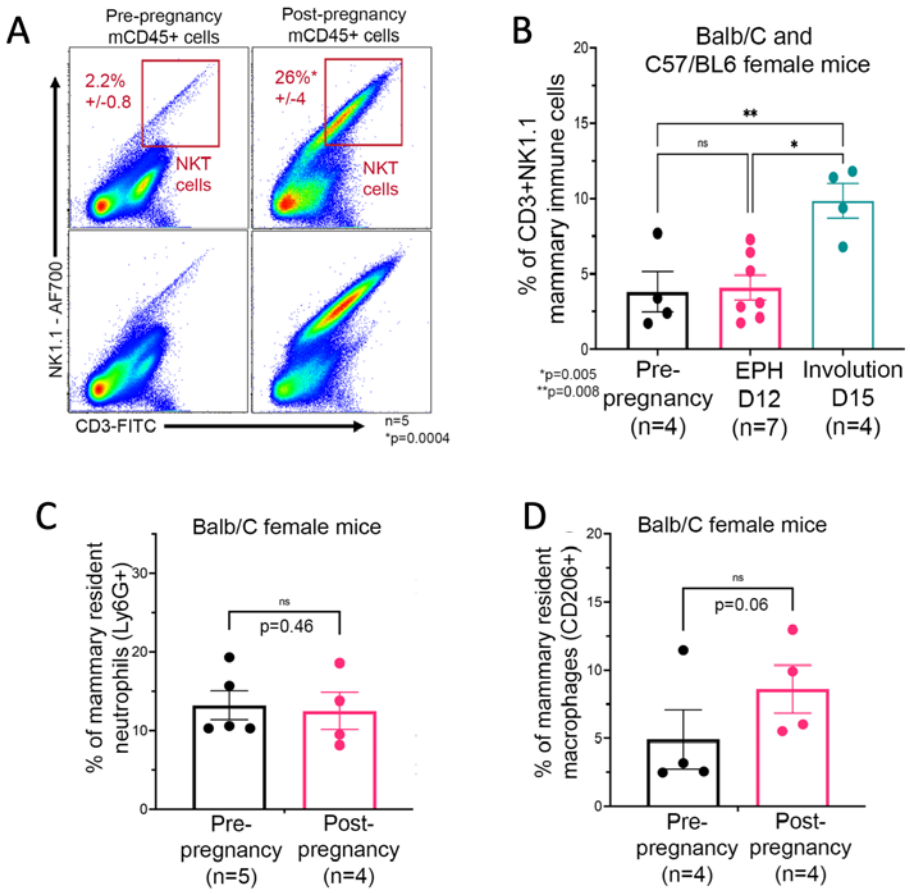


***Figure 2-8 Pregnancy induces expansion of specific populations of NKT cells.***

(**A**) Flow cytometry analysis of resident CD45+ cells harvested from pre- and post-pregnancy mammary tissue, and their distribution of NKT cells (NK1.1+CD3+). n=5 nulliparous and 5 parous female mice. *p=0.0004.

(**B**) Quantification of NKT cells abundance in mammary tissue from nulliparous female mice (black bar, n=4), from female mice during Exposure to Pregnancy Hormone day 12 (pink bar, EPH D12, n=7), and from female mice at post-pregnancy involution D15 (blue bar, n=4). EPH D12 x Involution D15 *p=0.005; Involution D15 x Pre-pregnancy **p=0.008.

(**C**) Quantification of Ly6G+ mammary resident neutrophils abundance in tissue from pre- and post-pregnancy female mice. n=5 nulliparous and n=4 parous female mice. *p=0.46.

(**D**) Quantification of CD206+ mammary resident macrophages abundance in tissue from pre- and post-pregnancy female mice. n=4 nulliparous and n=4 parous female mice. *p=0.06.

**Figure 2-9**

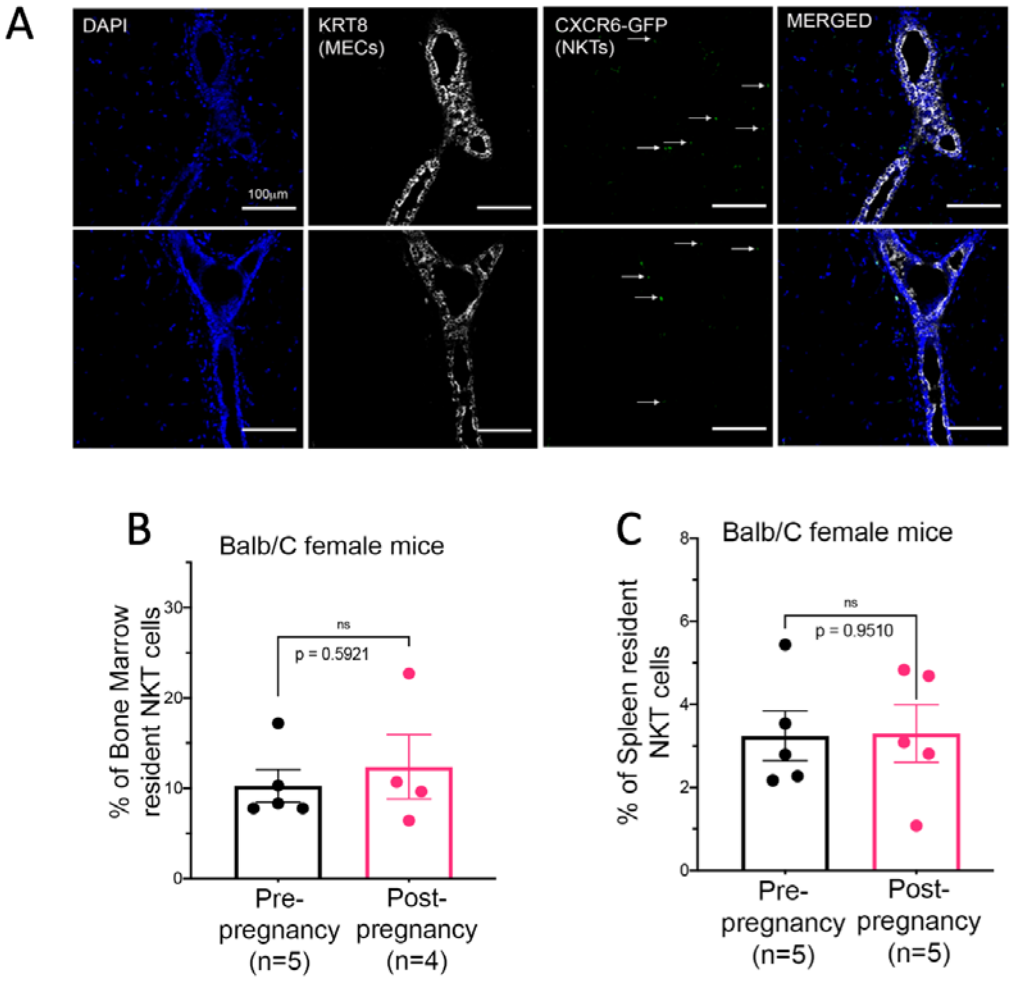


***Figure 2-9 Cellular characterization of post-pregnancy mammary immune microenvironment.***

(**A**) Immunofluorescence images (IF) of mammary tissue from Cxcr6-GFP-KI nulliparous mouse model showing the presence of GFP+ cells (NKT cells, green, white arrows) surrounding duct structures (Krt8+, white).
(**B**) Quantification of NKT cells abundance in bone marrow from pre- and post-pregnancy female mice. n=5 nulliparous and n=4 parous female mice. *p=0.5921.
(**C**) Quantification of NKT cells abundance in spleen from pre- and post-pregnancy female mice. n=5 nulliparous and n=5 parous female mice. *p=0.95.

To further characterize the identity of the post-pregnancy, mammary resident NKT cells, we combined cell surface and intracellular staining to detect canonical NKT lineage markers, including the NKT master regulator Tbet, the NKT/T-cell secreted factor IFNγ, and the NKT lineage marker Nkp46 (CD335) (Yu et al. 2011). Pre- and post-pregnancy, mammary resident NK1.1+CD3+ cells expressed all three markers, supporting their NKT identity. However, we detected a 2-fold increase in the percentage of post-pregnancy cells expressing Tbet, IFNγ, and CD335, suggesting that specific populations of NKTs are expanded in post-involuted mammary tissue (**Fig. 2-10 A**).

We also investigated whether pregnancy induced NKT cells represented a specialized population of CD8+ T-cells, a cytotoxic cell type reported to reside in mammary tissue (Wu et al., 2019) (Wu et al. 2019b). We found that a fraction of the NKT cells present in both pre- and post-pregnancy mammary tissue expressed CD8 on their surface, accounting for 41% and 35% of the total NKT cells, respectively (**Fig. 2-10 B**). To determine whether the triple-positive (CD3+NK1.1+CD8+) cells contributed significantly to the expanded population of post-pregnancy NKT cells, we analyzed mammary tissue of nulliparous and parous RAG1 KO mice, which lack mature CD8+ T-cells (Mombaerts et al. 1992). We observed a 10-fold expansion of NKT cells in RAG1 KO post-pregnancy mammary tissue, suggesting that CD8-expressing cells do not comprise a significant fraction of pregnancy-induced NKT cells (**Fig. 2-10 C**). These results are consistent with our scRNA-seq data, and further validate the existence of specific NKT subtypes in mammary glands after a full pregnancy cycle.

NKT cells have multiple roles, including tissue homeostasis, host protection, microbial pathogen clearance, and anti-cancer activity, mediated through their ability to recognize both foreign- and self-antigens via T-cell receptors (TCRs) (Balato et al. 2009). Therefore, we next investigated changes to the TCR repertoire of mammary resident, post-pregnancy NKT cells. We found that 17% of pre-pregnancy NKT cells expressed γδTCRs, in marked contrast to post-pregnancy NKT cells, which mostly expressed αβTCRs (44%) (**Fig. 2-10 D, top panels**). A pregnancy cycle did not alter TCR composition across all immune cells, given that mammary resident, pre- and post-pregnancy CD8+ T-cells mostly express

αβTCRs, suggesting that parity promotes expansion of subtypes of NKT cells that bear a specific TCR repertoire (**Fig. 2-10 D, bottom panels**).

**Figure 2-10**

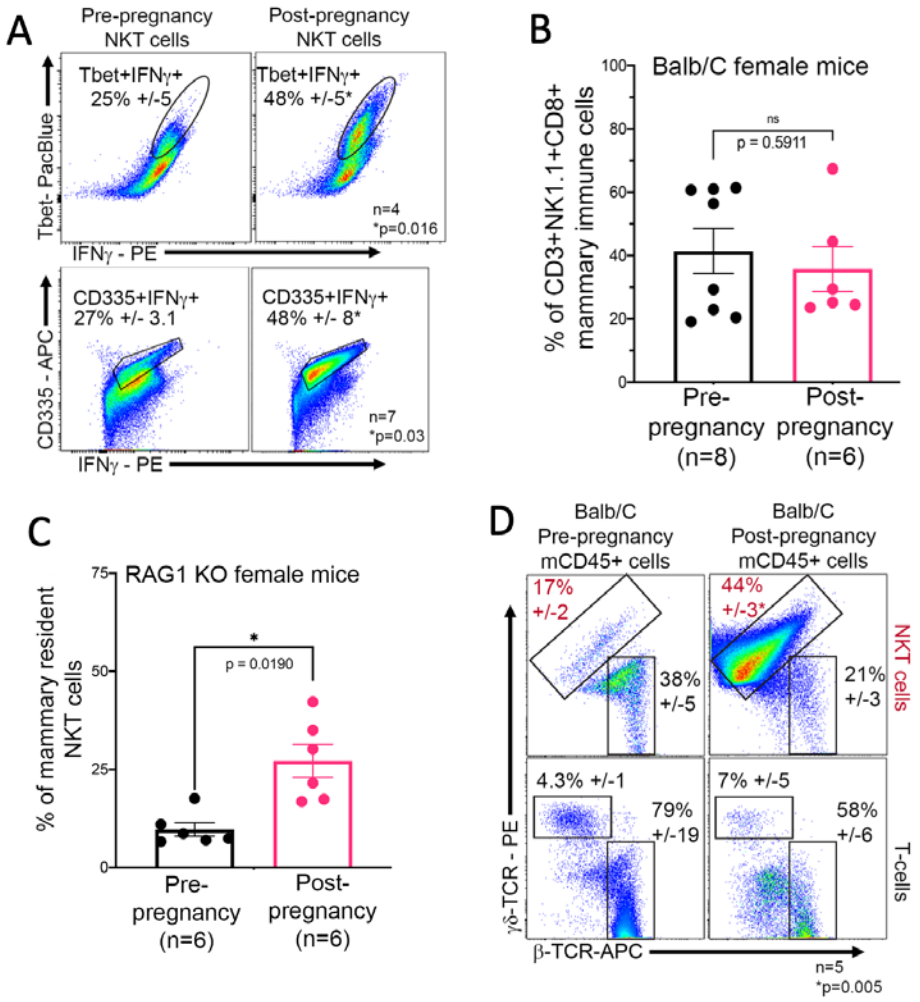


***Figure 2-10 Cellular characterization of post-pregnancy NKT cells shows altered TCR expression.***

(**A**) Flow cytometry analysis of the classical NKT cell markers T-bet, CD335, and IFNγ in NKT cells harvested from pre- and post-pregnancy mammary tissue. For Tbet analysis n=4 nulliparous and 4 parous female mice. *p=0.016. For CD335 analysis n=7 nulliparous and 7 parous female mice. *p=0.03.
(**B**) Quantification of CD8+ NKT cells abundance in mammary tissue from pre- and post-pregnancy female mice. n=8 nulliparous and n=6 parous female mice. *p=0.6
(**C**) Quantification of NKT cells abundance in mammary tissue from pre- and post-pregnancy RAG1 KO female mice. n=6 nulliparous and n=6 parous female mice. *p=0.019.
(**D**) Flow cytometry analysis of β and γδ T-cell receptors (TCRs) of pre- and post-pregnancy mammary NKT cells. n=5 nulliparous and 5 parous female mice. *p=0.005.

We next investigated the molecular signatures of FACS-isolated, mammary resident, NKT cells. Unbiased pathway analysis of bulk RNA-seq datasets revealed the enrichment of post-pregnancy NKT cells for processes controlling overall NKT development and activation, such as Notch signaling, TNFα signaling, TGFβ signaling, response to estrogen, and cMyc targets (Oh et al. 2015; Almishri et al. 2016; Doisne et al. 2009; Huber 2015; Mycko et al. 2009). Conversely, pre-pregnancy NKT cells were mainly enriched for processes previously associated with reduced immune activation, such as IFNα response (Bochtler et al. 2008) (**Fig. 2-11 A, Table 8-3**).

The activation of specific processes in post-pregnancy NKT cells was also evident from analysis of their accessible chromatin landscape. ATAC-seq profiles showed similar genomic distributions of accessible regions across pre- and post-pregnancy NKT cells, with a 93% overlap of their total accessible chromatin regions, suggesting that parity-induced changes did not substantially alter the chromatin accessibility associated with NKT lineage (**Fig. 2-11 B-C**). General TF motif analysis identified chromatin accessible regions bearing classical NKT regulator DNA binding motifs such as *T-bet*, *Plzf*, and *Egr2*, further supporting their NKT lineage identity (Seiler et al. 2012) (**Fig. 2-11 D**). Analysis of accessible chromatin exclusive to post-pregnancy NKT cells showed an enrichment for terms/genes associated with regulation of the adaptive immune response, killer cell activation and antigen presentation, such as *Pdk4*, *Maged1*, and *Lypla1*, all involved in enhanced immune-activation (Na et al. 2020; Connaughton et al. 2010; Lee et al. 2016; Jehmlich et al. 2013) (**Fig. 2-12 A and C**). DNA motif analysis at accessible regions exclusive to post-pregnancy NKT cells identified enrichment of specific TF motifs, including those recognized by Maf, a factor associated with an activated NKT state, and previously predicted by our scRNA-seq data to be expressed in cell clusters with an NKT identity (**Fig. 2-12 B**).

Overall, our analyses confirmed that post-pregnancy mammary tissue has an altered γδNKT cell composition, which bears molecular and cellular signatures of activated and mature adaptive immune cells.

**Figure 2-11**

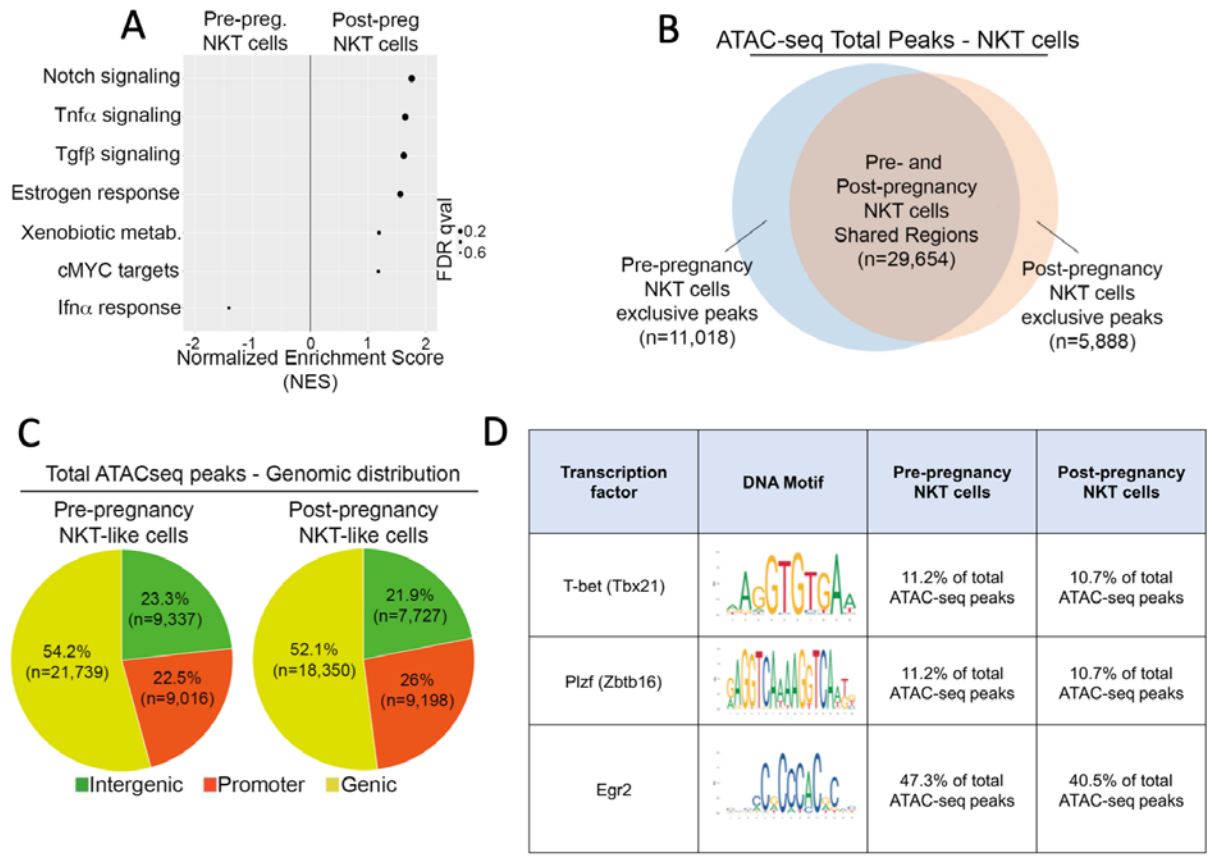


| Transcription factor | DNA Motif | Pre-pregnancy NKT cells | Post-pregnancy NKT cells |
|---|---|---|---|
| T-bet (Tbx21) | | 11.2% of total ATAC-seq peaks | 10.7% of total ATAC-seq peaks |
| Plzf (Zbtb16) | | 11.2% of total ATAC-seq peaks | 10.7% of total ATAC-seq peaks |
| Egr2 | | 47.3% of total ATAC-seq peaks | 40.5% of total ATAC-seq peaks |

***Figure 2-11 The molecular signature of post-pregnancy NKT cells.***

(**A**) Gene set enrichment analysis of differentially expressed genes in FACS-isolated NKT cells from pre- and post-pregnancy mammary tissue.
(**B**) Venn-diagram demonstrating the number of shared and exclusive ATAC-seq peaks of FACS-isolated NKT cells from nulliparous female mice (blue circle) and parous female mice (orange circle).
**(C)** Genomic distribution of total ATAC-seq peaks from FACS-isolated pre- and post-pregnancy NKT cells.
**(D)** TF motif analysis across total ATAC-seq peaks from FACS-isolated pre- and post-pregnancy NKT cells.

**Figure 2-12**

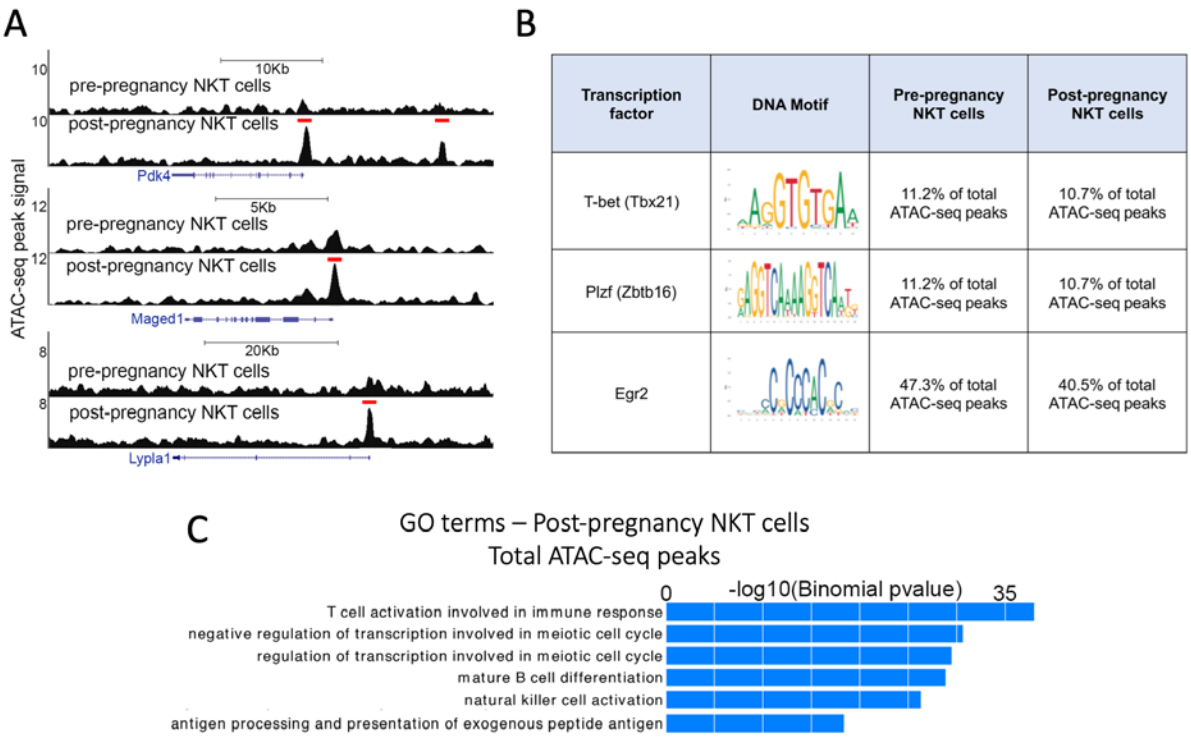


***Figure 2-12 The epigenetic signature of post-pregnancy NKT cells.***

(**A**) Genome browser tracks showing distribution of MACS-called ATAC-seq peaks at the *Pdk4*, *Maged1* and *Lypla1* genomic loci from pre- and post-pregnancy NKT cells.
**(B)** TF motif analysis across exclusive ATAC-seq peaks from FACS-isolated pre- or post-pregnancy NKT cells.
**(C)** GO term analysis of genes associated with total ATAC-seq peaks of FACS-isolated post-pregnancy NKT cells.

2.2.3 NKT expansion requires CD1d expression on post-pregnancy MECs

Classically, NKT cells are subdivided based on their activating antigens, including the main antigen-presenting molecules MHC class I, MHC class II, and the non-classical class I molecule, CD1d, which can be expressed on the surface of macrophages and dendritic cells, as well on the surface of epithelial cells (Gapin et al. 2013; Rizvi et al. 2015; Thibeault et al. 2009). Therefore, we next analyzed whether the expression of antigen-presenting factors on the surface of mammary epithelial and non-epithelial cells could underlie NKT cell expansion after pregnancy.

Flow cytometry analysis detected a 5-fold increase in the CD1d levels on the surface of post-pregnancy luminal and myoepithelial MECs (**Fig. 2-13 A-B**). In contrast, no differences in the expression of antigen-presenting factors MHC-I and MHC-II on the surface of pre- and post-pregnancy MECs were found (**Fig. 2-13 C-D**). No difference in surface expression of CD1d on mammary CD45+ immune cells was detected, suggesting that signals provided by CD1d+ MECs could promote the post-pregnancy expansion of mammary NKT cells (**Fig. 2-13 E**).

Gene expression analysis of scRNA-seq datasets and qPCR quantification of FACS-isolated epithelial cells confirmed that post-pregnancy MECs express higher levels of *Cd1d* mRNA, supporting that pregnancy induced molecular alterations may represent the basis for the observed increase in percentage of CD1d+ post-pregnancy MECs (**Fig. 2-13 A and Fig. 2-14 A**). In agreement, we observed increased levels of the active transcription marker histone H3 lysine 27 acetylation (H3K27ac) at the *Cd1d* genomic locus in FACS-isolated post-pregnancy MECs, suggesting that increased mRNA levels could be associated with parity-induced epigenetic changes at the CD1d locus (**Fig. 2-14 B**). These observations were confirmed in organoid systems that mimic the transcription and epigenetic alterations brought to MECs by pregnancy signals (Ciccone et al. 2020), where pregnancy hormones induced upregulation of *Cd1d* mRNA levels and increased H3K27ac levels at the *Cd1d* locus (**Fig. 2-14 C-D**). Thus, pregnancy-associated signals may induce epigenetic alterations at the *Cd1d* gene locus, that subsequently increase *Cd1d* mRNA and CD1d protein levels in post-pregnancy MECs.

**Figure 2-13**

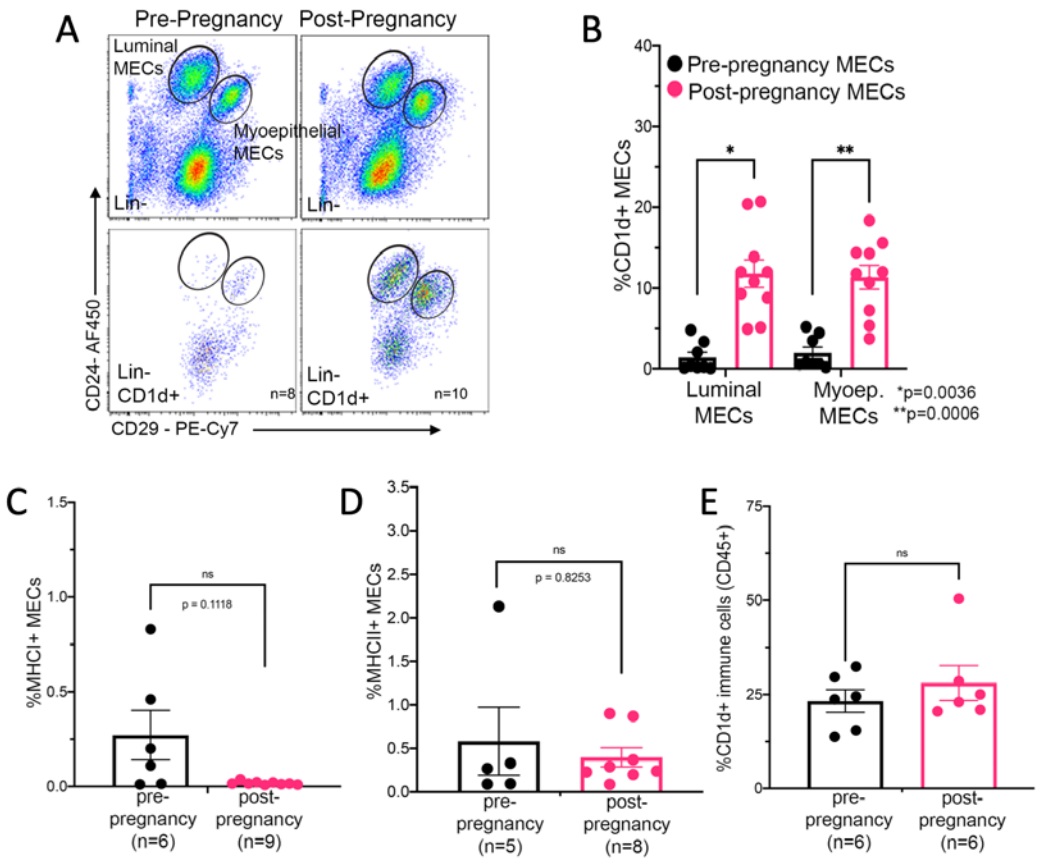


***Figure 2-13 Pregnancy alters CD1d transcription and expression on the surface of MECs.***

**(A)** Flow cytometry analysis of myoepithelial and luminal MECs harvested from pre-pregnancy (and post-pregnancy mammary tissue, and their distribution based on CD1d cell-surface expression.
**(B)** Flow cytometry quantification of CD1d+ MECs harvested from pre-pregnancy (black bars, n=8) and post-pregnancy (pink bars, n=10) mammary tissue. *p=0.0036 for luminal MECs and **p=0.0006 for myoepithelial MECs.
**(C)** Quantification of MHC-I+ MECs in pre- and post-pregnancy mammary tissue. n=6 nulliparous and n=9 parous female mice. *p=0.1.
**(D)** Quantification of MHC-II+MECs in pre- and post-pregnancy mammary tissue. n=5 nulliparous and n=8 parous female mice. *p=0.8.
**(E)** Quantification of CD1d+ immune cells in pre- and post-pregnancy mammary tissue. n=6 nulliparous and n=6 parous female mice. *p=0.28.

**Figure 2-14**

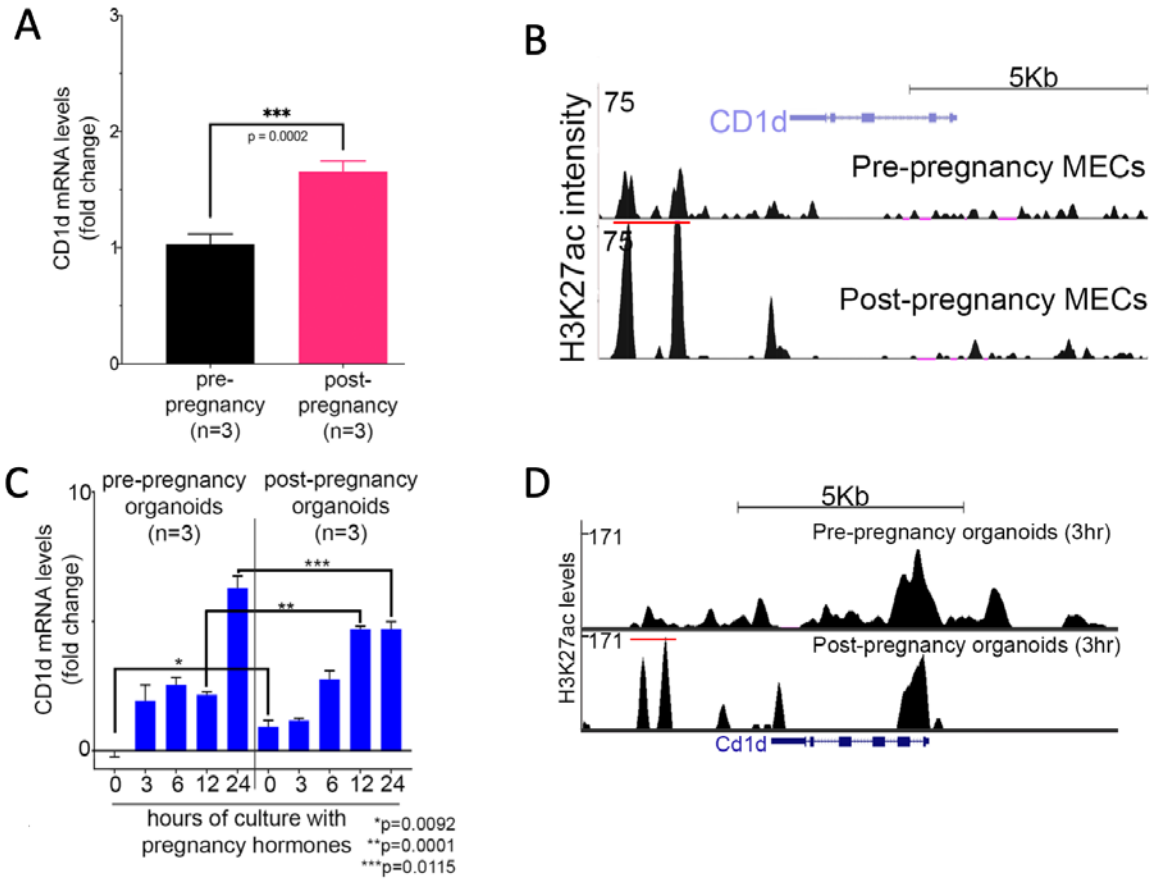


***Figure 2-14 The effects of pregnancy in controlling CD1d expression.***

**(A)** qPCR analysis of *Cd1d* mRNA levels in lineage depleted pre- and post-pregnancy MECs. n=3 biological replicates. p=0.0002.
**(B)** Genome browser tracks showing MACS-called, H3K27ac ChIP-seq peaks at the Cd1d genomic locus in FACS-isolated, pre- and post-pregnancy luminal MECs.
**(C)** qPCR analysis of *Cd1d* mRNA levels in organoid cultures derived from pre- and post-pregnancy MECs treated with pregnancy hormones. n=3 biological replicates. 0h, *p=0.0092; 12h, **p=0.0001; 24h, ***p=0.01.
**(D)** Genome browser tracks showing distribution of SEACR-called, H3K27ac Cut&Run, peaks at the Cd1d genomic locus in organoid cultures derived from pre- and post-pregnancy MECs treated for 3 hours with pregnancy hormones.

To investigate whether CD1d expression is required for the expansion of NKT cells after parity, we analyzed mammary glands from CD1d KO mice, which bear reduced levels of activated NKT cells (Faunce et al. 2005; Macho-Fernandez and Brigl 2015; Mantell et al. 2011). Mammary glands from nulliparous and parous CD1d KO mice displayed similar numbers of ductal structures and MEC populations as CD1d wild-type (WT) female mice, suggesting that loss of CD1d does not majorly alter mammary tissue homeostasis (**Fig. 2-15 A**). Further flow cytometry analysis indicated no statistically significant changes in the percentage of NKT cells in mammary glands of nulliparous CD1d KO mice (2.2% +/- 0.8), compared to nulliparous CD1d WT mice (3% +/- 1.6) (**Fig. 2-8 A, left panel, and Fig. 2-15 B, left panel**). Conversely, we found a 7-fold decrease in the percentage of NKT cells in mammary tissue from fully involuted, parous CD1d KO female mice (3% +/- 1.5) compared to parous CD1d WT mammary tissue (26% +/- 4), supporting the role of CD1d in regulating NKT activation (**Fig. 2-8 A, right panel, and Fig. 2-15 B, right panel**). Moreover, we found no difference in the abundance of NKT cells in glands from pre- and post-pregnancy CD1d KO female mice, consistent with lack of CD1d expression reducing the activation of NKT cells (**Fig. 2-15 B**). The analysis of an additional mouse strain that is deficient in mature/activated NKT cells, due to the deletion of the histone-demethylase *Kdm6* (UTX KO mouse model), failed to detect an expansion of NKT cells post-pregnancy, supporting that pregnancy induces the expansion of mature/active subtypes of NKT cells (Beyaz et al. 2017) (**Fig. 2-15 C**). Moreover, NKT cells observed in post-pregnancy CD1d KO mammary tissue mainly expressed αβTCR on their surface, in contrast to the γδ NKT cells observed in CD1d WT post-pregnancy glands, further confirming that loss of CD1d expression affects the expansion and activation of specific populations of NKT cells in post-pregnancy mammary tissue (**Fig. 2-15 D**).

Collectively, our studies identify pregnancy-induced epigenetic changes that may control the expression of *Cd1d* mRNA in MECs, and elucidate a role for CD1d in mediating communication between MECs and the γδTCR-expressing NKT cells, unique to post-pregnancy mammary glands.

**Figure 2-15**

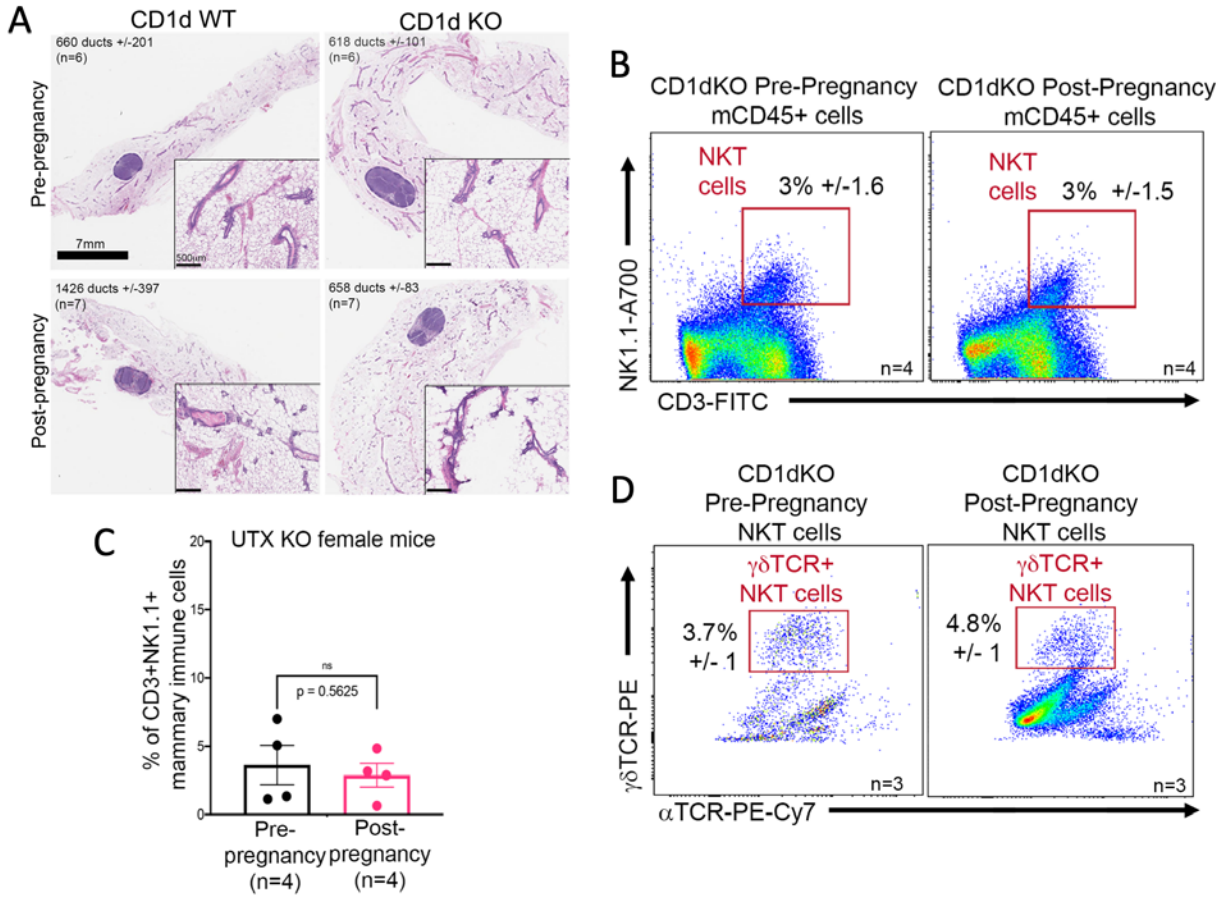


***Figure 2-15 NKT expansion depends on CD1d expression on post-pregnancy MECs.***

**(A)** H&E stained histological images and duct quantification from mammary glands harvested from nulliparous (top left, n=6) and parous (bottom left, n=7) CD1d WT female mice, and nulliparous (top right, n=6) and parous (bottom right, n=7) CD1d KO female mice. p=0.86 for pre-pregnancy glands and p=0.78 for post-pregnancy glands. Scale: 7mm. Zoom in panels, scale 500µm.

**(B)** Flow cytometry analysis of mammary resident CD45+ cells harvested from pre- and post-pregnancy CD1d KO female mice, and their distribution of NKT cells (NK1.1+CD3+). n=4 nulliparous and n=4 parous female mice. *p=0.3.

**(C)** Quantification of NKT cells abundance in mammary tissue from nulliparous and parous UTX KO female mice, which are deficient for activated NKT cells. n=4 nulliparous and n=4 parous female mice. *p=0.5.

**(D)** Flow cytometry analysis of β and γδ T-cell receptors (TCRs) of CD1d KO NKT cells from nulliparous (left, n=3) and parous (right, n=3) female mice. *p=0.5.

# 3. Pregnancy and oncoprotection in genetic models of mammary cancer

## 3.1 Author contributions

I acknowledge the following people who assisted with this project. Mary Feigman performed the initial flow cytometry and histology experiments on the CAGMYC mice, and transplant experiments with the double transgenic CD1d KO CAGMYC mouse model. Chen Chen and City Yang generated the K5-Brca1 KO mouse line. City Yang and Michael Ciccone maintained the mouse colony. Siran Li and Jude Kendall performed the whole genome DNA sequencing and CNV analyses. Matt Moss and Marygrace Trousdell analyzed the bulk RNA-seq data and generated the GSEA plots. Chen Chen performed the western blots on CAGMYC organoid cultures. J. Erby Wilkinson performed the histopathological analyses. Camila dos Santos oversaw the project, and participated in experimental design and data analyses.

## 3.2 A brief introduction to the GEMMs used in this section

### 3.2.1 The CAGMYC mouse model

To characterize the oncoprotective epigenetic changes induced by pregnancy, the dos Santos lab created a transgenic mouse strain (CAGMYC) of doxycycline (DOX) inducible *cMyc* overexpression as an oncogenic stressor. *Myc* is a key regulator of vital cellular processes such as growth, differentiation, proliferation, metabolism, and apoptosis. *Myc* deregulation has been widely shown to be associated with breast cancer progression and poor prognosis (Xu et al. 2010; Escot et al. 1986; Deming et al. 2000; Aulmann et al. 2002). We opted to use the CAGMYC model in which overexpression of *cMYC* is controlled by the CAG promoter, which is independent of pregnancy/lactation signals (Feigman et al. 2020), as opposed to classical promoters such as *MMTV, BLG*, and *WAP* as previously described. Pregnancy was found to elicit oncogenic protection in response to cMYC overexpression. Pre-pregnancy MECs showed abnormal growth, while post-pregnancy MECs resisted this phenotype and blocked malignant transformation.

Analysis of the pregnancy-induced epigenome revealed that genes that retained active histone marks (H3K27ac) after pregnancy, and are downregulated during re-exposure to pregnancy hormones, were associated with immune regulation. Further analysis of global gene expression of CAGMYC MECs demonstrated that post-pregnancy MECs have greater expression of genes associated with immune recruitment, thus suggesting that a full pregnancy cycle alters the communication between epithelial and immune cells. Here, we use this model to further understand epithelial-immune communication and cMyc driven oncogenesis.

### 3.2.2 The K5-CreERT2 Brca1$^{fl/fl}$ p53$^{-/+}$ (Brca1 KO) mouse model

cMYC overexpression is present in approximately 60% of basal-like breast cancers, with *cMYC* gain of function commonly found in *BRCA1* mutated breast cancers (Chen and Olopade 2008; Grushko et al. 2004). Interestingly, women harboring *BRCA1* mutations with a full-term pregnancy before the age of 25 benefit from pregnancy-induced breast cancer protection (Medina 2009; Terry et al. 2018). Therefore, we developed an inducible mouse model of *Brca1* loss of function, for the purpose of investigating how pregnancy-induced changes influence *Brca1* null mammary tumor development.

In this model, tamoxifen (TAM) induces homozygous loss of Brca1 function in cells that express the cytokeratin 5 gene (Krt5+ cells), which include MECs (dos Santos et al. 2013), cells from gastrointestinal tract (Sulahian et al. 2015), reproductive organs (Ricciardelli et al. 2017), and additional epithelial tissue (Castillo-Martin et al. 2010; Majumdar et al. 2012), in p53 heterozygous background (*Krt5*$^{\text{CRE-ERT2}}$*Brca1*$^{\text{fl/fl}}$*p53*$^{-/+}$, hereafter referred to as the Brca1 KO mouse).

Nulliparous Brca1 KO mice exhibited signs of mammary hyperplasia approximately 12 weeks post TAM treatment, which gradually progressed into mammary tumors at around 20 weeks after *Brca1* deletion (**Fig. 3-1 A-B**). Brca1 KO mammary tumors display cellular and molecular features similar to those previously described in human breast tissue from *BRCA1* mutation carriers and animal models of Brca1 loss of function, including high EGFR and KRT17 protein levels and altered copy number variation marked by gains and losses of genomic regions (Annunziato et al. 2019) (**Fig. 3-1 C-D**).

**Figure 3-1**

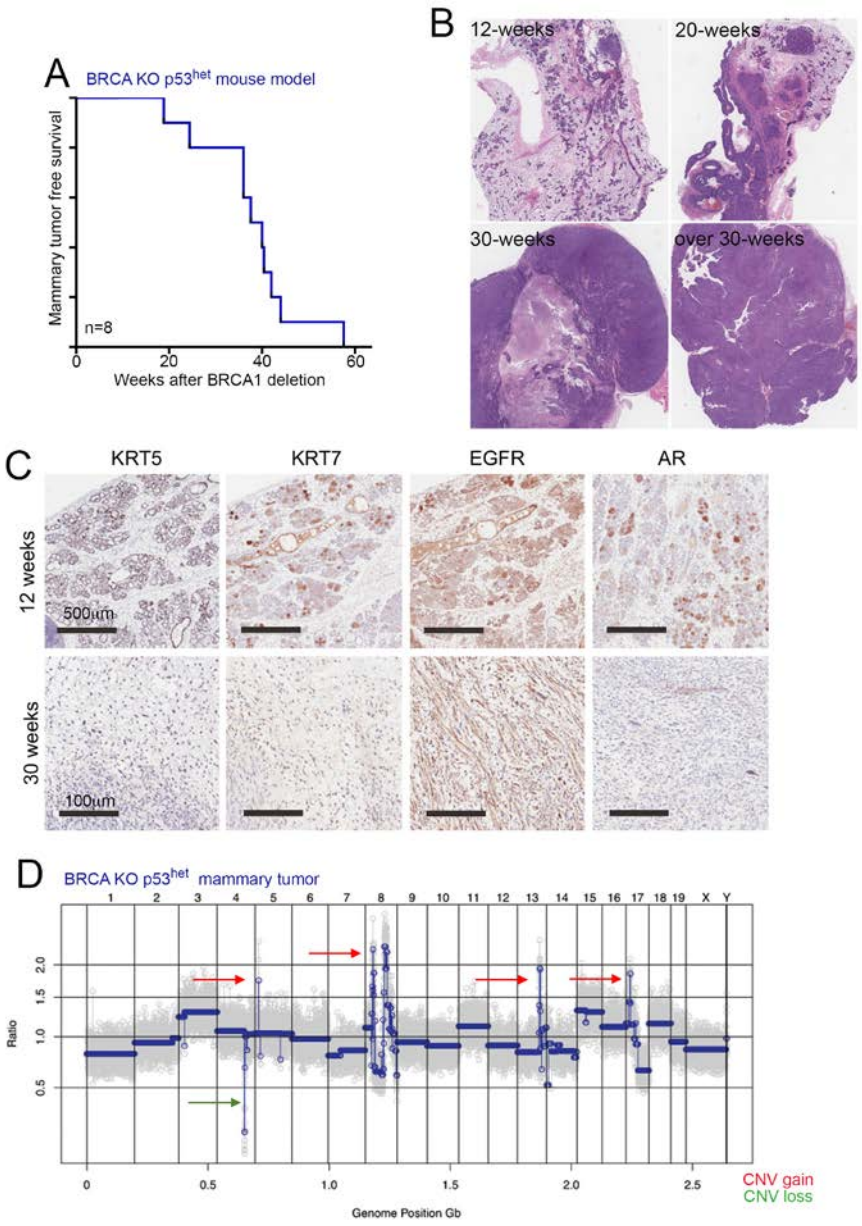


***Figure 3-1 Characterization of Krt5$^{CRE\text{-}ERT2}$Brca1$^{ko}$p53$^{het}$ (Brca1 KO) mouse model.***

**(A)** Tumor-free survival plot of nulliparous Brca1 KO female mice in weeks after TAM-treatment (to induce Brca1 deletion) (n=8).
**(B)** Mammary tissue and tumors from Brca1 KO nulliparous female mice at specific time points after TAM-treatment.
**(C)** Immunohistochemistry (IHC) analysis of mammary tissue and tumors from Brca1 KO nulliparous female mice for marker of basal-like mammary tumors KRT5, KRT7, EGFR and AR.
**(D)** Genomic segment plot showing Copy Number Variation (CNV) in mammary tumor from nulliparous Brca1 KO female mice.

## 3.3 Results

Parity resulted in the expansion of a specific population of γδNKT cells in the mammary gland in response to the upregulation of surface CD1d on MECs, pointing to a mechanistic connection between pregnancy-associated MECs and immune cell biology. Pregnancy has also been demonstrated to induce molecular modifications to MECs associated with an oncogene-induced senescence response to cMyc overexpression, and thus suppression of MEC malignant transformation (Feigman et al. 2020). Therefore, we next investigated whether pregnancy-induced mammary cancer protection was associated with the expansion of NKT cells.

### 3.3.1 Lack of mammary oncogenesis is marked by NKT expansion and CD1d+ MECs in CAGMYC and Brca1 KO parous mice

Flow cytometry analysis of pre- and post-pregnancy mammary tissue from cMyc overexpressing female mice (DOX-treated, CAGMYC model) demonstrated a 1.5-fold increase in the abundance of total CD3+ T-cells (**Fig. 3-2 A**). CD3+ T-cell expansion was also observed in mammary tissue transplanted with CAGMYC post-pregnancy MECs and organoid cultures derived from post-pregnancy CAGMYC MECs, both conditions previously demonstrated to lack mammary oncogenesis, and therefore suggesting a link between pregnancy-induced tumorigenic inhibition and specific changes to the adaptive immune system (**Fig. 3-2 B-C**). This selective expansion of CD3+ T cells was further supported by the analysis of markers that define mammary resident neutrophils (Ly6G+) and macrophages (CD206+), which were largely unchanged in mammary tissue transplanted with either pre- or post-pregnancy CAGMYC MECs (**Fig. 3-2 B**).

**Figure 3-2**

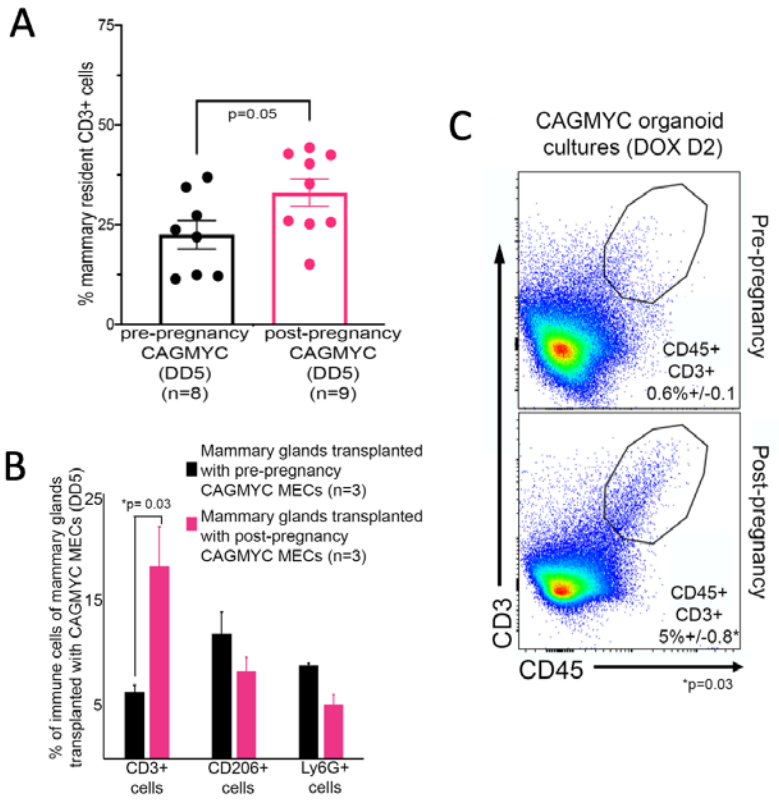


***Figure 3-2 The effects of cMYC-overexpression on pregnancy-induced immune changes and CD1d+ post-pregnancy MECs.***

**(A)** Quantification of CD3+ immune cell abundance in mammary tissue from DOX-treated (DD5), pre- and post-pregnancy CAGMYC female mice. n=8 nulliparous and n=9 parous female mice. p=0.05.
**(B)** Quantification of CD3+ (T/NKT cells), CD206+ (macrophages) and Ly6G+ (neutrophils) in mammary tissue of DOX-treated nulliparous female mice transplanted with pre-pregnancy CAGMYC MECS (black bars, n=3) or post-pregnancy CAGMYC MECs (pink bar, n=3) *p=0.03.
**(C)** Quantification of CD45+CD3+ immune cell abundance in DOX-treated (2-days), organoid cultures derived from pre-pregnancy CAGMYC mammary tissue (top panel, n=3) or from post-pregnancy CAGMYC mammary tissue (bottom panel, n=3) *p=0.03.

Further flow cytometry analysis identified a 6-fold increase in the percentage of NKT cells in mammary tissue from parous CAGMYC female mice, which predominantly expressed γδTCRs (**Fig. 3-3 A-B**). No change in the abundance of CD8+ T-cells or CD4+ T-cells was observed between mammary tissue from nulliparous and parous CAGMYC female mice, supporting the parity-induced expansion of γδNKT cells (**Fig. 3-3 C-D**), and suggesting that specific constituents of the mammary immune microenvironment may control tumorigenesis. In agreement, we also found a 5-fold higher percentage of CD1d+ luminal MECs in post-pregnancy mammary tissue, thus linking gain of CD1d expression and the expansion of γδTCR-expressing NKT cells, which may collectively play a role in blocking tumorigenesis (**Fig. 3-3 E**).

To investigate the effects of pregnancy on the mammary immune microenvironment and oncogenesis, age matched, TAM-treated, Brca1 KO nulliparous and parous (1 pregnancy, 21-days of gestation, 21-days of lactation/nursing, and 40-days post offspring weaning) female mice were monitored for tumor development (**Fig. 3-4 A**). Our study demonstrated that 100% of nulliparous Brca1 KO female mice (5 out of 5 mice) developed mammary tumors, compared to only 20% of the parous Brca1 KO female mice that developed mammary tumors (1 out of 5), thus indicating that a full pregnancy cycle decreases the frequency of Brca1 KO mammary tumors by 80% (**Fig. 3-4 B-C**).

Histopathological analysis suggested that pre-pregnancy mammary tumors were quite diverse, as previously reported for tumors from Brca1 KO mice (Brodie et al. 2001). These included poorly differentiated tumors, such as micro-lobular carcinomas with squamous trans-differentiation (**Fig. 3-4 C – top rows, far left panel**), medullary like carcinomas (**Fig. 3-4 C – top rows, right panel**), and solid carcinomas resembling high-grade invasive ductal carcinoma (IDC) in humans (**Fig. 3-4 C – top rows, left and far right panels**). Accordingly, the only tumor-bearing parous Brca1 KO female mouse developed a poorly differentiated carcinoma with extensive squamous trans-differentiation and with extensive necrosis, also previously reported for tumors from Brca1 KO mice (**Fig. 3-4 C – bottom rows, far right panels**). Additional histopathological analysis confirmed that mammary tissues from the remaining parous Brca1

KO female mice (4 out of 5) were largely normal (**Fig. 3-4 C – bottom rows, far left, left and right panels and Fig. 3-4 D**).

**Figure 3-3**

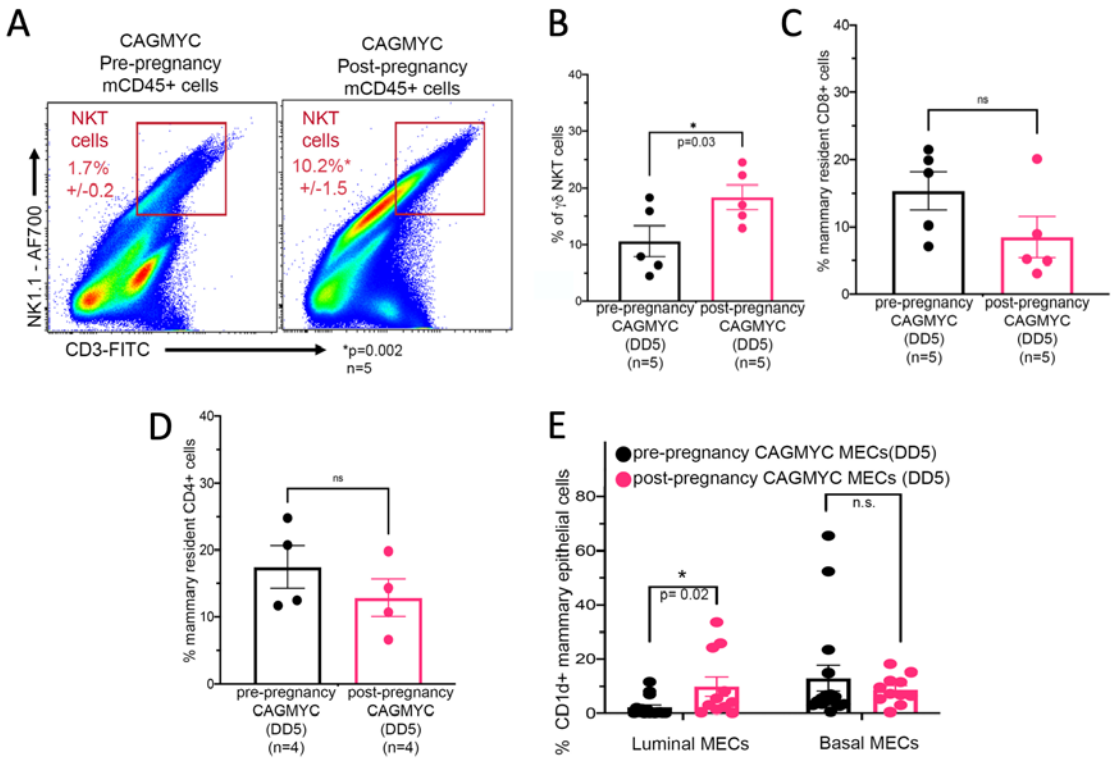


***Figure 3-3 Lack of mammary oncogenesis is marked by NKT expansion and CD1d+ MECs in CAGMYC parous female mice.***

(**A**) Flow cytometry analysis of mammary resident NKT cells (CD45+NK1.1+CD3+) from DOX-treated nulliparous (left panel, n=5) and parous (right panel, n=5) CAGMYC female mice. *p=0.002. (**B**) Flow cytometry quantification of CD1d+ luminal and myoepithelial MECs from DOX-treated nulliparous (left panel, n=16) and parous (right panel, n=11) CAGMYC female mice. *p=0.02.
**(B)** Quantification of γδTCR expression at the surface of NKT cells in mammary tissue from DOX-treated (DD5), pre- and post-pregnancy CAGMYC female mice. n=5 nulliparous and n=5 parous female mice. *p=0.03.
**(C)** Quantification of total CD8+ T-cells in mammary tissue from DOX-treated (DD5), pre- and post-pregnancy CAGMYC female mice. n=5 nulliparous and n=5 parous female mice. *p=0.24.
**(D)** Quantification of total CD4+ T-cells in mammary tissue from DOX-treated (DD5), pre- and post-pregnancy CAGMYC female mice. n=4 nulliparous and n=4 parous female mice. *p=0.41.
(**E**) Flow cytometry quantification of CD1d+ luminal and myoepithelial MECs from DOX-treated nulliparous (left panel, n=16) and parous (right panel, n=11) CAGMYC female mice. *p=0.02.

**Figure 3-4**

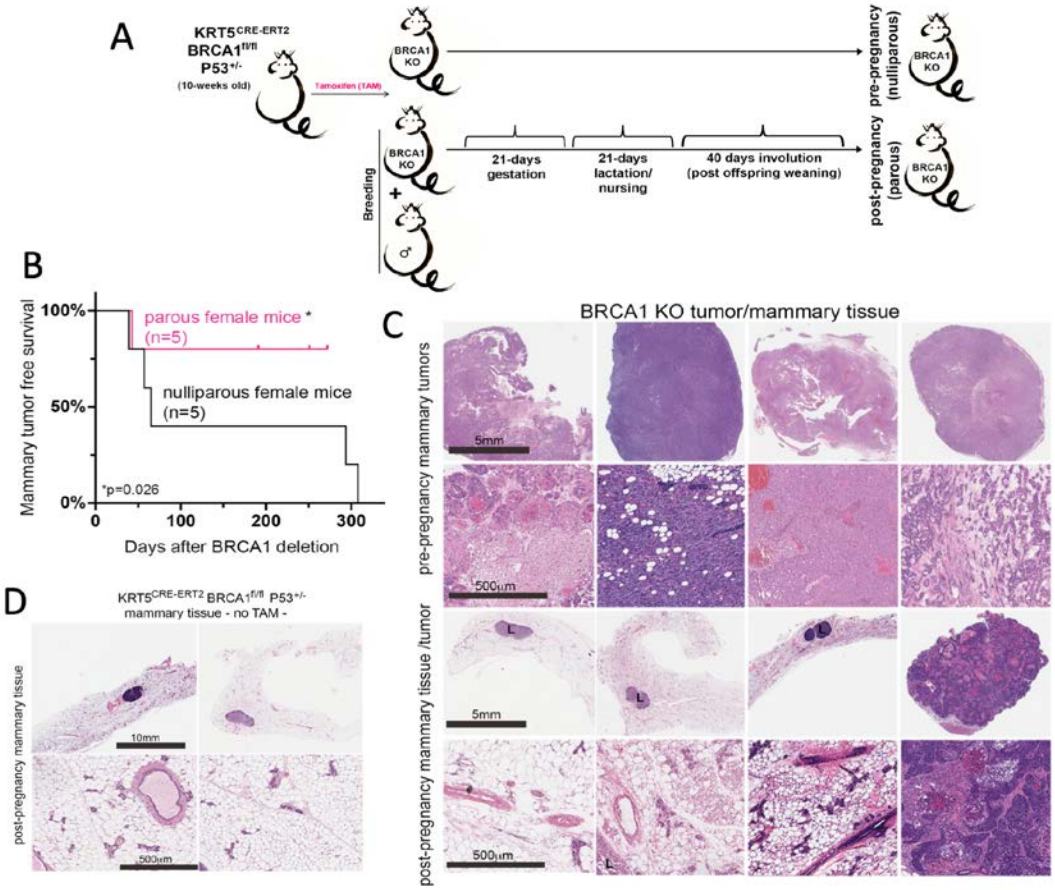


***Figure 3-4 Pregnancy decreases the frequency of Brca1 KO mammary tumor development.***

**(A)** Experimental approach showing the strategy for Brca1 deletion, and analysis of tumor development in pre- and post-pregnancy Brca1 KO female mice.

(**B**) Mammary tumor-free survival plot of nulliparous (black line, n=5) and parous (pink line, n=5) Brca1 KO female mice.

(**C**) H&E stained histological images from mammary tissue and mammary tumor harvested from nulliparous (top panels) and parous (bottom panels) Brca1 KO female mice. Scale: 5mm. Zoom-in panels, scale: 500µm.

**(D)** H&E histological images of normal mammary tissue harvested from parous, non-TAM treated, $Krt5^{CRE\text{-}ERT2}Brca1^{fl/fl}p53_{het}$ (therefore Brca1 WT) female mice.

Immunofluorescence analysis confirmed that both pre-pregnancy mammary tumors and post-pregnancy normal mammary tissue were indeed deficient for Krt5+ Brca1+ epithelial cells, indicating that the lack of mammary tumors in parous female mice was not due to inefficient *Brca1* deletion (**Fig. 3-5 A**).

Flow cytometry analysis of Brca1 KO MECs demonstrated a progressive loss of myoepithelial cells in tumor tissue from nulliparous (2.5-fold) and parous (2-fold) Brca1 KO female mice, defined by an increase in the percentage of $CD24^{high}CD29^{low}$ luminal-like MECs, (**Fig. 3-5 B**). These results suggest that tumor progression in this model is accompanied by changes to the population of $CD24^{high}$ MECs, which has been associated with poor clinical outcomes in patients with triple negative breast cancer (Chan et al. 2019). Further cellular analysis indicated a 2.7-fold increase in the percentage of $CD24^{high}$/luminal CD1d+ cells in healthy, post-pregnancy Brca1 KO mammary tissue compared to tissue from tumor-bearing nulliparous and parous Brca1 KO mice, supporting that parity induces the expression of CD1d at the surface of MECs (**Fig. 3-5 C**).

Given the increased levels of CD1d expression at the surface of post-pregnancy Brca1 KO MECs, we next investigated the presence of NKT cells in mammary tissue from nulliparous and parous Brca1 KO female mice. Flow cytometry analysis demonstrated a 3.8-fold increase in the percentage of NKT cells in healthy, post-pregnancy Brca1 KO mammary tissue compared to non-affected normal mammary tissue from tumor-bearing, nulliparous and parous Brca1 KO mice (**Fig. 3-6 A-B**). Additional flow cytometry analysis demonstrated that approximately 70% of total NKT cells from healthy, post-pregnancy Brca1 KO mammary tissue expressed γδTCR, in marked contrast to NKT cells from healthy (2.7%) and tumor mammary tissue (8.6%) from nulliparous Brca1 KO mice (**Fig. 3-6 C**).

Collectively, our findings show that pregnancy-induced gain of CD1d expression at the surface of MECs and expansion of NKT cells associates with lack of mammary oncogenesis in response to cMyc overexpression or loss of Brca1 function, thus supporting to the link between pregnancy-induced molecular changes, mammary tissue immune alteration, and inhibition of mammary tumorigenesis in clinically relevant mouse models.

**Figure 3-5**

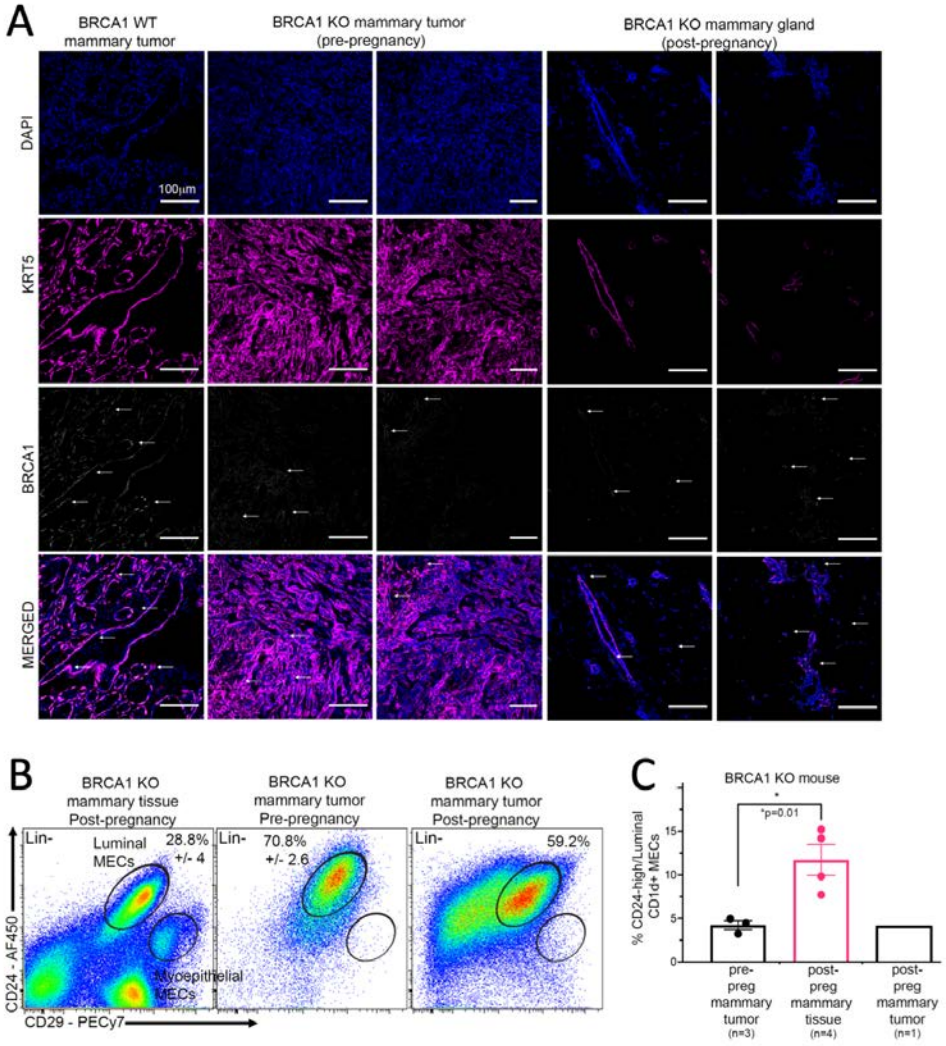


***Figure 3-5 Lack of mammary oncogenesis is marked by increased CD1d expression on MECs in Brca1 KO parous mammary tissue.***

**(A)** Immunofluorescence analysis (IF) of BRCA1 protein levels (white signal) in mammary epithelial cells (KRT5+, pink signal) from Brca1 WT mammary tumor (far left panels), pre-pregnancy Brca1 KO mammary tumors (left and middle panels), and from normal mammary tissue from parous Brca1 KO female mice (right and far right panels). Arrows indicate cells positive for BRCA1 and KRT5.
**(B)** FACS plots showing the abundance of luminal mammary epithelial MECs ($CD24^{high}CD29^{low}$) and myoepithelial mammary epithelial MECs ($CD24^{low}CD29^{high}$) in mammary tissue from parous Brca1 KO female mice (left panel), mammary tumor from nulliparous Brca1 female mice (middle panel), and mammary tumor from parous Brca1 female mice (right panel).
(**C**) Flow cytometry quantification of CD1d+ $CD24^{high}$ luminal MECs from Brca1 KO pre-pregnancy mammary tumors (black bar, n=3), Brca1 KO post-pregnancy healthy mammary tissue (pink bar, n=4), and Brca1 KO post-pregnancy mammary tumor (blue bar, n=1). *p=0.02.

**Figure 3-6**

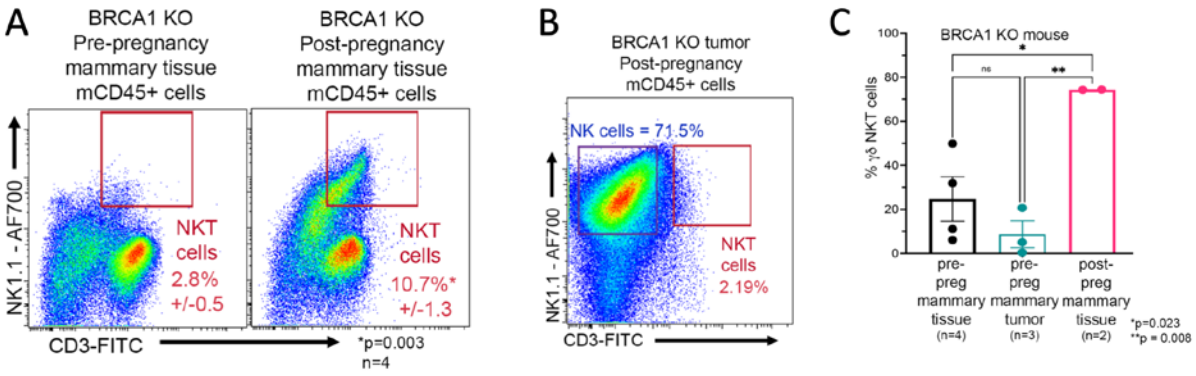


***Figure 3-6 Lack of mammary oncogenesis is marked by NKT expansion in Brca1 KO parous mammary tissue.***

(**A**) Flow cytometry analysis of mammary resident NKT cells in normal mammary tissue from nulliparous, tumor-bearing, Brca1 KO female mice (left panel, n=4) and normal mammary tissue from healthy parous Brca1 KO female mice (right panel, n=4). *p=0.003.
**(B)** FACS plots showing the abundance of NKT cells in mammary tumors from parous Brca1 KO female mice.
(**C**) Quantification of γδNKT cells in normal mammary tissue from nulliparous, tumor-bearing, Brca1 KO female mice (black bar panel, n=4), in mammary tumor tissue from nulliparous Brca1 KO female mice (blue bar, n=3), and in normal mammary tissue from healthy parous Brca1 KO female mice (black bar panel, n=2). *p=0.023 and **p=0.008.

### 3.3.2 Functionally active NKT cells are required to block malignant progression of post-pregnancy MECs

Given that we demonstrated that pregnancy-induced changes block mammary oncogenesis in two distinct models (**Fig. 3-3 and 3-4**), and that *cMyc* gain of function is commonly found in *Brca1* mutated breast cancers, we utilized the cMyc overexpression model to further characterize the effects of the immune microenvironment on the malignant progression of post-pregnancy MECs.

Analysis of fat-pad transplantations into severely immune deficient NOD/SCID female mice, which lack T-cells, B-cells, NK and NKT cells, indicated that 100% of mammary tissue injected with pre-pregnancy (n=5) or post-pregnancy (n=5) CAGMYC MECs developed adeno-squamous-like carcinomas with acellular lamellar keratin, high levels of cell proliferation (Ki67 staining), and increased collagen deposition (Trichrome blue staining) (**Fig. 3-7 A-C**). Therefore, NKT cells, or associated adaptive immune cells, are required for the parity associated protection from oncogenesis in the CAGMYC model.

Bulk RNA-seq analysis demonstrated that post-pregnancy CAGMYC MECs transplanted into the fat-pad of NOD/SCID female mice were less effective at activating the expression of canonical cMyc targets and estrogen response genes, compared to transplanted pre-pregnancy CAGMYC MECs, in agreement with the previously reported transcriptional state of post-pregnancy CAGMYC MECs (Feigman et al. 2020) (**Fig. 3-7 D**). We also found that organoid cultures derived from post-pregnancy CAGMYC MECs transplanted into NOD/SCID female mice retained a senescent-like state, characterized by reduced p300 protein levels and moderately increased p53 protein levels, in agreement with the previously reported senescent state of post-pregnancy CAGMYC MECs (Feigman et al. 2020) (**Fig. 3-7 E**). Together, these findings indicate that oncogenic progression of post-pregnancy CAGMYC MECs is associated with the immune deficient mammary microenvironment of NOD/SCID mice.

**Figure 3-7**

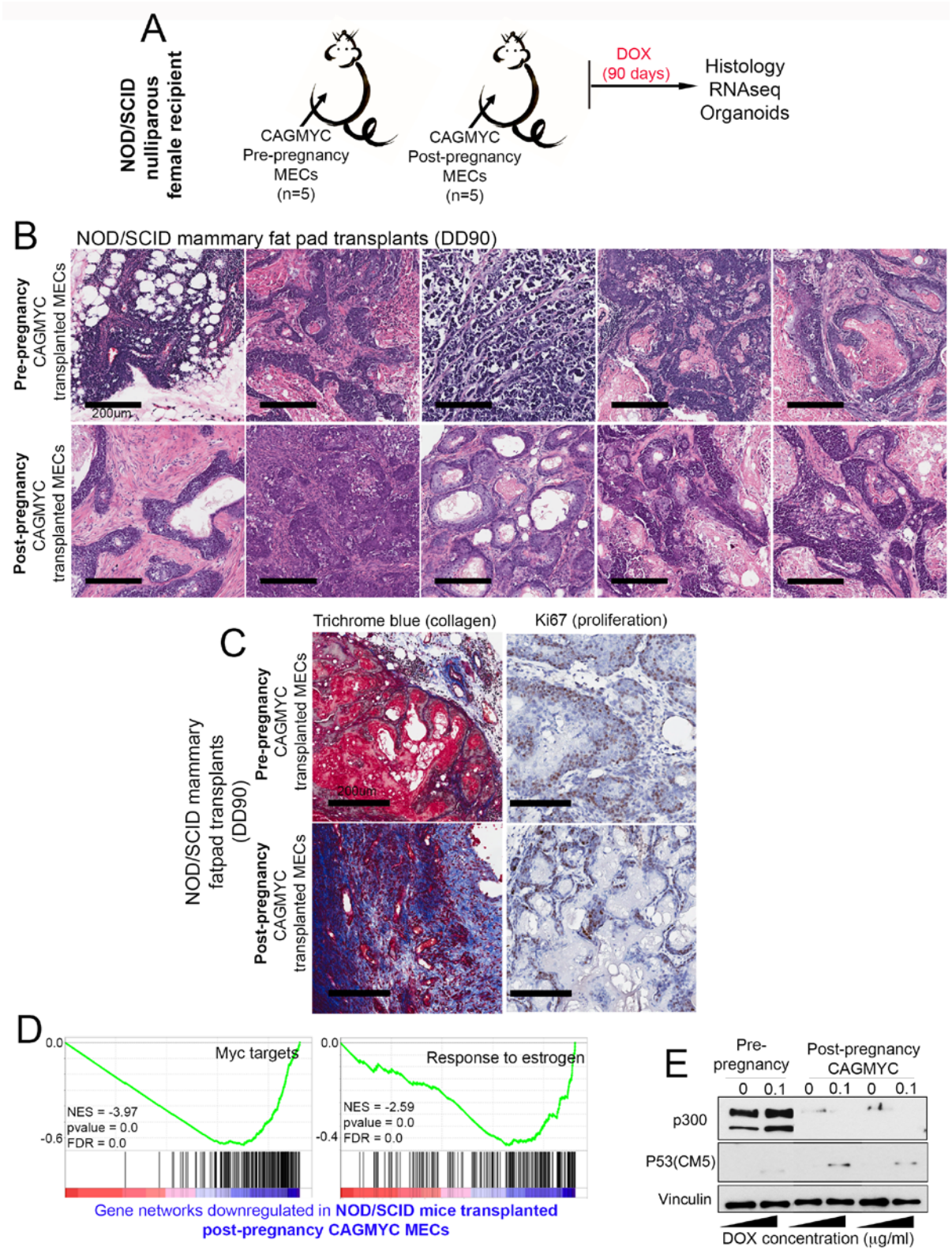
A
NOD/SCID nulliparous female recipient
CAGMYC Pre-pregnancy MECs (n=5)
CAGMYC Post-pregnancy MECs (n=5)
DOX (90 days)
Histology
RNAseq
Organoids
B
NOD/SCID mammary fat pad transplants (DD90)
Pre-pregnancy CAGMYC transplanted MECs
Post-pregnancy CAGMYC transplanted MECs
200um
C
Trichrome blue (collagen)
Ki67 (proliferation)
NOD/SCID mammary fatpad transplants (DD90)
Pre-pregnancy CAGMYC transplanted MECs
Post-pregnancy CAGMYC transplanted MECs
200um
D
Myc targets
NES = -3.97
pvalue = 0.0
FDR = 0.0
Response to estrogen
NES = -2.59
pvalue = 0.0
FDR = 0.0
Gene networks downregulated in NOD/SCID mice transplanted post-pregnancy CAGMYC MECs
E
Pre-pregnancy
Post-pregnancy CAGMYC
0 0.1 0 0.1 0 0.1
p300
P53(CM5)
Vinculin
DOX concentration (μg/ml)

***Figure 3-7 cMYC-overexpression induces oncogenesis of post-pregnancy MECs transplanted into NOD/SCID mammary fatpads.***

(**A**) Experimental approach showing strategy for the transplantation of pre- and post-pregnancy CAGMYC MECs into the fatpad of nulliparous NOD/SCID female mice, and tissue analysis.
(**B**) H&E stained histology images from DOX-treated (DD90) NOD/SCID mammary tissue transplanted with pre- and post-pregnancy CAGMYC MECs. n=5 nulliparous and 5 parous female mice. Scale: 200μm.
(**C**) Immunohistochemistry (IHC) analysis of Masson's Trichrome levels (collagen deposition) and Ki67 levels (proliferation) in DOX-treated (DD90) NOD/SCID mammary tissue transplanted with pre- and post-pregnancy CAGMYC MECs. n=5 nulliparous and 5 parous female mice. Scale: 200μm.
(**D**) Gene set enrichment analysis of gene networks down-regulated in NOD/SCID mice transplanted with post-pregnancy CAGMYC MECs.
(**E**) Western blot of p300, and p53 proteins in organoid cultures derived from NOD/SCID transplanted pre- and post-pregnancy CAGMYC tumor cells, with and without DOX treatment (2 days). Vinculin protein levels were used as endogenous control.

While our investigation of post-pregnancy CAGMYC MECs that were transplanted into the mammary tissue of immunosuppressed animals alluded to the importance of a robust immune system in blocking mammary tumorigenesis, it did not uncouple whether functionally active NKT cells, or CD1d expression at the surface of MECs, act to block oncogenesis in post-pregnancy mammary tissue. To determine whether signaling between CD1d+ MECs and NKT cells is critical for the development of mammary oncogenesis after pregnancy, we developed a double transgenic mouse model, by crossing the DOX-inducible CAGMYC mice into a CD1d KO background, hereafter referred as CAGMYC CD1d KO.

Tissue histology analysis indicated that mammary tissue from DOX-treated, nulliparous and parous CAGMYC CD1d KO female mice showed signs of tissue hyperplasia with atypia and abnormal ductal structures, demonstrating that loss of Cd1d expression is accompanied by mammary oncogenesis in a parity-independent fashion (**Fig. 3-8 A, left and far right panels and Fig. 3-8 B**). Conversely, analysis of DOX-treated, CAGMYC CD1d WT mice showed that mammary tissue from parous female mice lacked malignant lesions in response to cMyc overexpression (**Fig. 3-8 A, right panels and Fig. 3-8 B**). Flow cytometry analysis showed a lack of NKT cells in mammary tissue from both nulliparous and parous CAGMYC CD1d KO female mice, in marked contrast to the observed expansion of γδNKT cells in healthy post-pregnancy CAGMYC CD1d WT mammary glands that lacked tissue hyperplasia suggesting that CD1d expression may control pregnancy-induced expansion/activation of NKTs, and thus block mammary tumorigenesis. (**Fig. 3-8 C and Fig. 3-3 A**).

**Figure 3-8**

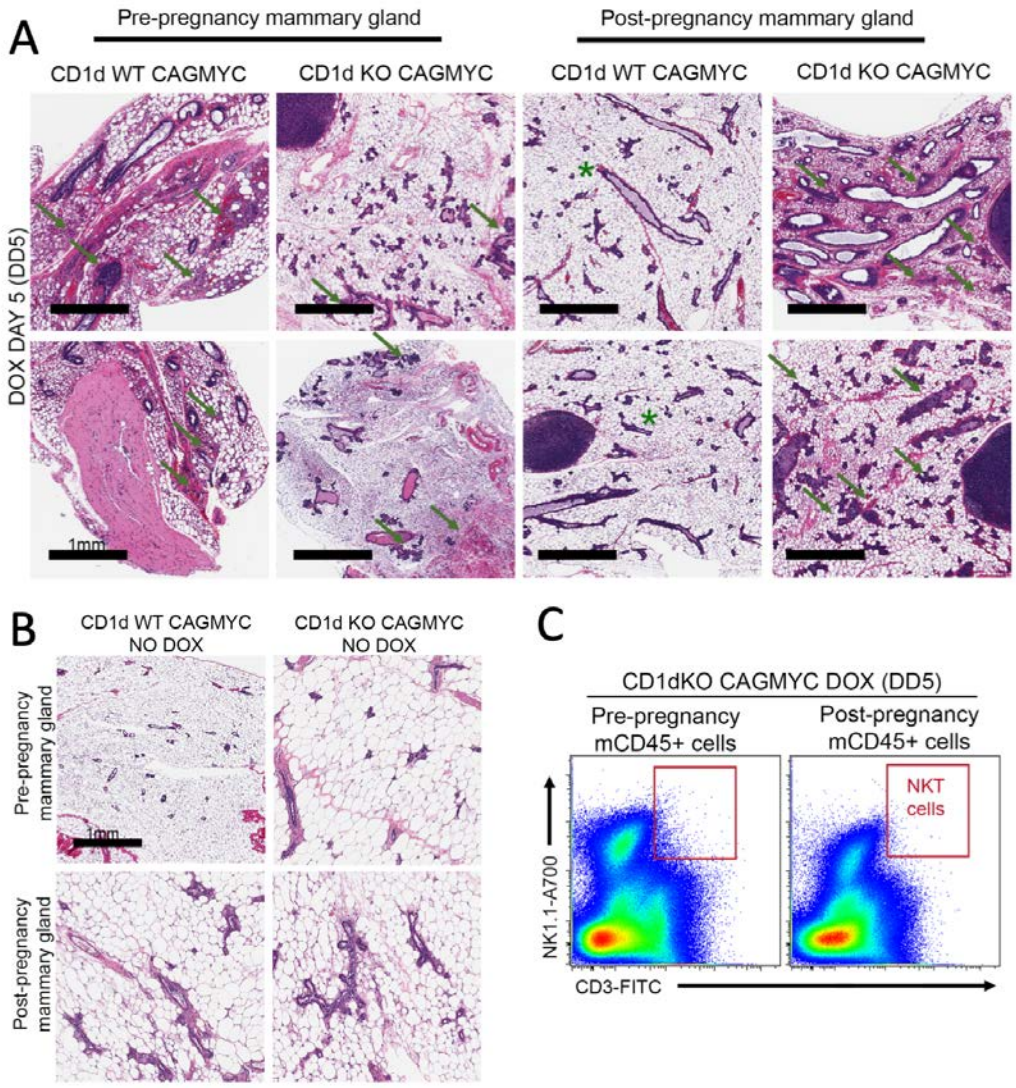


***Figure 3-8 Functionally active NKT cells are required to block malignant progression of post-pregnancy MECs.***

**(A)** H&E stained histological images of mammary tissue harvested from DOX-treated (DD5), nulliparous CD1d WT CAGMYC (far left panels), nulliparous CD1d KO CAGMYC (left panels), parous CD1d WT CAGMYC (right panels), and parous CD1d KO CAGMYC (far right panels) female mice. Green arrows indicate signs of malignant lesions/mammary hyperplasia. Green asterisks indicate normal-like ductal structures. Scale: 1mm.
**(B)** H&E stained histology images from mammary tissue from pre- and post-pregnancy CD1d WT CAGMYC and CD1d KO CAGMYC female mice without DOX treatment. Scale: 1mm.
**(C)** Flow cytometry analysis of mammary resident NKT cells harvested from pre- and post-pregnancy CD1d KO CAGMYC female mice (DOX D5).

To further determine whether loss of CD1d expression underlies the malignant transformation of post-pregnancy CAGMYC MECs, we performed mammary transplantation assays of CAGMYC CD1d KO MECs into the fat-pad of syngeneic animals (CD1d WT female mice). We found that 100% of mammary tissue injected with pre-pregnancy CAGMYC CD1d KO MECs and 70% of mammary glands injected with post-pregnancy CAGMYC CD1d KO MECs developed signs of malignant lesions, supporting that the loss of CD1d expression impacts pregnancy-induced breast cancer protection (**Fig. 3-9 A - black font**, and **Fig. 3-9 B-C**). This last observation was in marked contrast to the finding in glands injected with post-pregnancy CAGMYC CD1d WT MECs which, as previously reported, did not present signs of malignant transformation (Feigman et al. 2020) (**Fig. 3-9 A, blue font and Fig. 3-9 D-E**).

Altogether, these results suggest that loss of CD1d, with concomitant loss of pregnancy-induced expansion of NKT cells, supports the development of mammary malignant lesions, independently of parity. Moreover, our study elucidates that parity blocks the malignant transformation of MECs, both by inducing cell-autonomous, epigenetic alterations within the MECs, and non-autonomous, communication between CD1d+ MECs cells and NKT cells in the mammary gland.

**Figure 3-9**

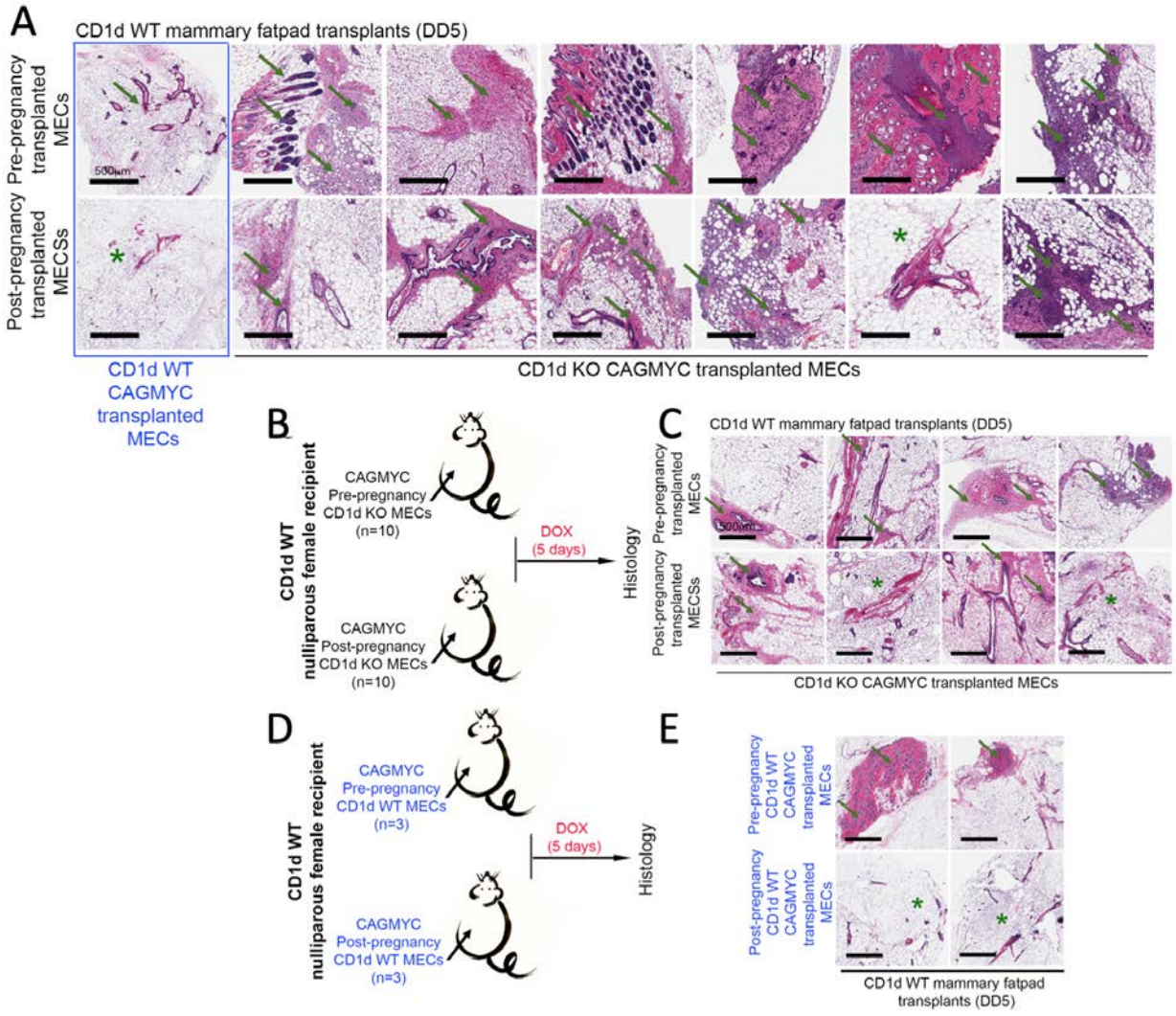
A
CD1d WT mammary fatpad transplants (DD5)
Pre-pregnancy transplanted MECs
Post-pregnancy transplanted MECSs
500μm
CD1d WT CAGMYC transplanted MECs
CD1d KO CAGMYC transplanted MECs
B
CD1d WT nulliparous female recipient
CAGMYC Pre-pregnancy CD1d KO MECs (n=10)
CAGMYC Post-pregnancy CD1d KO MECs (n=10)
DOX (5 days)
Histology
C
CD1d WT mammary fatpad transplants (DD5)
Pre-pregnancy transplanted MECs
Post-pregnancy transplanted MECSs
500μm
CD1d KO CAGMYC transplanted MECs
D
CD1d WT nulliparous female recipient
CAGMYC Pre-pregnancy CD1d WT MECs (n=3)
CAGMYC Post-pregnancy CD1d WT MECs (n=3)
DOX (5 days)
Histology
E
Pre-pregnancy CD1d WT CAGMYC transplanted MECs
Post-pregnancy CD1d WT CAGMYC transplanted MECs
CD1d WT mammary fatpad transplants (DD5)

***Figure 3-9 Loss of CD1d expression supports the malignant transformation and oncogenesis of post-pregnancy CAGMYC MECs.***

**(A)** H&E stained histological images of DOX-treated, CD1d WT mammary tissue transplanted with pre-pregnancy CD1d WT CAGMYC MECs (blue font, top far left panel), pre-pregnancy CD1d KO CAGMYC MECs (black font, top panel), post-pregnancy CD1d WT CAGMYC MECs (blue font, bottom far left panel), or post-pregnancy CD1d KO CAGMYC MECs (black font, bottom panel). Green arrows indicate signs of malignant lesions/mammary hyperplasia. Green asterisks indicate normal-like ductal structures. Scale: 500μm.
**(B)** Experimental approach showing the strategy for the transplantation of pre- and post-pregnancy CD1d KO CAGMYC MECs into the fatpad of nulliparous CD1d WT female mice, and tissue analysis.
**(C)** H&E stained histology images from mammary tissue from DOX-treated (DD5) CD1d WT nulliparous female mice transplanted with pre- and post-pregnancy CD1d KO CAGMYC MECs. Scale: 500μm.
**(D)** Experimental approach showing the strategy for the transplantation of pre- and post-pregnancy CD1d WT CAGMYC MECs into the fatpad of nulliparous CD1d WT female mice, and tissue analysis.
**(E)** H&E stained histology images from mammary tissue from DOX-treated (DD5) CD1d WT nulliparous female mice transplanted with pre- and post-pregnancy CD1d WT CAGMYC MECs. Scale: 500μm. Green arrows indicate signs of malignant lesions/mammary hyperplasia. Green asterisks indicate normal-like ductal structures.

# 4. Establishing an *in vitro* system to reprogram and assay pregnancy naïve MECs

## 4.1 Author contributions

I acknowledge the following people who assisted with this project. James Rail and Michael Ciccone performed the screen for CD1d inducing compounds *in vitro* in organoids. Charlie Chung provided an early protocol which was the basis for the organoid-immune cell co-culture imaging system, and helped with troubleshooting the analysis pipeline. Mackenzie Callaway provided critical feedback. Erika Wee from the CSHL Microscopy Shared Resource provided training and assisted during the setup of the imaging assays. Camila dos Santos oversaw the project, and participated in experimental design and data analyses.

## 4.2 Introduction

Given that our results indicate that pregnancy can induce an expansion of γδNKTs, and inhibit mammary oncogenesis in the presence of CD1d expression, we sought to understand ways in which we could extend the pregnancy protection to never pregnant conditions.

We hypothesized that inducing CD1d expression in MECs could eventually support the expansion of NKT cells. We also wanted to further understand the specific γδ chains that were more abundant in parous NKT cells. Our long term goal with this is to make engineered NKT cells that specifically express the γδTCRs that provide pregnancy protection, and to edit epithelial cells to express more CD1d in order to attract these NKT cells and enhance their oncoprotective effect.

We started developing *in vitro* assays in order to assess any changes in cytotoxicity of mammary resident immune cells after pregnancy. The reasoning behind this was twofold – we would be able to pinpoint immune cells involved in pregnancy protection against oncogenesis, and we would be able to use the assay as a platform to screen engineered NKT cells in the future.

## 4.3 Results

### 4.3.1 Pregnancy hormones are the most effective inducers of CD1d expression on MECs and may increase NKT abundance *in vivo*

We set up a low throughput screening assay to search for chemical compounds or culturing conditions that would increase the expression of CD1d at the surface of MECs. 3D organoid cultures derived from mammary tissue from never pregnant female mice were treated with a series of compounds previously described to induce CD1d expression in other model systems (**Table 4-1**) (Brutkiewicz 2006; Zhou et al. 2004; Jahng et al. 2004; Wu et al. 2003; Amprey et al. 2004; Maira et al. 2012; Li et al. 2010). Treated organoid cultures were then harvested and CD1d expression at the surface of MECs was quantified by flow cytometry. Based on the expression of CD1d via flow cytometry, pregnancy hormones appear to be the most efficient in inducing CD1d expression on the surface of MECs, once again linking pregnancy signals with induction of CD1d at the surface of MECs (**Fig. 4-1 A)**. Additionally, we determined that the timepoint for maximal CD1d induction by pregnancy hormones at the surface of MECs to be 48 hours of culturing in media with hormones (**Fig. 4-1 B)**.

In order to understand whether increased CD1d expression due to exposure of MECs to pregnancy hormones is sufficient to cause an increase in NKT cell abundance in mammary glands, we transplanted organoids treated with pregnancy hormones into the mammary glands of 8 week old wild-type Balb/C mice, in addition to untreated organoids, and a matrigel only control. 3 weeks post-transplant, we harvested mammary gland tissues and analyzed the abundance of NKT cells. This approach was chosen with the goal to allow organoid cultures grown with pregnancy hormones to involute from their exposure to pregnancy hormones, thus mimicking a mammary developmental program where NKTs became expanded.

***Table 4-1 CD1d inducing compounds used in the screen, related to Figure 4-1***

| | |
|---|---|
| Estrogen, Progesterone, Prolactin (EPP) | (Ciccone et al. 2020) |
| 18:0(2R-OH) SulfoGalCer (Sulfatide) | (Brutkiewicz 2006; Jahng et al. 2004) |
| 18:0(2S-OH) SulfoGalCer (PC) | |
| Dactolisib (BEZ-235) | (Shissler and Webb 2019; Maira et al. 2012) |
| Buparlisib (BKM-120) | |
| 7DW8-5 | (Li et al. 2010) |
| C17:0 Globotriaosylceramide (GB3) | (Brutkiewicz 2006) |
| Ganglioside GD3 (Bovine Milk) | |
| Ganglioside GM3 (Bovine Milk) | |
| 15:0 Lyso PG-d5 (15:0 LPG) | (Amprey et al. 2004) |
| 17:0 Lyso PG-d5 (17:0 LPG) | |
| 19:0 Lyso PG-d5 (19:0 LPG) | |

**Figure 4-1**

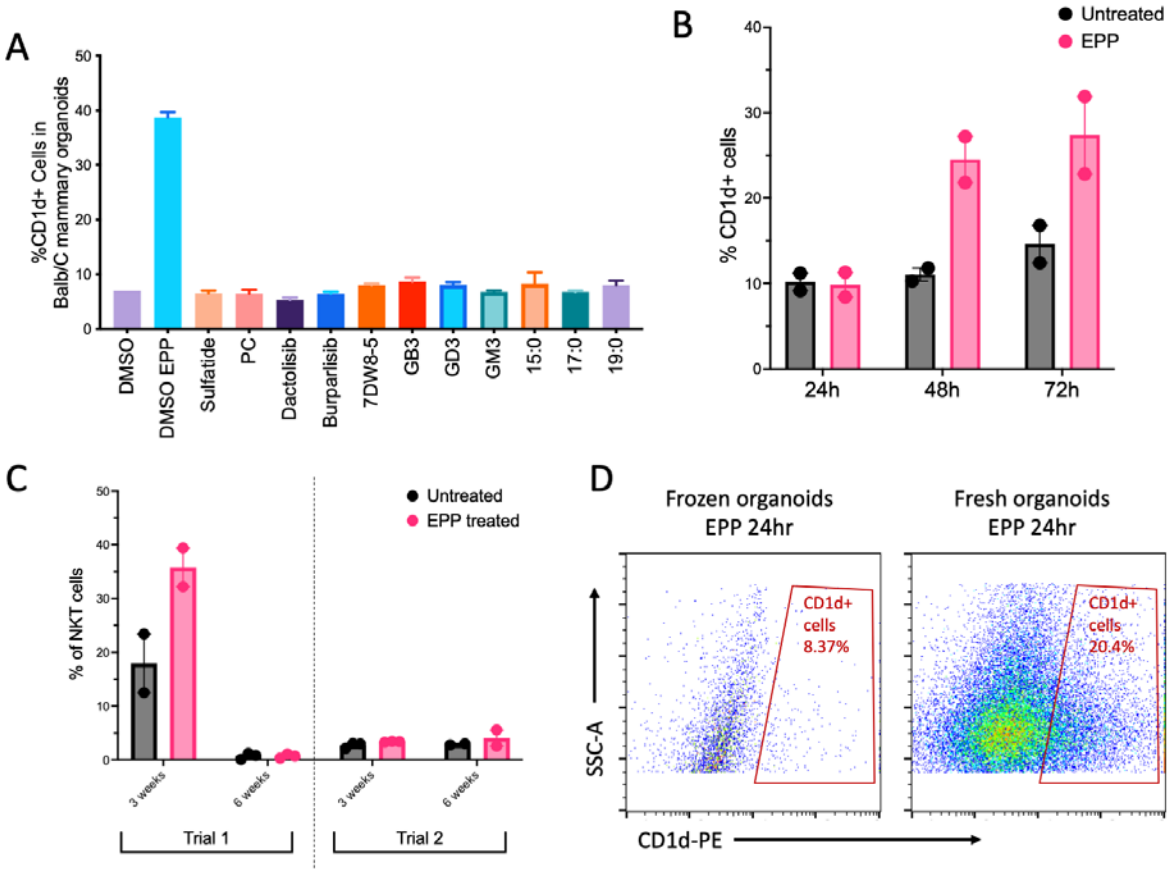


***Figure 4-1 Pregnancy hormones induce an increased CD1d expression on the surface of MECs in mammary organoid cultures derived from healthy Balb/C mice.***

**(A)** Flow cytometry quantification of CD1d expression on the surface of mammary organoids cultured with CD1d-inducing treatments.
**(B)** Flow cytometry quantification of CD1d expression on the surface of control untreated mammary organoids (black) and those cultured with pregnancy hormones (EPP – pink) at 24hr, 48hr, and 72hr of treatment.
**(C)** Flow cytometry quantification of NKT cells from mammary glands of mice transplanted with cultured, untreated organoids (black) or organoids treated with pregnancy hormones (EPP – pink). Two independent trials of the experiment are shown.
**(D)** Flow cytometry quantification of CD1d at the surface of MECs from frozen organoids from healthy Balb/C mice (left), or freshly obtained organoids from age-matched healthy Balb/C mice (right).

Our preliminary results confirmed that exposure of organoids to pregnancy hormones induces an expansion in the NKT cell population in the transplanted mammary glands at 3 weeks after transplanting. But this expansion disappears by 6 weeks post-transplant (**Fig. 4-1 C, left**) – indicating that serial infusions of treated cells might be necessary to keep the NKT cells around in the transplanted glands. Interestingly, when we attempted to repeat this experiment, we were unable to recapitulate the same results (**Fig. 4-1 C, right**).

It has been shown that freeze-thaw cycles of mammary tumor tissue can affect the overall epithelial cell profiles (Le Gallo et al. 2018). We used frozen organoids in our second experiment but fresh isolated organoids the first time. We hypothesized that this could be affecting how the cells react to pregnancy hormone treatment. We tested this hypothesis by treating freshly obtained organoids and frozen organoids from healthy Balb/c mice with pregnancy hormones and measuring CD1d expression via flow cytometry. And indeed, the overall viability and health of cells from frozen organoids was much lower and the freshly isolated organoids seemed to express CD1d more robustly after exposure to pregnancy hormones (**Fig. 4-1 D**).

### 4.3.2 Post-pregnancy immune cells exhibit an enhanced ability to induce cell death in Brca1 KO tumor organoids

To determine whether pregnancy enhances the overall cytotoxic abilities of mammary resident immune cells, we isolated pre- and post-pregnancy NKT cells (CD3+ NK1.1+) from mammary glands by magnetic bead aided separation (MACS). We placed these in 2D culture with Brca1 KO tumor cells (primary tumor cells from our mouse model described previously), and assayed Caspase 3/7 activity by flow cytometry using the Magic Red Caspase 3/7 Assay kit (Abcam) after 24 hours of co-culture. However, we did not notice any differences in the Caspase activity caused by pre- and post-pregnancy NKT cells in this system (**Fig. 4-2 A**). Interestingly, we noted that most of the NKT cells seemed to be dying while being processed for flow cytometry, as the co-culture needed to be dissociated into single cells by enzymatic digestion (**Fig. 4-2 B**). Moreover, 2D culture does not truly recapitulate how immune cells would interact

with MECs *in vivo*. Finally, NKT cells might need other immune cells and/or CD1d expression, or other environmental cues that we cannot reproduce in 2D culture.

**Figure 4-2**

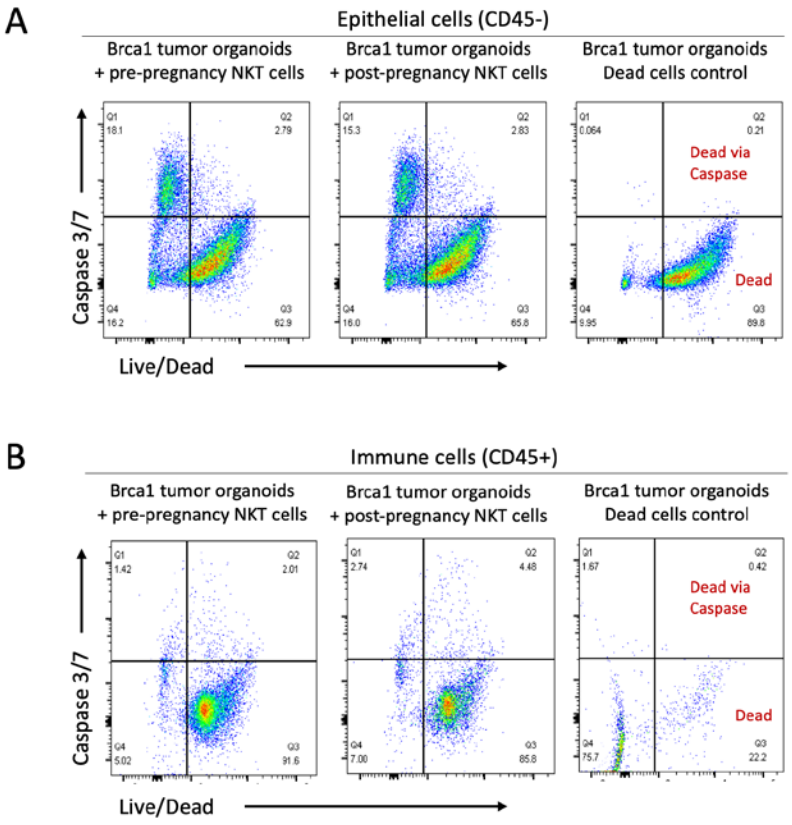


***Figure 4-2 2D co-culture of primary tumor organoids with primary NKT cells is not an informative system to assess changes in NKT cytotoxicity***

Flow cytometry analysis of Caspase 3/7 mediated killing of 2D cultured Brca1 tumor organoids by NKT cells isolated from pre- or post-pregnancy wild-type mice (n=2 per condition) showing NKT mediated killing represented in gate Q2.
**(A)** epithelial cells from the co-culture (CD45-)
**(B)** NKT cells from the co-culture (CD45+).

Based on these observations, we determined that a 3D co-culture system in Matrigel medium that we use to culture mammary organoids would be a better system. For this assay, tumor cells and immune cells were labeled with different fluorescent dyes (non-specific binding) and then plated together in a glass-bottom imaging plate with a Caspase 3/7 substrate in the culture media. Sequential images were captured to track the progression of colocalization of immune cells with tumor cells and killing on a spinning-disk confocal microscope (**Fig. 4-3 A**). This is a more direct readout of the killing ability and motility of immune cells than measuring Caspase 3/7 activity by flow cytometry, where there is no direct visualization of the interaction between the epithelial and immune cells.

An increase in colocalization of immune cells (green) with tumor cells (red) can be observed in the case of post-pregnancy immune cells at the peak of cell death (**Fig. 4-3 B**). Quantifying the relative colocalization of red fluorescence (tumor cells) with blue fluorescence (Caspase activity – i.e. cell death), shows that post-pregnancy immune cells elicit an increased rate of cell death in the tumor organoids (**Fig. 4-3 C**).

Though preliminary observations, our results from this section have the potential to be used as a therapeutic avenue to increase immune surveillance and curb oncogenesis in pregnancy naïve mammary glands. Once optimized to be reproducible, we can use our transgenic models of mammary oncogenesis to understand the protective potential of MECs treated with pregnancy hormones. We can also investigate whether combining treated MECs with immune cells from post-pregnancy mammary glands would be an effective intervention to arrest and/or cause regression in tumor growth.

**Figure 4-3**

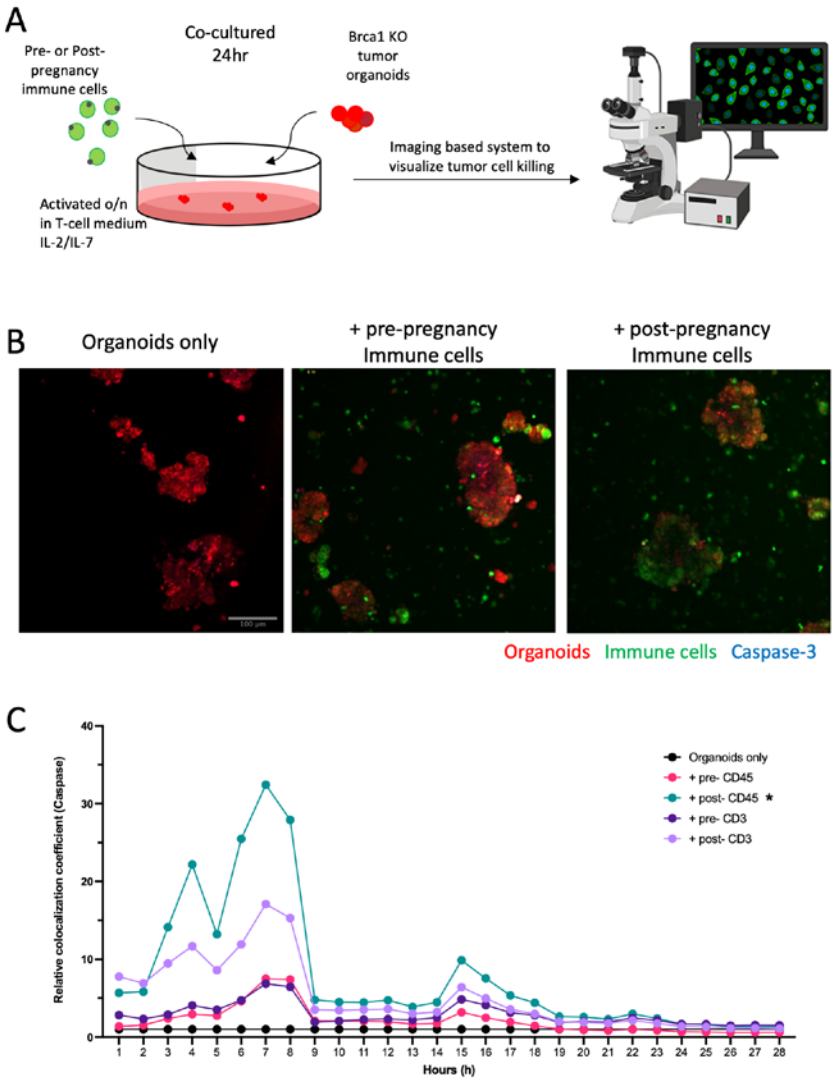


***Figure 4-3 3D co-culture of primary tumor organoids with primary immune cells shows increased cell death caused by post-pregnancy immune cells***

**(A)** Schematic of the 3D co-culture live imaging setup. Fluorescently labeled *Brca1* KO tumor organoids (red) and mammary resident immune cells (green) are mixed in an imaging medium containing a Caspase 3/7 substrate (blue) and serially imaged over 28 hours.
**(B)** Representative images demonstrating increased colocalization of post-pregnancy immune cells with *Brca1* KO tumor organoids at 6hr of co-culture. Scale: 100µm.
**(C)** Relative colocalization (normalized to organoids only) of Red/Blue for Caspase activity. Post-pregnancy immune cells cause an increased rate of cell death.

## 5. Conclusions and Perspectives

Our findings suggest that post-pregnancy mammary homeostasis does not rely on the presence of γδNKT cells, given the largely normal histology and cellular content of mammary tissue in mice deficient for this cell type. It is possible that NKT cells expand in response to the re-setting of whole-body immunity post-partum, with the child-bearing event providing signals that alter antigens across all maternal tissues as well as expanding specific immune cell populations. γδNKT cells have been found in the pregnant uterus across many mammalian species, linking NKT specialization and the pregnancy cycle (Mincheva-Nilsson 2003). Our results support that the expansion of NKT cells was predominantly observed in post-lactating, post-involution tissue, thus suggesting that the immune reprogramming of mammary tissue takes place after giving birth. In addition to the NKT cell population expansion, parity also promotes a modification of the TCR repertoire in NKT cells. γδT-cells reside within the normal breast, and their presence has been associated with a better prognosis during triple-negative breast cancer development (Wu et al. 2019b). Here we report that pregnancy-induced changes in TCR expression was specific to NKT cells, given that we did not find pregnancy-induced TCR rearrangements in CD8+NK1.1- immune cells, pointing to the specific engagement of NKT-lineages during pregnancy-induced mammary development.

Several other immune subtypes have been described to be enriched in mammary tissue during gestation, lactation and involution stages of mammary gland development. These studies identified alterations in leukocyte interaction with mammary ductal structures, as well to specific transcriptional changes, suggesting that cell interaction and cellular identity of mammary resident cells are affected by pregnancy-induced development (Dawson et al. 2020; Hitchcock et al. 2020). Our analysis of leukocytes, specifically macrophages and neutrophils, did not show alterations in cell abundance either in from healthy parous murine mammary tissue or in post-pregnant CAGMYC mammary tissue lacking malignant lesions. Moreover, we found that CD1d expression on the surface of total CD45+ mammary resident immune cells were not altered by parity, thus supporting a role for post-pregnancy CD1d+ MECs in regulating CD1d-dependent NKT cells. However, given that leukocytes have been implicated in the activation of NKT cells

(Macho-Fernandez and Brigl 2015; Rizvi et al. 2015), it is possible that molecular alterations, rather than changes to cellular abundance or antigen presentation, could play a role in inducing or sustaining the population of NKT cells in post-pregnancy mammary tissue.

Our studies also provide evidence linking pregnancy-induced immune changes with the inhibition of mammary oncogenesis. Our previous research focused on how post-pregnancy MECs assume a senescence-like state in response to cMyc overexpression, an oncogene-induced response that activates the immune system via the expression of senescence-associated genes (Braig and Schmitt 2006). Here, we found that CD1d expression at the surface of post-pregnancy MECs, and the presence of γδNKT cells were linked with the inhibition of mammary oncogenesis in two independent models of breast cancer, illustrating how epithelial and immune cells communicate to support pregnancy-induced mammary cancer prevention. Given that NKT cells were previously shown to interact with senescent cells, it is possible that pregnancy-induced activation of CD1d expression and NKT cell expansion represent additional responses to oncogene-induced cellular senescence (Kale et al. 2020).

Women completing a full-term pregnancy before the age of 25 have a substantially reduced breast cancer risk, by approximately one-third (Medina 2009). This benefit applies to the risk of all breast cancer subtypes, including those from women harboring *BRCA1* mutations (Terry et al. 2018). Thus, our findings supporting a role for pregnancy in inhibiting the development of Brca1 KO mammary tumors lends a clinical relevance to our studies. Interestingly, the mammary tumor from parous Brca1 KO female mouse was associated with low abundance of γδNKT cells and CD1d+ MECs, suggesting that loss of the pregnancy-induced epithelial to immune microenvironment communication may support mammary tumorigenesis. In agreement, the genetically engineered loss of CD1d expression, with a consequent deficiency in activated NKTs, supported the malignant progression of cMyc overexpressing MECs, further illustrating a link between epithelial and immune cells in supporting pregnancy-induced mammary cancer prevention.

Finally, our studies are the first to attempt to induce pregnancy-associated changes to MECs with the long term goal to use them in a therapeutic setting to improve immune surveillance in pregnancy naïve mammary glands. This, in combination with our live imaging experimental setup, can be further exploited to study epithelial-immune interactions *in vitro* to understand the roles of individual types of immune cells in the mammary microenvironment. Understanding the causal factors of pregnancy-associated oncoprotection will enable us to translate this into future therapies against breast malignancies.

Our findings are based on studies performed in mice that became pregnant at a young age (~8 weeks old), which reinforced pregnancy-induced changes to epithelial cells, and their effect on immune recruitment and oncogenesis inhibition. However, it remains unclear why such strong, pregnancy-induced changes do not fully prevent the development of breast cancer (Nichols et al. 2019). It has been suggested that specific mammary epithelial clones with oncogenic properties reside within the mammary tissue after pregnancy, and may give rise to late-onset mammary oncogenesis in aged mice (Li et al. 2020b). It is possible that such populations of rare MECs lose some of their pregnancy-induced molecular signatures over time, thereby bypassing oncogene-induced senescence and immune recognition, and ultimately developing into mammary tumors. Moreover, given that pregnancy-induced breast cancer protection becomes apparent ~5-8-years after pregnancy, it is possible that additional immune reprogramming induced by genetic makeup, age at pregnancy, and/or overall post-partum health, may further modify breast tissue and erase pregnancy-induced changes that inhibit breast cancer development.

Nonetheless, the connection between pregnancy, immunity, and oncogenesis could be used to develop therapies to block cancer development. Strategies could be developed to induce NKT expansion in the absence of a true pregnancy. Indeed, a series of preclinical models have been developed to optimize the delivery of CD1d stimulatory factors, such as αGalcer and KRN7000, and induce expansion of NKT cells (Zhang et al. 2019). Such strategies are mostly side-effect free, and could be used in cases of high cancer risk, including in the event of genetic alterations that affect BRCA1 function and/or family history of breast cancer. Additionally, the characterization of specific, pregnancy-induced TCR rearrangements could be leveraged in CAR-NKT immunotherapy, for example, which could also efficiently target disease that has

already developed. Collectively, such strategies could improve breast health, nursing experience, and decrease cancer risk in women who experience their first pregnancy after 35 years of age, when they are at greater risk of requiring medical intervention to improve milk production, breastfeeding assistance, and to develop breast cancer.

### 5.1 Highlights

Parity influences mammary cancer progression. We demonstrate how pregnancy induced changes modulate the communication between MECs and immune cells and establish a causal link between pregnancy, the immune microenvironment, and mammary oncogenesis in models of cMYC overexpression and Brca1 loss of function.

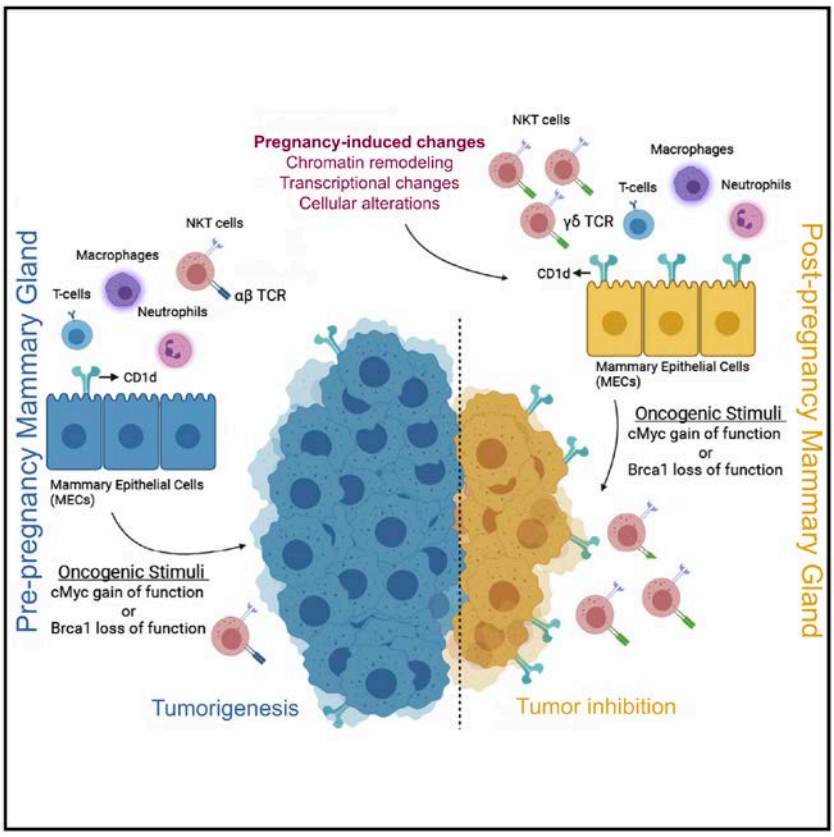


- Post-pregnancy MECs express higher levels of the antigen-presenting molecule CD1d
- γδTCR-expressing NKT cells are expanded in post-pregnancy mammary glands
- NKTs and CD1d expression associate with oncogenesis inhibition after pregnancy
- Loss of γδNKTs and CD1d expression supports mammary oncogenesis after pregnancy

## 5.2 Future directions

The work presented in this thesis paves the way for a number of follow up studies focused on understanding the role of pregnancy in the expansion γδ NKT cells in the mammary gland, and to further characterize the NKT cells.

*Identification of specific TCR rearrangements in pregnancy-induced mammary resident NKT cells*

NKT cells are known to assume multiple roles in maintaining tissue homeostasis, pathogen clearance, and cancer by recognizing self- and foreign-antigens using T-cell receptors (TCRs). We have shown that the TCRs expressed on post-pregnancy mammary NKT cells are different from those on pre-pregnancy NKT cells. Identifying the specific TCRs that are differentially expressed in post-pregnancy NKT cells may help us understand and replicate pregnancy associated oncoprotection.

In order to determine the specific changes to the TCR repertoire of mammary NKT cells, single cell TCR-sequencing by 5'-RACE may be employed. A caveat is that the existing single cell TCR sequencing reagents provided by 10X Genomics do not include γδ TCRs, but other groups have designed and validated primers for sequencing γδ TCRs with the 10X reagents, and this method can be used (Daniels et al. 2020).

*TCR replacement in NKT cells to assess changes in cytotoxicity*

The TCRs identified to be upregulated in post-pregnancy will then be overexpressed in NKT cells using a CRISPR-mediated TCR replacement strategy (Legut et al. 2018). With the help of CRISPR/Cas9, the endogenous TCRs from the recipient cells will be knocked out, and simultaneously the identified receptors will be transduced. Knocking out endogenous receptors ensures that mixed dimers of TCRs are not formed and the effects observed are solely due to the newly introduced TCRs. The TCR replacement strategy involves the use of two separate lentiviral transductions – one that encodes the chosen TCR transgenes (the desired γδ variable region sequences) in a pELNS transfer vector, and the other

CRISPR/Cas9 targeting the endogenous TCR-β constant region using a pLentiCRISPR v2 plasmid containing a puromycin-resistance marker gene. NKT cells will be isolated by magnetic enrichment for CD3+ and NK1.1+ cells, cultured overnight, and transduced with lentiviral particles in the presence of 5μg/ml polybrene. Cells that take up the virus will be selected by incubation with puromycin. The next step would be to test whether TCR replacement in pregnancy naïve NKT cells can increase the activation of cytotoxic CD8+ T cells as an effect of the secreted cytokines, or if the cytotoxic capabilities of the NKT cells themselves increases. These studies will be performed using *in vitro* killing assays in the 3D culture conditions described in section 4.3.2.

*Devise ways to upregulate CD1d in vivo to extend pregnancy protection in a never-pregnant setting*

NKT cells are classically activated by antigens presented by CD1d on the cell surface (Gapin et al. 2013; Rizvi et al. 2015). We find that CD1d expression on the surface of epithelial cells is elevated after pregnancy in healthy and in Brca1 KO mice. But the CD1d expression in Brca1 KO mice seems to be related to mammary tumorigenesis, as we observed more CD1d expression in non-tumor bearing mice. Moreover, approximately 70% of total NKTs from healthy, post-pregnancy Brca1 KO mammary tissue expressed γδTCR, in marked contrast to NKTs from healthy (2.7%) and tumor mammary tissue (8.6%) from nulliparous Brca1 KO mice (**Fig. 3-6**).

Our results show that there is a transient increase in the NKT cell population in mammary glands of mice transplanted with pregnancy hormone treated organoids. The next step would be to understand whether serial infusions of treated cells is required to sustain the expansion, and to determine the ideal route of delivery of these cells, since serial surgeries would not be ideal. We can use intraductal injections, where cells are injected into the nipples, as a local and minimally invasive delivery method.

Next, to confirm the necessity of CD1d expression on the surface of MECs, organoid cultures will be derived from CD1d KO mice, treated with pregnancy hormones, and transplanted into CD1d WT mice

to see if they can induce NKT expansion (Faunce et al. 2005; Macho-Fernandez and Brigl 2015; Mantell et al. 2011).

Taking it a step further, we would ask the question of whether ex-vivo treated organoids can bring in NKTs to mammary glands in our breast cancer mouse models and if they provide protection against oncogenesis. To do this, we would harvest one of the mammary glands from Brca1 KO mice, derive organoid cultures, treat with pregnancy hormones, and transplant them back into the same mouse and monitor to see whether this would provide protection against tumorigenesis. Alternatively, normal organoids treated with pregnancy hormones could be transplanted into Brca1 KO females and monitored for tumor growth over time.

# 6. Experimental Procedures

## 6.1 Data and Code Availability

scRNA-seq, RNA-seq, ATAC-seq datasets were deposited into BioProject database under number PRJNA708263 [https://www.ncbi.nlm.nih.gov/bioproject/PRJNA708263].

Results shown in Fig. 2-2 (pre-pregnancy scRNA-seq) were deposited into BioProject database number PRJNA677888 [https://www.ncbi.nlm.nih.gov/bioproject/?term=PRJNA677888].

Results shown in Fig. 2-3 C (pre- and post-pregnancy RNA-seq), and Fig. 2-9 C (pre- and post-pregnancy H3K27ac ChIP-seq) were deposited in the BioProject database under numbers PRJNA192515 [https://www.ncbi.nlm.nih.gov/bioproject/?term=PRJNA192515] and PRJNA544746 [https://www.ncbi.nlm.nih.gov/bioproject/PRJNA544746].

Results shown in Fig. 2-10 F (H3K27ac Cut&Run of organoid cultures) were deposited in the BioProject database under number PRJNA656955 [https://www.ncbi.nlm.nih.gov/sra/?term=PRJNA656955].

This thesis does not report original code.

## 6.2 Experimental Model and Subject Details

*Animal Studies*

All experiments were performed in agreement with approved CSHL Institutional Animal Care and Use Committee (IACUC). All animals were housed at a 12 hour light/12 hour dark cycle, with a controlled temperature of 72°F and 40-60% of humidity. Balb/C female mice were purchased from The Jackson Laboratory and Charles River. RAG1 KO mice (B6.129S7-Rag1$^{tm1Mom}$/J, IMSR Cat# JAX:002216, RRID:IMSR_JAX:002216) were purchased from The Jackson Laboratory. VavCre UTX KO were generated as previously described (Beyaz et al., 2017). CXCR6-KO-EGFP-KI mice (B6.129P2-Cxcr6$^{tm1Litt}$/J, IMSR Cat# JAX:005693, RRID:IMSR_JAX:005693) were purchased from The Jackson

Laboratory. CAGMYC transgenic mouse strain was generated as previously described (Feigman et al. 2020). CD1d KO CAGMYC transgenic mouse stain was generated by crossing CD1d KO (C.129S2-Cd1$^{tm1Gru}$/J, IMSR Cat# JAX:003814, RRID:IMSR_JAX:003814) mice with CAGMYC mice. Krt5$^{CRE-ERT2}$Brca1$^{fl/fl}$p53$^{het}$ (Brca1 KO) transgenic mouse strain was generated by crossing Blg$^{CRE}$Brca1$^{fl/fl}$p53$^{het}$ transgenic mouse strain (Trp53$^{tm1Brd}$Brca1$^{tmAash}$Tg(B-cre)74Acl/J, IMSR Cat# JAX:012620, RRID:IMSR_JAX:012620) with Krt5$^{CRE-ERT2}$ transgenic mouse strain (B6N.129S6(Cg)-Krt5$^{tm1.1(cre/ERT2)Blh}$/J, IMSR Cat# JAX:029155, RRID:IMSR_JAX:029155).

### 6.3 Method Details

*Antibodies*

All antibodies were purchased from companies as indicated below and used without further purification. Antibodies for lineage depletion: biotinylated anti-CD45 (Thermo Fisher Scientific Cat# 13-0451-85, RRID:AB_466447), biotinylated anti-CD31 (Thermo Fisher Scientific Cat# 13-0311-85, RRID:AB_466421), biotinylated anti-Ter119 (Thermo Fisher Scientific Cat# 13-5921-85, RRID:AB_466798) and biotinylated anti-CD34 (Thermo Fisher Scientific Cat# 13-0341-82, RRID:AB_466425). Antibodies for cell surface flow cytometry: eFluor 450 conjugated anti-CD24 (Thermo Fisher Scientific Cat# 48-0242-82, RRID:AB_1311169), PE-Cy7 conjugated anti-CD29 (BioLegend Cat# 102222, RRID:AB_528790), 7-AAD viability staining solution (BioLegend Cat# 420404, RRID:SCR_020993), PerCP-Cy5.5 conjugated anti-CD1d (BioLegend Cat# 123514, RRID:AB_2073523), PE conjugated anti-CD1d (BioLegend Cat# 140805, RRID:AB_10643277), APC conjugated anti-CD45 (BioLegend Cat# 103112, RRID:AB_312977), FITC conjugated anti-CD3 (BioLegend Cat# 100204, RRID:AB_312661), Alexa Fluor 700 conjugated. anti-NK1.1 (BioLegend Cat# 108730, RRID:AB_2291262), APC/Cy7 conjugated anti-CD8 (BioLegend Cat# 100714, RRID:AB_312753), PE conjugated anti-TCR γ/δ (BioLegend Cat# 118108, RRID:AB_313832), APC conjugated anti-TCR β (BioLegend Cat# 109212, RRID:AB_313435), APC conjugated anti-H-2Kb (BioLegend Cat# 116517,

RRID:AB_10568693), Pacific Blue conjugated anti-I-Ab (BioLegend Cat# 116421, RRID:AB_10613291), Brilliant Violet 421 conjugated anti-CD206 (BioLegend Cat# 141717, RRID:AB_2562232), Alexa Fluor 700 conjugated anti-Ly6G (BioLegend Cat# 127621, RRID:AB_10640452). Antibodies for intracellular flow cytometry: PE conjugated anti-IFNγ (BioLegend Cat# 505808, RRID:AB_315402), Pacific Blue conjugated anti-T-bet (BioLegend Cat# 644807, RRID:AB_1595586). Antibodies for negative controls: eFluor 450 conjugated mouse IgG (Thermo Fisher Scientific Cat# 48-4015-82, RRID:AB_2574060), FITC conjugated rat IgG (Thermo Fisher Scientific Cat# 11-4811-85, RRID:AB_465229), and PE-Cy7 conjugated mouse IgG (BioLegend Cat# 405315, RRID:AB_10662421). Antibody for MaSC enrichment: biotinylated anti-CD1d (BioLegend Cat# 123505, RRID:AB_1236543). Antibodies for Western Blot: anti-p300 antibody (Santa Cruz Biotechnology Cat# SC-585, RRID:AB_2231120), anti-Vinculin antibody (Abcam Cat# ab129002, RRID:AB_11144129), anti-p53 antibody (Leica Biosystems Cat# P53-CM5P, RRID:AB_2744683), goat anti-rabbit IgG HRP (Abcam Cat# ab6721, RRID:AB_955447) and goat anti-mouse IgG HRP (Abcam Cat# ab97051, RRID:AB_10679369). Antibodies for Immunohistochemistry (IHC) staining: anti-Cytokeratin 5 (KRT5) (BioLegend Cat# 905501, RRID:AB_2565050), anti-Cytokeratin 7/17 (KRT7/17) (Santa Cruz Biotechnology Cat# sc-8421, RRID:AB_627856), anti-EGFR (Santa Cruz Biotechnology Cat# sc-373746, RRID:AB_10920395), anti-AR (Santa Cruz Biotechnology Cat# sc-7305, RRID:AB_626671), and anti-Ki67 (Spring Bioscience Cat# M3062, RRID:AB_11219741). Antibodies for Immunofluorescence (IF) staining: Alexa Fluor 647 conjugated anti-Cytokeratin 5 (KRT5) (Abcam Cat# AB193895, RRID:AB_2728796), unconjugated rabbit anti-BRCA1 (Bioss Cat# bs-0803R, RRID:AB_10858843), Alexa Fluor 568 conjugated goat anti-rabbit IgG (Thermo Fisher Scientific Cat# A-11036, RRID:AB_10563566), Alexa Fluor 488 conjugated anti-GFP (BioLegend Cat# 338007, RRID:AB_2563287), Alexa Fluor 405 conjugated anti-Cytokeratin 8 (KRT8) (Abcam Cat# ab210139, RRID:AB_2890924).

*Mammary gland isolation*

Female mice classified as Pre-pregnancy (nulliparous, never pregnant), Post-pregnancy (parous, 1 gestation cycle, 21 days of lactation and 40 days of involution post offspring weaning), were housed together for 1-2 weeks to allow for estrous cycle synchronization prior to mammary gland isolation. For the experiments utilizing exposure to pregnancy hormones (EPH), never pregnant female mice (~8 weeks old) were implanted with 21 days-slow-release estrogen and progesterone pellets (17β-Estradiol (0.5 mg/pellet) + Progesterone (10 mg/pellet) – Innovative Research of America Cat# HH-112) prior to mammary gland isolation (at D12 post pellet implantation). Females classified as involution D15 had 1 gestation cycle, 21 days of lactation and 15 days of involution post offspring weaning. In all cases, mammary gland isolation was performed as previously described (dos Santos et al. 2013). In short, mammary glands (one to four pairs per mouse) were harvested, minced, and incubated for 2 hours with 1x Collagenase/Hyaluronidase (10x solution, Stem Cell Technology Cat# 07912) in RPMI 1640 GlutaMAX supplemented with 5% FBS. Digested mammary gland fragments were washed with cold HBSS (Thermo Fisher Scientific Cat# 14175103) supplemented with 5% FBS, followed by incubation with TrypLE Express (Thermo Fisher Scientific Cat# 12604-013) and an additional HBSS wash. Cells were incubated with 2 mL of Dispase (Stem Cell Technology Cat# 07913) supplemented with 40 µL DNAse I (Sigma Cat# D4263) for 2 minutes and then filtered through a 100µm Cell Strainer (BD Falcon Cat# c352360). The single cell suspension was incubated with lineage depletion antibodies and loaded onto a MACS magnetic column (Miltenyi Biotec Cat# 130-042-401). Lineage negative, flow-through cells (epithelial cells) were utilized for flow cytometry, and transcriptomic analysis. Lineage positive cells (immune cells) were eluted from column with 3ml of MACS buffer and utilized for flow cytometry, transcriptomic and epigenomic analysis. For cell analysis, Dual Fortessa II cell analyzer (BD Biosciences) was used. Data analysis was performed using BD FACSDiva Software (RRID:SCR_001456) or FlowJo (FlowJo, RRID:SCR_008520). Statistically significant differences were considered with Student's t-test *p*-value lower than 0.05 ($p<0.05$).

*Flow cytometry gating analysis*

Mammary resident cells (epithelial and non-epithelial) were harvested from both top and bottom mammary glands, and analyzed according to the bellow indicated strategy. For all flow cytometry analysis an average of 300,000 cells live cells (7-AAD negative) were recorded.

a) General innate immune cells analysis strategy:

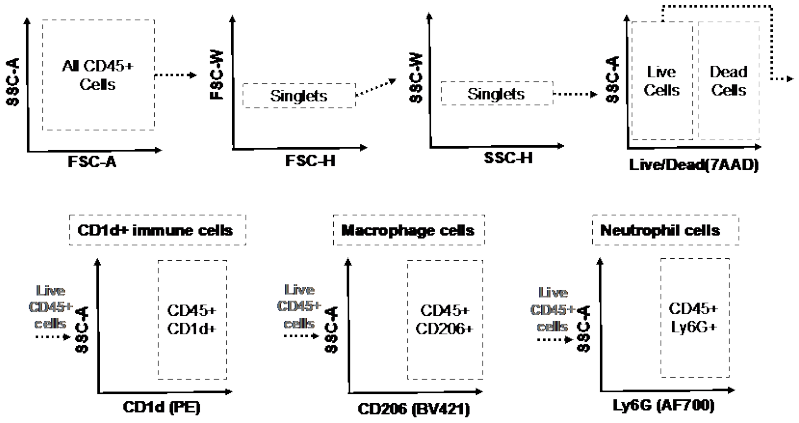


b) General adaptive immune cells analysis strategy:

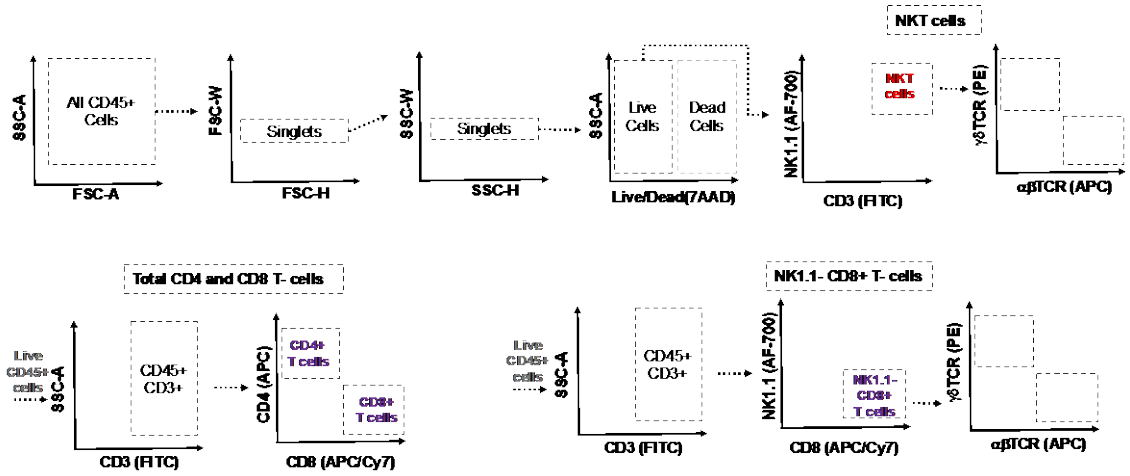

c) NKT intracellular analysis strategy:

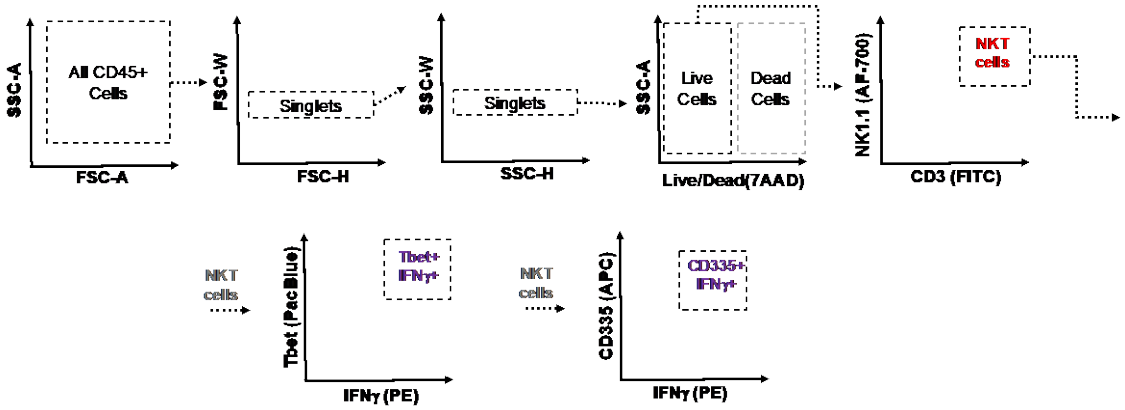


d) CD1d+ MECs analysis strategy:

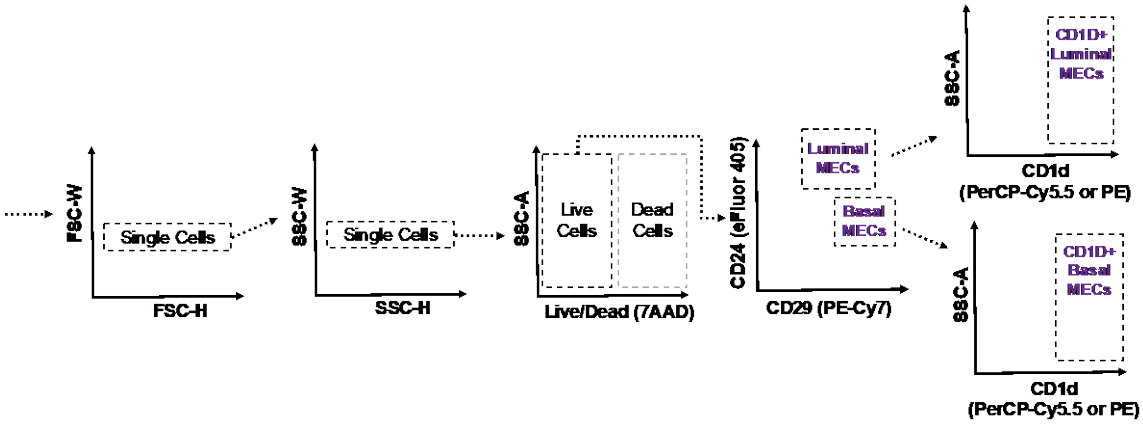


e) MHC-I and MHC-II MECs analysis strategy:

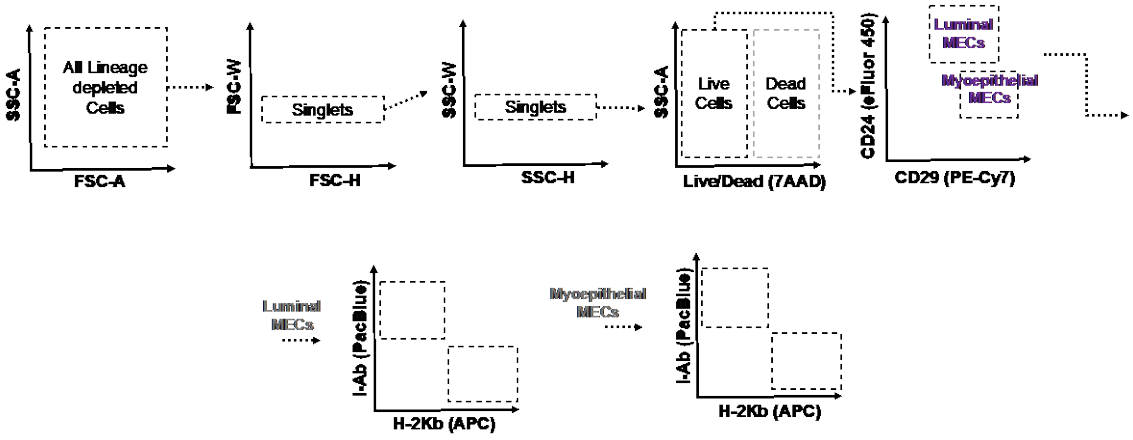

f) Magic Red Caspase 3/7 activity analysis strategy:

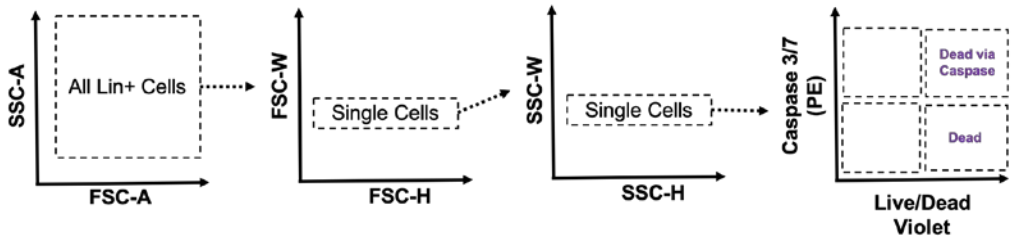


*Mammary Organoid Culture*

Mammary tissue dissected was minced and digested for ~40 minutes in Collagenase A, type IV solution (Sigma, Cat Cat# C5138-1G), following a series of centrifugations to enrich for mammary organoids. Freshly isolated mammary organoids were cultured with Essential medium (Advanced DMEM/F12, supplemented with ITS (Insulin/Transferrin/Sodium selenite, Gibco Cat# 41400-045, and FGF-2 (PeproTech, Cat# 450-33)) prior to analysis. For experiments shown in Fig. 2-10, organoid cultures were derived from normal mammary tissue from pre- or post-pregnancy Balb/C female mice (RRID:IMSR_CRL:028), cultured in the presence of FGF-2 for 6 days, following FGF-2 withdrawal for 24 hrs and then incubated with Complete medium (AdDF+++, supplemented with ITS (Final Concentration:1x, Insulin/Transferrin/Sodium Selenite, Gibco Cat# 41400-045), 17-β-Estradiol (Final concentration: 40ng/mL, Sigma Cat# E2758), Progesterone (Final concentration: 120ng/mL, Sigma Cat# P8783), Prolactin (Final concentration: 120ng/mL ,Sigma Cat# L4021), as previously described (Ciccone et al. 2020). For experiments shown in Fig. 3-2, organoid cultures were derived from pre- or post-pregnancy CAGMYC MECs, following treatment with doxycycline (DOX, 0.1mg/mL, Clontech Cat# 631311) for 2 days (DD2). For experiments shown in Fig. 3-8, organoid cultures were derived from NOD/SCID female mice, transplanted with either pre- or post-pregnancy CAGMYC MECs, following treatment with doxycycline (DOX, 0.1mg/mL) for 2 days (DD2). For experiments shown in Fig. 4-1, organoid cultures were derived from pre-pregnancy Balb/C female mice and incubated with CD1d inducing compounds described in Table 4-1 for 24 hours and then assayed by flow cytometry for CD1d expression. For

experiments shown in Fig. 4-2 and Fig. 4-3, organoid cultures were derived from a mammary gland tumor from a Tamoxifen treated Brca1 KO mouse.

*RT-qPCR*

Lineage depleted MECs or organoid cultures were washed with 0.5mL 1x PBS, following RNA extraction with Trizol (0.5mL, Thermo Fisher Scientific, Cat# 15596018). Reverse transcription was carried out using SuperScript III ™ kit (Thermo Fisher Scientific, Cat# 18080-051). RT-qPCR was performed using a Quantstudio 6 with SYBR Green Master mix (Applied Biosystems, Cat# 4368577). Relative mRNA expression of target gene was calculated via the ΔΔCt method and normalized to *β-actin* mRNA levels.

Cd1d qPCR primers: FWD: 5' TCC GGT GAC TCT TCC TTA CA 3' and REV: 5' CTG GCT GCT CTT CAC TTC TT 3'.

β-actin qPCR primers: FWD: 5' TGT TAC CAA CTG GGA CGA CA 3' and, REV: 5' GGG GTG TTG AAG GTC TCA AA 3'.

*Mammary fat pad transplantation*

MaSCs-enrichment was performed as previously described (dos Santos et al., 2013). In short, lineage depleted MECs were incubated with biotinylated anti-CD1d antibody, to allow for MaSC enrichment. CD1d-enriched MEC fractions were resuspended with 50% growth factor reduced matrigel solution (Corning, Cat# 356230) and injected into the cleared fat-pad of the inguinal mammary gland (anterior part of the gland). For experiments presented on Fig. 3-2 CD1d-enriched MECs fractions (~100K) were injected into the mammary fatpad of 12 weeks old CAG-only female mice, followed by DOX-treatment and histology analysis. For experiments presented on Fig. 3-6 CD1d-enriched MECs fractions (~100K) were injected into the mammary fatpad of 12 weeks old NOD/SCID (RRID:IMSR_JAX:001303) female mice, followed by DOX-treatment and histology analysis. For experiments presented on Fig. 3-7 and Fig. 3-8, pre- or post-pregnancy CD1d WT CAGMYC MECs (~10K) or CD1d KO CAGMYC MECs

(~10K) were injected into the mammary fatpad of 8-10 weeks old CD1d WT female mice, and allowed 3-days of tissue engraftment prior to DOX-treatment for 5 days.

*Histological analysis*

For histological analysis, the left inguinal mammary gland was harvested and fixed in 4% Paraformaldehyde overnight prior to paraffin embedding. For conventional histological analysis, mammary gland tissue slides were stained with Hematoxylin and Eosin (H&E). For ductal quantification, mammary gland H&E histological images were uploaded into Fiji (Fiji, RRID:SCR_002285), and ducts present in the posterior part of the gland were manually counted. Immunohistochemistry staining (IHC) was performed on a Roche Discovery Ultra Automated IHC/ISH stainer. For Masson's trichrome staining, Leica Multistainer Stainer/Coverslipper Combo (ST5020-CV5030) was used to stain slides according to standard reagents and protocols. Images were acquired using Aperio ePathology (Leica Biosystems) slide scanner in 40X lenses.

*Immunofluorescence (IF) analysis*

Paraffin-embedded mammary gland sections were deparaffinized in Xylene (Sigma Cat# 534056) and rehydrated, followed by antigen retrieval in Trilogy (Cell Marque Cat# 920P-10). Tissue was washed in 1x PBS (phosphate-buffered saline) for 1 min then blocked with blocking solution (10mM Tris-HCl pH 7.4, 100mM $MgCl_2$, 0.5% Tween 20, 10% FBS, 5% goat serum) for 4 hours in a humidified chamber. Sections were stained with the appropriate conjugated primary antibodies in blocking solution for 16 hours at 4°C. After subsequent washings with 1x PBS and blocking solution, tissues were incubated with DAPI (Sigma Cat# 10236276001) for 10 minutes to stain nuclei, and slides were mounted in ProLong Glass Antifade Mountant (Invitrogen Cat# P36980). Cell visualization and image collection was performed on a Zeiss LSM780 confocal laser-scanning microscope utilizing Zen lite software, Blue edition (ZEN Digital Imaging for Light Microscopy, RRID:SCR_013672) version 2.0.0.0. Non-specific staining was defined as follows (Scale: 200μm).

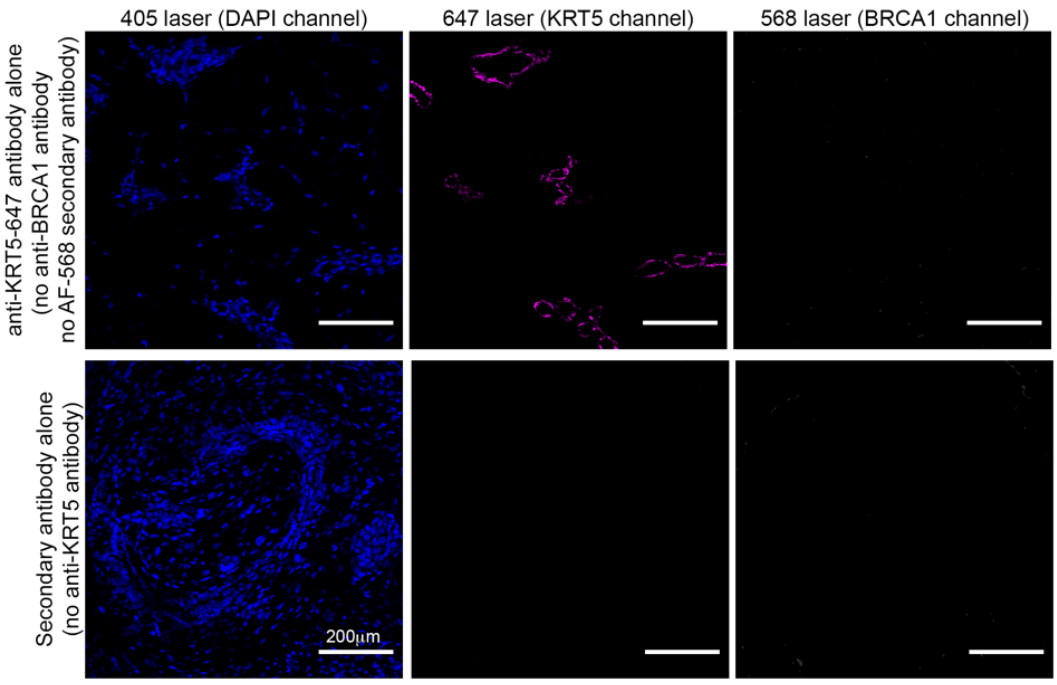


*Doxycycline (DOX) treatment*

Doxycycline was purchased from Takara Bio USA, Inc. (Cat# 631311) and sucrose was purchased from Sigma (Cat# S7903). DOX drinking solution (1 mg/mL) was prepared using sterile 1% sucrose water.

*Tamoxifen (TAM) treatment*

Tamoxifen USP grade was purchased from Sigma-Aldrich (Cat# 1643306) and sunflower seed oil (European Pharmacopoeia grade) was purchased from Sigma-Aldrich (Cat# 88921). To prepare the working solution, the Tamoxifen powder was weighed and dissolved in ethanol by vortexing. Heat sterilized sunflower oil was added at a ratio of 19:1 oil:ethanol mixture to a final concentration of 5mg/100ul (one dose), heated to 55°C and shaken vigorously to homogenize the mixture.

$Krt5^{CRE\text{-}ERT2}Brca1^{fl/fl}p53^{het}$ transgenic female mice received a total of three intraperitoneal doses of Tamoxifen warmed to 37°C on alternate days.

*Monitoring tumor growth*

3 week old $Krt5^{CRE\text{-}ERT2}Brca1^{fl/fl}p53^{-/+}$ female mice were treated with TAM. Half of TAM-treated female mice were housed together (pre-pregnancy/nulliparous group), and the other half were paired with a male (1 female and 1 male per breeding cage). Breeding TAM-treated females were allowed to give birth, nurse the offspring (21 days), and were considered post-pregnant (parous) after 40 days from offspring weaning. Both pre- and post-pregnancy mice were monitored for signs of tumor growth, and added to the Kaplan-Meier curve as soon as there was a palpable tumor. Mice with a tumor burden exceeding the limit of the animal's well-being (>2 cm), or mice showing signs of distress independently of tumor development were euthanized. At experimental end point, mammary tissue or mammary tumors were harvested for histological and flow cytometry analysis. Statistical analysis was performed with Logrank (Mantel-Cox) test.

*Western blot*

DOX-treated and control organoid cultures were homogenized in 1x Laemmli sample buffer (Bio-Rad, Cat# 1610747). Samples were loaded into homemade 10% SDS-PAGE gel and transferred overnight to PVDF membrane (Bio-Rad, Cat# 162-0177) using wet-transfer apparatus. Membranes were blocked with 1% BSA solution and incubated overnight with a diluted solution of primary antibody, followed by incubation with HRP-conjugated antibody for 40 minutes. HRP signal was developed with Luminata Crescendo Western HRP substrate (Millipore, Cat# WBLUR0100) in autoradiography film (Lab Scientific, Cat# XARALF2025). Developed films were scanned on Epson Perfection 2450 photo scanner.

*scRNA-seq data analysis*

Single cell data (pre-pregnancy mammary glands= 3,439 cells from n=2 biological replicates; post-pregnancy mammary glands= 4,412 cells from n=2 biological replicates) were aligned to mm10 using CellRanger v.3.1.0 (10x Genomics) (Cell Ranger , RRID:SCR_017344) (Zheng et al. 2017), and downstream processing was performed using Seurat v3.1.1 (SEURAT, RRID:SCR_007322) (Stuart et al.

2019). Cells with fewer than 250 features or higher than 10% mitochondrial gene content were removed prior to further analysis. Genes with fewer than 3 cells expressing them were removed, and the data were then log-normalized. Post-filtering analysis was performed on 3,075 cells (pre-pregnancy) and 4,029 cells (post-pregnancy). Principal component analysis was performed using the top 2,000 variable genes. This analysis was used to identify the number of significant components before clustering. Clustering was performed by calculating a shared nearest neighbor graph, using a resolution of 0.6. Subsetting into different cell types was performed using known markers for MECs, T-cells, Myeloid cells, B cells and NK cells. Epithelial cells for both datasets were defined by the expression of Epcam, Krt8, Krt18, Krt5 and Krt14 (cluster average expression > 2). Non-epithelial were cells considered having low expression of Epcam, Krt8, Krt18, Krt5 and Krt14. Epithelial lineage identification and T-cell lineage identification was performed utilizing a previously validated gene signature (Henry et al. 2021). Genes used to define each immune cluster (differentially expressed genes, DEGs) were determined using known cell type markers and using the FindAllMarkers function, which uses a Wilcoxon Rank Sum test to identify differentially expressed genes between all clusters in the dataset. Cell cycle scoring was performed with the CellCycleScoring function, using the default gene lists provided by Seurat. Cell dendrograms were generated using the BuildClusterTree function in Seurat, using default arguments. Diffusion mapping was performed using the DiffusionMap function from the "destiny" R package (Angerer et al. 2016). Gene Set Enrichment Analysis (GSEA, RRID:SCR_003199) (Subramanian et al. 2005) was used for global analyses of differentially expressed genes.

*RNA-seq library preparation and analysis*

FACS-isolated pre- and post-pregnancy NKT cells were collected and homogenized in TRIzol LS (Thermo Fisher Scientific, Cat# 10296010) for RNA extraction. Double stranded cDNA synthesis and Illumina libraries were prepared utilizing the Ovation RNA-seq system (V2) (Nugen Technologies, Cat# 7102-32). RNA-seq libraries were prepared utilizing the Ovation ultralow DR multiplex system (Nugen Technologies, Cat# 0331-32). Each library (n=2 biological replicates per experimental condition) was

barcoded with Illumina TruSeq adaptors to allow sample multiplexing, followed by sequencing on an Illumina NextSeq500, 76bp single-end run. Analyses were performed with command-line interfaced tools such as FastQC (FastQC, RRID:SCR_014583) for quality control and Trimmomatic (Trimmomatic, RRID:SCR_011848) (Bolger et al. 2014) for sequence trimming. We used STAR (STAR, RRID:SCR_004463) for mapping reads (Dobin et al. 2013), FeatureCounts (featureCounts, RRID:SCR_012919) for assigning reads to genomic features (Liao et al. 2014) and DESeq (DESeq, RRID:SCR_000154) to assess changes in expression levels simultaneously across multiple conditions and in multi-factor experimental designs, incorporating information from multiple replicates (Anders and Huber 2010). Genes with a statistically significant pvalue of $p< 0.05$ were considered differentially expressed. Gene Set Enrichment Analysis (GSEA) (Gene Set Enrichment Analysis, RRID:SCR_003199) was used for global analyses of differentially expressed genes (Subramanian et al. 2005). GSEA terms with statistically significant pvalue of $p<0.05$ were selected for data plotting and data interpretation. For experiments presented on Fig. 2-6 D, FACS-isolated, pre- and post-pregnancy CD45+NK1.1+CD3+ NKT cells (n=2 females per experimental group, n=4 pairs of mammary glands per female, n=2 biological replicates per experimental group) were utilized. For experiments presented on Fig. 3-6, total mammary tissue isolated from DOX-treated, NOD/SCID female mice transplanted with either pre- or post-pregnancy CAGMYC MECs (n=2 biological replicates per group) were utilized.

*ChIP-seq library analysis*

Previously published H3K27ac ChIP-seq datasets (Feigman et al. 2020) were mapped to the indexed mm9 genome using bowtie2 short-read aligner tool (Langmead and Salzberg 2012), using default settings. MACS2 peak-calling program (MACS, RRID:SCR_013291) (Zhang et al. 2008) was used to identify enriched genomic regions in this data by comparing the pulldown ChIP data to the control (Input) data using a q-value cutoff of $1.00^{-3}$ . Identification of genes closest to these differentially called peaks was performed using Genomic Regions Enrichment of Annotations Tool (GREAT, RRID:SCR_005807)

(McLean et al. 2010). Peak visualizations were generated using the UCSC Genome Browser (UCSC Genome Browser, RRID:SCR_005780) (Dreszer et al. 2012).

*Cut&Run library analysis*

Previously published H3K27ac Cut&Run datasets (Ciccone et al. 2020), were mapped to the indexed mm9 genome using bowtie2 short-read aligner tool using default settings (Langmead and Salzberg 2012). Sparse Enrichment Analysis for Cut&Run (SEACR) peak-calling program (Meers et al. 2019) was used to identify enriched genomic regions with an empirical threshold of n=0.01, returning the top n fraction of peaks based on total signal within peaks. The stringent argument was implemented, which used the summit of each curve. Identification of genes closest to these differentially called peaks was performed using Genomic Regions Enrichment of Annotations Tool (UCSC Genome Browser, RRID:SCR_005780) (McLean et al. 2010). Peak visualizations were generated using the UCSC Genome Browser (UCSC Genome Browser, RRID:SCR_005780) (Dreszer et al. 2012).

*ATAC-seq library preparation and analysis*

Nuclei of FACS-isolated, pre- and post-pregnancy NKT cells were isolated utilizing hypotonic lysis buffer and incubated with Tn5 enzyme from Nextera DNA sample Preparation kit (Illumina, Cat# FC-121-1031) for the preparation of ATAC libraries. Each library (n=2 per experimental condition) was amplified and barcoded as previously described (Buenrostro et al. 2015), then pooled for sequencing on an Illumina Nextseq500, 76bp single-end run. ATACseq library reads (n=2 per cell condition) were mapped to the indexed mm9 genome using Bowtie2 short read-aligner (Bowtie 2, RRID:SCR_016368) (Langmead and Salzberg 2012) and replicate alignment files were merged. MACS2 (MACS, RRID:SCR_013291) (Zhang et al. 2008) was used to identify enriched genomic regions in both conditions using a tag size of 25bp and a q-value cutoff of $1.00^{-2}$. Peaks were annotated using Homer (HOMER, RRID:SCR_010881) with standard mm9 genome reference. Location of peaks was then grouped into intergenic, promoter and genic (containing 5'UTR, Exons, Introns, Transcription Termination Sites, 3'UTR, ncRNA, miRNA,

snoRNA, and rRNA) regions. The UCSC genome browser (UCSC Genome Browser, RRID:SCR_005780) (Dreszer et al. 2012) was used to analyze genomic regions for overlap, using the Bedtools intersect function (BEDTools, RRID:SCR_006646) (Quinlan and Hall 2010). Any base pair overlap was enough to consider two regions "shared" and regions where no overlap existed defined the regions as exclusively being in one condition. The comparison was made into a Venn diagram using tool available at https://www.meta-chart.com/venn.

*DNA motif analysis*

Peaks from pre- and post-pregnancy NKT cells ATAC-seq libraries were utilized as input for unbiased transcription factor analyses using Analysis of Motif Enrichment (AME) (McLeay and Bailey 2010) and Find Individual Motif Occurrences (FIMO) (MEME Suite - Motif-based sequence analysis tools, RRID:SCR_001783) (Grant et al. 2011) was used to computationally define DNA binding motif regions to identify sequences of known motifs, with a statistical threshold of 0.0001.

*Genomic library preparation and Copy number variation (CNV) analysis*

Mammary normal tissue and tumor from nulliparous BRCA1 KO p53het female mice were dissociated as above described. Lineage depleted tumor cells were utilized for DNA extraction using DNeasy Blood & Tissue Kit (Qiagen Cat# 69504). Genomic DNA was sonicated to an average of 300 bp using Covaris E220 Focused-ultrasonicator. For library preparation, fragmented DNA went through standard end-repair (NEB Cat# E6050), dA-tailing (NEB Cat# E6053), and sequencing adapter ligation (NEB Cat# M2200) steps. Following universal adapter ligation, eight cycles of PCR was performed for each sample. During the PCR step, a unique pair of Illumina TruSeq i7 index and i5 index was added to each sample. The PCR library was purified with AMPure XP beads (Beckman Coulter Cat# A63881), and quantified using NanoDrop spectrophotometer and Agilent Technologies 2100 Bioanalyzer. Whole-genome-sequencing libraries with different combination of Illumina indexes were pooled together for one lane of Illumina MiSeq. 150 base pairs from both ends were sequenced along with two 8-bp indexes. For

CNV analysis, Read 1 of the sequence data was mapped to the mm9 reference genome using Hisat2 version 2.1.0 in single read alignment mode (Kim et al. 2015). The reference genome was divided into 5,000 variable-length bins with equal mappability as previously described (Baslan et al. 2012). The ratio of mapped reads in the tumor sample to mapped reads in the diploid sample (normal tissue) was used to compute a fitted piecewise constant function (segmentation). This segmentation used DNAcopy version 1.50.1 implementation of the circular binary segmentation algorithm (Seshan and Olshen 2022) and the copy number profiles were plotted using R version 3.4.4.

*2D co-culture system*

Brca1 KO tumor organoids were cultured in Matrigel (Corning, Cat# 356230), recovered with Cell Recovery Solution (Corning, Cat# 354253), and plated in 2D overnight to allow the cells to adhere, following which NKT cells (CD3+ NK1.1+ cells) isolated using MACS magnetic columns (Miltenyi Biotec Cat# 130-042-401) were added. After 24 hours of co-culture, organoids were dissociated into single cells by gentle agitation with TryPLE Express (ThermoFisher, Cat# 12604013), filtered, and cell death was quantified as a measure of Caspase 3/7 activity using the Magic Red assay kit (Abcam, Cat# ab270771) and Live/Dead Violet (Invitrogen Cat# L23105).

*3D co-culture system*

Single cell suspensions from pre- and post-pregnancy mammary glands (derived as described earlier) were incubated with a CD45 or CD3 biotin antibodies, incubated with anti-biotin magnetic beads (Miltenyi Biotec Cat# 130-090-485) and loaded onto a MACS magnetic column (Miltenyi Biotec Cat# 130-042-401). Positively labeled cells (immune cells ot T-cells) were eluted from column with 3ml of MACS buffer and incubated overnight in a T-cell activating medium (media composition below). Glass bottom 96-well imaging plates were warmed overnight in a 37°C incubator. Brca1 KO tumor organoids cultured in Matrigel and recovered with Cell Recovery Solution. Tumor organoids and immune cells were fluorescently labeled separately using non-specific CellTracker dyes (ThermoFisher, Red CMTPX Cat#

C34552 for organoids, Green CMFDA Cat# C7025 for immune cells) according to manufacturer protocols. Organoids and immune cells were then mixed at a ratio of 1:1000 and plated in imaging media composed of 10% Matrigel in 1:1 organoid:immune cell media containing 1mM NucView Blue Caspase-3 dye (Millipore-Sigma Cat# SCT104).

T-cell activating medium: RPMI + 10% FBS, P/S (100 U/μl), 5.5mM β-mercaptoethanol, 0.1M MEM nonessential amino acids, 10mM HEPES, 20 ng/ml IL-2 (PeproTech Cat# 212-12), 50 ng/ml IL-7 (PeproTech Cat# 217-17).

*3D time lapse live imaging*

Live cell imaging was set up on a Perkin-Elmer UltraVIEW VoX high speed spinning disk confocal microscope equipped with a high end CCD camera, a fully automated stage, and 6 laser lines (405, 440, 488, 514, 561, and 640nm). Temperature was held at 37°C, CO2 at 5%, and humidity at 80%. Plate setup included setting XY coordinates at 3 distinct points per well for serial imaging of the same organoids. Images were set to be collected at 1 hr intervals with exposure times of ~500ms. A 100μm z-stack was acquired at 10μm steps. The images were acquired, assembled, and analyzed using Volocity (Perkin-Elmer v.6.3) and FIJI (Schindelin et al. 2012) software.

*Quantification and Statistical Analysis*

Data represent results from three or more independent biological replicates, unless otherwise specified. Sequencing data are from two biological replicates from each condition. All statistical analyses were performed using GraphPad Prism V9 software. For all analyses, error bars indicate standard error of mean across samples of the same experimental group. Statistically significant differences were considered with *p*-values lower than 0.05 ($p<0.05$) from unpaired Student's t-tests, as described in the figure legends.

# 7. References


Albrektsen G, Heuch I, Hansen S, Kvåle G. 2005. Breast cancer risk by age at birth, time since birth and time intervals between births: exploring interaction effects. *British Journal of Cancer* **92**: 167–175.

Allouch S, Gupta I, Malik S, Al Farsi HF, Vranic S, Al Moustafa A-E. 2020. Breast Cancer During Pregnancy: A Marked Propensity to Triple-Negative Phenotype. *Frontiers in Oncology* **10**. https://www.frontiersin.org/articles/10.3389/fonc.2020.580345 (Accessed October 31, 2022).

Almishri W, Santodomingo-Garzon T, Le T, Stack D, Mody CH, Swain MG. 2016. TNFα Augments Cytokine-Induced NK Cell IFNγ Production through TNFR2. *JIN* **8**: 617–629.

Amprey JL, Im JS, Turco SJ, Murray HW, Illarionov PA, Besra GS, Porcelli SA, Späth GF. 2004. A Subset of Liver NK T Cells Is Activated during Leishmania donovani Infection by CD1d-bound Lipophosphoglycan. *Journal of Experimental Medicine* **200**: 895–904.

Anders S, Huber W. 2010. Differential expression analysis for sequence count data. *Genome Biology* **11**: R106.

Angerer P, Haghverdi L, Büttner M, Theis FJ, Marr C, Buettner F. 2016. destiny: diffusion maps for large-scale single-cell data in R. *Bioinformatics* **32**: 1241–1243.

Annunziato S, de Ruiter JR, Henneman L, Brambillasca CS, Lutz C, Vaillant F, Ferrante F, Drenth AP, van der Burg E, Siteur B, et al. 2019. Comparative oncogenomics identifies combinations of driver genes and drug targets in BRCA1-mutated breast cancer. *Nat Commun* **10**: 397.

Ao Z, Shah SH, Machlin LM, Parajuli R, Miller PC, Rawal S, Williams AJ, Cote RJ, Lippman ME, Datar RH, et al. 2015. Identification of Cancer-Associated Fibroblasts in Circulating Blood from Patients with Metastatic Breast Cancer. *Cancer Res* **75**: 4681–4687.

Asselin-Labat M-L, Sutherland KD, Barker H, Thomas R, Shackleton M, Forrest NC, Hartley L, Robb L, Grosveld FG, van der Wees J, et al. 2007. Gata-3 is an essential regulator of mammary-gland morphogenesis and luminal-cell differentiation. *Nat Cell Biol* **9**: 201–209.

Aulmann S, Bentz M, Sinn HP. 2002. C-myc oncogene amplification in ductal carcinoma in situ of the breast. *Breast Cancer Res Treat* **74**: 25–31.

Avagliano A, Fiume G, Ruocco MR, Martucci N, Vecchio E, Insabato L, Russo D, Accurso A, Masone S, Montagnani S, et al. 2020. Influence of Fibroblasts on Mammary Gland Development, Breast Cancer Microenvironment Remodeling, and Cancer Cell Dissemination. *Cancers (Basel)* **12**: 1697.

Bach K, Pensa S, Grzelak M, Hadfield J, Adams DJ, Marioni JC, Khaled WT. 2017. Differentiation dynamics of mammary epithelial cells revealed by single-cell RNA sequencing. *Nat Commun* **8**: 1–11.

Bach K, Pensa S, Zarocsinceva M, Kania K, Stockis J, Pinaud S, Lazarus KA, Shehata M, Simões BM, Greenhalgh AR, et al. 2021. Time-resolved single-cell analysis of Brca1 associated mammary tumourigenesis reveals aberrant differentiation of luminal progenitors. *Nature Communications* **12**: 1502.

Balato A, Unutmaz D, Gaspari AA. 2009. Natural killer T cells: an unconventional T-cell subset with diverse effector and regulatory functions. *J Invest Dermatol* **129**: 1628–1642.

Banerji S, Cibulskis K, Rangel-Escareno C, Brown KK, Carter SL, Frederick AM, Lawrence MS, Sivachenko AY, Sougnez C, Zou L, et al. 2012. Sequence analysis of mutations and translocations across breast cancer subtypes. *Nature* **486**: 405–409.

Barton M, Santucci-Pereira J, Russo J. 2014. Molecular Pathways Involved in Pregnancy-Induced Prevention Against Breast Cancer. *Front Endocrinol* **5**. https://www.frontiersin.org/articles/10.3389/fendo.2014.00213/full (Accessed April 15, 2020).

Baslan T, Kendall J, Rodgers L, Cox H, Riggs M, Stepansky A, Troge J, Ravi K, Esposito D, Lakshmi B, et al. 2012. Genome-wide copy number analysis of single cells. *Nat Protoc* **7**: 1024–1041.

Bassiri H, Das R, Guan P, Barrett DM, Brennan PJ, Banerjee PP, Wiener SJ, Orange JS, Brenner MB, Grupp SA, et al. 2014. iNKT Cell Cytotoxic Responses Control T-Lymphoma Growth In Vitro and In Vivo. *Cancer Immunol Res* **2**: 59–69.

Behbod F, Kittrell FS, LaMarca H, Edwards D, Kerbawy S, Heestand JC, Young E, Mukhopadhyay P, Yeh H-W, Allred DC, et al. 2009. An intraductal human-in-mouse transplantation model mimics the subtypes of ductal carcinoma in situ. *Breast Cancer Research* **11**: R66.

Beral V, Bull D, Doll R, Peto R, Reeves G, Collaborative Group on Hormonal Factors in Breast Cance. 2004. Breast cancer and abortion: collaborative reanalysis of data from 53 epidemiological studies, including 83 000 women with breast cancer from 16 countries. *The Lancet* **363**: 1007–1016.

Betterman KL, Paquet-Fifield S, Asselin-Labat M-L, Visvader JE, Butler LM, Stacker SA, Achen MG, Harvey NL. 2012. Remodeling of the Lymphatic Vasculature during Mouse Mammary Gland Morphogenesis Is Mediated via Epithelial-Derived Lymphangiogenic Stimuli. *The American Journal of Pathology* **181**: 2225–2238.

Betts CB, Pennock ND, Caruso BP, Ruffell B, Borges VF, Schedin P. 2018. Mucosal Immunity in the Female Murine Mammary Gland. *Journal of immunology (Baltimore, Md : 1950)* **201**: 734–746.

Blakely CM, Stoddard AJ, Belka GK, Dugan KD, Notarfrancesco KL, Moody SE, D'Cruz CM, Chodosh LA. 2006. Hormone-Induced Protection against Mammary Tumorigenesis Is Conserved in Multiple Rat Strains and Identifies a Core Gene Expression Signature Induced by Pregnancy. *Cancer Research* **66**: 6421–6431.

Boardman LA, Thibodeau SN, Schaid DJ, Lindor NM, McDonnell SK, Burgart LJ, Ahlquist DA, Podratz KC, Pittelkow M, Hartmann LC. 1998. Increased risk for cancer in patients with the Peutz-Jeghers syndrome. *Ann Intern Med* **128**: 896–899.

Bochtler P, Kröger A, Schirmbeck R, Reimann J. 2008. Type I IFN-Induced, NKT Cell-Mediated Negative Control of CD8 T Cell Priming by Dendritic Cells. *The Journal of Immunology* **181**: 1633–1643.

Bolger AM, Lohse M, Usadel B. 2014. Trimmomatic: a flexible trimmer for Illumina sequence data. *Bioinformatics* **30**: 2114–2120.

Bourges D, Meurens F, Berri M, Chevaleyre C, Zanello G, Levast B, Melo S, Gerdts V, Salmon H. 2008. New insights into the dual recruitment of IgA+ B cells in the developing mammary gland. *Mol Immunol* **45**: 3354–3362.

Braig M, Schmitt CA. 2006. Oncogene-induced senescence: Putting the brakes on tumor development. *Cancer Research* **66**: 2881–2884.

Breast Cancer Association Consortium, Mavaddat N, Dorling L, Carvalho S, Allen J, González-Neira A, Keeman R, Bolla MK, Dennis J, Wang Q, et al. 2022. Pathology of Tumors Associated With Pathogenic Germline Variants in 9 Breast Cancer Susceptibility Genes. *JAMA Oncol* **8**: e216744.

Brentjens RJ, Rivière I, Park JH, Davila ML, Wang X, Stefanski J, Taylor C, Yeh R, Bartido S, Borquez-Ojeda O, et al. 2011. Safety and persistence of adoptively transferred autologous CD19-targeted T cells in patients with relapsed or chemotherapy refractory B-cell leukemias. *Blood* **118**: 4817–4828.

Britt K, Ashworth A, Smalley M. 2007. Pregnancy and the risk of breast cancer. *Endocr Relat Cancer* **14**: 907–933.

Brodie SG, Xu X, Qiao W, Li W-M, Cao L, Deng C-X. 2001. Multiple genetic changes are associated with mammary tumorigenesis in Brca1 conditional knockout mice. *Oncogene* **20**: 7514–7523.

Brutkiewicz RR. 2006. CD1d Ligands: The Good, the Bad, and the Ugly. *The Journal of Immunology* **177**: 769–775.

Buenrostro J, Wu B, Chang H, Greenleaf W. 2015. ATAC-seq: A Method for Assaying Chromatin Accessibility Genome-Wide. *Curr Protoc Mol Biol* **109**: 21.29.1-21.29.9.

Callihan EB, Gao D, Jindal S, Lyons TR, Manthey E, Edgerton S, Urquhart A, Schedin P, Borges VF. 2013. Postpartum diagnosis demonstrates a high risk for metastasis and merits an expanded definition of pregnancy-associated breast cancer. *Breast Cancer Res Treat* **138**: 549–559.

Cancer Genome Atlas Network. 2012. Comprehensive molecular portraits of human breast tumours. *Nature* **490**: 61–70.
Cardiff RD, Kenney N. 2011. A Compendium of the Mouse Mammary Tumor Biologist: From the Initial Observations in the House Mouse to the Development of Genetically Engineered Mice. *Cold Spring Harb Perspect Biol* **3**: a003111.
Carroll LS, Capecchi MR. 2015. Hoxc8 initiates an ectopic mammary program by regulating Fgf10 and Tbx3 expression and Wnt/β-catenin signaling. *Development* **142**: 4056–4067.
Castillo-Martin M, Domingo-Domenech J, Karni-Schmidt O, Matos T, Cordon-Cardo C. 2010. Molecular pathways of urothelial development and bladder tumorigenesis. *Urologic Oncology: Seminars and Original Investigations* **28**: 401–408.
CDCBreastCancer. 2022. What Are the Risk Factors for Breast Cancer? *Centers for Disease Control and Prevention*. https://www.cdc.gov/cancer/breast/basic_info/risk_factors.htm (Accessed September 21, 2022).
Chaffer CL, Weinberg RA. 2010. Cancer Cell of Origin: Spotlight on Luminal Progenitors. *Cell Stem Cell* **7**: 271–272.
Chan S-H, Tsai K-W, Chiu S-Y, Kuo W-H, Chen H-Y, Jiang SS, Chang K-J, Hung W-C, Wang L-H. 2019. Identification of the Novel Role of CD24 as an Oncogenesis Regulator and Therapeutic Target for Triple-Negative Breast Cancer. *Mol Cancer Ther* **18**: 147–161.
Chan SR, Rickert CG, Vermi W, Sheehan KCF, Arthur C, Allen JA, White JM, Archambault J, Lonardi S, McDevitt TM, et al. 2014. Dysregulated STAT1-SOCS1 control of JAK2 promotes mammary luminal progenitor cell survival and drives ER α + tumorigenesis. *Cell Death & Differentiation* **21**: 234–246.
Chen S, Parmigiani G. 2007. Meta-analysis of BRCA1 and BRCA2 penetrance. *J Clin Oncol* **25**: 1329–1333.
Chen Y, Olopade OI. 2008. MYC in breast tumor progression. *Expert Review of Anticancer Therapy* **8**: 1689–1698.
Choudhury S, Almendro V, Merino VF, Wu Z, Maruyama R, Su Y, Martins FC, Fackler MJ, Bessarabova M, Kowalczyk A, et al. 2013. Molecular Profiling of Human Mammary Gland Links Breast Cancer Risk to a p27+ Cell Population with Progenitor Characteristics. *Cell Stem Cell* **13**: 117–130.
Chung C-Y, Ma Z, Dravis C, Preissl S, Poirion O, Luna G, Hou X, Giraddi RR, Ren B, Wahl GM. 2019. Single-Cell Chromatin Analysis of Mammary Gland Development Reveals Cell-State Transcriptional Regulators and Lineage Relationships. *Cell Reports* **29**: 495-510.e6.
Ciccone MF, Trousdell MC, Dos Santos CO. 2020. Characterization of Organoid Cultures to Study the Effects of Pregnancy Hormones on the Epigenome and Transcriptional Output of Mammary Epithelial Cells. *J Mammary Gland Biol Neoplasia* **25**: 351–366.
Ciriello G, Sinha R, Hoadley KA, Jacobsen AS, Reva B, Perou CM, Sander C, Schultz N. 2013. The molecular diversity of Luminal A breast tumors. *Breast Cancer Res Treat* **141**: 409–420.
Collins LC, Gelber S, Marotti JD, White S, Ruddy K, Brachtel EF, Schapira L, Come SE, Borges VF, Schedin P, et al. 2015. Molecular Phenotype of Breast Cancer According to Time Since Last Pregnancy in a Large Cohort of Young Women. *Oncologist* **20**: 713–718.
Connaughton S, Chowdhury F, Attia RR, Song S, Zhang Y, Elam MB, Cook GA, Park EA. 2010. Regulation of pyruvate dehydrogenase kinase isoform 4 (PDK4) gene expression by glucocorticoids and insulin. *Mol Cell Endocrinol* **315**: 159.
Coquet JM, Chakravarti S, Kyparissoudis K, McNab FW, Pitt LA, McKenzie BS, Berzins SP, Smyth MJ, Godfrey DI. 2008. Diverse cytokine production by NKT cell subsets and identification of an IL-17–producing CD4−NK1.1− NKT cell population. *PNAS* **105**: 11287–11292.
Coulie PG, Van den Eynde BJ, van der Bruggen P, Boon T. 2014. Tumour antigens recognized by T lymphocytes: at the core of cancer immunotherapy. *Nature Reviews Cancer* **14**: 135–146.
Coussens LM, Pollard JW. 2011. Leukocytes in Mammary Development and Cancer. *Cold Spring Harb Perspect Biol* **3**: a003285.

Couto JP, Bentires-Alj M. 2017. Mouse Models of Breast Cancer: Deceptions that Reveal the Truth. In *Breast Cancer: Innovations in Research and Management* (eds. U. Veronesi, A. Goldhirsch, P. Veronesi, O.D. Gentilini, and M.C. Leonardi), pp. 49–60, Springer International Publishing, Cham https://doi.org/10.1007/978-3-319-48848-6_6 (Accessed October 8, 2022).

Creighton CJ, Li X, Landis M, Dixon JM, Neumeister VM, Sjolund A, Rimm DL, Wong H, Rodriguez A, Herschkowitz JI, et al. 2009. Residual breast cancers after conventional therapy display mesenchymal as well as tumor-initiating features. *Proceedings of the National Academy of Sciences* **106**: 13820–13825.

Cristea S, Polyak K. 2018. Dissecting the mammary gland one cell at a time. *Nat Commun* **9**: 2473.

Dai X, Xiang L, Li T, Bai Z. 2016. Cancer Hallmarks, Biomarkers and Breast Cancer Molecular Subtypes. *Journal of Cancer* **7**: 1281–1294.

Daniels J, Doukas PG, Escala MEM, Ringbloom KG, Shih DJH, Yang J, Tegtmeyer K, Park J, Thomas JJ, Selli ME, et al. 2020. Cellular origins and genetic landscape of cutaneous gamma delta T cell lymphomas. *Nat Commun* **11**: 1806.

Davenport TG, Jerome-Majewska LA, Papaioannou VE. 2003. Mammary gland, limb and yolk sac defects in mice lacking Tbx3, the gene mutated in human ulnar mammary syndrome. *Development* **130**: 2263–2273.

Dawson CA, Pal B, Vaillant F, Gandolfo LC, Liu Z, Bleriot C, Ginhoux F, Smyth GK, Lindeman GJ, Mueller SN, et al. 2020. Tissue-resident ductal macrophages survey the mammary epithelium and facilitate tissue remodelling. *Nat Cell Biol* **22**: 546–558.

Deming SL, Nass SJ, Dickson RB, Trock BJ. 2000. C-myc amplification in breast cancer: a meta-analysis of its occurrence and prognostic relevance. *Br J Cancer* **83**: 1688–1695.

DeOme KB. 1967. The mouse mammary tumor system. *Proceedings of the Fifth Berkeley Symposium on Mathematical Statistics and Probability, Volume 4: Biology and Problems of Health* **5.4**: 649–656.

D'Esposito V, Liguoro D, Ambrosio MR, Collina F, Cantile M, Spinelli R, Raciti GA, Miele C, Valentino R, Campiglia P, et al. 2016. Adipose microenvironment promotes triple negative breast cancer cell invasiveness and dissemination by producing CCL5. *Oncotarget* **7**: 24495–24509.

Dirat B, Bochet L, Dabek M, Daviaud D, Dauvillier S, Majed B, Wang YY, Meulle A, Salles B, Le Gonidec S, et al. 2011. Cancer-associated adipocytes exhibit an activated phenotype and contribute to breast cancer invasion. *Cancer Res* **71**: 2455–2465.

Dobin A, Davis CA, Schlesinger F, Drenkow J, Zaleski C, Jha S, Batut P, Chaisson M, Gingeras TR. 2013. STAR: ultrafast universal RNA-seq aligner. *Bioinformatics* **29**: 15–21.

Doisne J-M, Bartholin L, Yan K-P, Garcia CN, Duarte N, Le Luduec J-B, Vincent D, Cyprian F, Horvat B, Martel S, et al. 2009. iNKT cell development is orchestrated by different branches of TGF-β signaling. *J Exp Med* **206**: 1365–1378.

Dos Santos CO, Dolzhenko E, Hodges E, Smith AD, Hannon GJ. 2015. An epigenetic memory of pregnancy in the mouse mammary gland. *Cell Rep* **11**: 1102–1109.

dos Santos CO, Rebbeck C, Rozhkova E, Valentine A, Samuels A, Kadiri LR, Osten P, Harris EY, Uren PJ, Smith AD, et al. 2013. Molecular hierarchy of mammary differentiation yields refined markers of mammary stem cells. *Proc Natl Acad Sci USA* **110**: 7123–7130.

Dreszer TR, Karolchik D, Zweig AS, Hinrichs AS, Raney BJ, Kuhn RM, Meyer LR, Wong M, Sloan CA, Rosenbloom KR, et al. 2012. The UCSC Genome Browser database: extensions and updates 2011. *Nucleic Acids Research* **40**: D918–D923.

Ebert LM, Meuter S, Moser B. 2006. Homing and Function of Human Skin γδ T Cells and NK Cells: Relevance for Tumor Surveillance. *The Journal of Immunology* **176**: 4331–4336.

Ellis MJ, Ding L, Shen D, Luo J, Suman VJ, Wallis JW, Van Tine BA, Hoog J, Goiffon RJ, Goldstein TC, et al. 2012. Whole-genome analysis informs breast cancer response to aromatase inhibition. *Nature* **486**: 353–360.

Escot C, Theillet C, Lidereau R, Spyratos F, Champeme MH, Gest J, Callahan R. 1986. Genetic alteration of the c-myc protooncogene (MYC) in human primary breast carcinomas. *Proc Natl Acad Sci USA* **83**: 4834–4838.

Fata JE, Chaudhary V, Khokha R. 2001. Cellular turnover in the mammary gland is correlated with systemic levels of progesterone and not 17beta-estradiol during the estrous cycle. *Biol Reprod* **65**: 680–688.

Faunce DE, Palmer JL, Paskowicz KK, Witte PL, Kovacs EJ. 2005. CD1d-Restricted NKT Cells Contribute to the Age-Associated Decline of T Cell Immunity. *The Journal of Immunology* **175**: 3102–3109.

Feigman MJ, Moss MA, Chen C, Cyrill SL, Ciccone MF, Trousdell MC, Yang S-T, Frey WD, Wilkinson JE, dos Santos CO. 2020. Pregnancy reprograms the epigenome of mammary epithelial cells and blocks the development of premalignant lesions. *Nature Communications* **11**: 2649.

Fisher B, Bauer M, Wickerham DL, Redmond CK, Fisher ER, Cruz AB, Foster R, Gardner B, Lerner H, Margolese R. 1983. Relation of number of positive axillary nodes to the prognosis of patients with primary breast cancer. An NSABP update. *Cancer* **52**: 1551–1557.

Florian S, Iwamoto Y, Coughlin M, Weissleder R, Mitchison TJ. 2019. A human organoid system that self-organizes to recapitulate growth and differentiation of a benign mammary tumor. *Proceedings of the National Academy of Sciences of the United States of America* **116**: 11444–11453.

Fornetti J, Martinson H, Borges V, Schedin P. 2012. Emerging targets for the prevention of pregnancy-associated breast cancer. *Cell Cycle* **11**: 639–640.

Foulkes WD, Stefansson IM, Chappuis PO, Bégin LR, Goffin JR, Wong N, Trudel M, Akslen LA. 2003. Germline BRCA1 mutations and a basal epithelial phenotype in breast cancer. *J Natl Cancer Inst* **95**: 1482–1485.

Freire-de-Lima CG, Xiao YQ, Gardai SJ, Bratton DL, Schiemann WP, Henson PM. 2006. Apoptotic Cells, through Transforming Growth Factor-β, Coordinately Induce Anti-inflammatory and Suppress Pro-inflammatory Eicosanoid and NO Synthesis in Murine Macrophages*. *Journal of Biological Chemistry* **281**: 38376–38384.

Fu NY, Nolan E, Lindeman GJ, Visvader JE. 2020. Stem Cells and the Differentiation Hierarchy in Mammary Gland Development. *Physiol Rev* **100**: 489–523.

Fujisaki K, Fujimoto H, Sangai T, Nagashima T, Sakakibara M, Shiina N, Kuroda M, Aoyagi Y, Miyazaki M. 2015. Cancer-mediated adipose reversion promotes cancer cell migration via IL-6 and MCP-1. *Breast Cancer Res Treat* **150**: 255–263.

Funnell T, O'Flanagan CH, Williams MJ, McPherson A, McKinney S, Kabeer F, Lee H, Salehi S, Vázquez-García I, Shi H, et al. 2022. Single-cell genomic variation induced by mutational processes in cancer. *Nature* 1–10.

Gapin L, Godfrey DI, Rossjohn J. 2013. Natural Killer T cell obsession with self-antigens. *Curr Opin Immunol* **25**: 168–173.

Gentles AJ, Newman AM, Liu CL, Bratman SV, Feng W, Kim D, Nair VS, Xu Y, Khuong A, Hoang CD, et al. 2015. The prognostic landscape of genes and infiltrating immune cells across human cancers. *Nature Medicine* **21**: 938–945.

Germanov E, Veinotte L, Cullen R, Chamberlain E, Butcher EC, Johnston B. 2008. Critical Role for the Chemokine Receptor CXCR6 in Homeostasis and Activation of CD1d-Restricted NKT Cells. *The Journal of Immunology* **181**: 81–91.

Gober H-J, Kistowska M, Angman L, Jenö P, Mori L, De Libero G. 2003. Human T Cell Receptor γδ Cells Recognize Endogenous Mevalonate Metabolites in Tumor Cells. *J Exp Med* **197**: 163–168.

Goddard ET, Bassale S, Schedin T, Jindal S, Johnston J, Cabral E, Latour E, Lyons TR, Mori M, Schedin PJ, et al. 2019. Association Between Postpartum Breast Cancer Diagnosis and Metastasis and the Clinical Features Underlying Risk. *JAMA Netw Open* **2**: e186997–e186997.

Godder KT, Henslee-Downey PJ, Mehta J, Park BS, Chiang K-Y, Abhyankar S, Lamb LS. 2007. Long term disease-free survival in acute leukemia patients recovering with increased γδ T cells after

partially mismatched related donor bone marrow transplantation. *Bone Marrow Transplantation* **39**: 751–757.
Godet I, Gilkes DM. 2017. BRCA1 and BRCA2 mutations and treatment strategies for breast cancer. *Integr Cancer Sci Ther* **4**. https://www.ncbi.nlm.nih.gov/pmc/articles/PMC5505673/ (Accessed April 10, 2020).
Godfrey DI, Kronenberg M. 2004. Going both ways: Immune regulation via CD1d-dependent NKT cells. *J Clin Invest* **114**: 1379–1388.
Godfrey DI, Le Nours J, Andrews DM, Uldrich AP, Rossjohn J. 2018. Unconventional T Cell Targets for Cancer Immunotherapy. *Immunity* **48**: 453–473.
Godfrey DI, MacDonald HR, Kronenberg M, Smyth MJ, Kaer LV. 2004. NKT cells: what's in a name? *Nat Rev Immunol* **4**: 231–237.
Godfrey DI, Uldrich AP, McCluskey J, Rossjohn J, Moody DB. 2015. The burgeoning family of unconventional T cells. *Nature Immunology* **16**: 1114–1123.
Gouon-Evans V, Rothenberg ME, Pollard JW. 2000. Postnatal mammary gland development requires macrophages and eosinophils. *Development* **127**: 2269–2282.
Grant CE, Bailey TL, Noble WS. 2011. FIMO: scanning for occurrences of a given motif. *Bioinformatics* **27**: 1017–1018.
Gray GK, Li CM-C, Rosenbluth JM, Selfors LM, Girnius N, Lin J-R, Schackmann RCJ, Goh WL, Moore K, Shapiro HK, et al. 2022. A human breast atlas integrating single-cell proteomics and transcriptomics. *Developmental Cell* **57**: 1400-1420.e7.
Green KA, Lund LR. 2005. ECM degrading proteases and tissue remodelling in the mammary gland. *Bioessays* **27**: 894–903.
Gregor MF, Misch ES, Yang L, Hummasti S, Inouye KE, Lee A-H, Bierie B, Hotamisligil GS. 2013. The Role of Adipocyte XBP1 in Metabolic Regulation during Lactation. *Cell Reports* **3**: 1430–1439.
Grushko TA, Dignam JJ, Das S, Blackwood AM, Perou CM, Ridderstråle KK, Anderson KN, Wei M-J, Adams AJ, Hagos FG, et al. 2004. MYC is amplified in BRCA1-associated breast cancers. *Clin Cancer Res* **10**: 499–507.
Guo Q, Betts C, Pennock N, Mitchell E, Schedin P. 2017. Mammary Gland Involution Provides a Unique Model to Study the TGF-β Cancer Paradox. *Journal of Clinical Medicine* **6**: 10.
Guo W, Keckesova Z, Donaher JL, Shibue T, Tischler V, Reinhardt F, Itzkovitz S, Noske A, Zürrer-Härdi U, Bell G, et al. 2012. Slug and Sox9 cooperatively determine the mammary stem cell state. *Cell* **148**: 1015–1028.
Guzman RC, Yang J, Rajkumar L, Thordarson G, Chen X, Nandi S. 1999. Hormonal prevention of breast cancer: Mimicking the protective effect of pregnancy. *PNAS* **96**: 2520–2525.
Hanasoge Somasundara AV, Moss MA, Feigman MJ, Chen C, Cyrill SL, Ciccone MF, Trousdell MC, Vollbrecht M, Li S, Kendall J, et al. 2021. Parity-induced changes to mammary epithelial cells control NKT cell expansion and mammary oncogenesis. *Cell Reports* **37**: 110099.
Harbeck N, Penault-Llorca F, Cortes J, Gnant M, Houssami N, Poortmans P, Ruddy K, Tsang J, Cardoso F. 2019. Breast cancer. *Nat Rev Dis Primers* **5**: 1–31.
Hartman EK, Eslick GD. 2016. The prognosis of women diagnosed with breast cancer before, during and after pregnancy: a meta-analysis. *Breast Cancer Res Treat* **160**: 347–360.
Harvey PW. 2012. Hypothesis Prolactin is tumorigenic to human breast: dispelling the myth that prolactin-induced mammary tumors are rodent-specific. *Journal of Applied Toxicology* **32**: 1–9.
Hatsell SJ, Cowin P. 2006. Gli3-mediated repression of Hedgehog targets is required for normal mammary development. *Development* **133**: 3661–3670.
Heczey A, Liu D, Tian G, Courtney AN, Wei J, Marinova E, Gao X, Guo L, Yvon E, Hicks J, et al. 2014. Invariant NKT cells with chimeric antigen receptor provide a novel platform for safe and effective cancer immunotherapy. *Blood* **124**: 2824–2833.
Heikkinen T, Kärkkäinen H, Aaltonen K, Milne RL, Heikkilä P, Aittomäki K, Blomqvist C, Nevanlinna H. 2009. The breast cancer susceptibility mutation PALB2 1592delT is associated with an aggressive tumor phenotype. *Clin Cancer Res* **15**: 3214–3222.

Henry S, Trousdell MC, Cyrill SL, Zhao Y, Feigman MJ, Bouhuis JM, Aylard DA, Siepel A, dos Santos CO. 2021. Characterization of Gene Expression Signatures for the Identification of Cellular Heterogeneity in the Developing Mammary Gland. *Journal of Mammary Gland Biology and Neoplasia* **26**: 43–66.

Hermans IF, Silk JD, Gileadi U, Salio M, Mathew B, Ritter G, Schmidt R, Harris AL, Old L, Cerundolo V. 2003. NKT Cells Enhance CD4+ and CD8+ T Cell Responses to Soluble Antigen In Vivo through Direct Interaction with Dendritic Cells. *The Journal of Immunology* **171**: 5140–5147.

Hill BS, Sarnella A, D'Avino G, Zannetti A. 2020. Recruitment of stromal cells into tumour microenvironment promote the metastatic spread of breast cancer. *Semin Cancer Biol* **60**: 202–213.

Hitchcock JR, Hughes K, Harris OB, Watson CJ. 2020. Dynamic architectural interplay between leucocytes and mammary epithelial cells. *The FEBS Journal* **287**: 250–266.

Hix LM, Shi YH, Brutkiewicz RR, Stein PL, Wang C-R, Zhang M. 2011. CD1d-Expressing Breast Cancer Cells Modulate NKT Cell-Mediated Antitumor Immunity in a Murine Model of Breast Cancer Metastasis. *PLOS ONE* **6**: e20702.

Hollern DP, Contreras CM, Dance-Barnes S, Silva GO, Pfefferle AD, Xiong J, Darr DB, Usary J, Mott KR, Perou CM. 2019. A mouse model featuring tissue-specific deletion of p53 and Brca1 gives rise to mammary tumors with genomic and transcriptomic similarities to human basal-like breast cancer. *Breast Cancer Res Treat* **174**: 143–155.

Hong S, Scherer DC, Singh N, Mendiratta SK, Serizawa I, Koezuka Y, Kaer LV. 1999. Lipid antigen presentation in the immune system; lessons learned from CD 1 d knockout mice. *Immunological Reviews* **169**: 31–44.

Hong S, Wilson MT, Serizawa I, Wu L, Singh N, Naidenko OV, Miura T, Haba T, Scherer DC, Wei J, et al. 2001. The natural killer T-cell ligand α-galactosylceramide prevents autoimmune diabetes in non-obese diabetic mice. *Nature Medicine* **7**: 1052–1056.

Hovey RC, Aimo L. 2010. Diverse and Active Roles for Adipocytes During Mammary Gland Growth and Function. *J Mammary Gland Biol Neoplasia* **15**: 279–290.

Howard BA, Lu P. 2014. Stromal regulation of embryonic and postnatal mammary epithelial development and differentiation. *Seminars in Cell & Developmental Biology* **25–26**: 43–51.

Huber S. 2015. ERβ and ERα Differentially Regulate NKT and Vγ4+ T-cell Activation and T-regulatory Cell Response in Coxsackievirus B3 Infected Mice. *J Clin Cell Immunol* **6**: 1–9.

Huh SJ, Clement K, Jee D, Merlini A, Choudhury S, Maruyama R, Yoo R, Chytil A, Boyle P, Ran FA, et al. 2015. Age- and Pregnancy-Associated DNA Methylation Changes in Mammary Epithelial Cells. *Stem Cell Reports* **4**: 297–311.

Humphries C. 2013. Adoptive cell therapy: Honing that killer instinct. *Nature* **504**: S13-15.

Husby A, Wohlfahrt J, Øyen N, Melbye M. 2018. Pregnancy duration and breast cancer risk. *Nat Commun* **9**: 4255.

Ibrahim AM, Moss MA, Gray Z, Rojo MD, Burke CM, Schwertfeger KL, dos Santos CO, Machado HL. 2020. Diverse Macrophage Populations Contribute to the Inflammatory Microenvironment in Premalignant Lesions During Localized Invasion. *Frontiers in Oncology* **10**.

Islami F, Liu Y, Jemal A, Zhou J, Weiderpass E, Colditz G, Boffetta P, Weiss M. 2015. Breastfeeding and breast cancer risk by receptor status—a systematic review and meta-analysis. *Annals of Oncology* **26**: 2398–2407.

Jahng A, Maricic I, Aguilera C, Cardell S, Halder RC, Kumar V. 2004. Prevention of autoimmunity by targeting a distinct, noninvariant CD1d-reactive T cell population reactive to sulfatide. *J Exp Med* **199**: 947–957.

Jamieson PR, Dekkers JF, Rios AC, Fu NY, Lindeman GJ, Visvader JE. 2017. Derivation of a robust mouse mammary organoid system for studying tissue dynamics. *Development (Cambridge, England)* **144**: 1065–1071.

Jehmlich U, Alahmad A, Biedenweg D, Hundt M. 2013. The role of palmitoyl-protein thioesterases in T cell activation (P1398). *The Journal of Immunology* **190**: 204.2-204.2.

Jena MK, Jaswal S, Kumar S, Mohanty AK. 2019. Molecular mechanism of mammary gland involution: An update. *Developmental Biology* **445**: 145–155.
Jindal S, Gao D, Bell P, Albrektsen G, Edgerton SM, Ambrosone CB, Thor AD, Borges VF, Schedin P. 2014. Postpartum breast involution reveals regression of secretory lobules mediated by tissue-remodeling. *Breast Cancer Res* **16**: R31.
Jonkers J, Meuwissen R, van der Gulden H, Peterse H, van der Valk M, Berns A. 2001. Synergistic tumor suppressor activity of BRCA2 and p53 in a conditional mouse model for breast cancer. *Nat Genet* **29**: 418–425.
Kale A, Sharma A, Stolzing A, Stolzing A, Desprez P-Y, Desprez P-Y, Campisi J, Campisi J. 2020. Role of immune cells in the removal of deleterious senescent cells. *Immunity and Ageing* **17**.
Kalos M, Levine BL, Porter DL, Katz S, Grupp SA, Bagg A, June CH. 2011. T Cells with Chimeric Antigen Receptors Have Potent Antitumor Effects and Can Establish Memory in Patients with Advanced Leukemia. *Sci Transl Med* **3**: 95ra73.
Karaayvaz M, Cristea S, Gillespie SM, Patel AP, Mylvaganam R, Luo CC, Specht MC, Bernstein BE, Michor F, Ellisen LW. 2018. Unravelling subclonal heterogeneity and aggressive disease states in TNBC through single-cell RNA-seq. *Nat Commun* **9**: 3588.
Kelsey JL, Gammon MD, John EM. 1993. Reproductive factors and breast cancer. *Epidemiol Rev* **15**: 36–47.
Khaled WT, Read EKC, Nicholson SE, Baxter FO, Brennan AJ, Came PJ, Sprigg N, McKenzie ANJ, Watson CJ. 2007. The IL-4/IL-13/Stat6 signalling pathway promotes luminal mammary epithelial cell development. *Development* **134**: 2739–2750.
Kim D, Langmead B, Salzberg SL. 2015. HISAT: A fast spliced aligner with low memory requirements. *Nature Methods* **12**: 357–360.
Kleinman HK, Martin GR. 2005. Matrigel: basement membrane matrix with biological activity. *Seminars in cancer biology* **15**: 378–86.
Klibi J, Amable L, Benlagha K. 2020. A focus on natural killer T-cell subset characterization and developmental stages. *Immunology & Cell Biology* **98**: 358–368.
Kobayashi S, Sugiura H, Ando Y, Shiraki N, Yanagi T, Yamashita H, Toyama T. 2012. Reproductive history and breast cancer risk. *Breast Cancer* **19**: 302–308.
Koledova Z, Lu P. 2017. A 3D Fibroblast-Epithelium Co-culture Model for Understanding Microenvironmental Role in Branching Morphogenesis of the Mammary Gland. *Methods in molecular biology (Clifton, NJ)* **1501**: 217–231.
Kordon EC, Coso OA, Kordon EC, Coso OA. 2017. *Postlactational Involution: Molecular Mechanisms and Relevance for Breast Cancer Development*. IntechOpen https://www.intechopen.com/state.item.id (Accessed October 13, 2022).
Koren S, Reavie L, Couto JP, De Silva D, Stadler MB, Roloff T, Britschgi A, Eichlisberger T, Kohler H, Aina O, et al. 2015. PIK3CA(H1047R) induces multipotency and multi-lineage mammary tumours. *Nature* **525**: 114–118.
Krause S, Maffini M V, Soto AM, Sonnenschein C. 2008. A novel 3D in vitro culture model to study stromal-epithelial interactions in the mammary gland. *Tissue engineering Part C, Methods* **14**: 261–71.
Kreso A, Dick JE. 2014. Evolution of the cancer stem cell model. *Cell Stem Cell* **14**: 275–291.
Kuperwasser C, Chavarria T, Wu M, Magrane G, Gray JW, Carey L, Richardson A, Weinberg RA. 2004. Reconstruction of functionally normal and malignant human breast tissues in mice. *Proc Natl Acad Sci U S A* **101**: 4966–4971.
Lakhani SR, Reis-Filho JS, Fulford L, Penault-Llorca F, van der Vijver M, Parry S, Bishop T, Benitez J, Rivas C, Bignon Y-J, et al. 2005. Prediction of BRCA1 status in patients with breast cancer using estrogen receptor and basal phenotype. *Clin Cancer Res* **11**: 5175–5180.
Langmead B, Salzberg SL. 2012. Fast gapped-read alignment with Bowtie 2. *Nat Methods* **9**: 357–359.
Le Gallo M, de la Motte Rouge T, Poissonnier A, Lavoué V, Tas P, Leveque J, Godey F, Legembre P. 2018. Tumor analysis: freeze–thawing cycle of triple-negative breast cancer cells alters tumor

CD24/CD44 profiles and the percentage of tumor-infiltrating immune cells. *BMC Res Notes* **11**: 401.
Le Nours J, Praveena T, Pellicci DG, Gherardin NA, Ross FJ, Lim RT, Besra GS, Keshipeddy S, Richardson SK, Howell AR, et al. 2016. Atypical natural killer T-cell receptor recognition of CD1d–lipid antigens. *Nature Communications* **7**: 1–14.
Lee MY, Sun L, Veltmaat JM. 2013a. Hedgehog and Gli Signaling in Embryonic Mammary Gland Development. *J Mammary Gland Biol Neoplasia* **18**: 133–138.
Lee YJ, Holzapfel KL, Zhu J, Jameson SC, Hogquist KA. 2013b. Steady-state production of IL-4 modulates immunity in mouse strains and is determined by lineage diversity of i NKT cells. *Nature Immunology* **14**: 1146–1154.
Lee YJ, Starrett GJ, Lee ST, Yang R, Henzler CM, Jameson SC, Hogquist KA. 2016. Lineage-Specific Effector Signatures of Invariant NKT Cells Are Shared amongst γδ T, Innate Lymphoid, and Th Cells. *JI* **197**: 1460–1470.
Legut M, Dolton G, Mian AA, Ottmann OG, Sewell AK. 2018. CRISPR-mediated TCR replacement generates superior anticancer transgenic T cells. *Blood* **131**: 311–322.
Lesterhuis WJ, Haanen JBAG, Punt CJA. 2011. Cancer immunotherapy--revisited. *Nat Rev Drug Discov* **10**: 591–600.
Lewandoski M. 2001. Conditional control of gene expression in the mouse. *Nat Rev Genet* **2**: 743–755.
Li CM-C, Shapiro H, Tsiobikas C, Selfors LM, Chen H, Rosenbluth J, Moore K, Gupta KP, Gray GK, Oren Y, et al. 2020a. Aging-Associated Alterations in Mammary Epithelia and Stroma Revealed by Single-Cell RNA Sequencing. *Cell Reports* **33**: 108566.
Li S, Gestl SA, Gunther EJ. 2020b. A Multistage Murine Breast Cancer Model Reveals Long-Lived Premalignant Clones Refractory to Parity-Induced Protection. *Cancer Prevention Research* **13**: 173–184.
Li X, Fujio M, Imamura M, Wu D, Vasan S, Wong C-H, Ho DD, Tsuji M. 2010. Design of a potent CD1d-binding NKT cell ligand as a vaccine adjuvant. *Proc Natl Acad Sci U S A* **107**: 13010–13015.
Liao Y, Smyth GK, Shi W. 2014. featureCounts: an efficient general purpose program for assigning sequence reads to genomic features. *Bioinformatics* **30**: 923–930.
Lilla JN, Werb Z. 2010. Mast cells contribute to the stromal microenvironment in mammary gland branching morphogenesis. *Dev Biol* **337**: 124–133.
Lim E, Vaillant F, Wu D, Forrest NC, Pal B, Hart AH, Asselin-Labat M-L, Gyorki DE, Ward T, Partanen A, et al. 2009. Aberrant luminal progenitors as the candidate target population for basal tumor development in BRCA1 mutation carriers. *Nat Med* **15**: 907–913.
Liu F, Pawliwec A, Feng Z, Yasruel Z, Lebrun J-J, Ali S. 2015. Prolactin/Jak2 directs apical/basal polarization and luminal linage maturation of mammary epithelial cells through regulation of the Erk1/2 pathway. *Stem Cell Res* **15**: 376–383.
Liu X, Holstege H, van der Gulden H, Treur-Mulder M, Zevenhoven J, Velds A, Kerkhoven RM, van Vliet MH, Wessels LFA, Peterse JL, et al. 2007. Somatic loss of BRCA1 and p53 in mice induces mammary tumors with features of human BRCA1-mutated basal-like breast cancer. *Proc Natl Acad Sci U S A* **104**: 12111–12116.
Liu X, Ory V, Chapman S, Yuan H, Albanese C, Kallakury B, Timofeeva OA, Nealon C, Dakic A, Simic V, et al. 2012. ROCK Inhibitor and Feeder Cells Induce the Conditional Reprogramming of Epithelial Cells. *The American Journal of Pathology* **180**: 599–607.
Lopez-Garcia MA, Geyer FC, Lacroix-Triki M, Marchió C, Reis-Filho JS. 2010. Breast cancer precursors revisited: molecular features and progression pathways. *Histopathology* **57**: 171–192.
Lord SJ, Bernstein L, Johnson KA, Malone KE, McDonald JA, Marchbanks PA, Simon MS, Strom BL, Press MF, Folger SG, et al. 2008. Breast Cancer Risk and Hormone Receptor Status in Older Women by Parity, Age of First Birth, and Breastfeeding: A Case-Control Study. *Cancer Epidemiology, Biomarkers & Prevention* **17**: 1723–1730.

Lühr I, Friedl A, Overath T, Tholey A, Kunze T, Hilpert F, Sebens S, Arnold N, Rösel F, Oberg H-H, et al. 2012. Mammary fibroblasts regulate morphogenesis of normal and tumorigenic breast epithelial cells by mechanical and paracrine signals. *Cancer Letters* **325**: 175–188.
Lynch ED, Ostermeyer EA, Lee MK, Arena JF, Ji H, Dann J, Swisshelm K, Suchard D, MacLeod PM, Kvinnsland S, et al. 1997. Inherited mutations in PTEN that are associated with breast cancer, cowden disease, and juvenile polyposis. *Am J Hum Genet* **61**: 1254–1260.
Lyons TR, O'Brien J, Borges VF, Conklin MW, Keely PJ, Eliceiri KW, Marusyk A, Tan A-C, Schedin P. 2011. Postpartum mammary gland involution drives progression of ductal carcinoma in situ through collagen and COX-2. *Nat Med* **17**: 1109–1115.
Macho-Fernandez E, Brigl M. 2015. The Extended Family of CD1d-Restricted NKT Cells: Sifting through a Mixed Bag of TCRs, Antigens, and Functions. *Frontiers in Immunology* **6**: 362.
Macias H, Hinck L. 2012. Mammary Gland Development. *Wiley Interdiscip Rev Dev Biol* **1**: 533–557.
MacMahon B, Cole P, Lin TM, Lowe CR, Mirra AP, Ravnihar B, Salber EJ, Valaoras VG, Yuasa S. 1970. Age at first birth and breast cancer risk. *Bull World Health Organ* **43**: 209–221.
Maira S-M, Pecchi S, Huang A, Burger M, Knapp M, Sterker D, Schnell C, Guthy D, Nagel T, Wiesmann M, et al. 2012. Identification and Characterization of NVP-BKM120, an Orally Available Pan-Class I PI3-Kinase Inhibitor. *Mol Cancer Ther* **11**: 317–328.
Majumdar D, Tiernan JP, Lobo AJ, Evans CA, Corfe BM. 2012. Keratins in colorectal epithelial function and disease. *International Journal of Experimental Pathology* **93**: 305–318.
Makarem M, Kannan N, Nguyen LV, Knapp DJHF, Balani S, Prater MD, Stingl J, Raouf A, Nemirovsky O, Eirew P, et al. 2013. Developmental Changes in the in Vitro Activated Regenerative Activity of Primitive Mammary Epithelial Cells. *PLOS Biology* **11**: e1001630.
Maller O, Hansen KC, Lyons TR, Acerbi I, Weaver VM, Prekeris R, Tan A-C, Schedin P. 2013. Collagen architecture in pregnancy-induced protection from breast cancer. *J Cell Sci* **126**: 4108–4110.
Mantell BS, Stefanovic-Racic M, Yang X, Dedousis N, Sipula IJ, O'Doherty RM. 2011. Mice Lacking NKT Cells but with a Complete Complement of CD8+ T-Cells Are Not Protected against the Metabolic Abnormalities of Diet-Induced Obesity. *PLOS ONE* **6**: e19831.
Martinson HA, Jindal S, Durand-Rougely C, Borges VF, Schedin P. 2015. Wound healing-like immune program facilitates postpartum mammary gland involution and tumor progression. *Int J Cancer* **136**: 1803–1813.
Marusyk A, Polyak K. 2010. Tumor heterogeneity: causes and consequences. *Biochim Biophys Acta* **1805**: 105–117.
Maus MV, Fraietta JA, Levine BL, Kalos M, Zhao Y, June CH. 2014. Adoptive Immunotherapy for Cancer or Viruses. *Annu Rev Immunol* **32**: 189–225.
McLean CY, Bristor D, Hiller M, Clarke SL, Schaar BT, Lowe CB, Wenger AM, Bejerano G. 2010. GREAT improves functional interpretation of cis-regulatory regions. *Nat Biotechnol* **28**: 495–501.
McLeay RC, Bailey TL. 2010. Motif Enrichment Analysis: a unified framework and an evaluation on ChIP data. *BMC Bioinformatics* **11**: 165.
Medina D. 2009. Breast Cancer: The Protective Effect of Pregnancy. *Clinical Cancer Research* **10**: 380s–384s.
Medina D. 2010. Of Mice and Women: A Short History of Mouse Mammary Cancer Research with an Emphasis on the Paradigms Inspired by the Transplantation Method. *Cold Spring Harb Perspect Biol* **2**: a004523.
Medina D, Kittrell FS. 2003. p53 function is required for hormone-mediated protection of mouse mammary tumorigenesis. *Cancer Res* **63**: 6140–6143.
Meers MP, Tenenbaum D, Henikoff S. 2019. Peak calling by Sparse Enrichment Analysis for CUT&RUN chromatin profiling. *Epigenetics & Chromatin* **12**: 42.
Meier-Abt F, Bentires-Alj M. 2014. How pregnancy at early age protects against breast cancer. *Trends in Molecular Medicine* **20**: 143–153.

Meier-Abt F, Milani E, Roloff T, Brinkhaus H, Duss S, Meyer DS, Klebba I, Balwierz PJ, van Nimwegen E, Bentires-Alj M. 2013. Parity induces differentiation and reduces Wnt/Notch signaling ratio and proliferation potential of basal stem/progenitor cells isolated from mouse mammary epithelium. *Breast Cancer Res* **15**: R36.

Melbye M, Wohlfahrt J, Olsen JH, Frisch M, Westergaard T, Helweg-Larsen K, Andersen PK. 1997. Induced Abortion and the Risk of Breast Cancer. *New England Journal of Medicine* **336**: 81–85.

Melhem-Bertrandt A, Bojadzieva J, Ready KJ, Obeid E, Liu DD, Gutierrez-Barrera AM, Litton JK, Olopade OI, Hortobagyi GN, Strong LC, et al. 2012. Early onset HER2-positive breast cancer is associated with germline TP53 mutations. *Cancer* **118**: 908–913.

Metelitsa LS, Naidenko OV, Kant A, Wu H-W, Loza MJ, Perussia B, Kronenberg M, Seeger RC. 2001. Human NKT Cells Mediate Antitumor Cytotoxicity Directly by Recognizing Target Cell CD1d with Bound Ligand or Indirectly by Producing IL-2 to Activate NK Cells. *The Journal of Immunology* **167**: 3114–3122.

Middleton LP, Amin M, Gwyn K, Theriault R, Sahin A. 2003. Breast carcinoma in pregnant women: assessment of clinicopathologic and immunohistochemical features. *Cancer* **98**: 1055–1060.

Mincheva-Nilsson L. 2003. Pregnancy and gamma/delta T cells: Taking on the hard questions. *Reproductive Biology and Endocrinology* **1**.

Molyneux G, Geyer FC, Magnay F-A, McCarthy A, Kendrick H, Natrajan R, MacKay A, Grigoriadis A, Tutt A, Ashworth A, et al. 2010. BRCA1 Basal-like Breast Cancers Originate from Luminal Epithelial Progenitors and Not from Basal Stem Cells. *Cell Stem Cell* **7**: 403–417.

Mombaerts P, Iacomini J, Johnson RS, Herrup K, Tonegawa S, Papaioannou VE. 1992. RAG-1-deficient mice have no mature B and T lymphocytes. *Cell* **68**: 869–877.

Monks J, Rosner D, Jon Geske F, Lehman L, Hanson L, Neville MC, Fadok VA. 2005. Epithelial cells as phagocytes: apoptotic epithelial cells are engulfed by mammary alveolar epithelial cells and repress inflammatory mediator release. *Cell Death Differ* **12**: 107–114.

Moore DM, Vogl AW, Baimbridge K, Emerman JT. 1987. Effect of calcium on oxytocin-induced contraction of mammary gland myoepithelium as visualized by NBD-phallacidin. *J Cell Sci* **88 ( Pt 5)**: 563–569.

Morsing M, Klitgaard MC, Jafari A, Villadsen R, Kassem M, Petersen OW, Rønnov-Jessen L. 2016. Evidence of two distinct functionally specialized fibroblast lineages in breast stroma. *Breast Cancer Res* **18**: 108.

Mycko MP, Ferrero I, Wilson A, Jiang W, Bianchi T, Trumpp A, MacDonald HR. 2009. Selective Requirement for c-Myc at an Early Stage of Vα14i NKT Cell Development. *The Journal of Immunology* **182**: 4641–4648.

Na YR, Jung D, Song J, Park J-W, Hong JJ, Seok SH. 2020. Pyruvate dehydrogenase kinase is a negative regulator of interleukin-10 production in macrophages. *J Mol Cell Biol* **12**: 543–555.

Nagato K, Motohashi S, Ishibashi F, Okita K, Yamasaki K, Moriya Y, Hoshino H, Yoshida S, Hanaoka H, Fujii S, et al. 2012. Accumulation of Activated Invariant Natural Killer T Cells in the Tumor Microenvironment after α-Galactosylceramide-Pulsed Antigen Presenting Cells. *J Clin Immunol* **32**: 1071–1081.

Nassour M, Idoux-Gillet Y, Selmi A, Côme C, Faraldo M-LM, Deugnier M-A, Savagner P. 2012. Slug controls stem/progenitor cell growth dynamics during mammary gland morphogenesis. *PloS one* **7**: e53498.

Nichols HB, Schoemaker MJ, Cai J, Xu J, Wright LB, Brook MN, Jones ME, Adami H-O, Baglietto L, Bertrand KA, et al. 2019. Breast Cancer Risk After Recent Childbirth. *Ann Intern Med* **170**: 22–30.

Nik-Zainal S, Davies H, Staaf J, Ramakrishna M, Glodzik D, Zou X, Martincorena I, Alexandrov LB, Martin S, Wedge DC, et al. 2016. Landscape of somatic mutations in 560 breast cancer whole-genome sequences. *Nature* **534**: 47–54.

Nowell PC. 1976. The clonal evolution of tumor cell populations. *Science* **194**: 23–28.

O'Brien J, Lyons T, Monks J, Lucia MS, Wilson RS, Hines L, Man Y, Borges V, Schedin P. 2010. Alternatively activated macrophages and collagen remodeling characterize the postpartum involuting mammary gland across species. *Am J Pathol* **176**: 1241–1255.

Oh SJ, Ahn S, Jin Y-H, Ishifune C, Kim JH, Yasutomo K, Chung DH. 2015. Notch 1 and Notch 2 synergistically regulate the differentiation and function of invariant NKT cells. *Journal of Leukocyte Biology* **98**: 781–789.

Ormandy CJ, Binart N, Kelly PA. 1997a. Mammary gland development in prolactin receptor knockout mice. *J Mammary Gland Biol Neoplasia* **2**: 355–364.

Ormandy CJ, Camus A, Barra J, Damotte D, Lucas B, Buteau H, Edery M, Brousse N, Babinet C, Binart N, et al. 1997b. Null mutation of the prolactin receptor gene produces multiple reproductive defects in the mouse. *Genes Dev* **11**: 167–178.

Pal B, Chen Y, Milevskiy MJG, Vaillant F, Prokopuk L, Dawson CA, Capaldo BD, Song X, Jackling F, Timpson P, et al. 2021. Single cell transcriptome atlas of mouse mammary epithelial cells across development. *Breast Cancer Research* **23**.

Pal B, Chen Y, Vaillant F, Jamieson P, Gordon L, Rios AC, Wilcox S, Fu N, Liu KH, Jackling FC, et al. 2017. Construction of developmental lineage relationships in the mouse mammary gland by single-cell RNA profiling. *Nat Commun* **8**: 1627.

Pang M-F, Georgoudaki A-M, Lambut L, Johansson J, Tabor V, Hagikura K, Jin Y, Jansson M, Alexander JS, Nelson CM, et al. 2016. TGF-β1-induced EMT promotes targeted migration of breast cancer cells through the lymphatic system by the activation of CCR7/CCL21-mediated chemotaxis. *Oncogene* **35**: 748–60.

Paul S, Lal G. 2016. Regulatory and effector functions of gamma–delta (γδ) T cells and their therapeutic potential in adoptive cellular therapy for cancer. *International Journal of Cancer* **139**: 976–985.

Pellicci DG, Uldrich AP, Le Nours J, Ross F, Chabrol E, Eckle SBG, de Boer R, Lim RT, McPherson K, Besra G, et al. 2014. The molecular bases of δ/αβ T cell–mediated antigen recognition. *J Exp Med* **211**: 2599–2615.

Pepper MS, Baetens D, Mandriota SJ, Di Sanza C, Oikemus S, Lane TF, Soriano JV, Montesano R, Iruela-Arispe ML. 2000. Regulation of VEGF and VEGF receptor expression in the rodent mammary gland during pregnancy, lactation, and involution. *Dev Dyn* **218**: 507–524.

Pilewskie M, Gorodinsky P, Fought A, Hansen N, Bethke K, Jeruss J, Scholtens D, Khan SA. 2012. Association between recency of last pregnancy and biologic subtype of breast cancer. *Ann Surg Oncol* **19**: 1167–1173.

Plaks V, Boldajipour B, Linnemann JR, Nguyen NH, Kersten K, Wolf Y, Casbon A-J, Kong N, van den Bijgaart RJE, Sheppard D, et al. 2015. Adaptive Immune Regulation of Mammary Postnatal Organogenesis. *Developmental Cell* **34**: 493–504.

Pollard JW, Hennighausen L. 1994. Colony stimulating factor 1 is required for mammary gland development during pregnancy. *Proc Natl Acad Sci U S A* **91**: 9312–9316.

Quinlan AR, Hall IM. 2010. BEDTools: a flexible suite of utilities for comparing genomic features. *Bioinformatics* **26**: 841–842.

Rahat MA, Coffelt SB, Granot Z, Muthana M, Amedei A. 2016. Macrophages and Neutrophils: Regulation of the Inflammatory Microenvironment in Autoimmunity and Cancer. *Mediators of Inflammation* **2016**.

Rahman N, Seal S, Thompson D, Kelly P, Renwick A, Elliott A, Reid S, Spanova K, Barfoot R, Chagtai T, et al. 2007. PALB2, which encodes a BRCA2-interacting protein, is a breast cancer susceptibility gene. *Nat Genet* **39**: 165–167.

Ran S, Volk L, Hall K, Flister MJ. 2010. Lymphangiogenesis and lymphatic metastasis in breast cancer. *Pathophysiology* **17**: 229–251.

Ray S, Chhabra A, Chakraborty NG, Hegde U, Dorsky DI, Chodon T, von Euw E, Comin-Anduix B, Koya RC, Ribas A, et al. 2010. MHC-I-restricted melanoma antigen specific TCR-engineered human CD4+ T cells exhibit multifunctional effector and helper responses, in vitro. *Clin Immunol* **136**: 338–347.

Reid JA, Mollica PA, Bruno RD, Sachs PC. 2018. Consistent and reproducible cultures of large-scale 3D mammary epithelial structures using an accessible bioprinting platform. *Breast cancer research : BCR* **20**: 122.

Renwick A, Thompson D, Seal S, Kelly P, Chagtai T, Ahmed M, North B, Jayatilake H, Barfoot R, Spanova K, et al. 2006. ATM mutations that cause ataxia-telangiectasia are breast cancer susceptibility alleles. *Nat Genet* **38**: 873–875.

Restifo NP, Dudley ME, Rosenberg SA. 2012. Adoptive immunotherapy for cancer: harnessing the T cell response. *Nat Rev Immunol* **12**: 269–281.

Ricciardelli C, Lokman NA, Pyragius CE, Ween MP, Macpherson AM, Ruszkiewicz A, Hoffmann P, Oehler MK. 2017. Keratin 5 overexpression is associated with serous ovarian cancer recurrence and chemotherapy resistance. *Oncotarget* **8**: 17819–17832.

Richter J, Neparidze N, Zhang L, Nair S, Monesmith T, Sundaram R, Miesowicz F, Dhodapkar KM, Dhodapkar MV. 2013. Clinical regressions and broad immune activation following combination therapy targeting human NKT cells in myeloma. *Blood* **121**: 423–430.

Rios AC, Fu NY, Lindeman GJ, Visvader JE. 2014. In situ identification of bipotent stem cells in the mammary gland. *Nature* **506**: 322–327.

Rizvi ZA, Puri N, Saxena RK. 2015. Lipid antigen presentation through CD1d pathway in mouse lung epithelial cells, macrophages and dendritic cells and its suppression by poly-dispersed single-walled carbon nanotubes. *Toxicol In Vitro* **29**: 1275–1282.

Robbins PF, Morgan RA, Feldman SA, Yang JC, Sherry RM, Dudley ME, Wunderlich JR, Nahvi AV, Helman LJ, Mackall CL, et al. 2011. Tumor Regression in Patients With Metastatic Synovial Cell Sarcoma and Melanoma Using Genetically Engineered Lymphocytes Reactive With NY-ESO-1. *J Clin Oncol* **29**: 917–924.

Robinson GW. 2007. Cooperation of signalling pathways in embryonic mammary gland development. *Nat Rev Genet* **8**: 963–972.

Robinson GW, McKnight RA, Smith GH, Hennighausen L. 1995. Mammary epithelial cells undergo secretory differentiation in cycling virgins but require pregnancy for the establishment of terminal differentiation. *Development* **121**: 2079–2090.

Rodriguez-Boulan E, Macara IG. 2014. Organization and execution of the epithelial polarity programme. *Nat Rev Mol Cell Biol* **15**: 225–242.

Rosenbluth JM, Schackmann RCJ, Gray GK, Selfors LM, Li CM-C, Boedicker M, Kuiken HJ, Richardson A, Brock J, Garber J, et al. 2020. Organoid cultures from normal and cancer-prone human breast tissues preserve complex epithelial lineages. *Nature communications* **11**: 1711.

Rosner B, Colditz GA, Willett WC. 1994. Reproductive Risk Factors in a Prospective Study of Breast Cancer: The Nurses' Health Study. *Am J Epidemiol* **139**: 819–835.

Russo IH, Russo J. 1996. Mammary gland neoplasia in long-term rodent studies. *Environ Health Perspect* **104**: 938–967.

Russo J, Balogh GA, Russo IH, and the Fox Chase Cancer Center Hospital Network Participants. 2008. Full-term Pregnancy Induces a Specific Genomic Signature in the Human Breast. *Cancer Epidemiology Biomarkers & Prevention* **17**: 51–66.

Russo J, Santucci-Pereira J, Cicco RL de, Sheriff F, Russo PA, Peri S, Slifker M, Ross E, Mello MLS, Vidal BC, et al. 2012. Pregnancy-induced chromatin remodeling in the breast of postmenopausal women. *International Journal of Cancer* **131**: 1059–1070.

Saeki K, Chang G, Kanaya N, Wu X, Wang J, Bernal L, Ha D, Neuhausen SL, Chen S. 2021. Mammary cell gene expression atlas links epithelial cell remodeling events to breast carcinogenesis. *Communications Biology* **4**.

Sag D, Krause P, Hedrick CC, Kronenberg M, Wingender G. 2014. IL-10–producing NKT10 cells are a distinct regulatory invariant NKT cell subset. *J Clin Invest* **124**: 3725–3740.

Salio M, Silk JD, Yvonne Jones E, Cerundolo V. 2014. Biology of CD1- and MR1-Restricted T Cells. *Annu Rev Immunol* **32**: 323–366.

Samocha A, Doh H, Kessenbrock K, Roose JP. 2019. Unraveling Heterogeneity in Epithelial Cell Fates of the Mammary Gland and Breast Cancer. *Cancers (Basel)* **11**. https://www.ncbi.nlm.nih.gov/pmc/articles/PMC6826786/ (Accessed June 1, 2020).
Santo CD, Salio M, Masri SH, Lee LY-H, Dong T, Speak AO, Porubsky S, Booth S, Veerapen N, Besra GS, et al. 2008. Invariant NKT cells reduce the immunosuppressive activity of influenza A virus–induced myeloid-derived suppressor cells in mice and humans. *J Clin Invest* **118**: 4036–4048.
Savage AK, Constantinides MG, Han J, Picard D, Martin E, Li B, Lantz O, Bendelac A. 2008. The transcription factor PLZF directs the effector program of the NKT cell lineage. *Immunity* **29**: 391–403.
Schedin P. 2006. Pregnancy-associated breast cancer and metastasis. *Nature Reviews Cancer* **6**: 281–291.
Schedin P, Mitrenga T, McDaniel S, Kaeck M. 2004. Mammary ECM composition and function are altered by reproductive state. *Molecular Carcinogenesis* **41**: 207–220.
Schindelin J, Arganda-Carreras I, Frise E, Kaynig V, Longair M, Pietzsch T, Preibisch S, Rueden C, Saalfeld S, Schmid B, et al. 2012. Fiji: an open-source platform for biological-image analysis. *Nat Methods* **9**: 676–682.
Schoppmann SF, Bayer G, Aumayr K, Taucher S, Geleff S, Rudas M, Kubista E, Hausmaninger H, Samonigg H, Gnant M, et al. 2004. Prognostic Value of Lymphangiogenesis and Lymphovascular Invasion in Invasive Breast Cancer. *Ann Surg* **240**: 306–312.
Schwertfeger KL, Richert MM, Anderson SM. 2001. Mammary gland involution is delayed by activated Akt in transgenic mice. *Molecular Endocrinology* **15**: 867–881.
Seiler MP, Mathew R, Liszewski MK, Spooner CJ, Spooner C, Barr K, Meng F, Singh H, Bendelac A. 2012. Elevated and sustained expression of the transcription factors Egr1 and Egr2 controls NKT lineage differentiation in response to TCR signaling. *Nat Immunol* **13**: 264–271.
Seshan VE, Olshen A. 2022. DNAcopy: DNA copy number data analysis. https://bioconductor.org/packages/DNAcopy/ (Accessed October 19, 2022).
Shakhar K, Valdimarsdottir HB, Bovbjerg DH. 2007. Heightened Risk of Breast Cancer Following Pregnancy: Could Lasting Systemic Immune Alterations Contribute? *Cancer Epidemiol Biomarkers Prev* **16**: 1082–1086.
Shamir ER, Ewald AJ. 2014. Three-dimensional organotypic culture: experimental models of mammalian biology and disease. *Nature Reviews Molecular Cell Biology* **15**: 647–664.
Sharp JA, Lefevre C, Brennan AJ, Nicholas KR. 2007. The Fur Seal—a Model Lactation Phenotype to Explore Molecular Factors Involved in the Initiation of Apoptosis at Involution. *J Mammary Gland Biol Neoplasia* **12**: 47–58.
Shimizu K, Kurosawa Y, Taniguchi M, Steinman RM, Fujii S. 2007. Cross-presentation of glycolipid from tumor cells loaded with α-galactosylceramide leads to potent and long-lived T cell–mediated immunity via dendritic cells. *J Exp Med* **204**: 2641–2653.
Shissler SC, Webb TJ. 2019. Inhibition of PI3K promotes anti-tumor immune responses to Mantle Cell Lymphoma. *The Journal of Immunology* **202**: 194.45-194.45.
Simian M, Hirai Y, Navre M, Werb Z, Lochter A, Bissell MJ. 2001. The interplay of matrix metalloproteinases, morphogens and growth factors is necessary for branching of mammary epithelial cells. *Development* **128**: 3117–3131.
Sinha DK, Pazik JE, Dao TL. 1988. Prevention of mammary carcinogenesis in rats by pregnancy: effect of full-term and interrupted pregnancy. *Br J Cancer* **57**: 390–394.
Sivaraman L, Conneely OM, Medina D, O'Malley BW. 2001. p53 is a potential mediator of pregnancy and hormone-induced resistance to mammary carcinogenesis. *Proc Natl Acad Sci U S A* **98**: 12379–12384.
Skibinski A, Kuperwasser C. 2015. The origin of breast tumor heterogeneity. *Oncogene* **34**: 5309–5316.
Skobe M, Hawighorst T, Jackson DG, Prevo R, Janes L, Velasco P, Riccardi L, Alitalo K, Claffey K, Detmar M. 2001. Induction of tumor lymphangiogenesis by VEGF-C promotes breast cancer metastasis. *Nat Med* **7**: 192–198.
Slade D. 2020. PARP and PARG inhibitors in cancer treatment. *Genes Dev* **34**: 360–394.

Slepicka PF, Cyrill SL, dos Santos CO. 2019. Pregnancy and Breast Cancer: Pathways to Understand Risk and Prevention. *Trends in Molecular Medicine*. http://www.sciencedirect.com/science/article/pii/S1471491419301650 (Accessed September 26, 2019).

Slepicka PF, Somasundara AVH, dos Santos CO. 2021. The molecular basis of mammary gland development and epithelial differentiation. *Seminars in Cell & Developmental Biology* **114**: 93–112.

Smyth MJ, Crowe NY, Pellicci DG, Kyparissoudis K, Kelly JM, Takeda K, Yagita H, Godfrey DI. 2002. Sequential production of interferon-γ by NK1.1+ T cells and natural killer cells is essential for the antimetastatic effect of α-galactosylceramide. *Blood* **99**: 1259–1266.

Sokolova A, Johnstone KJ, McCart Reed AE, Simpson PT, Lakhani SR. 2022. Hereditary breast cancer: syndromes, tumour pathology and molecular testing. *Histopathology* **n/a**. https://onlinelibrary.wiley.com/doi/abs/10.1111/his.14808 (Accessed December 7, 2022).

Sønderstrup IMH, Jensen M-BR, Ejlertsen B, Eriksen JO, Gerdes A-M, Kruse TA, Larsen MJ, Thomassen M, Lænkholm A-V. 2019. Subtypes in BRCA-mutated breast cancer. *Hum Pathol* **84**: 192–201.

Song L, Asgharzadeh S, Salo J, Engell K, Wu H, Sposto R, Ara T, Silverman AM, DeClerck YA, Seeger RC, et al. 2009. Vα24-invariant NKT cells mediate antitumor activity via killing of tumor-associated macrophages. *J Clin Invest* **119**: 1524–1536.

Sørlie T, Tibshirani R, Parker J, Hastie T, Marron JS, Nobel A, Deng S, Johnsen H, Pesich R, Geisler S, et al. 2003. Repeated observation of breast tumor subtypes in independent gene expression data sets. *Proc Natl Acad Sci U S A* **100**: 8418–8423.

Stacker SA, Caesar C, Baldwin ME, Thornton GE, Williams RA, Prevo R, Jackson DG, Nishikawa S, Kubo H, Achen MG. 2001. VEGF-D promotes the metastatic spread of tumor cells via the lymphatics. *Nat Med* **7**: 186–191.

Stein T, Morris JS, Davies CR, Weber-Hall SJ, Duffy M-A, Heath VJ, Bell AK, Ferrier RK, Sandilands GP, Gusterson BA. 2004. Involution of the mouse mammary gland is associated with an immune cascade and an acute-phase response, involving LBP, CD14 and STAT3. *Breast Cancer Res* **6**: R75–R91.

Stewart TA, Hughes K, Hume DA, Davis FM. 2019. Developmental Stage-Specific Distribution of Macrophages in Mouse Mammary Gland. *Frontiers in Cell and Developmental Biology* **7**.

Stordal B. 2022. Breastfeeding reduces the risk of breast cancer: A call for action in high-income countries with low rates of breastfeeding. *Cancer Medicine* **n/a**. https://onlinelibrary.wiley.com/doi/abs/10.1002/cam4.5288 (Accessed October 31, 2022).

Stuart T, Butler A, Hoffman P, Hafemeister C, Papalexi E, Mauck WM, Hao Y, Stoeckius M, Smibert P, Satija R. 2019. Comprehensive Integration of Single-Cell Data. *Cell* **177**: 1888-1902.e21.

Subramanian A, Tamayo P, Mootha VK, Mukherjee S, Ebert BL, Gillette MA, Paulovich A, Pomeroy SL, Golub TR, Lander ES, et al. 2005. Gene set enrichment analysis: A knowledge-based approach for interpreting genome-wide expression profiles. *Proceedings of the National Academy of Sciences* **102**: 15545–15550.

Sulahian R, Chen J, Arany Z, Jadhav U, Peng S, Rustgi AK, Bass AJ, Srivastava A, Hornick JL, Shivdasani RA. 2015. SOX15 Governs Transcription in Human Stratified Epithelia and a Subset of Esophageal Adenocarcinomas. *Cell Mol Gastroenterol Hepatol* **1**: 598-609.e6.

Sumbal J, Chiche A, Charifou E, Koledova Z, Li H. 2020. Primary Mammary Organoid Model of Lactation and Involution. *Front Cell Dev Biol* **8**. https://www.frontiersin.org/articles/10.3389/fcell.2020.00068/full#h1 (Accessed June 1, 2020).

Taneja P, Frazier DP, Kendig RD, Maglic D, Sugiyama T, Kai F, Taneja NK, Inoue K. 2009. MMTV mouse models and the diagnostic values of MMTV-like sequences in human breast cancer. *Expert Rev Mol Diagn* **9**: 423–440.

Terabe M, Swann J, Ambrosino E, Sinha P, Takaku S, Hayakawa Y, Godfrey DI, Ostrand-Rosenberg S, Smyth MJ, Berzofsky JA. 2005. A nonclassical non-Valpha14Jalpha18 CD1d-restricted (type II)

NKT cell is sufficient for down-regulation of tumor immunosurveillance. *J Exp Med* **202**: 1627–1633.

Terry MB, Liao Y, Kast K, Antoniou AC, McDonald JA, Mooij TM, Engel C, Nogues C, Buecher B, Mari V, et al. 2018. The Influence of Number and Timing of Pregnancies on Breast Cancer Risk for Women With *BRCA1* or *BRCA2* Mutations. *JNCI Cancer Spectrum* **2**. https://academic.oup.com/jncics/article/doi/10.1093/jncics/pky078/5370381 (Accessed April 7, 2019).

Thibeault SL, Rees L, Pazmany L, Birchall MA. 2009. At the crossroads: mucosal immunology of the larynx. *Mucosal Immunol* **2**: 122–128.

Thordarson G, Jin E, Guzman RC, Swanson SM, Nandi S, Talamantes F. 1995. Refractoriness to mammary tumorigenesis in parous rats: is it caused by persistent changes in the hormonal environment or permanent biochemical alterations in the mammary epithelia? *Carcinogenesis* **16**: 2847–2853.

Tickle C, Jung H-S. 2016. Embryonic Mammary Gland Development. In *eLS*, pp. 1–10, John Wiley & Sons, Ltd https://onlinelibrary.wiley.com/doi/abs/10.1002/9780470015902.a0026057 (Accessed October 24, 2022).

Tiede B, Kang Y. 2011. From milk to malignancy: the role of mammary stem cells in development, pregnancy and breast cancer. *Cell Res* **21**: 245–257.

Townsend MJ, Weinmann AS, Matsuda JL, Salomon R, Farnham PJ, Biron CA, Gapin L, Glimcher LH. 2004. T-bet Regulates the Terminal Maturation and Homeostasis of NK and Vα14i NKT Cells. *Immunity* **20**: 477–494.

Treiner E, Duban L, Bahram S, Radosavljevic M, Wanner V, Tilloy F, Affaticati P, Gilfillan S, Lantz O. 2003. Selection of evolutionarily conserved mucosal-associated invariant T cells by MR1. *Nature* **422**: 164–169.

Twigger A-J, Engelbrecht LK, Bach K, Schultz-Pernice I, Pensa S, Stenning J, Petricca S, Scheel CH, Khaled WT. 2022. Transcriptional changes in the mammary gland during lactation revealed by single cell sequencing of cells from human milk. *Nature Communications* **13**.

Uldrich AP, Le Nours J, Pellicci DG, Gherardin NA, McPherson KG, Lim RT, Patel O, Beddoe T, Gras S, Rossjohn J, et al. 2013. CD1d-lipid antigen recognition by the γδ TCR. *Nature Immunology* **14**: 1137–1145.

Ussher JE, Willberg CB, Klenerman P. 2018. MAIT cells and viruses. *Immunol Cell Biol* **96**: 630–641.

Van Keymeulen A, Lee MY, Ousset M, Brohée S, Rorive S, Giraddi RR, Wuidart A, Bouvencourt G, Dubois C, Salmon I, et al. 2015. Reactivation of multipotency by oncogenic PIK3CA induces breast tumour heterogeneity. *Nature* **525**: 119–123.

Van Keymeulen A, Rocha AS, Ousset M, Beck B, Bouvencourt G, Rock J, Sharma N, Dekoninck S, Blanpain C. 2011. Distinct stem cells contribute to mammary gland development and maintenance. *Nature* **479**: 189–193.

Waddell N, Arnold J, Cocciardi S, da Silva L, Marsh A, Riley J, Johnstone CN, Orloff M, Assie G, Eng C, et al. 2010. Subtypes of familial breast tumours revealed by expression and copy number profiling. *Breast Cancer Res Treat* **123**: 661–677.

Wagner K-U, Ward T, Davis B, Wiseman R, Hennighausen L. 2001. Spatial and temporal expression of the Cre gene under the control of the MMTV-LTR in different lines of transgenic mice. *Transgenic Res* **10**: 545–553.

Walsh T, Casadei S, Coats KH, Swisher E, Stray SM, Higgins J, Roach KC, Mandell J, Lee MK, Ciernikova S, et al. 2006. Spectrum of mutations in BRCA1, BRCA2, CHEK2, and TP53 in families at high risk of breast cancer. *JAMA* **295**: 1379–1388.

Wang X, Kaplan DL. 2012. Hormone-responsive 3D multicellular culture model of human breast tissue. *Biomaterials* **33**: 3411–3420.

Wang Y, Chaffee TS, LaRue RS, Huggins DN, Witschen PM, Ibrahim AM, Nelson AC, Machado HL, Schwertfeger KL. 2020. Tissue-resident macrophages promote extracellular matrix homeostasis

in the mammary gland stroma of nulliparous mice eds. S. Rath, C.V. Rothlin, and F. Davis. *eLife* **9**: e57438.
Webster J, Wallace RM, Clark AJ, Whitelaw CB. 1995. Tissue-specific, temporally regulated expression mediated by the proximal ovine beta-lactoglobulin promoter in transgenic mice. *Cell Mol Biol Res* **41**: 11–15.
Wen J, Kawamata Y, Tojo H, Tanaka S, Tachi C. 1995. Expression of whey acidic protein (WAP) genes in tissues other than the mammary gland in normal and transgenic mice expressing mWAP/hGH fusion gene. *Mol Reprod Dev* **41**: 399–406.
Wilson JRF, Bateman AC, Hanson H, An Q, Evans G, Rahman N, Jones JL, Eccles DM. 2010. A novel HER2-positive breast cancer phenotype arising from germline TP53 mutations. *Journal of Medical Genetics* **47**: 771–774.
Wohlfahrt J, Melbye M. 2001. Age at Any Birth Is Associated with Breast Cancer Risk. *Epidemiology* **12**: 68–73.
Wolf K, Alexander S, Schacht V, Coussens LM, von Andrian UH, van Rheenen J, Deryugina E, Friedl P. 2009. Collagen-based cell migration models in vitro and in vivo. *Seminars in cell & developmental biology* **20**: 931–41.
Wu B, Sun X, Gupta HB, Yuan B, Li J, Ge F, Chiang H-C, Zhang X, Zhang C, Zhang D, et al. 2018. Adipose PD-L1 Modulates PD-1/PD-L1 Checkpoint Blockade Immunotherapy Efficacy in Breast Cancer. *Oncoimmunology* **7**: e1500107.
Wu DY, Segal NH, Sidobre S, Kronenberg M, Chapman PB. 2003. Cross-presentation of disialoganglioside GD3 to natural killer T cells. *J Exp Med* **198**: 173–181.
Wu Q, Li B, Li Z, Li J, Sun S, Sun S. 2019a. Cancer-associated adipocytes: key players in breast cancer progression. *Journal of Hematology & Oncology* **12**: 95.
Wu Y, Kyle-Cezar F, Woolf RT, Naceur-Lombardelli C, Owen J, Biswas D, Lorenc A, Vantourout P, Gazinska P, Grigoriadis A, et al. 2019b. An innate-like Vδ1+ γδ T cell compartment in the human breast is associated with remission in triple-negative breast cancer. *Science Translational Medicine* **11**.
Xu J, Chen Y, Olopade OI. 2010. MYC and Breast Cancer. *Genes Cancer* **1**: 629–640.
Xu J, Lamouille S, Derynck R. 2009. TGF-β-induced epithelial to mesenchymal transition. *Cell Research* **19**: 156–172.
Yang J, Weinberg RA. 2008. Epithelial-mesenchymal transition: at the crossroads of development and tumor metastasis. *Dev Cell* **14**: 818–829.
Yang Y-H, Liu J-W, Lu C, Wei J-F. 2022. CAR-T Cell Therapy for Breast Cancer: From Basic Research to Clinical Application. *Int J Biol Sci* **18**: 2609–2626.
Ye X, Tam WL, Shibue T, Kaygusuz Y, Reinhardt F, Ng Eaton E, Weinberg RA. 2015. Distinct EMT programs control normal mammary stem cells and tumour-initiating cells. *Nature* **525**: 256–260.
Yu J, Mitsui T, Wei M, Mao H, Butchar JP, Shah MV, Zhang J, Mishra A, Alvarez-Breckenridge C, Liu X, et al. 2011. NKp46 identifies an NKT cell subset susceptible to leukemic transformation in mouse and human. *Journal of Clinical Investigation* **121**: 1456–1470.
Zeng D, Lewis D, Dejbakhsh-Jones S, Lan F, García-Ojeda M, Sibley R, Strober S. 1999. Bone Marrow NK1.1− and NK1.1+ T Cells Reciprocally Regulate Acute Graft versus Host Disease. *J Exp Med* **189**: 1073–1081.
Zhang H, Somasundaram K, Peng Y, Tian H, Zhang H, Bi D, Weber BL, El-Deiry WS. 1998. BRCA1 physically associates with p53 and stimulates its transcriptional activity. *Oncogene* **16**: 1713–1721.
Zhang J, Xia Y, Zhou X, Yu H, Tan Y, Du Y, Zhang Q, Wu Y. 2022. Current landscape of personalized clinical treatments for triple-negative breast cancer. *Frontiers in Pharmacology* **13**. https://www.frontiersin.org/articles/10.3389/fphar.2022.977660 (Accessed October 9, 2022).
Zhang R, Liu X, Huang W, Shao B, Yan Y, Liang X, Ran R, Song G, Di L, Jiang H, et al. 2021. Clinicopathological features and prognosis of patients with pregnancy-associated breast cancer: A matched case control study. *Asia-Pacific Journal of Clinical Oncology* **17**: 396–402.

Zhang Y, Liu T, Meyer CA, Eeckhoute J, Johnson DS, Bernstein BE, Nusbaum C, Myers RM, Brown M, Li W, et al. 2008. Model-based Analysis of ChIP-Seq (MACS). *Genome Biology* **9**: R137.

Zhang Y, Springfield R, Chen S, Li X, Feng X, Moshirian R, Yang R, Yuan W. 2019. α-GalCer and iNKT cell-based cancer immunotherapy: Realizing the therapeutic potentials. *Frontiers in Immunology* **10**.

Zheng GXY, Terry JM, Belgrader P, Ryvkin P, Bent ZW, Wilson R, Ziraldo SB, Wheeler TD, McDermott GP, Zhu J, et al. 2017. Massively parallel digital transcriptional profiling of single cells. *Nat Commun* **8**: 14049.

Zhou D, Mattner J, Cantu C, Schrantz N, Yin N, Gao Y, Sagiv Y, Hudspeth K, Wu Y-P, Yamashita T, et al. 2004. Lysosomal glycosphingolipid recognition by NKT cells. *Science* **306**: 1786–1789.

# 8. Appendix 1 – Supplementary tables

***Table 8-1 Differential gene-expression analysis (avg_log2FC) comparing selected pre- and post-pregnancy mammary epithelial scRNA-seq clusters, related to Figure 2-3.***

*Cluster EC2 x Cluster EC1*

| | | |
|---|---|---|
| Cluster EC2 | Pre-pregnancy alveolar like cells | Positive avg_log2FC |
| Cluster EC1 | Post-pregnancy alveolar like cells | Negative avg_log2FC |

| ID | avg_log2FC |
|---|---|
| HP | -3.41225 |
| RPS18 | 0.95423309 |
| RPS18-PS3 | 0.85295349 |
| CSN1S1 | -1.9926168 |
| GM10260 | -0.8173944 |
| RPL35 | -0.7285127 |
| SQSTM1 | -1.4970493 |
| CXCL1 | -2.4381099 |
| CSN3 | -1.4063395 |
| CSN1S2A | -1.2777775 |
| LGALS7 | 1.67539669 |
| SPP1 | -1.7734804 |
| CD200 | -1.3720457 |
| WFDC18 | 2.21187284 |
| GM10073 | -0.7484677 |
| LGALS3 | -1.4123553 |
| CSF3 | -2.3265594 |
| LTF | -2.2219596 |
| TM4SF1 | -1.1436616 |
| PLET1 | -0.8856469 |
| FCGBP | 1.17875924 |
| RPL15 | 0.76517913 |
| CSRP1 | 1.12668615 |
| DMKN | 1.32242531 |
| RPL23A-PS3 | 0.53010216 |
| PDK4 | -1.3128634 |
| TNFRSF12A | -0.7757174 |
| SLC7A2 | -0.9027661 |
| DKKL1 | -0.8177405 |
| UBALD2 | 0.78067012 |
| RPL6L | 0.58878136 |
| PLAUR | -0.9842945 |
| FABP5 | 1.79955594 |
| ANXA2 | -0.758103 |
| RPS28 | 0.35223714 |
| TMSB4X | 0.87902067 |
| EMID1 | 0.60013274 |
| TRF | -0.7353312 |
| ERDR1 | 0.86928857 |
| ITM2B | -0.6600402 |
| KIT | 0.76187512 |
| CD63 | -0.7277041 |
| EHD1 | -0.7459027 |
| CITED4 | 0.76045598 |
| CST3 | -1.7269527 |
| PLIN2 | -1.0621507 |
| RP23-278M8.1 | -0.5886355 |
| GM9493 | 0.58379215 |
| EEF2 | 0.50344529 |
| RNF19B | -0.9647511 |
| RHOJ | 0.99617701 |
| CAR2 | -1.0739367 |
| TNFAIP2 | -1.2408653 |
| SFN | -0.9458161 |
| ARRDC3 | 0.85177601 |
| LMO4 | 0.8362841 |
| C4B | -0.8514614 |
| PMEPA1 | -0.8647831 |
| EMP1 | -0.9158746 |
| PABPC1 | 0.49804445 |
| PRELP | -0.7346324 |
| LMNA | -0.6266127 |
| SRXN1 | -0.8147953 |
| RPS27RT | 0.34944042 |
| RPS27 | -0.5149663 |
| SLC2A1 | -0.928184 |
| TFAP2B | 0.38381511 |
| GM10709 | -0.5783823 |
| DBI | 0.60159515 |
| XBP1 | 1.08331436 |
| PIK3R1 | 0.96368608 |
| COMT | 0.5336296 |
| POLR2L | -0.7056183 |
| RPL6 | 0.37690283 |
| HILPDA | -1.0976729 |
| MFGE8 | -0.5539383 |
| SBSN | 0.76130029 |
| CIDEA | -0.7813266 |
| CX3CL1 | -0.8076444 |
| CYP1B1 | 0.53143687 |
| CGREF1 | -0.5920381 |
| IGSF8 | 0.67984248 |
| RPS26 | 0.30681624 |
| LAS1L | 0.78938915 |
| LCN2 | -0.5443904 |
| CEL | -1.0674076 |
| CRIP1 | -0.8142327 |
| 0610040J01RIK | 0.54050183 |
| PTTG1IP | -0.6817496 |
| MGAT4B | -0.4960538 |
| RPS11 | 0.26963681 |
| TNC | -0.5409597 |
| RSRP1 | 0.53485115 |
| RPL27 | 0.48710796 |
| S100A13 | -0.6244361 |
| IGFBP7 | -0.6457311 |
| BCAM | -0.6676489 |
| RSPO1 | 0.65861476 |
| IER2 | 0.75081181 |
| JCHAIN | -0.4094184 |
| CBR2 | -0.7848635 |
| FOXQ1 | 0.34182107 |
| FOS | 1.0583883 |
| GAPDH | 0.54979904 |
| BTG1 | 0.53533872 |
| PSAP | 0.44076867 |
| GM16136 | 0.46814484 |
| NEAT1 | 0.54571735 |
| PPP2CA | -0.4991189 |
| KRT8 | -0.4639008 |
| EHF | 0.7105334 |
| FAM107B | -0.6710583 |
| HMGN1 | 0.42460841 |
| CP | -0.6012948 |
| CAMK2N1 | -0.4090801 |
| QSOX1 | -0.6046003 |
| CRISPLD2 | 1.0300721 |
| APRT | -0.5160206 |
| LRG1 | 1.37454062 |
| CALM1 | -0.5182316 |
| PTGS2 | -1.0427087 |
| H3F3A | 0.37140594 |
| SLC31A2 | 0.43570049 |
| ARHGEF6 | -0.6759192 |
| CLTA | 0.55780014 |
| GM10076 | -0.4244255 |
| UBD | 0.50710925 |
| 9530053A07RIK | 0.27612258 |
| FOSL1 | -0.4820608 |
| UBA52 | 0.48291589 |
| CXADR | 0.62276051 |
| GM10036 | 0.39226964 |
| H1F0 | 0.68803391 |
| PRR13 | -0.5550719 |
| TIMP3 | -0.5760445 |
| CCK | -0.889174 |
| HBP1 | 0.35773448 |
| ERBB3 | 0.42608471 |
| CRIP2 | -0.4852684 |
| SLC35E4 | -0.4720801 |
| MAP3K1 | 0.53566684 |
| CDKN1A | -0.7639228 |
| 1500015O10RIK | -0.3435542 |
| ZC3H12A | -0.5359317 |
| ABCC3 | 0.30721929 |
| SCN1B | -0.3110158 |
| EZR | -0.4729411 |
| FRAT2 | 0.38174187 |
| EIF3F | 0.34084188 |
| EIF3H | 0.38251764 |
| CD44 | -0.6107016 |
| RPL13-PS3 | 0.34043176 |
| BAIAP2 | -0.5435382 |
| SGMS2 | -0.6073056 |
| CRABP2 | -0.6992823 |
| WNT7B | -0.4411393 |
| GM2A | 0.51816379 |
| MET | -0.5259474 |
| GIPC1 | 0.388673 |
| RFTN1 | -0.4529127 |
| COL16A1 | 0.35202565 |
| CXCL5 | -1.1883553 |
| TXN1 | -0.3993605 |
| GM266 | 0.34386915 |
| UBALD1 | 0.33515308 |
| F3 | -0.6314083 |
| VMP1 | -0.512585 |
| MCL1 | -0.5869433 |
| RNASET2A | 0.39990554 |
| DACT2 | 0.25705329 |
| COX7A2L | 0.39075435 |
| SLC39A14 | -0.5964625 |
| RGMA | 0.25603816 |
| HBEGF | -0.6166383 |
| TGM2 | 0.51496309 |
| NFKB1 | -0.5035646 |
| KCTD1 | 0.57646587 |
| PFKL | -0.3564594 |
| MAP1LC3B | 0.46680867 |
| S100A16 | -0.3510357 |
| F11R | 0.44921496 |
| FLRT3 | 0.33224128 |
| KLF4 | 0.47886011 |
| COL9A2 | 0.25993645 |
| GRB7 | 0.36944442 |
| TRPS1 | 0.5826528 |
| RPL3 | 0.27286246 |
| AHNAK | -0.41897 |
| NCOA7 | 0.34228615 |
| MAT2A | -0.4377527 |
| PHLDA1 | 0.5080431 |
| JDP2 | -0.5418526 |
| CXCL2 | -1.1870372 |
| PVRL4 | 0.38658609 |
| GM13889 | -0.7240565 |
| CEACAM10 | -0.3713838 |
| HS3ST1 | -0.6299339 |
| FTL1 | -0.3107629 |
| SOX4 | 0.6151711 |
| RALBP1 | 0.42496207 |
| EPHA2 | -0.3692702 |
| CELSR2 | 0.47901132 |
| SHISA2 | 0.36214805 |

| | |
|---|---|
| FTH1 | -0.4501944 |
| TUBB6 | -0.3502234 |
| RALY | 0.37048391 |
| UBE2C | 0.39428408 |
| SDC4 | -0.4271935 |
| RBP1 | 0.51637636 |
| CYP24A1 | 0.55703934 |
| TUBA1C | -0.4171137 |
| TBCC | -0.4899248 |
| S100A10 | -0.3926241 |
| FAM32A | 0.36250055 |
| PLA2G4A | -0.3332718 |
| WFDC2 | -0.3780653 |
| ALOX12E | 0.32632416 |
| SLPI | -0.6102408 |
| IL1RN | 0.64626012 |
| TSPAN3 | -0.3442177 |
| CD47 | 0.50617619 |
| EGR1 | 0.49385 |
| RPL27-PS3 | 0.34873231 |
| KLF13 | 0.42881199 |
| TNFRSF1B | -0.4612497 |
| RP9 | 0.46179308 |
| ZNRF1 | 0.40809964 |
| QARS | 0.37139715 |
| PHXR4 | -0.4562922 |
| SDC1 | 0.56791041 |
| ARMCX2 | 0.37943921 |
| GNG5 | 0.33081346 |
| PIEZO1 | -0.4249671 |
| BASP1 | -0.299978 |
| POR | -0.4363149 |
| ATOX1 | 0.34224381 |
| HOMER2 | -0.3709951 |
| ARPC4 | 0.35503639 |
| SLC6A6 | -0.2596367 |
| OGFRL1 | 0.69985122 |
| IGFBP5 | 0.64707378 |
| CLDN1 | 0.43933564 |
| TRIM8 | 0.43753854 |
| BSG | -0.3522088 |
| YPEL3 | 0.33983985 |
| TSC22D1 | 0.61834165 |
| RB1 | -0.3838559 |
| AHR | 0.40000467 |
| MTHFSL | 0.26017157 |
| FOXI1 | 0.34603328 |
| ANXA8 | -0.3502678 |
| PNRC1 | 0.4157556 |
| STX5A | 0.30234494 |
| ARID5B | 0.30161658 |
| EIF4EBP1 | 0.44270438 |
| RCHY1 | 0.30878347 |
| TUBB2A | -0.4019754 |
| GM10116 | -0.3972508 |
| CTSC | -0.3215553 |
| ARF5 | 0.32656296 |
| IFI202B | -0.8499241 |
| STMN1 | 0.67824401 |
| 4631405K08RIK | 0.37566258 |
| HSP90AA1 | -0.2673399 |
| GM8973 | 0.32049154 |
| TOP1 | -0.2868505 |
| KLF7 | 0.52905911 |
| XDH | 0.37355702 |
| PPP1CB | 0.31469134 |
| ANGPTL4 | -0.6103214 |
| MAST4 | -0.4342893 |
| NUS1 | -0.3704873 |
| NUPR1 | -0.5320468 |
| ACOT1 | 0.38646036 |
| ZFP36L2 | 0.63070253 |
| LALBA | 1.46236547 |
| GDI2 | 0.33563334 |
| PLB1 | 0.4190669 |
| ABHD17C | 0.38204019 |
| TNFRSF21 | 0.40617835 |
| ZFAND5 | 0.4328498 |
| GLTSCR2 | 0.3763282 |
| SLC5A8 | 0.28849913 |
| FOSL2 | 0.44146105 |
| LIF | -0.5037808 |
| P2RY6 | -0.3146484 |
| ATF7IP | 0.25493467 |
| S100A8 | 1.14763301 |
| DDI2 | 0.32916634 |
| AU020206 | -0.3412263 |
| S100A11 | -0.2687169 |
| SRSF7 | -0.3471977 |
| ETV6 | 0.33593341 |
| SMOX | -0.4320533 |
| TUBB4B | -0.3873203 |
| GAS6 | -0.3673182 |
| COL9A1 | 0.41095673 |
| MAF1 | 0.29241706 |
| CSF1 | -0.5908555 |
| GM10126 | -0.3377947 |
| SERPINE1 | -0.5088554 |
| OXA1L | 0.28637108 |
| LDHA | 0.50010519 |
| HMGN5 | 0.30534965 |
| TANC1 | 0.35938205 |
| MAT2B | 0.28401174 |
| FAM102A | -0.3615152 |
| PLEKHB1 | 0.30612316 |
| NGF | -0.4291502 |
| NOS1AP | 0.28530111 |
| ZFP637 | 0.26921015 |
| GM26917 | -0.330914 |
| KRT18 | -0.2747509 |
| PDGFA | -0.3520496 |
| S100A1 | -0.3223718 |
| NFKBIZ | -0.4028743 |
| HIST1H1E | 0.26071624 |
| CLCF1 | -0.2542899 |
| LZTS2 | 0.31236088 |
| VEGFA | -0.9070968 |
| DAB2 | -0.4019607 |
| ZFP36 | 0.3837823 |
| HMGB1 | 0.36841265 |
| TPM3 | 0.31072285 |
| BNIP3L | 0.36700092 |
| TAGLN | 0.35538996 |
| CITED2 | 0.6030088 |
| DDX5 | -0.2557279 |
| EIF3E | 0.32515081 |
| IER3 | -0.4319319 |
| TSPO | -0.3575336 |
| PKM | 0.34501178 |
| SECISBP2L | 0.30704951 |
| CHIC2 | 0.33078651 |
| SRGN | -0.2589423 |
| NFKBIA | -0.398926 |
| EFNA5 | 0.25471357 |
| HMOX1 | -0.6146459 |
| ANKRD11 | 0.38423583 |
| SNRPG | 0.30762884 |
| TMPRSS13 | 0.27203199 |
| CHMP2B | 0.30480499 |
| JUN | 0.50749064 |
| HIST1H1C | 0.31489971 |
| TAX1BP3 | 0.34998334 |
| TXNIP | 0.45864972 |
| PTX3 | -0.3768637 |
| ZFP36L1 | 0.35318112 |
| MAFB | 0.42708452 |
| PHPT1 | 0.32728633 |
| ALDOC | -0.3531481 |
| CARD19 | -0.2902602 |
| M6PR | 0.30079085 |
| GM42418 | -0.5267728 |
| ERRFI1 | -0.3043006 |
| CHIL1 | -0.4571045 |
| SERPINH1 | 0.34082078 |
| FHL2 | -0.2874073 |
| MBP | -0.3765734 |
| ZFP46 | 0.28494482 |
| CYSTM1 | -0.2988292 |
| HS2ST1 | 0.26958674 |
| GCH1 | -0.3461258 |
| MAP7D1 | -0.4160341 |
| NCL | -0.2680592 |
| PTGES | -0.4082996 |
| PTN | 0.5806618 |
| STAP2 | 0.27216495 |
| UQCRFS1 | 0.32525939 |
| TMEM120A | -0.3271727 |
| ZMIZ1 | -0.3318022 |
| AK2 | -0.2922428 |
| HEG1 | 0.25884961 |
| BTG2 | 0.48602494 |
| GPX1 | 0.28405723 |
| CSTB | -0.2868117 |
| RBM47 | 0.33105398 |
| LY6D | 0.2620322 |
| RIN2 | 0.28241235 |
| PDE4B | -0.3427502 |
| DUSP14 | -0.2735975 |
| HMGA1-RS1 | -0.2555186 |
| RSF1 | 0.26478857 |
| STAT3 | 0.3352457 |
| CTSD | -0.3110779 |
| KDM6B | -0.368726 |
| RB1CC1 | 0.26483381 |
| BZW2 | 0.2783197 |
| CTDSP2 | 0.33249325 |
| NOP56 | -0.3123795 |
| MPZL1 | 0.27898106 |
| C3 | 0.40079502 |
| SSR2 | 0.34712048 |
| SLC20A1 | -0.3206587 |
| CTBP1 | 0.25286113 |
| ETS1 | -0.3295536 |
| PTPN1 | 0.3351736 |
| CREB5 | 0.58631554 |
| PNRC2 | 0.26845156 |
| ERGIC3 | 0.25837039 |
| PDHA1 | 0.29174117 |
| ETS2 | -0.3271724 |
| SGMS1 | 0.36600606 |
| RRS1 | -0.3052903 |
| PDLIM4 | 0.32435107 |
| HMGB2 | 0.55497336 |
| PQLC1 | 0.30438279 |
| GABARAPL1 | 0.30204707 |
| ST6GALNAC4 | -0.286954 |
| TNF | -0.2689575 |
| GADD45B | -0.5367672 |
| CYB561 | 0.28910018 |
| HAGH | 0.32230037 |
| TGFBR1 | 0.34985606 |
| RHPN2 | -0.2792711 |
| GSTM1 | -0.2974814 |
| HES1 | 0.35998282 |
| GJA1 | 0.31525636 |
| MED24 | -0.3259472 |
| U2AF1 | -0.2822284 |
| UBB | 0.26409757 |
| PFKFB3 | -0.3957841 |
| PRKCA | 0.34014384 |
| SFI1 | 0.26748777 |
| 0610012G03RIK | 0.26301393 |
| FAM103A1 | 0.28919345 |
| GM7808 | -0.2988717 |
| SYNE4 | 0.25152708 |
| LURAP1L | -0.3423981 |
| PLPP2 | 0.28488562 |
| RALGDS | 0.40137463 |
| ENO1 | -0.3001817 |
| AKAP9 | 0.2589015 |
| IKZF2 | 0.38894087 |
| KRT7 | 0.52313111 |
| SLC28A3 | -0.4321609 |
| MRPL14 | -0.2676343 |
| 2200002D01RIK | -0.3131905 |
| VAT1 | -0.2697 |
| TMEM234 | 0.27013045 |
| RRAS | 0.26112937 |
| NFKBIB | -0.3040674 |
| SLC12A2 | 0.28958084 |
| ATXN7L3B | 0.2709961 |
| RABAC1 | -0.2576567 |
| CDCP1 | -0.2922656 |
| GJB2 | 0.37264187 |
| CD24A | -0.4017969 |
| TMBIM1 | -0.2610876 |
| ITGAV | -0.2803802 |
| CELF2 | -0.2971656 |
| ZFOS1 | 0.29612099 |
| ECM1 | -0.3128016 |
| IFITM2 | 0.29857567 |
| CISH | -0.2804749 |
| CNN3 | 0.30421046 |
| RBMS1 | -0.3175096 |
| KLC3 | 0.25248611 |
| WIPI2 | 0.25625356 |
| PEAK1 | -0.3070777 |
| CYCS | 0.28989905 |
| TCF7L2 | 0.30108475 |
| LITAF | 0.31333653 |
| TNIP1 | 0.25232102 |
| LOCKD | 0.30008829 |
| PNISR | 0.25396539 |
| TPST2 | -0.2849968 |
| CLDN3 | 0.38732362 |
| SSU72 | 0.26989651 |
| NAV2 | -0.302443 |
| MT2 | -0.4646665 |
| RAB10 | -0.2720932 |
| SLC39A1 | 0.3263839 |
| TNRC6A | 0.26957111 |
| ACLY | -0.3051099 |
| H2AFV | 0.40725129 |
| AEN | -0.2999965 |
| TUBB2B | -0.2937099 |
| PLEKHM2 | -0.2864394 |
| LRRC8A | 0.27965519 |
| MARCH7 | 0.32373008 |
| TRABD | 0.25479352 |
| NSMF | 0.28829313 |
| KLHL21 | -0.3357838 |
| CXCL16 | -0.3045125 |
| PIK3C2A | 0.3696741 |
| SUPT4A | 0.27761471 |
| BPTF | 0.25245585 |
| IFT43 | -0.2511782 |
| KRT17 | 0.31234665 |
| SCARB1 | 0.25523327 |
| MSRB1 | 0.30265914 |
| ARL6IP5 | -0.2596836 |
| LIMA1 | 0.26485213 |
| SNRPD1 | -0.268913 |
| ELF1 | 0.26047715 |
| TNIP3 | 0.28484656 |
| PLAT | -0.2879236 |
| SMPDL3A | 0.28371022 |
| TUBA4A | -0.2581073 |
| AY036118 | -0.2762664 |
| SUMO1 | 0.26652609 |
| CEBPB | -0.2716935 |
| SLC5A1 | 0.36017054 |
| SGK1 | 0.29682199 |
| PLEKHG3 | -0.3207291 |
| CEP170B | -0.2569257 |
| PTPRF | 0.25279701 |
| IRX1 | 0.31311492 |
| PRDX2 | 0.26431467 |
| TUBA1A | -0.309363 |
| SNW1 | 0.26550676 |
| IFNGR1 | 0.31214391 |
| WBP5 | 0.30115424 |
| ERP29 | 0.25056607 |
| TKT | 0.25670866 |
| EPHB3 | 0.30033295 |
| EGLN3 | 0.29929304 |
| SAA1 | -0.4700263 |
| MARCKS | -0.3331056 |
| CD14 | 0.5052468 |
| MKRN1 | 0.26270229 |
| LAP3 | 0.28036583 |
| TMEM176A | -0.3321555 |
| CLU | -0.2536262 |
| TSPAN8 | -0.2516312 |
| CALD1 | 0.42275897 |

| | |
|---|---|
| GSN | 0.32736505 |
| CYR61 | -0.6312425 |
| PPIF | -0.325058 |
| OSTC | 0.25442301 |
| MYC | -0.2649687 |
| PLSCR1 | 0.42440326 |
| HN1 | 0.25620642 |
| IFI203 | -0.4145351 |
| MSN | 0.25100561 |
| PPM1H | 0.29429954 |
| PVRL1 | -0.2822224 |
| HYPK | 0.254143 |
| KRT19 | 0.3741407 |
| ATP2B1 | 0.28993429 |

| | |
|---|---|
| BCL3 | 0.28982274 |
| MYH9 | 0.33685507 |
| MUC15 | 0.27633305 |
| MANF | 0.31417477 |
| ACTB | 0.60903947 |
| HK2 | -0.3102336 |
| SPPL2A | 0.25365488 |
| MNDAL | -0.3042569 |
| FLNB | 0.25695665 |
| ELF3 | -0.3522617 |
| BGLAP3 | 0.54309612 |
| RASSF1 | 0.28686589 |
| TRIM25 | -0.2772625 |
| MARCKSL1 | -0.3153275 |

| | |
|---|---|
| ID2 | 0.27232432 |
| ICAM1 | 0.37269107 |
| SEPP1 | 0.27175515 |
| POSTN | -0.2572193 |
| PDZK1IP1 | 0.25204479 |
| FOXC1 | -0.287111 |
| KLF5 | 0.28742002 |
| SOD2 | 0.42536864 |
| PRKCDBP | -0.3427673 |
| AQP3 | -0.4371909 |
| DCTN3 | -0.3939237 |
| PDLIM3 | 0.2747511 |
| NDRG1 | -0.3012046 |
| CEACAM1 | 0.35572358 |

| | |
|---|---|
| H2AFZ | 0.32994125 |
| AREG | 0.30950056 |
| TAGLN2 | 0.35824755 |
| SPRY2 | -0.2812402 |
| APOD | -0.7533769 |
| BTN1A1 | -0.4624796 |
| ADAMTS4 | -0.2758964 |
| ARRDC4 | 0.30074565 |
| TIMP1 | -0.2690303 |
| GADD45G | 0.25388697 |
| HSPB1 | 0.35888183 |

*Cluster EC4 x Cluster EC3*

| | | |
|---|---|---|
| Cluster EC4 | Pre-pregnancy myoepithelial progenitor MEC | Positive avg_log2FC |
| Cluster EC3 | Post-pregnancy myoepithelial progenitor MEC | Negative avg_log2FC |

| ID | avg_log2FC |
|---|---|
| SPARC | 2.31533684 |
| RPS18-PS3 | 0.93844188 |
| RPS18 | 0.91982817 |
| CSF3 | -3.5196402 |
| IGFBP3 | 1.85755426 |
| EMID1 | 1.12598284 |
| MT1 | -0.8993478 |
| MGP | 1.6753208 |
| COL9A3 | 1.20720255 |
| GAS1 | 1.66834078 |
| COL9A2 | 1.10333706 |
| MAFF | -1.3367986 |
| RPS28 | 0.51844485 |
| MT2 | -0.8072718 |
| IGFBP7 | 0.97804857 |
| MMP2 | 1.03063964 |
| HSPB1 | -1.6811946 |
| CDKN1A | -1.3011324 |
| ADAMTS4 | -2.0307597 |
| VEGFA | -1.2790844 |
| MAST4 | -0.9524079 |
| RPS8 | 0.44249643 |
| PLAUR | -1.3203245 |
| FST | -1.0554729 |
| POLR2L | -0.8855032 |
| MT-ATP6 | -0.4667118 |
| KRT14 | -0.8731447 |
| FTH1 | -0.8207371 |
| RPS4X | 0.48833952 |
| CTGF | 1.92716183 |
| GEM | -1.6646074 |
| MIA | 0.97744332 |
| CNN2 | 0.93898999 |
| EMB | 0.99997595 |
| GM10260 | -0.6025848 |
| PDPN | -1.0070121 |
| 1500015O10RIK | -1.2045197 |
| SOCS3 | -1.20897 |
| TSC22D1 | -0.9846283 |
| ELN | 0.9810055 |
| PLPP3 | -1.2186489 |
| RPL7 | 0.41065277 |
| MAT2A | -0.8053547 |
| ERDR1 | 0.77289846 |
| UBB | -0.6459221 |
| TM4SF1 | -1.2503979 |
| ADAMTS1 | -1.0981749 |
| RCAN1 | -1.4058609 |
| SDC1 | 0.90490115 |
| RPS3A1 | 0.36441531 |
| FZD1 | 0.69960277 |
| CRISPLD2 | 0.878397 |
| RGS2 | -1.4043259 |
| RPL35 | -0.5361239 |
| LGALS7 | 0.84250928 |
| EEF1G | 0.51770473 |
| RPS26 | 0.48163962 |
| SRM | 0.67153651 |
| COL4A2 | 0.76477759 |
| SLC43A2 | 1.0023914 |
| TNS1 | -0.9776525 |
| BCAM | 0.75356007 |
| RPL15 | 0.66090123 |
| TMEM165 | 0.69759769 |
| EIF1 | -0.346456 |
| NET1 | 0.84187384 |
| NFKBIA | -1.1983614 |
| RPL23A-PS3 | 0.54322523 |
| COL16A1 | 0.71172101 |
| MFGE8 | 0.77648684 |
| NEAT1 | 0.61165955 |
| APOE | 0.49057493 |
| PDE4B | -0.7058161 |
| PTX3 | -1.2862653 |
| COMT | 0.56490532 |
| RPL22L1 | 0.52361073 |
| LITAF | -0.7444526 |
| RPLP1 | 0.35900057 |
| MFAP2 | 0.54021457 |
| GM9493 | 0.63288626 |
| DLL1 | -1.0604585 |
| PHLDA3 | 0.67044447 |
| TXNRD1 | -0.8264388 |
| GNB2L1 | 0.43371403 |
| SERPINE1 | -1.2395515 |
| BRINP1 | -0.7215813 |
| SMAD7 | -0.8041567 |
| PAPPA | 0.54563931 |
| UCP2 | 0.60630776 |
| TUBB2A | -0.9317279 |
| RBP1 | 0.66437244 |
| SOX9 | -0.9740876 |
| XIST | 0.47191884 |
| PPIC | 0.53608313 |
| PHLDA1 | -1.0055703 |
| MT-CYTB | -0.3364994 |
| RPL6L | 0.55466562 |
| HACD1 | 0.58505046 |
| MT-CO3 | -0.3021533 |
| CD63 | -0.3671894 |
| SMIM3 | -0.6882912 |
| RPL36A | 0.37377545 |
| GM10354 | 0.58074988 |
| RPL37A | 0.280373 |
| IFRD1 | -1.0941353 |
| SPHK1 | -0.7111664 |
| KRT15 | 0.83262061 |
| RPL6 | 0.42041412 |
| OGT | 0.60528786 |
| HBEGF | -0.808186 |
| RPL10A | 0.38747415 |
| ERRFI1 | -0.6664904 |
| CYP1B1 | 0.6861433 |
| SH3PXD2B | 0.58426786 |
| ARC | -0.8342408 |
| SPRY2 | -1.1145088 |
| SNHG11 | -0.6080732 |
| B2M | -0.5298562 |
| RPS20 | 0.34271813 |
| SQSTM1 | -0.7667289 |
| CAV2 | 0.64058548 |
| FAM110A | -0.6517043 |
| CD24A | -0.8677453 |
| GADD45G | -1.0702124 |
| FOSL2 | -0.7965096 |
| HSP90AA1 | -0.4797294 |
| PPIB | 0.54063238 |
| CXCL14 | -0.6045752 |
| BGN | 0.6462825 |
| SLC2A1 | -0.7942687 |
| SFN | -0.5260975 |
| CNIH4 | 0.55628832 |
| KRT18 | -0.7362266 |
| CNDP1 | 0.47432199 |
| CXCL1 | -2.0747369 |
| H3F3B | -0.2720352 |
| CDA | -0.9688632 |
| RPS15A | 0.27096931 |
| IFITM3 | -0.3650145 |
| GSN | 0.59272819 |
| PTMA | -0.3315391 |
| FRMD6 | -0.7595661 |
| RPL14 | 0.26747713 |
| URAH | -0.8050883 |
| GPR153 | 0.33944661 |
| COL4A1 | 0.66007096 |
| EPHA2 | -0.5938618 |
| EFHD2 | -0.5659558 |
| MT-ND4 | -0.3135075 |
| DDIT4 | -1.0068922 |
| TRP63 | 0.81112026 |
| CCL2 | -1.3752987 |
| RPSA | 0.33189487 |
| WNT5B | 0.48803126 |
| TNS3 | 0.5979923 |
| HES1 | -0.6662436 |
| COL4A5 | 0.46764622 |
| ADAMTS5 | -0.832783 |
| CHADL | 0.48697472 |
| ARF6 | -0.4654558 |
| KLF7 | 0.64132675 |
| FTL1 | -0.3460791 |
| RPL12 | 0.32448236 |
| RNF19B | -0.6411261 |
| ICAM1 | -0.6696807 |
| HP | -0.670264 |
| CEBPB | -0.4041555 |
| 4631405K08RIK | 0.58329099 |
| NEDD9 | -0.6062499 |
| NPM1 | 0.38004012 |
| CHD7 | 0.55037146 |
| XYLT1 | 0.49650518 |
| GCNT2 | -0.6387185 |
| MAN1A | -0.6659465 |
| ATP2B1 | 0.53395439 |
| TSPAN5 | 0.48842022 |
| PMEPA1 | -0.4685796 |
| FRMD4B | -0.5669053 |
| TNFRSF12A | -0.5109 |
| SCN7A | -0.6312598 |
| LDHA | 0.36190965 |
| PDGFRL | 0.43547576 |
| RPL3 | 0.30551659 |
| EIF3F | 0.51933994 |
| TXNIP | 0.52084788 |
| SRSF5 | 0.44500396 |
| PRPF19 | 0.45223762 |
| P2RY1 | 0.37140954 |
| RPL4 | 0.27676966 |
| ECE1 | -0.5987072 |
| JAM2 | -0.4661935 |
| RCN1 | 0.47084665 |
| TNFSF10 | 0.34644 |
| PGM5 | -0.445634 |
| NONO | 0.54552869 |
| HMOX1 | -0.8856775 |
| TPT1 | -0.2609572 |
| PLEKHB1 | 0.40835234 |
| RAB20 | -0.6880616 |
| FHL2 | 0.51202847 |
| SERF1 | 0.34685372 |
| PSMA4 | 0.42848742 |
| WDR89 | 0.39773657 |
| NABP1 | -0.5605526 |
| SRSF6 | 0.49418054 |
| TFAP2B | 0.51336205 |
| CRLF2 | 0.30380665 |
| PEBP1 | 0.40710043 |
| RAMP1 | 0.29496676 |
| SDC4 | -0.4699373 |
| THSD7A | -0.4177646 |
| ELL2 | -0.5023646 |
| JCHAIN | -0.3783936 |
| F11R | 0.46162011 |
| NPW | 0.4074802 |
| LHFPL2 | 0.44793518 |
| NDUFV2 | 0.47199861 |
| DSTN | 0.35178272 |
| BCAR1 | -0.5868095 |
| FGFR2 | -0.6113653 |
| EIF4EBP1 | 0.57437562 |
| AFF1 | -0.5176102 |
| ZFP637 | 0.4697336 |
| RERG | 0.32082093 |
| PHPT1 | 0.48258605 |
| RPL23 | 0.25121188 |
| RPS27RT | 0.31039414 |
| RASL12 | 0.37046823 |
| FBLN2 | 0.33285403 |
| SERPINH1 | 0.32980026 |
| WFDC18 | 0.75080132 |
| SBSPON | 0.29906632 |
| SLC7A5 | 0.44200303 |
| FERMT2 | -0.6853473 |
| RNF122 | -0.5604109 |
| PRSS23 | 0.61700477 |
| ZFAND5 | 0.43163879 |
| AJUBA | 0.26497697 |
| LAMB3 | 0.47746315 |
| TEAD1 | 0.53602904 |
| PRELID1 | 0.39313129 |
| JOSD2 | 0.42959797 |
| LMOD1 | 0.48853126 |
| MSRB1 | 0.55284846 |
| NDUFA3 | 0.43962502 |
| ZFP260 | 0.36563007 |
| CDK4 | 0.426703 |
| UBALD2 | 0.50781208 |
| EPRS | 0.45454923 |
| TIMM44 | 0.38420928 |
| KRIT1 | 0.41800746 |
| UHRF2 | 0.41785218 |
| DEPDC7 | -0.586058 |
| RPL27 | 0.39692026 |
| APOL10B | 0.33410419 |
| TMEM147 | 0.45024579 |
| MAT2B | 0.34075028 |
| ACSL4 | 0.58112396 |
| DYNLL1 | -0.4780073 |
| NACC2 | 0.40226332 |
| FOSL1 | -0.5666335 |
| IGFBP5 | 0.56145017 |
| CLCA3A2 | 0.53746288 |
| ZFP36L1 | -0.5738934 |
| TIGD2 | 0.30712765 |
| FAM43A | -0.3422713 |
| COL7A1 | 0.40223898 |

| | |
|---|---|
| CUL4A | 0.34232447 |
| IER5 | -0.6757285 |
| RPL31 | 0.25380973 |
| ARPC4 | 0.39976332 |
| BRD3 | 0.45287809 |
| LMAN1 | 0.44866407 |
| CST3 | -0.5569612 |
| KEAP1 | 0.35624593 |
| CSRNP1 | -0.5836823 |
| BCLAF1 | 0.38881578 |
| FOXC1 | -0.5212569 |
| EEF1B2 | 0.33393866 |
| PCDH7 | -0.5709166 |
| ANXA6 | 0.38063561 |
| AATF | 0.39449673 |
| MTHFD2 | 0.44674565 |
| ACTG1 | 0.31228593 |
| GJA1 | -0.5333332 |
| TRIM29 | 0.41057539 |
| TMEM51 | -0.4844163 |
| PXDC1 | -0.7909189 |
| ERP29 | 0.39700372 |
| CTSF | 0.35621831 |
| RPS27 | -0.4274824 |
| GOLIM4 | 0.3130729 |
| AEBP1 | 0.37627045 |
| CD9 | -0.3025922 |
| PDAP1 | 0.37191478 |
| KLF4 | -0.589869 |
| CSN1S1 | -0.5766556 |
| FBLN7 | 0.25958328 |
| LIF | -0.6083555 |
| PHXR4 | -0.504854 |
| GADD45A | -0.7145401 |
| TGFA | -0.5262129 |
| TIMM9 | 0.39914248 |
| CDK2AP1 | 0.3922054 |
| CALM2 | -0.4449998 |
| SUPT4A | 0.41790276 |
| CAPRIN1 | 0.40534059 |
| NCL | 0.34339354 |
| DUSP5 | -0.713894 |
| GFRA1 | 0.45763336 |
| FAM103A1 | 0.3152435 |
| PDIA6 | 0.43508388 |
| CIR1 | 0.33946913 |
| PLS3 | 0.48245323 |
| FOXO1 | 0.52862089 |
| TXNDC5 | 0.38774984 |
| H2AFJ | 0.39548501 |
| PLEKHA1 | 0.33547894 |
| PMM1 | 0.32905662 |
| PINX1 | 0.31393275 |
| ACTA2 | 0.56448816 |
| RPS26-PS1 | 0.36754392 |
| POLR2E | 0.37354047 |
| NFE2L2 | 0.46342246 |
| SPP1 | -0.6121358 |
| HNRNPA2B1 | -0.3213263 |
| TANC2 | 0.425398 |
| TAX1BP3 | 0.39588865 |
| MEDAG | -0.6400996 |
| NOCT | -0.5408565 |
| RUNX1 | -0.4430038 |
| CCDC6 | 0.32457028 |
| KIF1A | 0.29156081 |
| CDC16 | 0.36769992 |
| FSTL1 | 0.38540657 |
| GARS | 0.33739441 |
| TPBG | -0.574881 |
| RUSC2 | -0.2720314 |
| SLC25A4 | 0.39774954 |
| SRP72 | 0.34480645 |
| ERH | 0.29878681 |
| FAM83A | -0.4517431 |
| BTG2 | -0.8584152 |
| PSAP | 0.37168572 |
| PEX11B | 0.30081339 |
| SAE1 | 0.35777803 |
| TAGLN | 0.52444022 |
| KDM6B | -0.6416266 |

| | |
|---|---|
| SEC61B | 0.37870012 |
| ACAD9 | 0.30806691 |
| IER3 | -0.6830465 |
| TSPAN7 | 0.30069923 |
| SDHD | 0.37571699 |
| RPS12-PS3 | 0.36544885 |
| GM10116 | -0.4371065 |
| LMNA | -0.3316212 |
| ANP32B | 0.32172679 |
| TAGLN2 | -0.4480851 |
| UQCC3 | 0.37288685 |
| PIGT | 0.39027094 |
| HDDC2 | 0.2588352 |
| RBM5 | 0.41102126 |
| RNPEP | 0.30080457 |
| IL11 | -0.5088407 |
| SFRP1 | -0.4449052 |
| H2-Q6 | -0.4049656 |
| SLC38A2 | 0.34250873 |
| PERP | 0.35709232 |
| BNC1 | -0.2664369 |
| KLC1 | 0.40708266 |
| MAF1 | 0.29348089 |
| TOPORSOS | 0.30800575 |
| ATG101 | 0.31243432 |
| TNFRSF18 | 0.29652422 |
| GM11713 | -0.3573909 |
| ATP5C1 | 0.39357475 |
| OST4 | 0.34164821 |
| LAMC1 | 0.33023107 |
| SPTBN1 | 0.38486574 |
| YBX3 | 0.38865125 |
| WIF1 | 0.48657687 |
| UBA52 | 0.35184243 |
| TRIB1 | -0.5917682 |
| NUDCD2 | 0.26134308 |
| UQCRQ | 0.31565564 |
| MYBBP1A | 0.36714805 |
| LSM1 | 0.29191815 |
| SSR2 | 0.41874809 |
| RPL9-PS6 | 0.33654384 |
| IMMT | 0.36951128 |
| PXN | -0.4647902 |
| MANF | 0.41468346 |
| PHB2 | 0.39203273 |
| SERBP1 | 0.2828969 |
| SOX10 | -0.4798252 |
| COPE | 0.39442061 |
| 2810004N23RIK | 0.34740187 |
| NRIP1 | -0.3386643 |
| MORC4 | 0.25095288 |
| RAE1 | 0.37164297 |
| ECHDC2 | 0.31523672 |
| GPATCH4 | 0.37068642 |
| EMP1 | -0.696586 |
| ARGLU1 | 0.40718827 |
| STX11 | -0.4366108 |
| UBAC1 | 0.30345463 |
| BTG3 | -0.3947181 |
| STARD3NL | 0.31227141 |
| DAB2 | -0.2954445 |
| BRI3BP | 0.27921262 |
| RELN | 0.27798043 |
| NUDT21 | 0.36157685 |
| RTCB | 0.38383592 |
| SEC31A | 0.35929852 |
| FRG1 | 0.34292623 |
| EIF1A | -0.3911459 |
| YIPF3 | 0.36021646 |
| ZFP706 | 0.33440768 |
| GAS6 | 0.39181917 |
| 1810037I17RIK | -0.4875338 |
| KCTD4 | 0.30616561 |
| NIPAL4 | 0.28310065 |
| TINAGL1 | -0.6310722 |
| UBE2D3 | -0.3044025 |
| ILK | 0.31327639 |
| FAM162A | 0.44557318 |
| CCT4 | 0.32219454 |
| COA3 | 0.35707481 |
| LAP3 | 0.38093417 |

| | |
|---|---|
| SSNA1 | 0.3081824 |
| HRAS | 0.32139642 |
| CSTB | 0.3355974 |
| TGIF1 | -0.4018765 |
| NTNG1 | 0.34091013 |
| MATN4 | 0.39958731 |
| EPCAM | -0.2696682 |
| MINA | 0.29914148 |
| CCT5 | 0.35450689 |
| RNF10 | 0.34570631 |
| EIF3M | 0.33814594 |
| SLC4A7 | 0.32777162 |
| GAPDH | 0.28635784 |
| RRAD | -0.6094345 |
| BSG | 0.30357164 |
| DAG1 | 0.35655236 |
| EXOSC7 | 0.30813708 |
| AKAP2 | -0.459156 |
| EIF4E2 | 0.30710229 |
| PPP1R14B | 0.3657822 |
| NR4A2 | -0.5779799 |
| RPL13-PS3 | 0.30730943 |
| UNC5B | -0.4437752 |
| CCT3 | 0.33701293 |
| 1810058I24RIK | 0.36160031 |
| DDX27 | 0.32674642 |
| PAICS | 0.26274236 |
| IL17B | 0.54322222 |
| ASXL2 | 0.27597167 |
| FGFR1OP2 | 0.36655766 |
| ETS2 | -0.4703247 |
| NFKB1 | -0.4344701 |
| TRIM28 | 0.29330919 |
| PPP3R1 | 0.27405411 |
| FAM195B | 0.33584045 |
| BAX | 0.30761806 |
| RRP15 | 0.31936193 |
| RGCC | -0.4381616 |
| ATP13A1 | 0.28829229 |
| LTF | -0.3732564 |
| CLINT1 | 0.3103585 |
| CFL2 | 0.32976322 |
| C1QBP | 0.33632 |
| PARM1 | 0.37811999 |
| RPL10 | 0.32939948 |
| CCNJL | -0.2552777 |
| KTN1 | 0.33428696 |
| TLR2 | 0.36383299 |
| GPX8 | 0.2883108 |
| SERPINA3N | -0.6318531 |
| RAB24 | 0.30831828 |
| THOC7 | 0.36224132 |
| ATAD3A | 0.30651805 |
| ZBTB7A | 0.38935402 |
| PABPC4 | 0.33731556 |
| IKZF4 | -0.5053935 |
| PCBP4 | 0.33314422 |
| ID4 | 0.52341058 |
| CHIL1 | 0.59775596 |
| MBD3 | 0.3675118 |
| DCTPP1 | 0.29335745 |
| STX16 | 0.26421627 |
| GLRX | -0.5465164 |
| ITPKB | -0.506864 |
| DYNC1I2 | 0.31652263 |
| HDLBP | 0.35242735 |
| TUFM | 0.30706302 |
| SSBP1 | 0.33278462 |
| SMC1A | 0.41174748 |
| COPS6 | 0.27280278 |
| AK1 | -0.477259 |
| 1110004F10RIK | 0.28073955 |
| PTPRE | -0.4994545 |
| MAP3K7 | 0.28167803 |
| PSMD6 | 0.3302106 |
| DUSP7 | -0.3711356 |
| NRBP2 | 0.26889204 |
| LSM2 | 0.30310515 |
| GM7676 | -0.4055085 |
| RBM6 | 0.36019144 |
| UAP1 | -0.5684793 |

| | |
|---|---|
| REST | 0.31120158 |
| ELOVL7 | 0.36507809 |
| TAF1D | 0.28911219 |
| TMEM167 | 0.27620036 |
| WDR77 | 0.28877813 |
| WDR26 | 0.28008568 |
| ZFP292 | 0.30172772 |
| ZFP106 | 0.27283828 |
| PPP2CB | -0.4556738 |
| PRMT7 | 0.295475 |
| CSNK2A1 | 0.25778915 |
| EZR | -0.4328437 |
| ITGB4 | 0.28084443 |
| ADGRG1 | -0.4421174 |
| UQCRC1 | 0.30019907 |
| 0610012G03RIK | 0.2927798 |
| MPZL2 | -0.4552464 |
| GM8973 | 0.2502512 |
| EBNA1BP2 | 0.28710592 |
| ADPRHL2 | 0.31786817 |
| SLC39A14 | -0.4354608 |
| RAP2B | 0.38862021 |
| MRPS17 | 0.27526535 |
| CXCL2 | -1.7614319 |
| LYSMD2 | 0.27802615 |
| CTAGE5 | 0.32390617 |
| TCN2 | 0.30472465 |
| FAM60A | 0.28031402 |
| COLGALT1 | 0.2633101 |
| POLB | 0.28008404 |
| TSPO | -0.4213732 |
| CAMK2N1 | -0.4815123 |
| NRP2 | -0.3932933 |
| CP | -0.5303249 |
| SGMS2 | -0.4601589 |
| CDCA7 | 0.3483478 |
| 1810011O10RIK | -0.5290126 |
| CDC42EP4 | -0.3962075 |
| PBDC1 | 0.36183479 |
| TIMM13 | 0.3115409 |
| R3HDM4 | 0.27083187 |
| LGALS3 | -0.4872663 |
| TJP2 | -0.4549103 |
| CHTF8 | 0.27062033 |
| VIMP | 0.32301812 |
| RGS19 | 0.27111727 |
| RALGDS | -0.4993997 |
| ATRX | 0.31035105 |
| HK2 | -0.5812297 |
| ARF3 | 0.34633373 |
| HERPUD1 | 0.34617543 |
| MZT2 | 0.36664695 |
| LYAR | 0.35710477 |
| PPIL2 | 0.35133399 |
| METTL1 | 0.32997665 |
| SSB | 0.31559358 |
| LZTS2 | 0.29626 |
| PYCR2 | 0.2887178 |
| POLR1A | 0.25198401 |
| LBP | 0.30360189 |
| MRPL34 | 0.29327553 |
| SPRY1 | 0.2593321 |
| ZFOS1 | 0.36412275 |
| SUSD6 | -0.432964 |
| COPS7A | 0.29932026 |
| SEMA4C | -0.4428507 |
| CNPY2 | 0.32042431 |
| MOXD1 | 0.30420897 |
| HEG1 | 0.41127993 |
| 2-Sep | 0.33103339 |
| TENM2 | 0.33883669 |
| SLPI | -0.5543372 |
| IL19 | 0.36507232 |
| BLMH | 0.25995015 |
| SYNCRIP | 0.30231097 |
| RDX | 0.34059444 |
| PGLS | 0.28953013 |
| DCTN2 | 0.32020427 |
| TMEM173 | -0.3121298 |
| HADHA | 0.29649667 |
| MKRN1 | 0.30118109 |

| | |
|---|---|
| PUS7 | 0.26884441 |
| ZC3H12A | -0.3084632 |
| TIMM10B | 0.3039074 |
| RPL27-PS3 | 0.26511831 |
| TUBA1B | 0.34105002 |
| SOX4 | -0.3770179 |
| MRTO4 | 0.28729525 |
| MYDGF | 0.28759299 |
| EIF3A | 0.28189265 |
| DUT | 0.25480828 |
| NSUN2 | 0.31109974 |
| CTSD | 0.34680005 |
| UBTF | 0.28835974 |
| PRDX2 | 0.33812661 |
| IMPDH2 | 0.29509665 |
| ZFP36L2 | -0.4482765 |
| FARSB | 0.32129396 |
| KRCC1 | 0.26102589 |
| DKC1 | 0.2876327 |
| RAB2A | 0.26013704 |
| FAF2 | 0.27020559 |
| GABARAPL1 | 0.33255972 |
| DST | -0.4095084 |
| GNG5 | 0.28376148 |
| EIF5B | 0.25104829 |
| SDHB | 0.34203588 |
| GPS1 | 0.3339113 |
| CSPP1 | 0.25466682 |
| GORASP2 | 0.34408839 |
| IFRD2 | 0.27091401 |
| IGFBP6 | -0.3070253 |
| KLF13 | 0.32147109 |
| FABP5 | 0.36547102 |
| RABL6 | 0.28541043 |
| URI1 | 0.27170986 |
| POLR2J | 0.26253636 |
| PNN | 0.29758303 |
| SH2D5 | -0.4609008 |
| PDIA3 | 0.33569238 |
| MAFK | -0.3983459 |
| BMP7 | 0.29374638 |
| PPID | 0.28913241 |
| ATP5G3 | 0.29764128 |
| RNF166 | 0.25850692 |
| BRK1 | 0.30447817 |
| ADH5 | 0.27457244 |
| MRPL14 | 0.31346617 |
| RPS6KA1 | 0.25918788 |
| PPP1CA | 0.26578586 |
| JUP | -0.372577 |
| LUZP1 | -0.3343226 |
| EIF3I | 0.35657155 |
| OSTC | 0.2943919 |
| MAF | 0.3354657 |
| MRPS34 | 0.27892591 |
| S100A6 | -0.3808668 |
| CD200 | -0.4983864 |
| PNISR | 0.314966 |
| RRBP1 | 0.29117117 |
| PES1 | 0.31104103 |
| IER2 | -0.4005167 |
| 1110065P20RIK | 0.25273141 |
| GLRX5 | 0.27815202 |
| PCGF2 | 0.25988125 |
| RSU1 | 0.33145684 |
| EMG1 | 0.29275472 |
| ARF5 | 0.25791704 |
| MT-ND4L | -0.3857562 |
| MDH2 | 0.29443577 |
| DNAJC2 | 0.29807656 |
| UBA5 | 0.26083595 |
| KRT8 | -0.4374715 |
| IARS | 0.28236859 |
| PPIL4 | 0.27306153 |
| PRKCA | 0.30587186 |
| METAP2 | 0.261197 |
| ACTR1A | 0.26132854 |
| UTP11L | 0.28610594 |
| MICAL2 | 0.28001954 |
| ZFP280C | 0.25384681 |
| SSRP1 | 0.29358092 |
| RPL13A-PS1 | 0.28067437 |
| FXYD2 | -0.7811718 |
| PEX19 | 0.27525296 |
| ATF3 | -0.5896153 |
| AHR | 0.31695045 |
| ATP5A1 | 0.25554229 |
| 1110008P14RIK | 0.28796553 |
| PTOV1 | 0.31042106 |
| MAP1LC3A | -0.3617765 |
| LAMTOR5 | 0.25471769 |
| SLC7A2 | 0.41472158 |
| OSGIN1 | -0.4987429 |
| AIMP2 | 0.27001796 |
| CHMP2B | 0.29457881 |
| ANXA1 | 0.41619062 |
| ARHGEF40 | 0.28136028 |
| ENY2 | 0.29462073 |
| RABGEF1 | -0.3722777 |
| ATP5O | 0.28262356 |
| ITGB3 | 0.4665733 |
| LYPD3 | -0.4220152 |
| BAK1 | 0.26959336 |
| ADSL | 0.28100369 |
| PSMD9 | 0.25905926 |
| WDFY1 | 0.28038882 |
| GADD45GIP1 | 0.3194576 |
| SNAI2 | 0.27557276 |
| AIMP1 | 0.26152968 |
| SLC25A51 | 0.26686323 |
| MAP2K3 | -0.2943596 |
| PPM1H | 0.26909874 |
| P4HB | 0.25430814 |
| FAM83G | -0.3468894 |
| NFIC | 0.25840333 |
| TCEA1 | 0.27045886 |
| ARL6IP5 | 0.31923587 |
| SPPL3 | 0.26619412 |
| BIRC3 | -0.3669547 |
| TXNDC9 | 0.2641789 |
| PPP1R18 | -0.397703 |
| MRPL57 | 0.26482153 |
| MAP7D1 | -0.4762334 |
| GM10036 | 0.2524142 |
| YPEL3 | 0.28265688 |
| ANAPC2 | 0.27004058 |
| CALM1 | -0.3391943 |
| STRAP | 0.25767591 |
| UQCRFS1 | 0.2905505 |
| CRIM1 | -0.4382513 |
| JUNB | -0.3766895 |
| YWHAH | 0.28080339 |
| GABARAPL2 | -0.4316758 |
| NLE1 | 0.26215605 |
| LTBP2 | 0.26240883 |
| UBE3A | 0.271055 |
| ANKRD12 | 0.25835874 |
| SOCS1 | -0.4390789 |
| GALNT18 | 0.29079108 |
| LY6E | 0.26553968 |
| CISD1 | 0.31007628 |
| PTPN14 | -0.2934405 |
| C4B | -0.318458 |
| BRD7 | 0.25556092 |
| TPR | 0.28869399 |
| NAA20 | 0.28653849 |
| BTG1 | 0.26525725 |
| KCTD1 | 0.34354026 |
| 1110008F13RIK | 0.30454105 |
| RTN3 | 0.25488168 |
| TCEB1 | -0.3526374 |
| DHX30 | 0.25471763 |
| ARL1 | 0.26596153 |
| GMPS | 0.28290706 |
| 2810474O19RIK | 0.32223164 |
| PDGFC | 0.25424277 |
| TOMM70A | 0.25571258 |
| PLAGL1 | 0.28448598 |
| MRPL52 | -0.3500249 |
| SF3B5 | 0.28926677 |
| HTR1D | -0.2584835 |
| H1F0 | 0.45418799 |
| TRIM32 | 0.2589827 |
| GTF2F2 | 0.34418362 |
| CLMP | -0.3555079 |
| HAS2 | -0.4719543 |
| PGAM1 | 0.25347273 |
| PFKFB3 | -0.2841986 |
| RNF187 | 0.28324877 |
| HDAC2 | 0.26066118 |
| RRAGA | 0.25804136 |
| H2-Q4 | -0.3758206 |
| SNX10 | -0.366059 |
| SMARCB1 | 0.26420055 |
| BCL3 | -0.523212 |
| GSR | -0.3496278 |
| XPOT | 0.28341554 |
| FHAD1 | -0.4351905 |
| MRPL3 | 0.25404685 |
| MTX2 | 0.26875255 |
| TMA7 | 0.26122839 |
| SYNGR2 | 0.28891296 |
| TOMM5 | 0.31197582 |
| ABCF1 | 0.28198095 |
| CHD2 | 0.25708688 |
| NFKBIZ | -0.3164092 |
| GM6133 | 0.26682526 |
| CYC1 | 0.3124549 |
| RNF7 | 0.25380471 |
| TSN | 0.27802403 |
| NSA2 | 0.25856491 |
| 5730559C18RIK | -0.4728983 |
| CCL7 | -0.504884 |
| FKBP4 | 0.2673495 |
| LAMP1 | 0.28208354 |
| UQCRC2 | 0.28467361 |
| PROCR | -0.4595694 |
| MRPS24 | 0.27176402 |
| SAC3D1 | 0.27731375 |
| GPN1 | 0.25076828 |
| RPS2 | 0.26176479 |
| HNRNPA1 | -0.3123329 |
| ANKRD11 | 0.27219913 |
| FABP4 | -0.8815584 |
| ACP1 | 0.265252 |
| NPTN | 0.27737128 |
| NPTX2 | -0.3074983 |
| TIA1 | 0.26598959 |
| GM10709 | -0.3762732 |
| CALU | 0.25552986 |
| RBPJ | -0.3348149 |
| BZW2 | 0.25269565 |
| ARPC5 | 0.26046012 |
| FLNC | -0.5051666 |
| TMEM238 | 0.30503277 |
| CCAR1 | 0.30990657 |
| RND1 | -0.4117352 |
| PTK7 | 0.26412503 |
| ARHGAP42 | -0.3426682 |
| TMEM33 | 0.2623349 |
| SNTB2 | -0.3247926 |
| ANAPC5 | 0.30482345 |
| CLTB | -0.2511393 |
| LRRC58 | 0.26295995 |
| CRLF1 | 0.27504382 |
| FLNA | 0.2847464 |
| NUDC | 0.28976751 |
| GLUL | -0.447331 |
| LGALS1 | 0.42695736 |
| MIR143HG | 0.28861547 |
| ASPH | 0.27760104 |
| VPS37B | -0.3922518 |
| LTV1 | 0.2606141 |
| JMJD1C | -0.4378552 |
| ITGA5 | -0.3887217 |
| SMAD1 | 0.30941261 |
| ETHE1 | -0.3351722 |
| NDUFA10 | 0.25770263 |
| NDUFS7 | 0.2832036 |
| ARID5A | -0.4162362 |
| SNX17 | 0.28532048 |
| AHSA1 | 0.26227417 |
| ITM2B | -0.2538379 |
| ARMC1 | 0.2581443 |
| ARPC3 | -0.4043713 |
| MTCH2 | 0.25865473 |
| DUSP1 | -0.7816019 |
| GABARAP | -0.2827577 |
| MRPL36 | 0.26988939 |
| MED21 | 0.29751108 |
| OLA1 | 0.26643749 |
| KNOP1 | 0.29048826 |
| MAPK1 | 0.25390048 |
| ZFP462 | -0.3887111 |
| RAP1A | 0.25224894 |
| CSF1 | -0.7271172 |
| GM10053 | -0.3131711 |
| S100A16 | 0.28209942 |
| USP36 | 0.25673012 |
| TRNAU1AP | 0.26789372 |
| GRWD1 | 0.26441605 |
| FZD7 | 0.32093415 |
| NRG1 | -0.3828285 |
| WASF2 | 0.27223762 |
| FGG | -0.5146343 |
| WNT5A | -0.3233618 |
| HNRNPH1 | -0.3858656 |
| MRPL54 | 0.27041759 |
| TXN1 | -0.3636133 |
| LRRFIP1 | -0.3299886 |
| ADARB1 | -0.2993121 |
| RER1 | 0.27644351 |
| EPS8 | 0.29285819 |
| RPL7L1 | 0.28495885 |
| SNRPE | 0.25023731 |
| CALR | 0.25107548 |
| MPHOSPH8 | 0.28507556 |
| NDUFA8 | 0.26864457 |
| PIN1 | 0.26395498 |
| RB1CC1 | 0.2841917 |
| HCAR2 | -0.2910127 |
| WBSCR22 | 0.25379804 |
| HADHB | 0.29390143 |
| YAP1 | -0.3468991 |
| KRT23 | 0.25165482 |
| ZFP91 | 0.25444789 |
| JAK1 | 0.28908155 |
| COL14A1 | 0.25701656 |
| GADD45B | -0.6779728 |
| PPP3CA | 0.27750842 |
| ZFP703 | -0.3144785 |
| RNH1 | -0.4153291 |
| CKB | -0.4033804 |
| SYNM | -0.3797559 |
| LAMB2 | 0.25778733 |
| POLE4 | -0.3700228 |
| SCAP | 0.25891013 |
| SLC6A6 | -0.3956762 |
| PPDPF | 0.28524098 |
| NR4A3 | -0.3153713 |
| TCP1 | 0.25782616 |
| CAV1 | 0.35720543 |
| H2-T23 | -0.371192 |
| 1700025G04RIK | 0.29973804 |
| CBR3 | 0.26144267 |
| ENAH | -0.3571742 |
| PRKCDBP | 0.27685229 |
| KAZN | -0.363265 |
| SMC3 | 0.25357415 |
| CEBPZ | 0.25801958 |
| IRX3 | 0.28079631 |
| 2700060E02RIK | 0.2503269 |
| HIVEP2 | -0.3817948 |
| DNAJB1 | -0.8025256 |
| DDX3X | -0.2765232 |
| LDHB | 0.32541194 |
| NDUFB5 | 0.25697518 |
| PRMT1 | 0.28152081 |
| CLIC1 | -0.2741242 |
| ZFP207 | 0.25464338 |
| CX3CL1 | 0.25057288 |
| S100A1 | 0.32312934 |
| SUCO | -0.2638043 |
| NR1D1 | -0.2809194 |

| | |
|---|---|
| MID1IP1 | -0.2866345 |
| FGFR1 | -0.305203 |
| SLC41A1 | -0.3340476 |
| MRPS30 | 0.25146644 |
| TRIM27 | 0.25390091 |
| KLHL21 | -0.3108227 |
| PLSCR1 | -0.2808647 |
| RNASE4 | 0.28765903 |
| PIM1 | -0.3350008 |
| COQ10B | -0.3763347 |
| CXCL12 | -0.4387291 |
| RSRP1 | 0.26312431 |
| LIPE | -0.2567864 |
| NDUFS6 | 0.25784205 |
| CNN1 | 0.30499414 |
| TIPARP | -0.4112152 |
| IFI202B | 0.35593479 |
| GSTM5 | 0.26277025 |
| ITM2C | 0.30748972 |
| EFNB1 | -0.3939123 |
| IRS2 | -0.3087484 |
| YTHDC1 | -0.3589166 |
| FERMT1 | -0.4100528 |
| CYP51 | 0.26323189 |
| CBR2 | -0.3962188 |
| KLF10 | -0.363313 |
| TRIP12 | 0.25081132 |
| ANGPTL4 | 0.34181698 |
| BHLHE40 | -0.3613637 |
| MARCKS | -0.3821772 |
| KRT5 | 0.26961365 |
| YPEL5 | -0.2802858 |
| DBI | 0.32342532 |
| GM5786 | -0.2574996 |

| | |
|---|---|
| CSN3 | -0.2968789 |
| ANXA7 | -0.2955547 |
| ZFP36 | -0.5121517 |
| JUND | -0.3596601 |
| PRORSD1 | 0.25255265 |
| HSP90B1 | 0.26275558 |
| XBP1 | 0.25410387 |
| ID3 | -0.4219109 |
| GPX3 | -0.4160527 |
| EHD4 | -0.2800302 |
| OSMR | -0.2823905 |
| TMEM120A | -0.296411 |
| MED13L | -0.3168404 |
| ANXA2 | -0.294842 |
| AY036118 | -0.2645271 |
| SOD2 | -0.3621312 |
| MAP3K2 | -0.3275486 |
| MOCS2 | -0.3203483 |
| ITPK1 | -0.2675809 |
| CD44 | -0.285081 |
| ARL4C | 0.26311693 |
| SNX18 | -0.2522661 |
| GCLM | -0.3160262 |
| CYSTM1 | -0.2892793 |
| CREM | -0.2791787 |
| SPOP | -0.2627009 |
| ATXN7 | -0.3655965 |
| TSC22D2 | -0.3353653 |
| UBE2H | -0.2983197 |
| GM20186 | -0.39789 |
| ODC1 | -0.2504866 |
| IDI1 | 0.25054512 |
| SERTAD2 | -0.3127763 |
| PURA | -0.2733728 |

| | |
|---|---|
| ITPKC | -0.2501931 |
| PAWR | -0.2524261 |
| HACD2 | -0.2720441 |
| DYNLRB1 | -0.286995 |
| MGST3 | -0.2584638 |
| GRB2 | -0.2884103 |
| MDM2 | -0.3645892 |
| GJB3 | -0.3001574 |
| MEG3 | 0.2541342 |
| HTRA1 | 0.2764651 |
| NFATC2 | -0.2566964 |
| LGMN | -0.3421986 |
| AHNAK | -0.253099 |
| SEC14L1 | -0.2776982 |
| KRT16 | -0.48625 |
| SRXN1 | -0.3056399 |
| ETS1 | -0.3411989 |
| LACTB | -0.281461 |
| SLC16A1 | -0.3061881 |
| TMBIM1 | -0.2738378 |
| CGREF1 | -0.2630399 |
| FNDC4 | -0.2958394 |
| STEAP4 | 0.32917848 |
| SFR1 | -0.2953137 |
| FHOD3 | -0.257756 |
| MYC | -0.2759724 |
| BCR | -0.2936909 |
| EPAS1 | -0.2523975 |
| KLF6 | -0.2702859 |
| PPP1R15A | -0.3390034 |
| CRIP1 | -0.2631821 |
| RHOU | -0.3048126 |
| USP50 | -0.2501396 |
| TIMP2 | -0.2767852 |

| | |
|---|---|
| MICALL1 | -0.2540084 |
| DEK | -0.2751447 |
| NOTCH2 | -0.2546141 |
| PRR13 | -0.2678446 |
| TRP53INP1 | -0.2541585 |
| FEM1B | -0.2887525 |
| REEP5 | -0.276574 |
| TGOLN1 | -0.2907745 |
| TMSB4X | -0.3530559 |
| VIM | -0.4420188 |
| RBMS3 | -0.2590783 |
| PLET1 | 0.54782958 |
| CHKA | -0.2727559 |
| WFDC2 | -0.2585037 |
| SLC5A3 | -0.260472 |
| TNIP1 | -0.2703667 |
| MBP | -0.3661046 |
| BAG3 | -0.2850318 |
| PDLIM3 | -0.3337658 |
| HILPDA | -0.3226099 |
| PMP22 | -0.2929944 |
| VCAM1 | -0.4649157 |
| ELF3 | -0.2572267 |
| CYR61 | 0.25169352 |
| THBS1 | 0.30056578 |
| HSPA1A | -1.4447849 |
| NR4A1 | -0.3236005 |
| SGK1 | -0.3334334 |
| NUPR1 | -0.48738 |
| EGR1 | -0.3041719 |
| HSPA1B | -0.7375439 |
| FOS | -0.2745653 |
| FOSB | -0.266892 |

*Cluster EC8 x Cluster EC5*

| | | |
|---|---|---|
| Cluster EC8 | Pre-pregnancy ductal-like MEC | Positive avg_log2FC |
| Cluster EC5 | Post-pregnancy ductal-like MEC | Negative avg_log2FC |

| ID | avg_log2FC |
|---|---|
| RPS18-PS3 | 1.18992122 |
| RPS18 | 1.26388637 |
| RPS28 | 0.8618869 |
| FXYD2 | -1.9250332 |
| LY6D | 2.54194062 |
| RPS26 | 0.84120746 |
| DCN | 2.38411347 |
| HP | -2.2748495 |
| NRXN3 | 1.32871626 |
| RPL10A | 0.72121968 |
| RPL32 | 0.63809086 |
| PTN | 1.18253047 |
| EMB | -1.2415353 |
| TMPRSS6 | -0.9886125 |
| RPS27RT | 0.59065672 |
| 2210407C18RIK | -2.3893773 |
| RPL3 | 0.49567543 |
| LTC4S | -1.2573627 |
| RPS8 | 0.46709917 |
| FAM3C | -1.075416 |
| RPS27A | 0.43796626 |
| RPS20 | 0.63072393 |
| R3HDML | 1.12771004 |
| RPS3A1 | 0.48473335 |
| RPS26-PS1 | 0.70743652 |
| CST3 | -1.0302361 |
| ITM2B | -0.7741654 |
| RPL23A-PS3 | 0.65744914 |
| PABPC1 | 0.72907796 |
| RPL23 | 0.42674955 |
| RPLP0 | 0.50880619 |
| RPLP1 | 0.48755774 |
| RPL37A | 0.39911891 |
| SOX9 | 1.16737231 |
| RPL17 | 0.45692419 |
| RPL37 | 0.41587614 |
| H2-K1 | -1.0256533 |
| TM4SF1 | -1.5094496 |
| RPS15A | 0.45067426 |
| RPL15 | 0.63524675 |
| TOX2 | 0.7974272 |
| RPL12 | 0.63069255 |
| PCOLCE | -0.9207665 |
| ATOX1 | -0.5910612 |
| RPL18 | 0.39360442 |
| COMT | 0.65569565 |
| CLCA3A2 | -1.3647923 |
| RPL36 | 0.41638775 |
| RPL6 | 0.47622587 |
| TMEM158 | 0.9064517 |
| FUCA1 | -0.805027 |
| FTL1 | -0.6488383 |
| RPL35A | 0.36829896 |
| EEF2 | 0.42868848 |
| GNB2L1 | 0.56382118 |
| GM8730 | 0.44458698 |
| CRIM1 | -0.8055155 |
| NAV2 | 0.73859137 |
| H2-D1 | -0.8441993 |
| RPS4X | 0.43817281 |
| SGMS1 | 0.88851498 |
| WFDC12 | -0.7239626 |
| MAN1A | -1.1171824 |
| RGS20 | 0.54281344 |
| BMP3 | -0.9091897 |
| RPS19 | 0.36535408 |
| POLR2L | -0.7504381 |
| RPS17 | 0.37428292 |
| TSPAN1 | -0.9691037 |
| RPL13 | 0.39570293 |
| RPL39 | 0.34738731 |
| HSPB1 | -1.2010745 |
| BTF3 | 0.47275331 |
| TMED3 | -0.8586651 |
| RPS3 | 0.35350051 |
| RPL36A | 0.44326677 |
| RPL24 | 0.34438727 |
| SMIM22 | -0.6963714 |
| CALCA | 1.71855172 |
| GSN | 0.78232932 |
| ERRFI1 | 0.97012886 |
| RPS5 | 0.36878438 |
| GM9493 | 0.61859878 |
| RPS24 | 0.3872358 |
| ERDR1 | 0.89063282 |
| AREG | 0.75630221 |
| TSPAN13 | -0.6051338 |
| RPL22L1 | 0.5594345 |
| RPL7 | 0.39298197 |
| RPS9 | 0.3267333 |
| UBE2Q2 | 0.73498743 |
| AQP3 | 0.92562487 |
| GPX4 | -0.514277 |
| OAZ1 | -0.4226787 |
| RPL34 | 0.33433024 |
| RPL28 | 0.39872847 |
| COPG2 | -0.7133057 |
| RPSA | 0.4595774 |
| GM10263 | 0.38023062 |
| RPS29 | 0.2902955 |
| RPS14 | 0.32664833 |
| RPL14 | 0.32367454 |
| KIF5C | 0.6145501 |
| HIF1A | 0.71327378 |
| RPL19 | 0.29316566 |
| RPS2 | 0.52893089 |
| RPS13 | 0.34091859 |
| GM10036 | 0.45622388 |
| EEF1B2 | 0.4820212 |
| EEF1A1 | 0.30611073 |
| RPL5 | 0.4092854 |
| TSPO | -0.5364546 |
| RPL8 | 0.32090655 |
| RPS15 | 0.31625636 |
| HMGCS2 | 0.97914016 |
| TMEM176B | -0.6174452 |
| RPS10 | 0.36549744 |
| MUC1 | -0.5797397 |
| MALAT1 | -0.3547237 |
| RPL11 | 0.32341954 |
| TMPRSS2 | 0.65416519 |
| PNRC1 | 0.57063559 |
| RPL6L | 0.45766681 |
| CD81 | -0.6570352 |
| SAMD5 | -0.5542301 |
| ANAPC13 | -0.4791306 |
| RPL4 | 0.36028972 |
| SNHG11 | -1.1042267 |
| HEPACAM2 | -0.6661256 |
| RPS16 | 0.27812016 |
| UBA52 | 0.56725577 |
| TNS3 | -0.4357214 |
| ENO1 | -0.6408969 |
| TMSB4X | -0.6191246 |
| RPL18A | 0.28013432 |
| RPS21 | 0.33179284 |
| PLCB1 | -0.5829767 |
| NFIB | 0.5638651 |
| 5330417C22RIK | 0.44789575 |
| MFGE8 | -0.5577449 |
| CALR | -0.6672341 |
| MASP2 | -0.3703753 |
| CRIP1 | -0.6813086 |
| RPL26 | 0.29704517 |
| GSTA4 | -0.6383727 |
| PIRA2 | 0.87690026 |
| RPS6 | 0.30135317 |
| APP | -0.6138135 |
| RPL13-PS3 | 0.48799412 |
| CRYM | -1.3657359 |
| WDR89 | 0.42464941 |
| PTMA | -0.3032444 |
| AGPS | -0.8364079 |
| CXCL17 | 0.65407753 |
| MORF4L1 | -0.411987 |
| ABCC3 | 0.62346604 |
| RPS12-PS3 | 0.45395573 |
| TMEM59 | -0.4808266 |
| SOCS2 | -0.6533881 |
| TRP53INP1 | 0.71133098 |
| IFITM3 | -0.4782109 |
| ADRBK2 | 0.51105176 |
| SV2C | -0.6079549 |
| ITIH5 | 0.49230396 |
| UQCC2 | -0.4266572 |
| RPL31 | 0.2854199 |
| OST4 | -0.4304637 |
| TMEM176A | -0.5606968 |
| RPL27A | 0.26454219 |
| 5930412G12RIK | 0.52326026 |
| PRSS23 | -0.6783544 |
| FBXO2 | -0.4595704 |
| GJB3 | -0.7376795 |
| RPS7 | 0.33552708 |
| ACHE | -0.412324 |
| SH3PXD2B | 0.45600695 |
| PDLIM1 | -0.4697243 |
| CALM2 | -0.4648533 |
| NET1 | 0.92432368 |
| NACA | 0.26616553 |
| HAGH | -0.5064756 |
| YWHAQ | -0.4735318 |
| GM9843 | 0.29502448 |
| LCP1 | -0.5009999 |
| SMDT1 | -0.4284063 |
| EIF3F | 0.35908056 |
| LDHD | -0.5786977 |
| ATP6V1F | -0.347671 |
| PLEKHG3 | 0.49286046 |
| WBP5 | -0.4591178 |
| VDAC1 | -0.4601759 |
| B2M | -0.4926122 |
| NDRG1 | 0.53511242 |
| CHCHD2 | -0.3245578 |
| ARID5B | 0.6110499 |
| BTG3 | -0.4946694 |
| PCBD1 | -0.3876396 |
| CXADR | 0.67542794 |
| DBP | -0.6763226 |
| CD63 | -0.423267 |
| NABP1 | 0.53050603 |
| FGB | 1.20992864 |
| DAD1 | -0.3976842 |
| ECM1 | -0.7107852 |
| PHYH | 0.5355907 |
| POLR2G | -0.4878713 |
| LRG1 | 0.37796361 |
| S100A16 | 0.53600967 |
| PFKL | -0.44899 |
| UBL5 | -0.3185216 |
| IL6RA | 0.33208637 |
| CELF4 | 0.45549687 |
| PKM | -0.4436203 |
| ALDOA | -0.3637458 |
| CYSTM1 | -0.3421409 |
| RABAC1 | -0.3721842 |
| ARPC2 | -0.3827931 |
| ABCC8 | 0.30037024 |
| 1700025G04RIK | -0.2950847 |
| TAP2 | -0.6736999 |
| BEX1 | 0.28819542 |
| MDFI | 0.41714241 |
| RPL9-PS6 | 0.34134613 |
| CNN3 | -0.4272618 |
| SCARF2 | -0.4458248 |
| GNAI2 | -0.4048364 |
| PRDX6 | -0.4657721 |
| ITIH2 | 0.43114586 |
| AKR1B3 | -0.4014325 |
| SPHK1 | 0.49375587 |
| ATP6V1G1 | -0.3152623 |
| CD24A | 0.52105915 |
| RPL10 | 0.41975797 |
| UFSP1 | -0.4086446 |
| IL6ST | 0.485334 |
| HSPA5 | -0.6485635 |
| RPL27-PS3 | 0.36178619 |
| ID2 | 0.70514834 |
| GJB4 | -0.6707199 |
| F3 | 0.62139297 |
| CSN1S1 | -0.4571236 |
| GM6133 | 0.39795033 |
| PSMC4 | -0.4365438 |
| PCP4 | -1.2876637 |
| TNIP3 | 0.91970039 |
| CD82 | -0.4248255 |
| TOP1 | 0.39934446 |
| RPL27 | 0.42323425 |
| TMEM56 | -0.4415401 |
| ACTG1 | 0.42113947 |
| CDKN1A | 0.41060402 |
| SPINT2 | -0.2675067 |
| NEAT1 | 0.44320544 |
| SYNGR2 | -0.4471871 |
| MRPL14 | -0.3800478 |
| LAPTM4A | -0.3775298 |
| ATP5H | -0.3049357 |
| CTSE | -0.5835866 |
| PRDX1 | -0.3094062 |
| UBL3 | -0.4757524 |
| MYL12A | -0.292468 |
| CTSB | -0.4247592 |
| ABHD12 | -0.448543 |
| PER3 | -0.5622943 |
| ZFOS1 | 0.44527727 |
| CEACAM1 | 0.47728257 |
| CCDC124 | -0.4028937 |
| INHBB | 0.46590391 |
| DNAJA4 | -0.5678117 |
| TMEM116 | -0.2677182 |
| MYO1E | 0.42416459 |

| | |
|---|---|
| FZD10 | 0.40168503 |
| INSL6 | -0.337511 |
| GM10116 | -0.4789945 |
| CAPNS1 | -0.3721853 |
| TMED10 | -0.3234307 |
| CISD1 | -0.4396111 |
| NDUFB6 | -0.4050791 |
| BSG | -0.2966119 |
| ALDOC | -0.3694125 |
| ZFP36 | 0.34547289 |
| UBB | -0.492613 |
| INPPL1 | 0.48619911 |
| AY036118 | -0.5414036 |
| DNAJA1 | -0.9119501 |
| PSMA2 | -0.4227833 |
| EIF4EBP1 | 0.36896881 |
| TROVE2 | -0.3492607 |
| CLDN8 | -0.3858389 |
| MT2 | 0.94926496 |
| NDUFA11 | -0.4252678 |
| HCFC2 | 0.30016671 |
| AHNAK2 | 0.33865778 |
| NRAS | 0.35283219 |
| ROMO1 | -0.3193179 |
| ATP1B1 | -0.4703144 |
| STXBP6 | -0.4289754 |
| GM13393 | -0.257271 |
| MPC1 | -0.421387 |
| AES | -0.361434 |
| FOSB | -1.0067064 |
| CAPN5 | 0.3588379 |
| RPL13A-PS1 | 0.35084702 |
| MIEN1 | -0.3708059 |
| S100A10 | 0.4102787 |
| CDC42EP5 | 0.34043773 |
| MRFAP1 | -0.3412783 |
| GALNT18 | -0.4990803 |
| GSTK1 | -0.3560957 |
| VAMP8 | -0.3465466 |
| ATP6V0E | -0.3677176 |
| NGF | 0.44635201 |
| CYP3A57 | -0.669751 |
| RER1 | -0.3401843 |
| GLRX5 | -0.3953919 |
| FITM2 | 0.30804073 |
| CCDC162 | 0.37666112 |
| MYADM | 0.43920601 |
| PSMB3 | -0.387222 |
| ADRM1 | -0.4285549 |
| SDF2L1 | -0.4053932 |
| NUPR1 | -0.5076809 |
| TMEM147 | -0.3645828 |
| SPTAN1 | 0.34907129 |
| DGAT2 | 0.7104496 |
| PDIA3 | -0.4281573 |
| GM17430 | 0.35258833 |
| ARF1 | -0.3078058 |
| RPL35 | -0.2759195 |
| N4BP1 | 0.3007646 |
| NDUFS5 | -0.3406087 |
| CDH13 | -0.2539134 |
| LARGE | -0.6578414 |
| URAH | 0.34948125 |
| PRKCA | 0.32913762 |
| AR | -0.281882 |
| PDE4B | 0.33835851 |
| FKBP2 | -0.3733531 |
| MT1 | 0.95092806 |
| TNFRSF21 | 0.43117743 |
| SPCS1 | -0.3243892 |
| HSPA1B | -1.3257733 |
| CLTB | -0.3368119 |
| CXCL16 | -0.4235144 |
| CHMP5 | -0.3498245 |
| TMEM205 | -0.4205774 |
| OAZ2 | -0.3474344 |
| BC031181 | -0.3307821 |
| GM10709 | -0.3212095 |
| RBX1 | -0.3010299 |
| AMD1 | 0.36213597 |
| GM11808 | 0.30626078 |
| MSN | 0.33642691 |
| PARD6G | -0.2908865 |
| S100A14 | 0.35395467 |
| SEC62 | -0.3627336 |
| TMEM159 | -0.5462207 |
| CDO1 | -0.3097039 |
| POLE3 | -0.3343585 |
| PTPN2 | 0.47042934 |
| TM2D1 | -0.3538362 |
| RNF5 | -0.3372868 |
| KLF9 | 0.31674452 |
| TONSL | -0.3857407 |
| NAB1 | 0.34188842 |
| TGIF1 | 0.43752468 |
| GM5160 | -0.2767176 |
| OSTF1 | -0.327465 |
| ACOT1 | 0.46840362 |
| CRISPLD2 | 0.45221509 |
| GSTT1 | -0.3428685 |
| JCHAIN | -0.2587859 |
| TSPAN17 | -0.4169673 |
| LASP1 | 0.32969216 |
| SRP14 | -0.2967375 |
| MAL | -0.3813902 |
| YIPF4 | -0.3298835 |
| CDK2AP1 | 0.3490344 |
| GSTP1 | -0.3384946 |
| GNG12 | -0.8039197 |
| KCNQ1OT1 | 0.36023827 |
| LY6A | -0.5616344 |
| HSP90B1 | -0.4680939 |
| TXNL1 | -0.360731 |
| PSMB5 | -0.3433695 |
| OAT | -0.4409555 |
| RPS2-PS6 | 0.25250022 |
| ORMDL2 | -0.372701 |
| LAMP1 | -0.2951512 |
| SLC35B1 | -0.3304246 |
| PLAC8 | 0.39045153 |
| TMEM123 | -0.3857128 |
| ANXA5 | -0.4584788 |
| UGP2 | -0.3316819 |
| ARG1 | 0.3879202 |
| PFKFB3 | 0.53263766 |
| UQCR10 | -0.293065 |
| BCL2L11 | 0.46953149 |
| SAT1 | -0.4234823 |
| SPP1 | -0.4604669 |
| CXXC5 | 0.38179185 |
| FAM83H | 0.31186295 |
| STUB1 | -0.3401348 |
| BHLHE40 | -0.3711905 |
| WDR26 | 0.3589136 |
| ITM2C | -0.3259819 |
| ISCU | -0.3388099 |
| MSRB1 | -0.3634143 |
| NDUFA1 | -0.2892189 |
| DSTN | -0.2754448 |
| METTL7A1 | 0.33685858 |
| GPR137B | -0.3153005 |
| DNAJC12 | -0.3739782 |
| ITGB3 | -0.3930528 |
| MGAT4B | -0.3192086 |
| PLIN2 | -0.367006 |
| SC5D | -0.315579 |
| LRP10 | -0.3483122 |
| FEZ2 | -0.2741846 |
| TIRAP | 0.26063218 |
| PSMC5 | -0.3368527 |
| GOT1 | -0.3831788 |
| PEPD | -0.29292 |
| SERINC3 | -0.2994849 |
| CRAMP1L | 0.25673154 |
| UQCRQ | -0.260438 |
| DBI | -0.3318247 |
| LITAF | 0.34450975 |
| HSP90AA1 | -0.9472682 |
| TALDO1 | -0.3379679 |
| HSP90AB1 | -0.3064295 |
| 1500011K16RIK | -0.3482527 |
| RPL36-PS3 | 0.31667722 |
| MAD2L2 | -0.3425921 |
| FAU | 0.29292763 |
| TMBIM4 | -0.3438819 |
| UBE2F | -0.3091939 |
| ADM | 0.34334868 |
| PAPSS1 | -0.329373 |
| PINK1 | -0.3830007 |
| PFDN2 | -0.2855621 |
| MBOAT7 | 0.31717533 |
| H1F0 | 0.53137118 |
| ETS2 | 0.32105219 |
| PIR | 0.47937978 |
| FAM134C | 0.26683228 |
| 4833439L19RIK | -0.4010284 |
| NDUFAB1 | -0.3183634 |
| FAM110A | -0.3449546 |
| HIPK1 | 0.29367441 |
| MIDN | 0.36903155 |
| EIF2S2 | 0.29218196 |
| MAFG | 0.28870861 |
| BDNF | 0.30295803 |
| PRSS22 | 0.53830135 |
| H1FX | 0.30485366 |
| LTF | -0.3499346 |
| MANBA | 0.38489209 |
| JUND | -0.4074126 |
| STK40 | 0.29546553 |
| BNIP3 | -0.2592173 |
| SCAMP3 | -0.3206791 |
| MRPS14 | -0.2788464 |
| MLPH | 0.36375568 |
| ID3 | -0.9512744 |
| SUMO1 | -0.2986105 |
| FAM174A | -0.3290689 |
| ATP6AP1 | -0.3562517 |
| NDUFB7 | -0.3347969 |
| CIB1 | -0.3214876 |
| EHD1 | 0.28315836 |
| SUB1 | 0.34225072 |
| RAB7B | -0.2521833 |
| FAT1 | 0.36683852 |
| DYNLRB1 | -0.3141866 |
| RHOC | -0.2927152 |
| DUSP4 | -0.3522378 |
| NBL1 | -0.3711691 |
| NDUFA13 | -0.2544114 |
| SLC7A7 | -0.251905 |
| MBNL2 | -0.327004 |
| VCP | -0.3478645 |
| EFHD2 | 0.41309337 |
| FAM96A | -0.2957327 |
| PDGFA | -0.4037185 |
| ISG20 | 0.3445121 |
| ARL2 | -0.3036659 |
| BCR | -0.4503348 |
| NEK7 | 0.26640008 |
| F11R | 0.31101532 |
| DHCR24 | -0.2822631 |
| MALL | 0.32541564 |
| ATP2C1 | -0.3352041 |
| SCP2 | -0.3158216 |
| OSMR | 0.32902817 |
| GFPT2 | 0.29992806 |
| HCFC1R1 | -0.3022909 |
| CDH1 | 0.27960117 |
| TNFAIP8 | 0.33583097 |
| EPHB3 | 0.34138346 |
| GADD45G | 0.57471317 |
| MRPS21 | -0.3039096 |
| NME1 | -0.3150892 |
| RAB5C | -0.3276518 |
| SNRPG | 0.3342037 |
| OGT | 0.35197995 |
| PPP1R2 | -0.3356636 |
| GLUL | -0.7346685 |
| KLF13 | 0.31055154 |
| ANO6 | 0.29755697 |
| OGDH | -0.2893836 |
| ATP6V0B | -0.3122884 |
| ZBTB7A | 0.30268727 |
| DMPK | -0.2567292 |
| CPQ | -0.2554211 |
| PI4K2B | 0.29886119 |
| TMED4 | -0.3198525 |
| EPS8L1 | 0.25142445 |
| 2310030G06RIK | -0.3213565 |
| CIRBP | -0.3129272 |
| BST2 | -0.3584873 |
| VAV3 | -0.3338524 |
| ZYX | 0.32726388 |
| PDLIM4 | 0.28542685 |
| REEP5 | -0.3103433 |
| TRAPPC4 | -0.2672446 |
| CHCHD5 | 0.2739542 |
| RAB5A | -0.2654195 |
| CLIP4 | 0.43360439 |
| PSMB6 | -0.2530964 |
| HIST1H2AL | -0.3592269 |
| H2-T23 | -0.2993322 |
| PPP1R11 | -0.3273171 |
| NDUFA12 | -0.2632034 |
| ATP1A1 | -0.3426402 |
| PRKAB1 | 0.26177678 |
| SEC13 | -0.2877947 |
| PTPN1 | 0.40098748 |
| CERS2 | -0.3553563 |
| UBALD2 | 0.26798826 |
| CAV1 | 0.37255469 |
| BABAM1 | -0.3131349 |
| RALBP1 | -0.2690528 |
| TET3 | 0.29581884 |
| KANK3 | 0.26245318 |
| LRRC10B | -0.2564646 |
| MTHFD2L | 0.28964469 |
| TRAK1 | 0.29311963 |
| CTSH | -0.3085751 |
| ATP6V0E2 | -0.2764871 |
| LAMTOR2 | -0.2932975 |
| KRT7 | -0.262736 |
| EMP1 | 0.5235891 |
| HOXB2 | -0.2656055 |
| STEAP4 | 0.28665366 |
| CCDC12 | -0.2790385 |
| 2810474O19RIK | 0.28835985 |
| LAMC2 | 0.31153022 |
| IMPDH2 | 0.27168319 |
| DPM3 | -0.2635387 |
| ADCK5 | -0.2853413 |
| DYNLT1C | 0.30296315 |
| PNKD | -0.2562621 |
| SKP1A | -0.2767257 |
| 2200002D01RIK | -0.334315 |
| CUTA | -0.2892114 |
| MARCKS | -0.3059918 |
| SLC9A3R2 | -0.2987631 |
| DYNLL2 | -0.3232239 |
| SCN1B | -0.2816656 |
| JAG1 | -0.2639284 |
| MAD2L1 | 0.345974 |
| ATP6V1D | -0.2703738 |
| TPM3 | 0.2677618 |
| SSR2 | 0.28557938 |
| 4930523C07RIK | 0.32721467 |
| NDUFAF3 | -0.2800843 |
| RCAN1 | 0.38180351 |
| ITGB6 | -0.3160982 |
| NEDD8 | -0.2533862 |
| ANXA1 | -0.4357169 |
| NDFIP1 | -0.3125609 |
| PSMC3 | -0.2887129 |
| BC005624 | -0.3040177 |
| MVP | -0.2695987 |
| NISCH | 0.25701133 |
| AFG3L1 | 0.25768203 |
| SHB | 0.27248808 |
| UNC5B | -0.2784144 |
| SSNA1 | 0.27498457 |
| AHSA1 | -0.2761647 |
| YWHAH | 0.29952418 |
| SNRPB | -0.2680773 |
| STAT5A | 0.3271492 |
| TMEM50A | -0.2763808 |

| | |
|---|---|
| FOS | -0.5486435 |
| UCHL5 | -0.2661158 |
| RCN2 | -0.2931804 |
| CTSA | -0.2559055 |
| SEMA4C | 0.34560881 |
| AHR | -0.349568 |
| NDUFB10 | -0.2763413 |
| PIEZO2 | 0.26842995 |
| TPI1 | -0.2834934 |
| TESC | 0.25541943 |
| NDUFB4 | -0.3020919 |
| SLC48A1 | -0.2740522 |
| RAD23A | -0.2812474 |
| LMO7 | 0.34194259 |
| CAB39L | -0.255705 |
| CSN3 | -0.3973642 |
| CDIPT | -0.2683502 |
| POLR2F | -0.2594806 |
| PLBD2 | -0.26209 |
| PIGP | -0.2681886 |
| GIPC1 | 0.31679885 |
| RP9 | 0.26454173 |
| KRT4 | 0.51741384 |
| TPPP3 | -0.3738329 |
| WFS1 | -0.2717045 |
| FIS1 | -0.2616459 |
| MRPL20 | -0.2658254 |
| AMN1 | 0.25606103 |
| MPV17 | -0.2562361 |
| MAPK13 | -0.2901268 |
| DEFB1 | 0.43344867 |
| LAMA5 | 0.2514355 |
| SAR1B | -0.2576068 |
| SHISA4 | -0.2648458 |
| TRAPPC2L | -0.2716963 |
| RAPH1 | 0.2510971 |

| | |
|---|---|
| LEPROTL1 | -0.2771392 |
| PODXL | 0.25157772 |
| OCIAD1 | -0.2555998 |
| SSRP1 | -0.301622 |
| TNFAIP2 | -0.2588996 |
| CTSD | -0.2890844 |
| TMEM65 | 0.28954671 |
| SLC25A39 | -0.27518 |
| EPB41L3 | -0.2740754 |
| TNFAIP1 | 0.2508641 |
| SFI1 | 0.28982417 |
| 2210016F16RIK | -0.2517191 |
| UBE2K | -0.265805 |
| ACLY | -0.277086 |
| TRIM25 | 0.28318653 |
| CALM1 | -0.3171159 |
| 0610040J01RIK | 0.25522141 |
| CD151 | -0.2743827 |
| EBPL | -0.2637168 |
| BCL3 | 0.32728281 |
| KLF3 | 0.27549059 |
| HDAC11 | 0.25253409 |
| ARHGEF17 | 0.29746427 |
| RNF187 | -0.2540578 |
| CYB5R3 | -0.2697194 |
| SPR | -0.2882224 |
| ETFB | -0.2846293 |
| ANGPTL4 | -0.466305 |
| DDIT4 | -0.4483809 |
| SYF2 | -0.2639814 |
| ACSL3 | -0.2750066 |
| LAMTOR4 | -0.2658535 |
| ARGLU1 | 0.26546397 |
| NARS | -0.2537528 |
| LAS1L | 0.32060842 |
| KRT6A | 0.61208089 |

| | |
|---|---|
| COA3 | -0.2834306 |
| COPE | -0.2508306 |
| IP6K1 | 0.25549266 |
| ADGRG6 | -0.2633153 |
| HSPA1A | -2.3401206 |
| LY6E | 0.28652118 |
| SARAF | -0.2523618 |
| PTS | -0.2597013 |
| HSPH1 | -0.3159717 |
| SRA1 | -0.2794053 |
| PLET1 | 0.39038235 |
| DUSP1 | -0.5804819 |
| HMGCL | -0.2722476 |
| PABPN1 | 0.26280452 |
| UQCRC1 | -0.2646616 |
| ST3GAL1 | 0.2914429 |
| CAR8 | -0.2684072 |
| TSC22D2 | -0.266153 |
| FGF13 | -0.2540955 |
| H2-Q7 | -0.2703138 |
| FXYD3 | -0.2864313 |
| PSMB8 | -0.254063 |
| EMC7 | -0.2557059 |
| EIF5 | 0.29273069 |
| SOD2 | -0.2610739 |
| DNAJC3 | -0.2858517 |
| CAPSL | -0.3332189 |
| SOX4 | -0.4267755 |
| RASD1 | -0.4934225 |
| FAM213B | -0.2543962 |
| SMIM3 | 0.25991546 |
| GATA3 | -0.2989811 |
| ZWINT | 0.26953359 |
| ETS1 | -0.2956004 |
| HERPUD1 | -0.295105 |
| TRF | -0.3039322 |

| | |
|---|---|
| HIST1H1C | 0.50922176 |
| HSPB8 | -0.2917692 |
| ITGB5 | -0.2636675 |
| VEGFA | 0.31093751 |
| SQSTM1 | -0.2887921 |
| PADI4 | 0.3190473 |
| FGG | 0.4728174 |
| KLF2 | -0.6628286 |
| LY6C1 | -0.2703588 |
| NFKBIZ | -0.3074371 |
| PLPP3 | -0.2917038 |
| ATF3 | -0.7236957 |
| HK2 | 0.26183913 |
| ABHD2 | -0.5063073 |
| CCL5 | -0.5475305 |
| IDO1 | -0.467186 |
| TMEM86A | -0.2952127 |
| RHOB | -0.3518169 |
| HSPE1 | -0.3289985 |
| NOCT | -0.2788543 |
| DNAJB1 | -1.3023746 |
| CXCL15 | -0.4334838 |
| TOB1 | -0.2959279 |
| CTSL | 0.35667912 |
| TPH1 | 0.311058 |
| SERPINH1 | -0.5159763 |
| APOC1 | -0.3106238 |
| CLU | -0.3200278 |
| KRT14 | -0.4057282 |
| UPK3A | 0.5663947 |
| CHIL1 | 0.25652983 |
| EGR1 | -0.3836938 |
| JUN | -0.7707645 |
| BTG2 | -0.2923109 |

***Table 8-2 Differential gene-expression analysis (avg_log2FC) comparing FACS-isolated pre- and post-pregnancy luminal mammary epithelial cells, related to Figure 2-3.***

*Post-pregnancy x Pre-pregnancy luminal MECs*

| | |
|---|---|
| Pre-pregnancy luminal MECs | Negative avg_log2FC |
| Post-pregnancy luminal MECs | Positive avg_log2FC |

Table 8-2 can be found at https://doi.org/10.1016/j.celrep.2021.110099 as Table S2.

***Table 8-3 Differential gene-expression analysis (log2FoldChange) comparing FACS-isolated pre- and post-pregnancy mammary resident NKT cells, related to Figure 2-11.***

*Post-pregnancy x Pre-pregnancy NKT cells*

Pre-pregnancy NKT cells Negative avg_log2FC

Post-pregnancy NKT cells Positive avg_log2FC

| ID | log2FoldChange |
|---|---|
| Klhdc8a | -10.396616 |
| Mrpl28 | -10.354259 |
| Nup43 | -10.222935 |
| Emc6 | -9.8011804 |
| Dnase1l1 | -9.5569436 |
| Tbc1d31 | -9.3022889 |
| Rfx2 | -9.2570242 |
| Cstad | -9.1275339 |
| Rbm10 | -8.917264 |
| Man1b1 | -8.7521811 |
| Clec12a | -8.5855052 |
| Gpr15l | -8.56871 |
| Mettl26 | -8.5414241 |
| Pfkfb4 | -8.3813645 |
| Iscu | -8.3463175 |
| Abcg3 | -8.2099961 |
| Pold4 | -8.1160199 |
| Nlrp10 | -8.1113885 |
| Ecscr | -8.0690224 |
| Ap5b1 | -8.0400711 |
| Triap1 | -8.0005427 |
| Zfp994 | -7.990489 |
| Magohb | -7.990489 |
| Zfp691 | -7.9854358 |
| Cyp2e1 | -7.9752759 |
| Stk11 | -7.9701691 |
| Zkscan14 | -7.9074333 |
| Txn2 | -7.8967069 |
| Ndufa1 | -7.8640407 |
| Comtd1 | -7.8306177 |
| Bcl2a1a | -7.8193024 |
| Vmn1r43 | -7.8136113 |
| Snx24 | -7.7254355 |
| Thap4 | -7.6698215 |
| Rab42 | -7.6635077 |
| Stoml3 | -7.6185203 |
| Slc6a1 | -7.6119774 |
| Smim20 | -7.6119774 |
| Osbpl7 | -7.5855052 |
| Fam185a | -7.5379768 |
| Abhd4 | -7.5310574 |
| Oprk1 | -7.4959536 |
| Krba1 | -7.4816694 |
| Tfpt | -7.4744739 |
| Vamp8 | -7.4526695 |
| Dcaf11 | -7.4453275 |
| Usp17lb | -7.4230747 |
| Zfp975 | -7.4155802 |
| Ppp6r2 | -7.4155802 |
| Tha1 | -7.3541797 |
| Mgat1 | -7.3541797 |
| Mrs2 | -7.3384123 |
| Ntn3 | -7.3304636 |
| Cnih1 | -7.3224708 |
| Extl2 | -7.3144335 |
| Ubl7 | -7.3063511 |
| Sf3b6 | -7.3063511 |
| Olfr126 | -7.2900493 |
| Fzd6 | -7.2568825 |
| Slc9a7 | -7.2400086 |
| Slfn1 | -7.2229351 |
| Zfpm1 | -7.2056571 |
| Mydgf | -7.1969399 |
| Gins3 | -7.1809291 |
| Poli | -7.1793459 |
| Fgl1 | -7.1704677 |
| Mepce | -7.1343984 |
| Fam92b | -7.1252384 |
| Il5 | -7.1160199 |
| Gnat1 | -7.1160199 |
| Adhfe1 | -7.1067421 |
| Emcn | -7.1067421 |
| Fbxw4 | -7.1067421 |
| Adal | -7.0974042 |
| Ercc5 | -7.0974042 |
| Gnao1 | -7.0974042 |
| Rpp40 | -7.0690224 |
| Habp2 | -7.0690224 |
| Rtn4rl1 | -7.0690224 |
| Tysnd1 | -7.0690224 |
| Cox6b2 | -7.0594364 |
| Ggn | -7.03029 |
| Apold1 | -7.0005427 |
| Nacc2 | -7.0005427 |
| Tpd52l2 | -6.9803648 |
| Ankrd40 | -6.9701691 |
| Tmem258 | -6.9495588 |
| S100a13 | -6.9391422 |
| Naip5 | -6.9286498 |
| Thnsl1 | -6.9180805 |
| Dgki | -6.9074333 |
| Fam45a | -6.8967069 |
| Olfr134 | -6.8967069 |
| Cry1 | -6.8967069 |
| Mustn1 | -6.8859001 |
| Tmem101 | -6.8750118 |
| Ubd | -6.8750118 |
| Exo1 | -6.8529855 |
| Hpse | -6.8529855 |
| Aqp6 | -6.841845 |
| Lynx1 | -6.8306177 |
| R3hcc1 | -6.8193024 |
| Slc12a9 | -6.8193024 |
| Eml3 | -6.8193024 |
| Plin1 | -6.8078976 |
| Nphp3 | -6.8078976 |
| Abt1 | -6.784814 |
| Rnf7 | -6.7731322 |
| Coq6 | -6.7731322 |
| Cdt1 | -6.761355 |
| Hic1 | -6.761355 |
| Spx | -6.761355 |
| Unc45b | -6.761355 |
| Gata5os | -6.761355 |
| Hlx | -6.761355 |
| Habp4 | -6.7494809 |
| Parp11 | -6.7494809 |
| Ly96 | -6.7254355 |
| Cldn26 | -6.7132607 |
| Zfp444 | -6.7132607 |
| Ndufb8 | -6.7009824 |
| Ppapdc1b | -6.7009824 |
| Ccdc136 | -6.7009824 |
| Grwd1 | -6.6885987 |
| Tpcn2 | -6.6761077 |
| Rdh16 | -6.6761077 |
| Ehd3 | -6.6635077 |
| Cldn5 | -6.6635077 |
| Gdf15 | -6.6507967 |
| Clcn2 | -6.6250336 |
| Map3k21 | -6.6250336 |
| Prss42 | -6.6250336 |
| Rnf41 | -6.6250336 |
| Fam198b | -6.6119774 |
| Batf2 | -6.6119774 |
| Cdk6 | -6.6119774 |
| Pygo2 | -6.6119774 |
| Fkbp2 | -6.598802 |
| Racgap1 | -6.598802 |
| Gpr26 | -6.598802 |
| Sf3b5 | -6.5855052 |
| Mmp13 | -6.5720847 |
| Runx3 | -6.5585382 |
| Vps4a | -6.5310574 |
| Ufl1 | -6.5310574 |
| Cmpk2 | -6.5310574 |
| Zfp229 | -6.5171182 |
| Gbp3 | -6.5171182 |
| Fxyd1 | -6.5171182 |
| Oxtr | -6.503043 |
| Mief1 | -6.4888292 |
| Pde10a | -6.4888292 |
| Zfp329 | -4.2472736 |
| Rn45s | 2.06786142 |
| Gas6 | 9.92948258 |

## 9. Appendix 2 – List of publications

Slepicka PF, **Somasundara AVH**, dos Santos CO. 2021. The molecular basis of mammary gland development and epithelial differentiation. *Seminars in Cell & Developmental Biology* **114**: 93–112.

**Hanasoge Somasundara AV**, Moss MA, Feigman MJ, Chen C, Cyrill SL, Ciccone MF, Trousdell MC, Vollbrecht M, Li S, Kendall J, et al. 2021. Parity-induced changes to mammary epithelial cells control NKT cell expansion and mammary oncogenesis. *Cell Reports* **37**: 110099.

Seminars in Cell and Developmental Biology 114 (2021) 93–112

Contents lists available at ScienceDirect

Seminars in Cell and Developmental Biology

journal homepage: www.elsevier.com/locate/semcdb

Review

# The molecular basis of mammary gland development and epithelial differentiation

Priscila Ferreira Slepicka [a], Amritha Varshini Hanasoge Somasundara [b], Camila O. dos Santos [c,*]

[a] Stem Cell Transplantation and Regenerative Medicine, Department of Pediatrics, Stanford University School of Medicine, Palo Alto, CA 94305, USA
[b] Cold Spring Harbor Laboratory, CSHL School of Biological Sciences, 1 Bungtown Road, Cold Spring Harbor, NY 11724, USA
[c] Cold Spring Harbor Laboratory, 1 Bungtown Road, Cold Spring Harbor, NY 11724, USA

ARTICLE INFO

*Keywords:*
Mammary development
Gene expression
Transcription regulation
Cell heterogeneity

ABSTRACT

Our understanding of the molecular events underpinning the development of mammalian organ systems has been increasing rapidly in recent years. With the advent of new and improved next-generation sequencing methods, we are now able to dig deeper than ever before into the genomic and epigenomic events that play critical roles in determining the fates of stem and progenitor cells during the development of an embryo into an adult. In this review, we detail and discuss the genes and pathways that are involved in mammary gland development, from embryogenesis, through maturation into an adult gland, to the role of pregnancy signals in directing the terminal maturation of the mammary gland into a milk producing organ that can nurture the offspring. We also provide an overview of the latest research in the single-cell genomics of mammary gland development, which may help us to understand the lineage commitment of mammary stem cells (MaSCs) into luminal or basal epithelial cells that constitute the mammary gland. Finally, we summarize the use of 3D organoid cultures as a model system to study the molecular events during mammary gland development. Our increased investigation of the molecular requirements for normal mammary gland development will advance the discovery of targets to predict breast cancer risk and the development of new breast cancer therapies.

## 1. Introduction

Mammals are a diverse class of warm-blooded vertebrates with class-specific features that include the presence of hair and the nourishment of young offspring through the secretion of milk by the mammary glands of females. The structure and development of the mammary gland, as well as the nutritional constituents of milk (fat globules, casein micelles, whey proteins, and sugars) are highly conserved across mammals. The evolutionary origin of the mammary gland dates to 310 million years ago (mya), during the Carboniferous period [1,2], long before the appearance of mammals (190 mya). In the Carboniferous period, synapsids (mammalian ancestors evolved from basal amniotes) developed a glandular integument. During the various radiations of synapsids (mammals and mammaliaforms, therapsids), the ancestral integument became highly specialized to produce an abundant and nutritive secretion (milk) during lactation, leading to what is currently defined as the mammary gland. The primitive apocrine glands from which mammary glands originated played an initial role in keeping terrestrially-laid parchment-shelled eggs moist, and in protecting the skin of early synapsids from infection and injury [3].

More recently in evolution, emergence of the placenta diversified mammary gland structures in eutherians in terms of the number of glands and lobuloalveolar structures per nipple [4]. For instance, unlike nipples in mice and humans, cattle or ruminants have a teat formed by epithelial proliferation and gland cisterns that accumulate milk in between each milk harvest, offering a substantial yield of milk for the offspring and an economically advantageous milk supply [5].

During the first days or months of life, milk contributes significantly to nourishment, as well as to the regulation of basal metabolism and temperature of mammalian offspring. As lactation proceeds, caseins are synthetized, phosphorylated, and aggregated into large micelles that are insoluble in the milk and that function to carry calcium phosphate nanoclusters directly to the offspring's body [6]. The presence of casein micelles correlates with an improvement in offspring nutrition, reducing the demand for egg yolk, and potentially leading to the inactivation of genes associated with yolk formation during evolution [7]. The three primary caseins, α-, β-, or κ-casein, present in the milk of monotremes, marsupials, and eutherians, respectively, diverged before these three

* Corresponding author.
*E-mail address:* dossanto@cshl.edu (C.O. dos Santos).

https://doi.org/10.1016/j.semcdb.2020.09.014
Received 19 July 2020; Received in revised form 28 September 2020; Accepted 30 September 2020
Available online 17 October 2020

taxa originated [8,9].

All the above processes arose more than 150 million years ago and shaped not only a new evolutionary feature to nourish offspring but also the development and anatomy of mammals. As the mammary gland specialized over time, molecular mechanisms have also evolved to control cellular differentiation of mammary epithelial cells and to support their production of milk during lactation. In this review, we will further discuss several molecular switches that control the identity of mammary epithelial cells (MECs) and the development of a fully-functional, milk-producing mammary gland.

## 2. Understanding fetal mammary gland development

Embryonic development of the mammary gland (Fig. 1) is initiated during mid-gestation in many mammalian species. Several mammary gland features associated with sexual dimorphism differ among mammals: the number of primary and secondary sprouts, formation of teats and cisterns in cattle and ovines, and the timing of each developmental event [5].

In rodents, thick bands of ectodermal cells form bilateral and vertical mammary lines at embryonic day (E) E11.25 whereupon clumps of ectoderm (placodes) bloom along the mammary line at day E11.75, and these ultimately determine the number of breasts in each mammalian species. At day E12.5 the placodes intumesce into the mesoderm, forming an early mammary bud surrounded by a basement membrane (BM) and the first traces of a mammary mesenchyme. Between E13 and E14, the bud will give rise to mammary bulbs with an ectodermal stalk that will elongate into a sprout surrounded by the mesenchyme (fat pad) at E15.5. Lumen formation commences at day E17–18, involving the programmed death of ectodermal cells localized at the center of the mammary branches.

### 2.1. Signaling networks in the placode and mammary tissue formation

The first stage of mammary development occurs at the same time as the specialization and maturation of the embryonic mesoderm and ectoderm. The ectoderm shapes the structural organization of the mammary gland whereas mesenchymal signaling networks guide ectodermal modifications and expansion during mammary line positioning, placode assembly, and mammary bud formation and elongation. Members of the Fibroblast growth factor (FGF) and the Wingless-related integration site (WNT) protein families govern signaling in mammary embryonic tissues, and they regulate transcription factors (TFs) from the Homeobox gene family (HOX), GATA binding protein 3 (GATA3), and the T-box family (TBX), which are intermittently expressed either in the endoderm or mesoderm [10–12].

*Hoxc8* is expressed until E12.5 and defines the location of mammary placodes, whereas *Hox9* is expressed until shortly after birth, and their depletion results in mammary ductal hypoplasia [10,13]. Hox genes have been suggested to be the founders of the enhancer landscape in

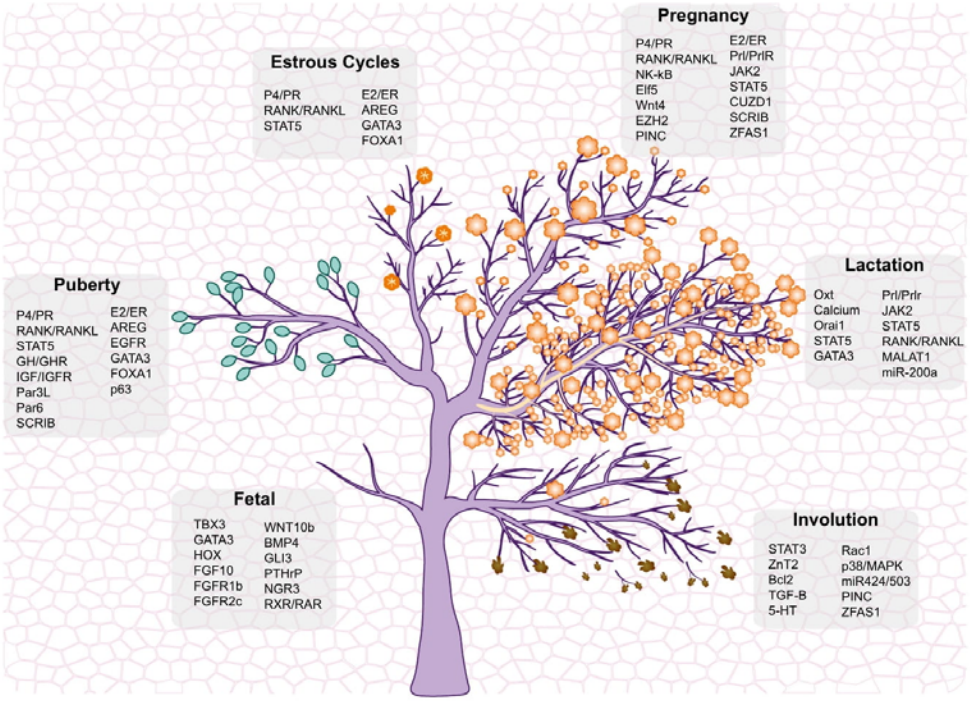


**Fig. 1.** The blooming of mammary gland development. Schematic illustration of mammary gland developmental stages, showing fetal, puberty, estrous cycles, pregnancy, lactation and involution (from left to right). In puberty, green buds represent TEBs. Mammary alveoli are shown as orange flowers in estrous cycles, pregnancy and lactation. In lactation, the milk is represented as yellow sap flowing from the alveoli (flowers) to the ducts (branches). During involution, the regression of the mammary tissue is depicted with falling dead flowers and branches into the background, which portrays the fat pad. The basal compartment and luminal compartment are delineated with darker and lighter colors in the tree, respectively. The main molecular regulators of each developmental stage are highlighted in the grey squares.

mammary epithelial cells, acting directly via mammary bud regulatory elements (MBRE) [14]. Such elements, including those associated with the *Hoxd9* gene, have been identified in eutherians but not in monotremes or marsupials, suggesting that mammary gland development and a specific pool of regulatory factors perhaps guided evolution in eutherians.

Across all mammals, the TF TBX3 plays a role during fetal mammary gland development. The expression of Fibroblast growth factor receptor 1b (FGFR1b), Fibroblast growth factor receptor 2c (FGFR2c), and Fibroblast growth factor 10 (FGF10) initially promote *Tbx3* gene expression in mammary line mesenchyme and subsequently in the placodes [15]. Conversely, Bone morphogenic protein 4 (BMP4) negatively regulates *Tbx3*, which influences the orientation of ectodermal cells, mammary line specification, and placode formation [16]. Furthermore, loss of *Tbx3* expression in mice results in the absence of mammary placodes and abnormal gland development, due to loss of expression of Wnt10b and Lymphoid enhancer-binding factor 1 (Lef1), key factors in mammary embryogenesis [17–20]. A similar phenotype is observed in FGF10$^{+/-}$ mice which have lost one of the master regulators of TBX3 [21,22].

Ectopic expression of the Wnt inhibitor Dickkopf (Dkk1) in the ectoderm compromises the formation of mammary placodes and impairs the localization of Wnt10b [23]. As abrogation of placode development is more severe in embryos ectopically expressing Dkk1 compared to FGF10- or FGFR-null mice, Wnt networks may be critical for placode initiation [23]. Later in mammary development, mutations in Wnt10b have been correlated with aggressive clinical outcomes for breast cancer, and rapid development of mammary tumors [24].

Other regulators of mammary embryogenesis include TFs that are part of the Hedgehog (Hh) pathway. For instance, mutations in the GLI family Zinc Finger 3 (Gli3) TF lead to the loss of specific placodes, which can cause ductal defects in later stages of mammary development [22]. Through a signaling cascade with members of the Hh network, Gli3 activates gene-specific transcription that controls bud formation [25–27]. GLI family Zinc Finger 2 (Gli2) functions in ductal branching through its localization in the tissue surrounding mammary branches (stroma) from embryogenesis to adulthood, but it becomes stromal and epithelial during pregnancy and lactation [28].

### 2.2. The nest of embryonic mammary tissue

The microenvironment surrounding mammary tissue plays a pivotal role in the gland development, predominantly via regulation of epithelial-to-mesenchymal transition (EMT), during which epithelial cells lose cell polarity and cell adhesion to become mesenchymal cells with migration and invasion properties. Both EMT and mesenchymal-epithelial transition (MET), the reverse of EMT, are associated with normal mammary development, such as the placodes during embryogenesis, and with cancer, as mammary tumor-initiating cells acquire stem-cell properties through the EMT [29,30]. EMT-inducing TFs (i.e. Zeb1, Slug, Twist) have been detected in cells at terminal end buds (TEBs) during puberty, and Wnt and Transforming growth factor beta (TGF-β) signaling pathways in TEBs have also been reported as regulators of EMT [31]. More specifically, EMT-driven signals can determine the expression of extracellular matrix (ECM) components and epithelial cell adhesion receptors through Neuregulin-3 (Nrg3), a member of the EGF family, which also localizes in the mesenchyme underlying the mammary line [32]. In Nrg3 mutant mice, FGF10 and mesenchymal Tbx3 expression levels were normal, however, Wnt10b and Lef1 levels were reduced or undetectable in specific placodes [33,34]. Nrg3 signaling through its receptor Erb-B2 receptor tyrosine kinase 4 (Erbb4) has been suggested to modulate cell adhesion, thus promoting transduction of somatic FGF10 signaling to the developing placodes.

From E15.5−E16.5 to the end of embryonic development, mammary buds continue to elongate and form rudimentary ductal sprouts that embed into the mesenchymal layer. Throughout this developmental time, transcriptional regulation and cellular signaling mediated by Tbx2–3, Wnt genes, Parathyroid related hormone (PTHrP), Msh homeobox 2 (MSX2), and Nuclear factor kappa B (NF-κB) function in concert to promote branching morphogenesis and expansion [27].

Specific immune cell populations are involved in mammary gland development, with recent studies demonstrating the presence of macrophages in the embryonic mammary gland. During embryonic development, macrophages invade and partially remove the mammary epithelium of males, implicating the microenvironment in the sexual dimorphism of the gland [35]. Macrophage-derived progenitor cells from the fetal liver or yolk sac persist in the gland from embryogenesis to adulthood, thus composing the majority of the macrophage population in the postnatal mammary fat pad [36]. Conversely, during puberty, mammary macrophages mostly originate from precursor cells located in the bone marrow, an observation that may suggest constant remodeling of the gland and the requirement for cellular renewal [37].

Macrophages have been observed in the mesenchyme surrounding the mammary buds, but not in close proximity to the epithelial cells during embryogenesis [35]. This is in marked contrast to postnatal stages of mammary development, in which macrophages are found in periductal locations, indicating their role as scavengers as part of the immune surveillance in the mammary microenvironment [35–38]. During postnatal stages, macrophages reach the intraductal niche through dendritic cell movements whereupon they have direct contact with both luminal and basal ductal compartments [37]. Thus, it is possible that fetal macrophages play a role that is distinct from their "sentinel" function during embryonic mammary development, which still remains to be elucidated. Accordingly, we still lack a clear picture of whether macrophages that populate fetal mammary glands remain dormant during post-birth mammary gland development, and whether they contribute to tissue surveillance after birth.

### 2.3. Not everything is about symmetry

Mammary gland development is bilateral and asymmetrical, like other paired organs [19]. Although the rate of asymmetry is relatively low for the mammary gland, molecular factors can contribute to left-right (L-R) asymmetry in somites during embryogenesis, including the Retinoic acid receptors, RARs and RXRs. Lack of RXRα induces defects in the ductal networks, with thoracic mammary glands (TMGs) showing asymmetry marked by decreased ductal branching in the left gland, whereas inguinal mammary glands (IMGs) remain symmetric, with no alterations in the ductal profile [39].

Retinoic acid (RA) regulates the expression of *Tbx3*, *Fgf8*, sonic hedgehog protein (*Shh*), and human epidermal growth factor receptor 2 (*ErbB2*), all genes associated with MEC differentiation and proliferation [40,41]. In addition, forkhead box protein M1 (*FoxM1*) and *Gata3* are highly expressed in the left mammary gland, in contrast to retinoic acid-inducible G-protein coupled receptor 5D (*Gprc5d*) and Neurogenic locus notch homolog protein 1 (Notch1), which are more abundant in the right gland [39]. Both pairs of genes play a role in luminal progenitor cell fate commitment, and in chemoresistance to cancer treatment, suggesting that asymmetrical development of the gland may engage programs that could alter the commitment and malignance of MECs. In fact, women whose breasts significantly vary in size have been reported to have an increased risk of developing breast cancer, with the left breast often being the most affected tissue [42,43], thus suggesting that misregulation of genes associated with left-sided breast development could play an important role as a prognostic marker of aggressive cancer development.

## 3. The "teen" years

During embryogenesis, the maternal hormones provide the initial stimuli to the rudimentary mammary gland for ductal development. However, after birth, cessation of maternal signaling reduces ductal and

branching genesis in the postnatal mammary gland. This activity resumes with the start of puberty, a stage marked by the production of female sexual hormones, which will complete mammary morphogenesis and prepare the gland for milk production in the event of pregnancy.

Puberty varies widely, from a few weeks to several years post-birth, in different mammalian species (5 weeks old in mice and 9–18 years old in humans). The onset of puberty is triggered by the increase in gonadotropin levels that lead to the secretion of ovarian hormones, mainly Estrogen (E2) and Progesterone (P4). Peak levels of E2 production are between the follicular phase and ovulation and, depending on the vertebrate, E2 synthesis occurs every 2–4 days in mice and once every month in humans [44].

In the pubertal and adult female, the mammary gland undergoes developmental modifications tightly correlated with ovarian/uterine reproductive cyclical repetitions (4–5 days in mice and 26–32 days in humans). The cycle (Fig. 1) is divided between two major phases: Follicular (proestrus and estrus in mice) and luteal (metestrus and diestrus in mice) phases. In humans, the follicular phase begins on the first day of menstruation when P4 levels decrease, the previous corpus luteum degenerates, and a new preovulatory folliculum grows. During ovulation (also called estrus in mice), peak levels of E2 stimulate the high production of luteinizing hormone from the pituitary gland, causing the release of the ovum from the ovary whereupon the luteal phase begins. In mice, and in preparation for a potential pregnancy, the corpus luteum keeps up P4 production for a few days thus triggering mammary tissue expansion and lobuloalveologenesis. The percentage of dense tissue in women's breasts (mammographic density), is amplified during this phase given the augmented mammary ductal branching and, in mice, high levels of P4 positively correlate with lobuloalveologenesis and tertiary branching [44,45]. The degradation of the corpus luteum and reduced levels of P4 mark the end of a cycle, which induces clearance of MECs through cell death and lobuloalveolar shedding.

The investigation of the molecular underpinnings of both mammary gland pubertal development and the fluctuations during the reproductive cycle will contribute to evaluate the effects of molecular and signaling perturbations in response to disease and cancer initiation, ductal alveologenesis, stromal composition, and in immune microenvironment studies.

### 3.1. Pubescent structure of the gland

The rapid increase in mammary morphogenesis through branch initiation, invasion of the fat pad, and ductal elongation, transforms a pre-formed, rudimentary mammary epithelium into an extensive ductal network. Hormonal signaling promotes differentiation and proliferation of MECs, culminating in an extensively branched mammary morphology, with pro-apoptotic factors, such as BH3-only BCL-2 protein (BIM), triggering apoptosis and cell clearance to allow lumen formation in the newly developed ducts [46]. The pubescent emergence of mammary ducts depends on TEBs, which emerge at the tip of the ducts and are responsible for promoting the invagination of ducts into the fat pad at a rate of ~0.5 mm/day in mice [47]. TEBs (Fig. 1) are elongated-shaped structures with an outer layer of cap cells and an inner multilayer of body cells.

The TEB cap cells have stem cell-like features such as self-renewal properties, being morphologically undifferentiated, and the ability to give rise to both luminal and myoepithelial cells in cleared fat pad transplants. In the "neck" region of TEBs, cap cells tend to differentiate into myoepithelial cells, while a fraction of the cap cells have high mobility, penetrate the lumen of the TEBs, and commit to a luminal cell fate [48,49]. Additional studies of cells expressing the Tumor protein 63 (TP63), a master regulator of MEC development, identified cap cells with a unipotent differentiation capacity towards a myoepithelial cell fate [50], thus suggesting a cellular hierarchy within mammary differentiation and cellular commitment. Conversely, and with the combination of biostatistical modeling and lineage tracing, recent studies dispute the contribution of cap-in-body cells to the luminal lineage. These migratory cap cells are more apoptotic and unlikely to contribute overall to either the luminal or the myoepithelial lineages [47,50]. Therefore, the role of TEB cap cells in ductal elongation remains controversial and warrants further studies.

As an additional cellular stage, the cap-in-body cells are mostly exclusive to the body of TEBs. These cells have a delayed cell cycle progression and increased apoptotic rate when compared to cap cells localized at the outer layer of the TEBs. Molecular analysis of cap-in-body cells identified the TF Forkhead box O protein 1 (FOXO1), and its downstream targets, as major regulators of apoptosis in cap-in-body cells, which contributed to the formation of the lumen during ductal expansion [50]. Collectively, these studies indicate that TEB cap and cap-in-body mammary cells may represent a pool of plastic, heterogeneous, undifferentiated cells that guide pubescent ductal expansion.

Moreover, signaling between MECs and the stroma plays a crucial role in ductal elongation during puberty. TEBs can secrete factors (i.e. eotaxin and interleukin 5) that recruit eosinophils to the tip of TEBs, thus orchestrating side branching [51,52]. Additionally, macrophages spread throughout the mammary ductal system encasing TEBs and perfusing the epithelial bilayer, where they perform a range of functions in guiding ductal outgrowth into the fat pad and phagocytizing body cells to form the lumen of the ducts [35,52,53].

### 3.2. Estrogen network

During embryogenesis, estrogen receptor (ER)α-depleted glands showed normal primitive mammary ducts, however, during puberty and the following stages of mammary development, lack of ER expression severely compromised ductal network development [54]. Transplantation of ERα$^{-/-}$ MECs, together with wild-type (WT) MECs, resulted in ductal elongation, suggesting that ER may also act in a paracrine manner, stimulating neighbor cells [55–57]. Local paracrine signals act downstream of ovarian hormones, as stroma-derived growth factors. Among these factors is Amphiregulin (AREG), a ligand of the Epidermal growth factor receptor (EGFR) in stromal cells, which functions as a membrane-anchored precursor and is expressed in luminal MECs and cells throughout the TEBs. AREG-depleted mice lack a mammary ductal network during puberty, similar to the phenotype observed in ERα$^{-/-}$ glands, and ectopic AREG overexpression rescues the ductal network phenotype in ERa knock out (KO) mice. [58,59]. AREG is cleaved by Desintegrin and metalloproteinase domain-containing protein 17 (ADAM17) to promote signaling in stromal cells. The ADAM17 KO phenocopies the ablation of mammary ductal outgrowth seen in AREG- and EGFR-depleted mice during puberty, indicating that the E2-AREG-ADAM17 axis is a key network of paracrine signaling responsible for ductal outgrowth during mammary pubertal development [60]. Moreover, the epithelial expression of AREG is sufficient to induce mammary ductal formation, independently of the stromal signals. In contrast, stromal expression of EGFR is crucial for mammary tree formation compared to epithelial EGFR expression, demonstrating that depletion of EGFR family members also delayed ductal expansion with hyperplasia of cap-in-body cells and reduced body cell levels [60–62].

E2 binds to its receptor, ER, which translocates from the cytoplasm to the nucleus, where it activates the transcription of genes associated with expansion and growth of the mammary epithelium. ER executes its TF functions in both a ligand-independent (Activation function-1, AF-1) and ligand-dependent (Activation function-2, AF-2) manner, and both mechanisms support the transcriptional activation of paracrine factors which are crucial for ductal outgrowth and side branching [58]. Beyond its transcription activation role, ER can mediate a series of cellular signaling via its membrane localization. In fact, site-specific mutations in ERα protein that block its anchoring to cellular membrane resulted in delayed mammary development during puberty and an inability of MaSCs to repopulate mammary fat pads in transplantation assays. This phenotype was accompanied by alterations to the transcriptional state of

MECs, thus bringing together a complex regulatory network of endogenous and secreted factors orchestrated by ERα [63].

Another TF, Forkhead box A protein 1 (FOXA1), mediates E2 signaling by facilitating chromatin accessibility and, therefore, the interaction between ER and its gene targets. FOXA1 has been identified as a target of the GATA3 regulatory network in branching morphogenesis during puberty [64–67]. Loss of GATA3 has been shown to abrogate TEB formation and to reduce ductal outgrowth, and impair development of ER + MECs, and perturb pathways regulated by P4, consistent with its role as a master regulator of hormone sensing during mammary gland development [11,67,68]. More recently, a reorganization of the chromatin landscape has been detected in cancer cells, leading to redistribution of ER- and FOXA1-binding sites and disruption of GATA3-ER-FOXA1 signaling network, implicating these TFs and their downstream targets in disease-related pathways [69].

As part of its function during mammary development, ER also recruits other coregulators. The ER co-factor abrogation of glutamic acid [E] and aspartic acid [D]-rich C-terminal domain 1 (CITED1) induced ductal hyperplasia, little to no lumen formation, and dilated ductal structures, thus delaying mammary maturation, although these effects were less pronounced in comparison to ERα$^{-/-}$ [70]. CITED1 also functions as a downstream target of the TGF-β family of TFs, suggesting that its role as a cofactor in these two major signaling pathways, ER and TGF-β, ensures a balance between proliferative and non-proliferative signals during puberty [71].

### 3.3. Progesterone signaling

In mammals there are two main nuclear progesterone receptor (PR) isoforms (PR-A and PR-B) and multiple variants that homodimerize or heterodimerize to perform distinct gene transcription functions. The ratio of PR-A:PR-B varies in humans (1:1) and in mice (2:1–3:1), and perturbation of the PR ratio has been associated with mammary oncogenesis in humans and atypical side-branching development and proliferation in mice [72,73]. Although PR-A can act as a dominant repressor of PR-B during murine puberty, ablation of PR-B results in the lack of conventional pubertal structures in the mammary gland [74,75]. Overexpression of PR-A in the pubertal gland induces mammary ductal hyperplasia and the development of abnormal TEBs [73]. In mice, during puberty, overall depletion of PR resulted in impaired mammary side branching and lobuloalveolar development [76,77]. Using mammary transplantation assays, injection of PR-depleted MECs resulted in impaired lobuloalveolar development in response to E2/P4 treatment, a phenotype mostly rescued with the co-transplantation of WT MECs and PR$^{-/-}$ MECs [77].

Increased P4 levels result in induction of side-branching morphogenesis, through the activation of a subset of quiescent ductal MECs and their reorganization into a multilayered epithelium that buds laterally [76,78]. Given the role of P4 signaling in side branching, we speculate that PR signaling is essential for MaSCs to promote tissue expansion and differentiation, although MaSCs have not been demonstrated to express PR [79–82]. PR is commonly expressed in luminal epithelial cells in mice and humans, and such cell types also engage in tissue expansion during puberty in response to elevated P4 levels, suggesting that a combination of paracrine and non-paracrine functions are regulated by the PR/P4 axis [79,80].

One of the P4-induced paracrine signaling mechanisms involves release of the Receptor activator of nuclear factor kappa-B-ligand (RANKL) and its interaction with Receptor activator of nuclear factor kappa-B (RANK) in PR-negative cells, which together control mammary alveologenesis during much of mammary gland development [83,84]. In addition to its paracrine function, P4 induces the proliferation of PR-positive MECs, potentially through the activation of its downstream target Cyclin D1 (CCND1), a mitogenic regulator [83]. Ccnd1-depleted mice show similar phenotypes as PR-null mice [85,86]. The abrogation of PR reduces Ccnd1 expression, resulting in cell cycle changes in highly proliferative cells. P4 also mediates Wnt4 signaling during puberty to promote ductal expansion, revealing that an additional signaling network is involved in mammary branching during major mammary development stages [87]. The balance between P4-induced cell proliferation and side branching may also rely on mediators and downstream targets of P4 signaling.

At puberty, P4 and Insulin growth factor 1 (IGF-1) synergistically promote side branching, TEB expansion, and lobulo alveologenesis, with the combination of P4 and IGF-1 treatment having a 3-fold greater effect on ductal branching compared to IGF-1 treatment alone [76,88]. In prepubertal glands, IGF-1 and/or IGF1R have substantial, P4-independent effects on branching, as increased IGF-1 and/or IGF1R levels markedly enhanced ductal expansion, in some cases resulting in mammary tumors, whereas the transplantation of IGF−1R-depleted cells into mammary fat pads arrested MEC proliferation, causing defects in TEB formation [89–93].

The IGF-1 signaling network involves pituitary hormones required for TEB initiation. Growth hormone (GH) binds to its receptor (GHR) on stromal cells and activates IGF-1 transcription, which, in turn, is secreted and interacts with IGFR in epithelial cells. The depletion of IGF-1 leads to a delay in pubertal ductal outgrowth with few side branches, a similar phenotype as described in GHR KO glands [94]. As GH and E2 are upstream targets of IGF-1, the combination of GH and E2 treatment rescued the phenotype caused by IGF-1 depletion [94]. The expression of AREG, an E2-transcriptional target, is increased by P4 signaling and mediates TEB formation and expansion during puberty [95].

In summary, the P4 network involves a combination of paracrine signals and other hormonal pathways that coordinate mammary TEB development, ductal expansion into the fat pad, and side branching during puberty and adult reproductive cycles.

### 3.4. Regulation of cell polarity

The multicellular bi-layered organization of luminal and myoepithelial cells confers the mammary gland tissue with polarization, and polarity proteins regulate the differential apical-basal (A/B) asymmetry of MECs. Collectively, polarity proteins govern TEB expansion, likely through the regulation of MaSC homeostasis and mammary epithelial fate commitment. Golgi positioning and cytoskeleton organization ensures the orientation of vesicle trafficking, which also contributes to cell polarity. MEC cell polarity can also play a role in mammary lumen formation, in epithelial cell shape and, consequently, ductal branching [96,97]. Moreover, depletion of the TF TP63 blocked mammary lumen establishment, and reduced levels of cell-cell adhesion proteins, a phenotype commonly found in mammary tissues with loss of cell polarity [98]. The loss of polarity proteins, i.e. Partitioning-defective protein 3 (Par3), triggers atypical hyperplastic ductal morphology due to loss of A/B symmetry, deregulation of progenitor cell differentiation, and increases in cell proliferation and apoptosis [99]. This results in expansion of the diameter of primary ducts and limits the growth of secondary branches, thus arresting mammary branching.

The exogenous Par3-Like (Par3L) protein is another key polarity factor involved in mammary duct expansion. Par3L localizes in cap cells of TEBs and controls stem cell maintenance, as lack of Par3L significantly depleted a subset of MaSCs [100]. Mechanistically, Par3L has been suggested to interact with and inhibit Protease-activated receptor 4/Liver kinase B1 (Par4/LKB1) kinase activity, thus controlling stem cell maintenance and cell apoptosis [100]. In addition, the depletion of the focal adhesion protein Paxillin, induces loss of A/B cell polarity, misallocation of apical proteins, loss of microtubule acetylation, and disturbed acinar orientation [101].

Moreover, cell polarity determines the orientation of the mitotic spindle and, consequently, the plane of cell division. This also affects the differentiation and architecture of the expanding TEB during pubertal mammary development. In addition to the factors discussed above, a number of signaling pathways are involved in cell fate decisions. Notch/

Numb/Musashi1 signaling, Wnt/β-catenin signaling, and p53 and its downstream effectors are all key pathways that regulate the symmetry of cell divisions based on microenvironmental cues at various developmental stages in the mammary gland (reviewed in detail by Santoro et al. [102]).

The deregulation of proteins that control cell polarity is often associated with tumorigenesis. The ablation of Par3, besides impairing ductal growth, also induces Signal transducer and activator of transcription 3 (STAT3)-dependent cell invasion and migration, and it contributes to the invasiveness and metastasis of mammary tumors from ErbB2 mice [103]. Partitioning-defective protein 6 (Par6) is overexpressed in $ER^+$ human breast tumors and in MCF10A human mammary cell lines, and the inhibition of ErbB2-Par6 signaling axis is sufficient to arrest cell invasion [104]. Although expression of Par6 does not alter A/B polarity, it does cause hyperplasia and induces EGF-independent cell proliferation [105]. Additionally, upregulation of Scribble (SCRIB) as well as its mislocalization away from cell-cell junctions is correlated with poor breast cancer prognosis, and ectopic expression of SCRIB can activate oncogenic pathways (i.e. PTEN and mTOR) [106]. Pubertal rats subjected to 7,12-dimethylbenz(α)anthracene (DMBA) treatment developed more TEBs, which showed a higher proliferation rate compared to other mammary developmental stages, and these TEBs eventually underwent oncogenic transformation [107]. Therefore, TEB development and organization share some characteristics with oncogenic phenotypes (i.e. cell invasion, proliferation and an increase in vascular supply) and investigation of TEBs and pubertal development of the mammary gland may be relevant to breast cancer research.

Microtubule organization also plays a key role in determining the apicobasal polarity of MECs, orienting the mitotic spindle, and forming the mammary lumen structure during development and in response to pregnancy signals. Loss of Stathmin (STM), a microtubule destabilizing protein, causes a significant delay in postnatal development and maturation of the mammary gland in mice, thus depriving them of the ability to nurse offspring. STM loss leads to decreased Prolactin receptor (PrlR) trafficking and Signal transducer and activator of transcription 5 (STAT5) signaling, both known to be essential for normal functioning of the gland and to be involved in breast cancer [108]. Huntingtin (HTT) is another protein that regulates apicobasal polarity through microtubule-based dynamics. HTT has been shown to be required for the microtubule dependent apical localization of Par3 through vesicular transport and controls lumen formation in virgin, pregnant, and lactating mice [109]. Integrins also play a critical role in determining the apicobasal polarity of MECs through the Integrin linked kinase (ILK)-microtubule network, by regulating tight junction proteins, basolateral surface, Golgi orientation, and consequently mammary acinar morphogenesis [110].

Additional components of the basement membrane, have also been reported in determining MEC cell polarity. For instance, loss of p120, a complex subunit essential for normal functioning of E-cadherin (epithelial cadherin), induced alterations to ductal architecture and TEB function, phenotypes that were likely resultant of an abnormal interaction of cadherin complexes with polarity proteins [111]. More recently, it was shown that depletion of the laminin-binding integrins α3α6 resulted in abnormal baso-apical polarization of luminal progenitor cells, and blocked alveologenesis during pregnancy, thus illustrating that maintenance of polarity via basement membrane function can influence the secretory potential of MECs [112].

Overall, several molecular pathways and factors act during puberty to promote mammary ductal maturation, and these pathways remain active throughout adulthood. As each reproductive cycle promotes lobulo alveologenesis and side branching, we speculate that the constant promotion of mammary cell differentiation and proliferation may induce tumorigenesis over time or otherwise elicit oncogenic pathways that are dormant in the first years of adulthood.

## 4. Parity signals and mammary development

A complete pregnancy cycle involves gestation, lactation, and involution and, collectively represents the second postnatal stage of mammary gland development, which prepares the gland to produce nourishment to support the offspring. Given the complexity and importance of each of these steps and their molecular programs in mammary gland development and maturation, we will discuss each of them separately.

As well as their role in sexual maturation and mammary development, increased E2 and P4 levels during early gestation are the main factors that induce and regulate MEC proliferation, differentiation, ductal branching, and alveolar development [113,114]. These effects on mammary gland development can be mimicked with subcutaneous implantation of slow-release 17-β-estradiol and progesterone pellets, which provide a temporally controlled approach for studies of the mammary gland in response to pregnancy hormones [115]. Similar to the pubertal mammary gland development, ER dimerizes and translocates to the nucleus in response to elevated E2 levels, thus acting as (a) a paracrine signal transducer that activates FGF and EGF pathways, and (b) a TF of that induces the expression of ER−responsive genes, during pregnancy [116,117].

During pregnancy (Fig. 1), P4 and prolactin (Prl) orchestrate the differentiation of MECs into specialized alveolar structures, which are capable of synthetizing and secreting milk during lactation. Like its function during puberty, the main role of P4 during pregnancy is to promote extensive ductal side-branching but, in pregnancy, P4 signals substantially increase the number of alveolar structures to promote a lactation-competent gland. The absence of PRs in MECs impairs alveolar and side-branching formation, and its paracrine signaling is associated with Wnt4 and RANKL [114]. The RANKL receptor (RANK) expressed in $ER^+$ $PR^+$ luminal cells increases WNT paracrine signaling in $ER^-PR^-$ luminal progenitor cells, wherein P4 mediates Wnt4 and RANKL expression in luminal cells, promoting alveologenesis, expansion of mammary epithelium and milk-secreting acini during pregnancy [118–120]. In progenitor cells, P4-RANK/L signals upregulate R-spondin, a receptor agonist for Wnt. Thus, the Wnt and RANK pathways work in combination to control MEC differentiation [118]. As a consequence, Wnt4 KO does not completely abrogate alveologenesis, as other factors are able to compensate for the absence of Wnt4, promoting alveoli formation in late pregnancy [119]. However, RANKL and RANK KO pregnant mice have no lobuloalveolar milk-secreting structures and experience increased levels of apoptosis in alveolar MECs [121,122].

RANKL activates NF-kB in combination with IkB kinase (IKK), inducing the expression of Ccnd1 and promoting MEC proliferation during pregnancy [123]. The impairment of this pathway leads to underdeveloped ductal structures during pregnancy and a subsequent lactation deficiency due to the lack of MEC expansion [124]. RANKL expression in PR + luminal cells induces mitogenic paracrine signaling to MaSCs and RANKL-expressing luminal progenitors. Elf5 is a downstream factor for the P4-RANK/L network that can induce progenitor specification towards luminal secretory cell fate [79,125]. The purification of subpopulations of MECs and organoid culture strategies will potentially help identify the specific cell lineages affected by RANK/L, its downstream targets, and the mechanisms and molecular switches triggered by P4.

The release of oxytocin (peptide and neuropeptide hormone, OXT) is one of the factors that control parturition (the act of giving birth) and lactation (Fig. 1). OXT controls calcium uptake and contractibility of myoepithelial cells and induces mechanical constriction of luminal alveolar cells to eject milk droplets into the lumen of alveoli [126]. Abrogation of oxytocin production and release does not impact milk production, instead affecting myoepithelial cell contraction. This results in an accumulation of milk droplets in the luminal alveolar cells, nursing impairment, and the death of pups [127]. The inhibition of oxytocin master regulators, such as ORAI calcium release-activated calcium

channel protein 1 (Orai1), delays alveolar contraction due to interference with calcium influx, and impairs lactation [128,129].

Lactation and milk production yield during late pregnancy have been associated with the presence of binucleated alveolar cells [130,131]. Aurora kinase A (AURKA) and polo-like kinase (PLK1), essential kinases that control cell cycle progression, were found to be upregulated during the onset of lactation, and binucleated cells were suggested to be a byproduct of cytokinesis failure during cell division [130]. These binucleated MECs not only have an altered ploidy index, but also display an enlarged cell volume, indicating the synthesis of high levels of milk protein. They are postulated to play a critical role during milk production, given that AURKA-depleted mammary glands lacked cells with increased DNA content, and were impaired for milk protein production, resulting in stunting of the pups. Similarly, small molecule inhibition of AURKA and PLK1 kinase activity reduced binucleation in luminal alveolar cells and impacted lactogenesis [130]. Such binucleated cells were also detected in the mammary tissue of humans, cows, seals, and wallabies, indicating their evolutionary conservation across mammalian species [146]. However, recent studies have yielded conflicting results, with some indicating that mitotic events are not involved in promoting alterations in DNA synthesis and milk protein production in murine MECs, while others have suggested that DNA synthesis and lactogenesis are directly associated. This highlights the complexity of mechanisms supporting polyploidy in mammary alveolar cells during pregnancy and lactation, which still remain to be elucidated [132–134].

### 4.1. Prolactin's role in mammary gland development and lactation

Prolactin (Prl) was first described in 1929 when virgin rabbits injected with pituitary extracts from lactating mice showed pregnancy-like mammary architecture and lactating glands [135]. During the early stages of pregnancy, markedly increased Prl levels play a role in maintaining the *corpus luteum*, expression of E2 and P4, and in inducing mammary morphogenesis [136,137]. Prl KO mice suffer from impaired alveolar bud formation and reduced tertiary ductal branches, demonstrating the role of Prl during pregnancy-induced development of the mammary gland [138]. The defective mammary branching phenotype was restored by administration of P4 in $Prl^{-/-}$ ovariectomized mice, revealing that P4 and Prl potentially coordinate lobuloalveolar development [138]. Impaired alveologenesis, but not ductal branching, was rescued when the mammary fat pads of WT mice were transplanted with $Prl^{-/-}$ MECs, revealing that prolactin alone drives mammary alveologenesis. While the placental hormones regulate Prl function mid-pregnancy, Prl levels increase during lactation. Prl is mainly expressed by lactotrophic cells in the pituitary gland and released into the bloodstream, but it is also expressed locally in several tissues, including by MECs in the mammary glands. RANKL also acts downstream of PrlR signaling and its overexpression in virgin glands induces pregnancy-like mammary architecture. RANKL is also responsive to P4, and depletion of RANKL results in similar mammary phenotypes as in $PR^{-/-}$ and $Prl^{-/-}$ glands [48,84,139].

Prolactin binds to its receptor (PrlR), resulting in the activation of several signaling cascades, including the Janus Kinase (JAK)/STAT5 pathway in MECs [140,141]. Upon Prl binding, JAK1 and JAK2 are recruited to PrlR, and their activation triggers the phosphorylation and nuclear localization of STAT5 [142]. STAT5(A/B) was first described as one of the progenitors and master regulators of stem cells in normal and leukemic hematopoiesis, and its activation allows for its binding to GAS motif responsive elements (TTCnnnGAA) at gene regulatory regions [143,144]. In MECs, STAT5 controls the expression of an array of genes, including whey acidic protein (*Wap*), *β-casein,* and others that together regulate differentiation and proliferation across multiple developmental stages [145,146]. STAT5 also binds to super-enhancers of mammary lineage-specific target genes, which then act collectively with additional TFs to control gene expression [147].

A downstream target of the PrlR pathway is the ETS transcription factor 5(ELF5), a major regulator of alveolar cell fate and lobuloalveolar expansion, as mammary glands from $Elf5^{+/-}$ mice show arrested alveologenesis during pregnancy and lactation failure [148,149]. Elf5 expression increases during pregnancy and lactation, and falls immediately after lactation (involution), when alveolar structures are cleared [149,150]. Accordingly, induction of Elf5 expression in virgin mice leads to an increased expression of milk genes (β-casein and Wap), secretion of milk, inhibition of ductal expansion, and alveolar differentiation [148]. The depletion of Elf5 impacts other downstream targets of the prolactin pathway, as female mice and cultured cells that are haploinsufficient for Elf5 showed impairment of STAT5 activation during pregnancy. Elf5 responsive elements were found near the promoter region of *STAT5*, suggesting that ELF5 controls STAT5 expression [150]. Genome-wide analysis showed that ELF5 and STAT5 colocalize at mammary-specific STAT5-bound enhancers, including an intergenic enhancer that controls STAT5 activity, suggesting that they cooperate to induce gene expression [151–153].

Additional factors, such as Cub and zona pellucida-like domain-containing protein 1 (CUZD1) operate downstream of the JAK2/STAT5 pathway. Loss of CUZD1 induces abnormal mammary TEBs, and impairs the development of tertiary branches and alveologenesis, resulting in a critical reduction of milk proteins and milk production in pregnant and lactating mice [154]. CUZD1 deletion resulted in enhanced STAT5-mediated transcription activation of members of the EGF family, such as *Areg, Nrg1* (neuregulin-1), and *Epgn* (epigen), which interact with ErbB receptors and promote MEC proliferation [152,154–156].

During early (5–7 days) and mid (11–14 days) pregnancy in mice, the downregulation of SCRIB expression delayed alveologenesis though the reduction of Prl-induced activation of the JAK2/STAT5 pathway [157]. Loss of SCRIB induced PrlR accumulation in the Golgi complex and in recycling endosomes in both mouse and human cells. Given that lactation and milk flow were normal, it was hypothesized that SCRIB levels are restored in late pregnancy [157], however SCRIB depletion has not been fully investigated during involution, when A/B cell polarity is lost [158]. Late during gestation and early during lactation, formation of tight junctions during luminal cell specification controls cellular polarity, which is crucial for directional secretion of milk droplets into the lumen [159], which is principally coordinated by Prl/JAK2 modulation of Extracellular signal-regulated kinases (ERK)1/2 function [160].

### 4.2. The back-and-forth of mammary involution

Offspring weaning removes the suckling stimulus and causes milk stasis, which triggers a series of remodeling processes leading to regression of mammary tissue to a pre-pregnancy state, also known as involution (Fig. 1). In humans involution lasts an average of 24 months, while in rodents it lasts for ~10–20 days and encompasses two main phases, the reversible phase (days 0–2 of involution) and the irreversible phase (days 8–18) [161,162].

The reversible phase is characterized by reduced milk production, milk absorption, epithelial cell shedding, alveolar cell death, phagocytosis of apoptotic cells by non-specialized epithelial cells, leukocyte infiltration, and breakdown of tight junctions. As the name implies, resumption of suckling restores lactation through the release of accumulated milk. During lactation, the mammary gland may commence reversible involution after a few hours of milk accumulation, which restores milk-producing cells and avoids over production of milk.

Cell death in the reversible phase of involution occurs via non-apoptotic signals, where residual milk fat globules are taken up by the MECs through lysosomes, which induces lysosomal-mediated cell death (LCD) [163,164]. Of the factors that control LCD, the Zinc transporter zinc transporter 2 (ZnT2) is involved in regulating mammary gland development during lactation and involution [165]. During lactation, ZnT2 regulates cell polarization, orientation of vesicles, lumen formation, and prolactin signaling, while induction of ZnT2 expression in MECs induced premature activation of involution and increased zinc

concentration in mitochondria and lysosomes [166]. Mutations in ZnT2 have been found in women who produce milk deficient in zinc, which is an important nutritional constituent for newborns [167]. From day 0–6, ~80% of the mammary epithelium undergoes tightly regulated cell death [168]. Serotonin (5-HT) synthetized by MECs [169] regulates tight junction homeostasis through the activation of p38-MAPK signaling, with long-term exposure to 5-HT inducing tight junction breakdown and promoting cell death [170].

Such events occur concomitantly to the recruitment of STAT3-mediated signals, which is initially activated by Leukemia inhibitor factor (LIF) in response to milk stasis during the first 3 days of involution [171,172]. Activation of LIF-STAT3 pathways induces the expression of Oncostatin M (OSM), one of the main cytokines induced by STAT3-regulatory network, and essential factor for the control of the irreversible phase of involution [173]. In fact, mammary glands from either TGF-$\beta^{-/-}$, interleukin $6^{-/-}$ ($IL6^{-/-}$), $lLIF^{-/-}$, or $STAT3^{fl/fl}$ mice showed stalled involution and lower levels of cell death [171,172,174,175]. Similarly, STAT5 overexpression during early involution activates *Akt1* transcription, a direct target of STAT5, and both proteins abrogate pro-apoptotic STAT3 signaling, leading to the survival of mammary cells and delayed involution, indicating that the Prl/JAK2/STAT5 pathway must be terminated during involution [176,177]. Understanding the mechanisms by which STAT3 functions during involution could lead to therapeutic strategies targeting STAT3 during breast cancer development and progression [178].

During the irreversible phase (days 2–6), the mammary Extracellular matrix (ECM) undergoes substantial remodeling, with the activation of wound healing processes, via increased activity of Matrix metalloproteases (MMPs), deposition of collagen and BM, in addition to changes in many signaling pathways [179]. For example, the metalloprotease Disintegrin and metalloproteinase domain-containing protein 12 (ADAM12) directly activates the STAT3 pathway, one of the involution signals in MECs. In addition, MECs of both rodents and humans express the inflammatory activator gene Cyclooxygenase-2 (COX-2) in response to collagen accumulation during involution, a signal that supports immune infiltration, but may also be associated with postpartum breast tumor development [180,181]. Finally, the drop of systemic Prl levels, and the increase of leptin hormone levels induces adipogenesis starting on involution day 2, allowing for the initial reestablishment of pre-pregnancy cellular density and architecture in the mammary gland [182,183].

In the irreversible phase of involution, macrophages and non-professional phagocytic MECs clear the remainder of the cellular debris, resulting in a second wave of inflammation and immune cell recruitment [184,185]. Activation of Ras-related C3 botulinum toxin substrate 1 (Rac1), a member of Rho-GTPase family, in MECs sustains their phagocytic activity, while chemotactic factors promote macrophage infiltration in order to eliminate dead cells [186,187]. Concordantly, Rac1-/- female mice showed accumulation of dead cells and milk protein in the mammary lumen due to loss of adhesion proteins in dying MECs, and inhibition of the phagocytic function of MECs.

The ECM also plays a role in immune cell recruitment and activation, as well as broader immune system functions, as collagen and laminin fragments may also induce an influx of macrophages and neutrophils to the involuting gland [188]. Accordingly, TGF-β regulates MEC cell death and phagocytosis, and helps in the maintenance of ECM integrity, thus also playing a role during the final stages of involution [189,190]. Signaling pathways and the high cell-turnover modulate mammary involution, and they also promote an increase in self-antigen reactions, creating an immune tolerant environment and a mucosal barrier. Increased numbers of T regulatory cells ($ROR\gamma T^{+}$ $FoxP3^{+}$ $CD4^{+}$), dendritic cells, and memory Treg (Th17) cells are observed during involution. The immune environment then reverts to its nulliparous state when involution comes to an end [191].

The immune tolerance observed during involution and lactation may be relevant for understanding postpartum breast cancer, which has a very poor clinical prognosis, as well as suggest potential routes to explore in cancer treatment [192]. For example, T-lymphocytes expressing the T-cell receptor γδ TCR, also called γδ T cells, may be potential targets for genetic engineering to treat a variety of cancers, including breast tumors [193]. γδ T-cells are involved in both innate and adaptive immune responses, and the mechanism of activation for γδ T-cells is major histocompatibility complex (MHC)-independent creating an opportunity for the development of pan-population immunotherapy.

Despite involution being both a complex and extensive developmental process, the post-involution gland is phenotypically indistinguishable from a mammary gland that has never been exposed to pregnancy hormones, and is competent to re-engage in the lactation process *de novo*, by repeating the process with each pregnancy. Part of this ability is based on stable molecular changes brought about by the first pregnancy cycle, which enhance milk production during a consecutive pregnancy, indicating that MECs undergo stable molecular changes that function as a memory of prior pregnancy [194,195]. These changes involve remodeling of the MEC epigenome, including alteration of the DNA methylation landscape and gain of the histone 'active' mark, H3K27ac, at genomic regions associated with early activation of milk-related genes during a subsequent exposure to pregnancy hormones [196–198]. These gene activation mechanisms are MEC-autonomous, given that a robust response to pregnancy hormones was also observed using fatpad transplantation and organoid cultures [198].

Involution shares many biological processes and gene networks with those implicated in breast cancer progression and metastasis [188,199]. Thus, research on involution-related processes will provide insights on the orchestration of mechanisms associated with ECM remodeling, regulation of gene transcription, maintenance of the epigenomic landscape, and immune surveillance in the normal environment of the gland, while also exploring their deregulation in contribution to cancer development.

## 5. Beyond tissue development – The transcriptional regulation of MEC differentiation

Two main theories have been advanced concerning the cellular states between MaSCs and fully differentiated MECs [200]. The first hypothesis is based on a MaSC that differentiates directly into luminal or myoepithelial progenitors, thereby producing the respective differentiated MECs. The second theory postulates the existence of a bipotent stem cell generated by a multipotent stem cell that gives rise to basal and luminal progenitors. However, it is difficult to analyze lineage commitment and differentiation in a system where cell surface markers and signals are highly interchangeable. To address this point, several studies have focused on understanding determinants of cell identity and state, with the goal of defining gene expression dynamics that could identify bi- or unipotent cells and their ability to commit to a lineage during the process of mammary gland differentiation (summarized in Fig. 2 and Table 1).

### 5.1. Working forces of MEC differentiation

Axis inhibition protein 2 (Axin2) is one such factor whose role in MEC differentiation has been investigated. Axin2 is a target of the Wnt/β-Catenin pathway and has been shown to mark stem cells localized at the bottom of intestinal crypts and to generate entire crypt/villus structures [201–203]. In the mammary gland, $Axin2^{+}$ MECs exclusively give rise to MECs committed to the myoepithelial lineage in pre-pubescent mice. However, $Axin2^{+}$ MECs demonstrated multipotent cell fates in mammary transplantation assays, suggesting that signals present during wound healing, or those coming from specific localization at TEBs during mammary branching, may dictate stemness (Table 1) [203,204].

In addition to signaling molecules, epigenetic factors have also been shown to play a role in lineage commitment and differentiation during

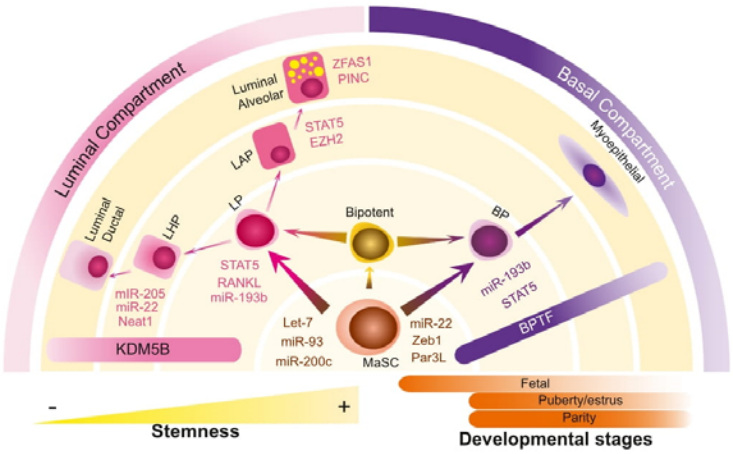


**Fig. 2.** Molecular regulators of mammary hierarchy. Schematic representation of molecular regulators of mammary cell lineage commitment. Two main differentiation pathways have been reported in literature. In one of them, mammary stem cell (MaSCs) can differentiate into luminal progenitors (LP) and basal progenitors (BP), which are committed to originate either luminal alveolar progenitor (LAP) and luminal hormone progenitors (LHP), or myoepithelial cells, respectively. Another possibility is that MaSCs differentiate into a bipotent MaSC that will give rise to LPs and BPs, subsequently driving luminal and basal differentiated cells. Signaling molecules regulating one MEC subpopulation are color coded according to the cell color and are adjacent to the cell type, whereas molecules regulating more than one cell fate are represented with a bar. Lighter yellow semi-circles indicate high cellular stemness whereas the darker yellow is representative of a differentiated state. The orange bars on the right highlight the most common MECs specification networks identified in each stage of the mammary gland. The gradient colors in the bars representing BPTF (Bromodomain Protein Transcription Factor) and KDM5B (Lysine-Specific Demethylase 5B) are directly related to the function of these proteins at the specified cell lineage.

mammary gland development. For instance, Lysine-specific demethylase 5B (KDM5B), a Jumonji protein, is a histone demethylase that removes H3K4me3 methyl marks and regulates ductal development during puberty and pregnancy through the control of the transcription of genes for luminal lineage maintenance [205]. Using a single-cell approach, KDM5B was identified as a regulator of epigenetic and transcriptomic states of differentiated luminal epithelial cells, as well as a regulator of transcriptomic heterogeneity in ER + luminal breast cancer (Table 1) [206]. The inhibition of KDM5B was associated with a pattern of H3K4me3 marks that overall altered the transcriptomic profile in single cells. The KDM5 family of proteins has been implicated in the development of cancer, poor cancer survival, and cancer therapy resistance (e.g. lung, melanoma and breast) [207–210]. Recent studies have attempted to identify small molecules that target KDM5 [211–213].

Many components of the master epigenetic regulator Polycomb complex (PcG) have been implicated during mammary gland development. The H3K27me3 histone methyltransferase Enhancer of zest homolog 2 (EZH2), the catalytic subunit of the polycomb repressive complex 2 (PRC2), and a key factor in stem cell differentiation, regulates the timing of alveologenesis and luminal differentiation during mammary development [79,214–216]. Loss of EZH2 induced premature cell differentiation and luminal alveolar lineage commitment due to enhanced STAT5 occupancy at its genomic binding sites and increased expression of its downstream targets, suggesting that loss of a repressive marker catalyzed by EZH2 facilitated STAT5-dependent gene expression activation and luminal-biased differentiation (Table 1) [217]. During pregnancy, activation of genes associated with milk production and cellular differentiation was associated with loss of H3K27me3 signals, whereas genes that were repressed during pregnancy (and mammary morphogenesis) markedly gained H3K27me3, demonstrating a regulated gene expression switch that supports cellular commitment during pregnancy-development [79]. Conversely, the Polycomb repressive complex 1 (PRC1) ring finger protein 4, also known as BMI-1, plays an essential role in controlling the stemness of MECs [214,215]. Loss of Bmi-1 affected the pool of MaSCs and lineage committed progenitors, which resulted in defective mammary development in fat pad transplantation assays (Table 1), a phenotype that was rescued by further loss of Ink4a/Arf expression, one of the factors negatively regulated by PRC1/BMI-1 [218].

Another key regulator of MaSC self-renewal and differentiation is the Bromodomain protein transcription factor (BPTF). BPTF is the largest subunit of the Nucleosome remodeling factor (NURF) complex, classified as a histone acetylation reader that plays a role in the regulation of chromatin accessibility, modulating TF-DNA occupancy and gene expression levels. [219–223]. Conditional deletion of BPTF in cytokeratin K5 (KRT5+) MaSCs resulted in loss of accessibility at genomic regions occupied by many master regulators of mammary development, such as SRY-box (SOX) 2 [224], Transcription factor AP-2 (TFAP2) [225], Runt-related transcription factor 1 (RUNX1) [226], SOX10 [227], TEA domain transcription factor 1 (TEAD1) [228], SOX6 [229] and Zinc finger e-box binding homeobox 1 (ZEB1) [230], and impacted ductal alveologenesis during active stages of post-birth mammary gland development (Table 1) [231]. Pygopus 2 (PYGO2), is an additional epigenetic factor and histone methylation reader that in response to Wnt signaling controls gene expression, self-renewal and MEC differentiation. Conditional loss of Pygo2 in Cytokeratin 14 (KRT14) expressing cells resulted in reduced mammary repopulation activity in fat pad transplantation assays (Table 1) due to a luminal-biased state of MaSCs, suggesting its role in sustaining the basal-like fate commitment of MECs [232,233]. Further gene-focused chromatin immunoprecipitation assays (ChIP-qPCR) suggested a mechanism through which PYGO2 chromatin association induces the active transcription of *Notch3* mRNA, one of the drivers of luminal/alveolar cellular fate, indicating an epigenomic control of the timing of gene expression according to the cell differentiation state [234,235].

As well as epigenetic regulation of MEC differentiation, many TFs associated with DNA and gene expression regulation are required to determine lineage commitment and cellular differentiation. For example, STAT5 plays a role during pregnancy-development of the mammary gland, and has also been implicated in cellular differentiation [48,139,147,153–156]. Depletion of STAT5 expression in MaSCs resulted in loss of tissue engraftment in fat pad transplantation assays, abrogation of mammary branching, and reduced milk production, demonstrating a role for STAT5 in controlling lineage commitment

**Table 1**
Transcriptional regulation of MEC differentiation – overall summary of bulk and scRNAseq expression profiles and their contribution to elucidating cellular state, master regulators, and lineage commitment across mammary epithelial tress.

| Gene name | Cell types | Function | Identification method | References |
|---|---|---|---|---|
| Axin2 | Multipotent cell fates | Lineage commitment and stemness | Lineage tracing, transplantation assays | [203,204] |
| BPTF | Basal epithelial cells, MaSC pool | MaSC self-renewal, ductal alveologenesis, regulation of chromatin accessibility | Gene knockdown, transgenic mice, RNA-seq, ATAC-seq | [231,333] |
| HOTAIR | Ductal carcinoma cells | Hormonal regulation of cell proliferations | Human tumor tissue analysis, microarray expression analysis, gene knockdown, PDX models | [263,264,266] |
| KDM5B | Luminal epithelial cells | Regulator of epigenetic and transcriptomic states | Single cell RNA-seq, mathematical and molecular modeling, gene knockdown, human tumor cell line cultures, inhibitor resistance | [206,207,211,213] |
| Let-7/ miR-93/ miR-200c | MaSCs | Maintenance of stemness and regulation of differentiation | 3D cell culture assays, miRNA expression sequencing | [248] |
| NEAT1 | Luminal ductal progenitors | Ductal morphogenesis throughout postnatal mammary development | Mouse tissue analysis, RNA in situ hybridization | [260,261] |
| PER2 | MaSC pool | MaSC lineage commitment during pubertal development, regulation of MEC identity, epithelial-mesenchymal transition (EMT) | Transgenic mice, transplantation assays, RNA-seq, | [238,239] |
| PRC2 complex – EZH2 | Luminal alveolar progenitors | Regulator of timing of differentiation and alveologenesis | Gene knockdown, transgenic mice, ES cell differentiation studies | [214,216,217] |
| PRC1 complex – Bmi1 | MaSC pool | Mammary ductal expansion, alveolar cell differentiation, self-renewal of MaSCs | Human MaSC cultures, PDX models, transgenic mice | [218,243] |
| PROM1 | ER+ luminal progenitors | Development and long-term homeostasis of ER+ luminal cells, alveologenesis | Transgenic mice, lineage tracing, transplantation assays | [334] |
| Pygo2 | Basal epithelial cells, MaSC pool | MaSC self-renewal, regulation of chromatin accessibility, lineage commitment and differentiation | Gene knockdown, transgenic mice, transplantation assays, ChIP microarrays | [232,233,335] |
| SOX9 | ER- luminal and basal progenitors | Development and long-term homeostasis of ER- luminal cells | Transgenic mice, lineage tracing, transplantation assays | [240,334] |
| STAT5 | Luminal and basal progenitors | Lineage commitment and differentiation during pregnancy | Inhibitor assays, transgenic mice, microarray analysis, transplantation assays, 3D cell culture systems | [139,147,153–156,236,237] |
| miR-193b | Luminal progenitors | Control of MaSC activity and alveolar differentiation | Transplantation assays. RNA-seq, gene knockdown | [254] |
| miR-205/ miR-22 | MaSCs, MECs | Stemness, EMT, cell polarity, differentiation and specialization of MECs during late pregnancy through lactation, breast tumorigenesis | Transplantation assays, xenograft models, 3D cell culture, gene knockdown | [249–253] |
| miR-206/ miR-150 | Luminal alveolar cells, MaSCs | Regulation of cell proliferation, differentiation, and stemness during pregnancy, mammary positioning during embryogenesis | 3D cell culture, microarray expression analysis, gene overexpression, transgenic mice | [255–257] |
| ZFAS1, PINC | Luminal alveolar cells | Terminal secretory differentiation during pregnancy and lactation, epigenetic control of mammary development | Gene knockdown, microarray expression analysis, RNA in situ hybridization | [259,261] |

(Table 1) [236]. STAT5 overexpression in MaSCs induced precocious alveologenesis, further indicating that STAT5 is involved in the differentiation of luminal alveolar progenitor cells [237].

Based on observations of genes that control MEC lineage commitment, a "developmental clock" has been proposed for MEC fate specification, which functions independently of normal circadian clocks. Period 2 (PER2) is one such gene that regulates MaSC lineage commitment and cell fate determination during the pubertal development of the mammary gland, given that PER2 KO mice exhibited underdeveloped mammary glands with reduced ductal branching, and MECs displayed a dual luminal/myoepithelial phenotype, demonstrating PER2's role in cell fate determination (Table 1) [238]. Further studies showed that loss of PER2 resulted in alteration of MEC identity, with the deregulation of several factors that block or promote EMT progression and MaSC cell fate determination, suggesting that these MECs have increased cell fate plasticity and heterogeneity, which will need to be defined at the single cell level [239,240].

Additional TFs controlling MEC differentiation include the AP-1 complex, E2 factor (E2F), RUNX1, and BCL11B, which mainly control gene expression in response to changes in the levels of growth factors and hormones (such as FGF, EGF, and ER). For example, loss of function of the TFs AP-1and E2F suppressed mammary development at all postnatal stages, given their role in controlling genes such as Ccnd1, c-myelocytomatosis oncogene (c-Myc), Tissue inhibitor matrix metalloproteinase 1 (TIMP1), Vimentin (Vim), and Fibronectin (Fn), which together guide the proliferation, survival, and ECM remodeling of MECs [241,242].

Undoubtedly, this comprehensive overview of molecular regulators in murine MECs illustrates the intersection of complex events that guide murine mammary gland development. The need to understand how such processes take place in mammary tissue aims to answer outstanding questions regarding activation of programs associated with development and carcinogenesis in humans. For example, utilizing RNA interference targeting to induce Bmi-1 knockdown, severely impaired the mammary repopulating capacity of human MaSCs in humanized mammary fat pad transplantation assays, and reduced in vitro mammosphere formation, supporting an evolutionarily conserved role in controlling breast stem cell activity [243]. The notion of the evolutionarily conserved need for molecular regulators of breast development was further expanded in studies that defined cell specific cis-regulatory regions in isolated mammary cell populations from humans, implicating TP63, ELF5, and ESR1 as master regulators of human mammary epithelial lineage commitment [244]. In addition, the utilization of mouse and human comparative analyses revealed that pregnancy epigenetically modifies the Cyclin-dependent kinase inhibitor 1B ($p27^{Kip1}$) and TGFβ gene loci, an effect that influences the state of

luminal progenitor cells in culturing systems [245]. Still, there remains an acknowledged gap in bridging breast cellular function, lifespan, and life events (pregnancy, environmental exposures, habits, etc) with epigenomic and molecular alterations that can influence MEC homeostasis and cancer development.

### 5.2. ncRNA regulation of MEC development

Non-coding RNAs (ncRNAs) are known to play key roles during tissue development and cellular lineage commitment. MicroRNAs (miRNAs) and long non-coding RNAs (lncRNAs) have been implicated in fate specification and specialization of MECs. Profiling of miRNA expression in comma-Dβ cells, a normal-like mammary cell line revealed a number of miRNAs potentially involved in MEC differentiation, including miR-205 and miR-22, which are highly expressed in Sca1$^{high}$ progenitor cells, and let-7 and miR-93, present in mammary undifferentiated cells (Table 1) [246–248].

Several of these miRNAs have subsequently been shown to either promote or block MEC stemness. For example, loss of miR-205 expression resulted in a stemness phenotype in MECs, promoting EMT, and altering cell polarity and symmetric division, through increased Zeb1/2 and Notch expression [249]. During late-pregnancy through lactation, miR-200a stabilizes the levels of E-cadherin and other cell polarity proteins, such as Par6b, by potentially downregulating Zeb1/2, thereby inducing MEC differentiation and specialization [250]. Conversely, miR-22 overexpression resulted in Zeb1 upregulation, leading to the amplification of the MaSC pool, and breast tumorigenesis [251]. Zeb1 and Bmi-1 are also target of miR-200c, a microRNA detected in CD44$^{+}$CD24$^{-}$ mammary repopulating cells and downstream to the p53 oncogene [252,253]. miR-193b has been identified as a STAT5 target, and mice lacking miR-193b showed accelerated stem/progenitor cell activity and proliferation during puberty and pregnancy (Table 1) [254]. Given miR193b is downstream of prolactin signaling, other miRNAs may potentially be targets of hormonal pathways, and their signaling is yet to be elucidated.

Besides its expression in ER + breast cancers, miR-206 regulates the transcription of genes that control cell proliferation, differentiation, and stemness in non-tumorigenic mammary cells during pregnancy (Table 1) [255]. Among the genes upregulated by mir-206 in mammary buds are Tbx3 and Lef1, TFs required for mammary positioning during embryogenesis (see above) [256]. The levels of miR-206 and miR-150 decrease between pregnancy and lactation [255,257]. Constitutive expression of miR-150 in MECs resulted in the failure of alveoli formation, and therefore, lactation, liked caused by reduced the expression and phosphorylation of STAT5 [257], however the exact mechanism is currently not known. miR424–503 has been shown to activate apoptosis during involution [258]. As the offspring are weaned, the TGF-β pathway is activated, upregulating miR-424–503 and resulting in the expression of apoptotic factors while reducing the activity of Akt and ERK1–2 pathways [258].

Amongst the lncRNAs identified in MECs, ZNFX1 antisense RNA 1 (ZFAS1) and pregnancy induced non-coding RNA (PINC), are highly expressed in alveolar cells during pregnancy, however, their expression is significantly decreased during lactation with a subsequent increase during involution (Table 1). The reduction of PINC levels during lactation is crucial for terminal secretory differentiation of the gland as knockdown of PINC induces differentiation whereas its overexpression interferes negatively with lactogenic differentiation [259]. PINC inhibits the differentiation of alveolar secretory cells through its interaction with Retinoblastoma-associated protein 46 (RbAp46) and PRC2, which results in the deposition of H3K27me3 marks that repress the transcription of target genes [259]. PINC modulates the epigenetic control of mammary development to prevent overproduction of milk and uncontrolled differentiation of luminal progenitor cells into alveolar secretory cells.

Similarly, the lncRNA Nuclear paraspeckle assembly transcript 1 (Neat1) is expressed in luminal cells and is required for ductal morphogenesis throughout postnatal mammary gland development, as KO mice for Neat1 show impaired lactation progression (Table 1) [260]. In parous glands, PINC and ZFAS1 localize to the terminal ductal-lobular structures, where their function is associated with cell survival and cell division [261,262]. Taken together, ZFAS1, Neat1, and PINC expression is tightly regulated during mammary development, and collectively these ncRNAs control the differentiation of mammary alveolar structures.

Hox transcript antisense intergenic RNA (HOTAIR) is another lncRNA that recruits PRC2 to control and repress the transcription of target genes (Table 1) [263,264]. Given that E2 regulates HOTAIR, and that HOTAIR regulates cancer cell proliferation and cancer invasion in ER + breast tumors, this suggests that a feedback loop exists between HOTAIR and mammary hormones [265,266]. Metastasis associated lung adenocarcinoma transcript 1 (MALAT1) is a lncRNA upregulated by oxytocin during lactation and in the breast of postmenopausal women [267]. MALAT1 has also been reported to induce invasion and metastasis and to regulate the oncogene p53 [268].

With their wide-ranging role in gene expression regulation, miRNAs and lncRNAs have been considered as suitable drug targets to abrogate the establishment and progression malignant mammary development. While a series of strategies, including the development of tiny-LNAS, have been shown to be efficient in silencing programs regulated by miRNAs [269], recent studies utilizing anti-sense oligo targeting approaches have successfully reduced tumor growth and metastasis by inhibiting MALAT1 expression, thus providing a potential therapeutic strategy to target breast tumors.

### 5.3. New insights into mammary hierarchy – at single cell resolution

The need for more refined strategies to isolate MaSCs and differentiated MECs has led to the development of flow cytometry-based methods for the prospective isolation of mammary cells, the identification of multiple cellular markers that, coupled with molecular profiling, are starting to reveal the mechanistic basis of mammary lineage commitment [200,204,270–277]. These approaches are also filling in the gaps in our understanding of cell specification and plasticity, while raising questions about our appreciation of cellular heterogeneity in MECs. Recent advances in next generation sequencing coupled with bioengineering approaches for single-cell isolation (e.g. microfluidics) offer versatile and agnostic tools able to address global molecular classification and cell identity at high-resolution.

Single cell RNA-seq (scRNAseq) studies are beginning to analyze mammary epithelial cell developmental trajectories in order to address, for example, the existence of bipotent MaSCs and/or lineage-committed progenitors during mammary development, and the temporal switches that govern lineage segregation [278]. To investigate the onset of the mammary epithelial differentiation during embryogenesis, the transcriptomes of a limited pool of FACS-isolated E14 cells have been analyzed, using scRNAseq [279]. Although a transcriptional signature for multipotency was still detected in E13 mammary tissue, unsupervised analysis revealed a composite of gene expression signatures from both luminal and basal cells at E14 [279]. This data provides insight into the molecular regulation that shifts multipotency to unipotency in a developmentally timed fashion, and also indicates the presence of a rare population of bipotent cells early during mammary fetal development. Consistent with these results, scRNAseq data from mouse mammary tissue at E16 and E18 revealed hybrid transcriptional signatures consistent with both basal and luminal lineage specifiers within a single fMaSC cluster, in addition to signatures associated with chromatin remodeling, indicating a role of the epigenetic reprogramming of stemness during mammary embryogenesis [280]. Single-nucleus ATAC-seq (snATACseq) data revealed an epigenetically poised state in fMaSCs from E18, an observation consistent with earlier lineage tracing studies [281,282]. This poised state may guide bidirectional cell commitment to either the basal or luminal lineage after birth [283].

MEC specification accompanies mammary tissue remodeling during subsequent postnatal developmental stages, involving multiple repeated lineage segregation events. Single-cell transcriptome analyses of pre-pubertal glands revealed signs of an intermediate cellular state between embryonic and adult cells, with MECs assuming more luminal/alveolar features, which potentially indicates the emergence of a luminal precursor or immature state [280,284]. Such an intermediate cellular state was also observed in studies that analyzed MaSCs microdissected from TEBs, which demonstrated a heterogenous transcription state for lineage committed MaSCs, thus introducing the concept that perhaps pools of MaSCs are more likely to drive mammary expansion and growth [285]. High-resolution transcriptomics of sorted cells also captured a largely heterogeneous population of MECs wherein myoepithelial cells showed gene profiles correlated to luminal cells, thus suggesting a common ancestry [286].

Single-cell transcriptomics has also revealed and confirmed epithelial cell types within the mammary gland. For instance, scRNA-seq captured Protein C receptor (Procr +) cells, B-cell lymphoma/leukemia 11B (Bcl11 +) cells, and Cadherin 5 (Cdh5 +) cells within myoepithelial cell clusters, corroborating previous studies that characterized populations of MaSCs that reside within the basal compartment, consistent with their ability to fully reconstitute the mammary epithelium in transplantation assays [286–289]. A series of studies have described modifications in the transcriptional landscape of luminal MECs across mammary development. scRNA-seq studies revealed that parity stably affects the transcriptional program of luminal cells, and biases luminal differentiation towards an alveolar fate [288]. E2 treatment correlated with the enrichment of four populations within the luminal progenitor and mature luminal pools, consisting of: (a) $ER\alpha^{+}PR^{+}$; (b) $ER\alpha^{+}PR^{-}$; (c) $ER\alpha^{-}PR^{+}$; and (d) $ER\alpha^{-}PR^{-}$ cells, revealing hormone receptor expression in cells of the luminal fate [290]. Single-cell transcriptomics captured a shift within the hormone-sensing alveolar secretory luminal cells, from high numbers in young murine glands to very low numbers in nulliparous perimenopausal murine glands, indicating a role for aging in luminal cellular fate [291]. Pseudotemporal reconstruction of scRNAseq data from adult breast epithelial cells have also identified a linear trajectory that may give rise to three distinct cellular populations, connecting one myoepithelial cell cluster with two luminal-committed cell clusters [292]. These further divide into subpopulations that were all proliferative, indicating a specific progenitor cell-type for each cell subcluster.

Although single-cell RNA-seq and ATAC-seq are groundbreaking technologies, standardization and reproducibility are critical issues for these methods. Some of the potential pitfalls in these systems arise from single-cell isolation techniques, variation in cell counts, and computational data analysis that considers both technical and biological effects [293]. Furthermore, we still lack a clear general signature of all cells within mammary tissue, including stromal and immune cells, data that would allow effective cellular identification across developmental stages and could consider cellular fluctuations that could influence tumorigenesis. Regardless, single-cell transcriptomics has been critical in the reconstruction of the cell populations that constitute the mammary gland and in disentangling the transcriptional and epigenomic programs critical for mammary lineage segregation and development.

## 6. Organoids and modeling normal mammary gland development

Over the last several decades, it has become clear that the functional differentiation and development of tissues is dependent on three-dimensional architecture. Consequently, there has been a surge in studies that use three-dimentional (3D) cultures to model mammary gland development. Numerous protocols have been developed for the 3D culture of tissues and organs, and the resulting structures are collectively referred to as "organoids". However, the definition of the organoids depends on the source tissue. In the case of mammary glands, organoids are cultures derived from of mammary tissue fragments in 3D gels, whose composition is similar to the in vivo mammary ECM [294,295] .

Cultures of mammary epithelial cells in collagen I gels were first established in the late 1970s. Together with other contemporary studies, they demonstrated that the normal functional differentiation of MECs is dependent on their interaction with a flexible biological substrate [296–299]. MECs harvested from virgin female mice grown in collagen gels showed the ability to reorganize and form structures that can express milk proteins when stimulated with hormones [300–303]. There were also alterations in differentiation and proliferation of MECs depending on whether the collagen gel matrix was attached to a substrate or if it was suspended in dome-like structures [299,304–306].

Mammary organoids can also been grown in commercial 3D matrices such as Matrigel [307] or collagen I [308], which contain BM matrix proteins required for epithelial cell growth and differentiation. Culturing mammary organoids in Matrigel gives rise to organized clusters of bi-layered mammary epithelium, which can be stimulated into branching morphogenesis with growth factors, partially resembling normal in vivo mammary gland development [309,310]. Such organoid systems can also be used as models to study the modifications that pregnancy brings about to the mammary gland. By culturing organoids with pregnancy hormones, organoids can be stimulated to secrete milk proteins (lactation), and removal of such signals can mimic some of the stages seen during involution [198,311] (Fig. 3). Additionally, to understand the role of various stromal components during normal mammary gland development, several co-culture assays for MECs or primary mammary organoids with fibroblasts have been developed [312,313]. These assays involve culturing MECs or primary organoids in Matrigel containing fibroblasts isolated by enzymatic digestion and differential centrifugation. There are also 3D-printing strategies for controlled placement of cells in the hydrogel matrix, which allows for reproducible, high-throughput experiments [314].

3D mammary organoids cultures has led to the elucidation of many factors that drive signaling transduction, gene expression regulation, cell-to-cell junction and tissue remodeling, and that together influence mammary development and MEC differentiation [189,315–320]. More recently, mammary organoids have been used to define a role for Suppressor of zest 12 (SUZ12) and Embryonic ectoderm development (EED), core components of the PRC2 complex, in sustaining progenitor activity of MECs via regulation of cell type specific gene silencing [321]. In addition, high levels of R-spondin-1 (Rspo) induced the expansion of undifferentiated myoepithelial cells, revealing that the combination of Nrg1 treatment with low concentrations of Rspo can help maintaining mammary organoids in culture for extended periods of time [322]. Moreover, mammary organoid cultures have also been utilized to analyze the signals controlling mTOR regulation of MaSCs, and the specific contribution of EMT-associated genes in controlling MEC migration and invasion, demonstrating the use of such a system to understand signals that control stemness and cellular plasticity [323–325].

Recently, protocols have also been developed for modeling mammary gland developmental and molecular processes engaged during pregnancy, lactation and involution, and as well for culturing irradiated organoids to simulate radiotherapy, a standard protocol for treating many types of breast cancer [311,326,327]. Furthermore, it has been shown by single-cell analysis that normal and pre-malignant organoid cultures can retain the complex system of multiple MEC states (stem/progenitor and differentiated) and protein expression patterns [328]. Although lacking the complex interactions with the microenvironment, human tissue organoids can be used as a model system to characterize cellular and molecular changes during development and to test the susceptibility of an individual to a variety of therapies.

## 7. Final remarks

In this review we discuss many aspects of the molecular basis of

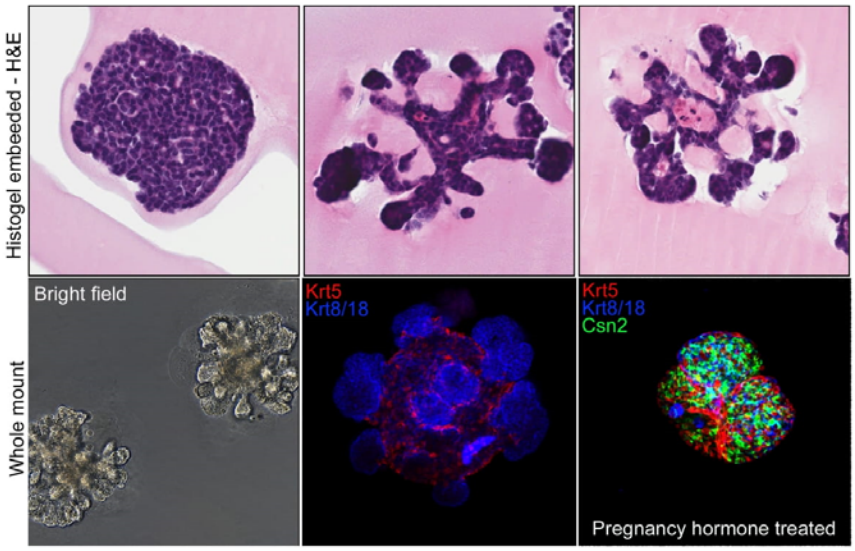


**Fig. 3.** Mammary organoid cultures can replicate characteristics of normal development. Representative images of mammary organoid culture derived from pre-pregnancy MECs (Balb/C mice), grown with either essential media or media with pregnancy hormones (containing estrogen (E2), progesterone (P4), and prolactin (Prl). (a) H&E stained organoids (b) light microscope image of organoids in culture (c) Immunofluorescence image of an organoid showing the branching morphogenesis phenotype (d) Immunofluorescence image of an organoid treated with pregnancy hormones expressing Csn2, a milk protein. Scale: 200 μm. Mammary organoid growth conditions and IF staining were performed as described on [198]. Images credits to Chen Chen and Michael F. Ciccone.

mammary epithelial differentiation, as well as the mechanisms that are engaged during the various mammary gland developmental stages. Our goal was to highlight many of the significant advances in mammary gland biology research from the last several decades, and to highlight important mechanisms that must be considered as we move toward addressing questions about lineage commitment, cellular differentiation, and mammary gland development. Many of the points discussed here have implications for either the initiation, maintenance or progression of mammary tumorigenesis, underlining the disease relevance in the understanding of normal breast development.

Technological developments – the exploration of 3D organoid cultures and single-cell strategies – are deepening our understanding of specific perturbations that influence the mammary tissue as a whole. Unquestionably, the combination of such strategies with novel mathematical models and lineage tracing has the means to provide quantifiable metrics of cell fate and expression heterogeneity and will yield valuable insights into the coordination of tissue development, as well as help in the prediction of novel factors that modulate risk and treatment response of breast tumors. For instance, quantification of MEC-specific apoptosis and proliferation rates, cell size, cell number, and duct morphology, offer parameters that sufficiently predicted the outcome of ductal elongation in TEBs during puberty [47]. In fact, previous studies have also successfully demonstrated the use of mathematical modeling and lineage tracing to correlate the number of cells and differentiation states with age, pregnancy, and the risk for breast cancer development [329–331]. Moreover, the integration of 3D imaging of breast tumor spheroids with the analysis of biophysical parameters using mathematical models has brought us a step closer toward assessing tumor aggressiveness and response to treatment [332], thus offering robustness and a method for the analysis of retrospective clinical data.

Altogether, these strategies hold the promise of answering long-standing questions about the connections between the regulation of gene expression and tissue maintenance, and microenvironment homeostasis and cellular diversity; evidence of which will hopefully elucidate, address, and perhaps even provide preventative strategies against malignant transformation.

## Declaration of Competing Interest

The authors declare that they have no known competing financial interests or personal relationships that could have appeared to influence the work reported in this paper.

## Acknowledgments

This work was performed with the support by the CSHL and Northwell Health Affiliation, the Rita Allen Scholar Award, the AACR-Breast Cancer Research Foundation Award, the Pershing Square Sohn Prize for Cancer Research, the NIH/NCI grant R01CA248158–01 (C.O.D.S.), and Bristol-Myers Squibb Fellowship (A.V.H.S.). We deeply apologize to all investigators whose works were not cited owing to space limitations. This work was also supported with editing services provided by Dr. Riddihough from Life Science Editors.

## References

[1] O.T. Oftedal, The origin of lactation as a water source for parchment-shelled eggs, J. Mammary Gland Biol. Neoplasia 7 (2002) 253–266.
[2] O.T. Oftedal, The mammary gland and its origin during synapsid evolution, J. Mammary Gland Biol. Neoplasia 7 (2002) 225–252.
[3] C. Vorbach, M.R. Capecchi, J.M. Penninger, Evolution of the mammary gland from the innate immune system? Bioessays 28 (2006) 606–616.
[4] A.V. Capuco, S.E. Ellis, Comparative aspects of mammary gland development and homeostasis, Annu. Rev. Anim. Biosci. 1 (2013) 179–202.
[5] A.R. Rowson, K.M. Daniels, S.E. Ellis, R.C. Hovey, Growth and development of the mammary glands of livestock: a veritable barnyard of opportunities, Semin. Cell Dev. Biol. 23 (2012) 557–566.
[6] E. Smyth, R.A. Clegg, C. Holt, A biological perspective on the structure and function of caseins and casein micelles, Int. J. Dairy Technol. 57 (2004) 121–126.

[7] D. Brawand, W. Wahli, H. Kaessmann, Loss of egg yolk genes in mammals and the origin of lactation and placentation, PLoS Biol. 6 (2008), e63.
[8] C.M. Lefèvre, J.A. Sharp, K.R. Nicholas, Characterisation of monotreme caseins reveals lineage-specific expansion of an ancestral casein locus in mammals, Reprod. Fertil. Dev. 21 (2009) 1015–1027.
[9] M. Rijnkels, Multispecies comparison of the casein gene loci and evolution of casein gene family, J. Mammary Gland Biol. Neoplasia 7 (2002) 327–345.
[10] L.S. Carroll, M.R. Capecchi, Hoxc8 initiates an ectopic mammary program by regulating Fgf10 and Tbx3 expression and Wnt/β-catenin signaling, Development 142 (2015) 4056–4067.
[11] M.-L. Asselin-Labat, K.D. Sutherland, H. Barker, R. Thomas, M. Shackleton, N. C. Forrest, L. Hartley, L. Robb, F.G. Grosveld, J. van der Wees, G.J. Lindeman, J. E. Visvader, Gata-3 is an essential regulator of mammary-gland morphogenesis and luminal-cell differentiation, Nat. Cell Biol. 9 (2007) 201–209.
[12] T.G. Davenport, Mammary gland, limb and yolk sac defects in mice lacking Tbx3, the gene mutated in human ulnar mammary syndrome, Development 130 (2003) 2263–2273.
[13] F. Chen, M.R. Capecchi, Paralogous mouse Hox genes, Hoxa9, Hoxb9, and Hoxd9, function together to control development of the mammary gland in response to pregnancy, Proc. Natl. Acad. Sci. 96 (1999) 541–546.
[14] R. Schep, A. Necsulea, E. Rodríguez-Carballo, I. Guerreiro, G. Andrey, T. H. Nguyen Huynh, V. Marcet, J. Zákány, D. Duboule, L. Beccari, Control of Hoxd gene transcription in the mammary bud by hijacking a preexisting regulatory landscape, Proc. Natl. Acad. Sci. 113 (2016) E7720–E7729.
[15] M.C. Eblaghie, S.J. Song, J.Y. Kim, K. Akita, C. Tickle, H.S. Jung, Interactions between FGF and Wnt signals and Tbx3 gene expression in mammary gland initiation in mouse embryos, J. Anat. 205 (2004) 1–13.
[16] K.-W. Cho, J.Y. Kim, S.J. Song, E. Farrell, M.C. Eblaghie, H.J. Kim, C. Tickle, H. S. Jung, Molecular interactions between Tbx3 and Bmp4 and a model for dorsoventral positioning of mammary gland development, Proc. Natl. Acad. Sci. USA 103 (2006) 16788–16793.
[17] C. van Genderen, R.M. Okamura, I. Farinas, R.G. Quo, T.G. Parslow, L. Bruhn, R. Grosschedl, Development of several organs that require inductive epithelial-mesenchymal interactions is impaired in LEF-1-deficient mice, Genes Dev. 8 (1994) 2691–2703.
[18] K. Boras-Granic, H. Chang, R. Grosschedl, P.A. Hamel, Lef1 is required for the transition of Wnt signaling from mesenchymal to epithelial cells in the mouse embryonic mammary gland, Dev. Biol. 295 (2006) 219–231.
[19] J.M. Veltmaat, et al., Positional variations in mammary gland development and cancer, J. Mammary Gland Biol. Neoplasia 18 (2013) 179–188.
[20] L.A. Jerome-Majewska, G.P. Jenkins, E. Ernstoff, F. Zindy, C.J. Sherr, V. E. Papaioannou, Tbx3, the ulnar-mammary syndrome gene, and Tbx2 interact in mammary gland development through a p19Arf/p53-independent pathway, Dev. Dyn. 234 (2005) 922–933.
[21] J.M. Veltmaat, F. Relaix, L.T. Le, K. Kratochwil, F.G. Sala, W. van Veelen, R. Rice, B. Spencer-Dene, A.A. Mailleux, D.P. Rice, J.P. Thiery, S. Bellusci, Gli3-mediated somitic Fgf10 expression gradients are required for the induction and patterning of mammary epithelium along the embryonic axes, Development 133 (2006) 2325–2335.
[22] S.J. Hatsell, P. Cowin, Gli3-mediated repression of Hedgehog targets is required for normal mammary development, Development 133 (2006) 3661–3670.
[23] E.Y. Chu, Canonical WNT signaling promotes mammary placode development and is essential for initiation of mammary gland morphogenesis, Development 131 (2004) 4819–4829.
[24] P. Wend, K. Wend, S.A. Krum, G.A. Miranda-Carboni, The role of WNT10B in physiology and disease, Acta Physiol. (Oxf. ) 204 (2012) 34–51.
[25] M.Y. Lee, L. Sun, J.M. Veltmaat, Hedgehog and Gli signaling in embryonic mammary gland development, J. Mammary Gland Biol. Neoplasia 18 (2013) 133–138.
[26] C. Tickle, H.-S. Jung. Embryonic Mammary Gland Development, John Wiley & Sons Ltd, 2016, pp. 1–10.
[27] G.W. Robinson, Cooperation of signalling pathways in embryonic mammary gland development, Nat. Rev. Genet. 8 (2007) 963–972.
[28] S.J. Hatsell, P. Cowin, Gli3-mediated repression of Hedgehog targets is required for normal mammary development, Development 133 (2006) 3661–3670.
[29] C.J. Creighton, X. Li, M. Landis, J.M. Dixon, V.M. Neumeister, A. Sjolund, D. L. Rimm, H. Wong, A. Rodriguez, J.I. Herschkowitz, C. Fan, X. Zhang, X. He, A. Pavlick, M.C. Gutierrez, L. Renshaw, A.A. Larionov, D. Faratian, S. G. Hilsenbeck, C.M. Perou, M.T. Lewis, J.M. Rosen, J.C. Chang, Residual breast cancers after conventional therapy display mesenchymal as well as tumor-initiating features, Proc. Natl. Acad. Sci. USA 106 (2009) 13820–13825.
[30] X. Ye, W.L. Tam, T. Shibue, Y. Kaygusuz, F. Reinhardt, E. Ng Eaton, R. A. Weinberg, Distinct EMT programs control normal mammary stem cells and tumour-initiating cells, Nature 525 (2015) 256–260.
[31] M. Nassour, Y. Idoux-Gillet, A. Selmi, C. Come, M.L.M. Faraldo, M.A. Deugnier, P. Savagner, Slug controls stem/progenitor cell growth dynamics during mammary gland morphogenesis, PLoS One 7 (2012), e53498.
[32] H. Panchal, O. Wansbury, S. Parry, A. Ashworth, B. Howard, Neuregulin3 alters cell fate in the epidermis and mammary gland, BMC Dev. Biol. 7 (2007) 105.
[33] B.A. Howard, B.A. Gusterson, The characterization of a mouse mutant that displays abnormal mammary gland development, Mamm. Genome 11 (2000) 234–237.
[34] B. Howard, Identification of the scaramanga gene implicates Neuregulin3 in mammary gland specification, Genes Dev. 19 (2005) 2078–2090.
[35] T.A. Stewart, K. Hughes, D.A. Hume, F.M. Davis, Developmental stage-specific distribution of macrophages in mouse mammary gland, Front. Cell Dev. Biol. 7 (2019) 250.
[36] N. Jäppinen, I. Félix, E. Lokka, S. Tyystjärvi, A. Pynttäri, T. Lahtela, H. Gerke, K. Elima, P. Rantakari, M. Salmi, Fetal-derived macrophages dominate in adult mammary glands, Nat. Commun. 10 (2019) 281.
[37] C.A. Dawson, B. Pal, F. Vaillant, L.C. Gandolfo, Z. Liu, C. Bleriot, F. Ginhoux, G. K. Smyth, G.J. Lindeman, S.N. Mueller, A.C. Rios, J.E. Visvader, Tissue-resident ductal macrophages survey the mammary epithelium and facilitate tissue remodelling, Nat. Cell Biol. 22 (2020) 546–558.
[38] D.E. Gyorki, M.L. Asselin-Labat, N. van Rooijen, G.J. Lindeman, J.E. Visvader, Resident macrophages influence stem cell activity in the mammary gland, Breast Cancer Res. 11 (2009) R62.
[39] J.P. Robichaux, R.M. Hallett, J.W. Fuseler, J.A. Hassell, A.F. Ramsdell, Mammary glands exhibit molecular laterality and undergo left-right asymmetric ductal epithelial growth in MMTV-cNeu mice, Oncogene 34 (2015) 2003–2010.
[40] C. Ginestier, J. Wicinski, N. Cervera, F. Monville, P. Finetti, F. Bertucci, M. S. Wicha, D. Birnbaum, E. Charafe-Jauffret, Retinoid signaling regulates breast cancer stem cell differentiation, Cell Cycle 8 (2009) 3297–3302.
[41] M. Rhinn, P. Dolle, Retinoic acid signalling during development, Development 139 (2012) 843–858.
[42] S.A. Cheng, L.Z. Liang, Q.L. Liang, Z.Y. Huang, X.X. Peng, X.C. Hong, X.B. Luo, G. L. Yuan, H.J. Zhang, L. Jiang, Breast cancer laterality and molecular subtype likely share a common risk factor, Cancer Manag. Res. 10 (2018) 6549–6554, https://doi.org/10.2147/CMAR.S182254.
[43] M.H. Amer, Genetic factors and breast cancer laterality, Cancer Manag. Res. (2014) 191, https://doi.org/10.2147/CMAR.S60006.
[44] J.E. Fata, V. Chaudhary, R. Khokha, Cellular turnover in the mammary gland is correlated with systemic levels of progesterone and not 17beta-estradiol during the estrous cycle, Biol. Reprod. 65 (2001) 680–688.
[45] G.W. Robinson, et al., Mammary epithelial cells undergo secretory differentiation in cycling virgins but require pregnancy for the establishment of terminal differentiation, Development 121 (1995) 2079–2090.
[46] A.A. Mailleux, M. Overholtzer, T. Schmelzle, P. Bouillet, A. Strasser, J.S. Brugge, BIM regulates apoptosis during mammary ductal morphogenesis, and its absence reveals alternative cell death mechanisms, Dev. Cell 12 (2007) 221–234.
[47] I. Paine, A. Chauviere, J. Landua, A. Sreekumar, V. Cristini, J. Rosen, M.T. Lewis, A geometrically-constrained mathematical model of mammary gland ductal elongation reveals novel cellular dynamics within the terminal end bud, PLoS Comput. Biol. 12 (2016), e1004839.
[48] S. Srivastava, M. Matsuda, Z. Hou, J.P. Bailey, R. Kitazawa, M.P. Herbst, N. D. Horseman, Receptor activator of NF-kappaB ligand induction via Jak2 and Stat5a in mammary epithelial cells, J. Biol. Chem. 278 (2003) 46171–46178.
[49] J.M. Williams, C.W. Daniel, Mammary ductal elongation: differentiation of myoepithelium and basal lamina during branching morphogenesis, Dev. Biol. 97 (1983) 274–290.
[50] A. Sreekumar, M.J. Toneff, E. Toh, K. Roarty, C.J. Creighton, G.K. Belka, D.K. Lee, J. Xu, L.A. Chodosh, J.S. Richards, J.M. Rosen, WNT-mediated regulation of FOXO1 constitutes a critical axis maintaining pubertal mammary stem cell homeostasis, Dev. Cell 43 (2017) 436–448.e6.
[51] A.N. Sferruzzi-Perri, S.A. Robertson, L.A. Dent, Interleukin-5 transgene expression and eosinophilia are associated with retarded mammary gland development in mice, Biol. Reprod. 69 (2003) 224–233.
[52] V. Gouon-Evans, et al., Postnatal mammary gland development requires macrophages and eosinophils, Development 127 (2000) 2269–2282.
[53] W.V. Ingman, J. Wyckoff, V. Gouon-Evans, J. Condeelis, J.W. Pollard, Macrophages promote collagen fibrillogenesis around terminal end buds of the developing mammary gland, Dev. Dyn. 235 (2006) 3222–3229.
[54] Y. Feng, D. Manka, K.U. Wagner, S.A. Khan, Estrogen receptor-alpha expression in the mammary epithelium is required for ductal and alveolar morphogenesis in mice, Proc. Natl. Acad. Sci. USA 104 (2007) 14718–14723.
[55] J. Russo, X. Ao, C. Grill, I.H. Russo, Pattern of distribution of cells positive for estrogen receptor alpha and progesterone receptor in relation to proliferating cells in the mammary gland, Breast Cancer Res. Treat. 53 (1999) 217–227.
[56] N. Zeps, J.M. Bentel, J.M. Papadimitriou, M.F. D'Antuono, H.J.S. Dawkins, Estrogen receptor-negative epithelial cells in mouse mammary gland development and growth, Differentiation 62 (1998) 221–226.
[57] R.B. Clarke, et al., Dissociation between steroid receptor expression and cell proliferation in the human breast, Cancer Res. 57 (1997) 4987–4991.
[58] L. Ciarloni, S. Mallepell, C. Brisken, Amphiregulin is an essential mediator of estrogen receptor alpha function in mammary gland development, Proc. Natl. Acad. Sci. USA 104 (2007) 5455–5460.
[59] N.J. Kenney, A. Bowman, K.S. Korach, J. Carl Barrett, D.S. Salomon, Effect of exogenous epidermal-like growth factors on mammary gland development and differentiation in the estrogen receptor-alpha knockout (ERKO) mouse, Breast Cancer Res. Treat. 79 (2003) 161–173.
[60] M.D. Sternlicht, Mammary ductal morphogenesis requires paracrine activation of stromal EGFR via ADAM17-dependent shedding of epithelial amphiregulin, Development 132 (2005) 3923–3933.
[61] J.F. Wiesen, et al., Signaling through the stromal epidermal growth factor receptor is necessary for mammary ductal development, Development 126 (1999) 335–344.
[62] A.J. Jackson-Fisher, G. Bellinger, R. Ramabhadran, J.K. Morris, K.F. Lee, D. F. Stern, ErbB2 is required for ductal morphogenesis of the mammary gland, Proc. Natl. Acad. Sci. USA 101 (2004) 17138–17143.

[63] L. Gagniac, M. Rusidzé, F. Boudou, S. Cagnet, M. Adlanmerini, P. Jeannot, N. Gaide, F. Giton, A. Besson, A. Weyl, P. Gourdy, I. Raymond-Letron, J.F. Arnal, C. Brisken, F. Lenfant, Membrane expression of the estrogen receptor ERα is required for intercellular communications in the mammary epithelium, Development 147 (2020), dev182303, https://doi.org/10.1242/dev.182303.

[64] A. Hurtado, K.A. Holmes, C.S. Ross-Innes, D. Schmidt, J.S. Carroll, FOXA1 is a key determinant of estrogen receptor function and endocrine response, Nat. Genet. 43 (2011) 27–33.

[65] J. Laganiere, G. Deblois, C. Lefebvre, A.R. Bataille, F. Robert, V. Giguere, From the Cover: location analysis of estrogen receptor alpha target promoters reveals that FOXA1 defines a domain of the estrogen response, Proc. Natl. Acad. Sci. USA 102 (2005) 11651–11656.

[66] J.S. Carroll, X.S. Liu, A.S. Brodsky, W. Li, C.A. Meyer, A.J. Szary, J. Eeckhoute, W. Shao, E.V. Hestermann, T.R. Geistlinger, E.A. Fox, P.A. Silver, M. Brown, Chromosome-wide mapping of estrogen receptor binding reveals long-range regulation requiring the forkhead protein FoxA1, Cell 122 (2005) 33–43.

[67] H. Kouros-Mehr, E.M. Slorach, M.D. Sternlicht, Z. Werb, GATA-3 maintains the differentiation of the luminal cell fate in the mammary gland, Cell 127 (2006) 1041–1055.

[68] M. Takaku, S.A. Grimm, J.D. Roberts, K. Chrysovergis, B.D. Bennett, P. Myers, L. Perera, C.J. Tucker, C.M. Perou, P.A. Wade, GATA3 zinc finger 2 mutations reprogram the breast cancer transcriptional network, Nat. Commun. 9 (2018) 1059.

[69] M. Takaku, S.A. Grimm, B. De Kumar, B.D. Bennett, P.A. Wade, Cancer-specific mutation of GATA3 disrupts the transcriptional regulatory network governed by Estrogen Receptor alpha, FOXA1 and GATA3, Nucleic Acids Res. 48 (2020) 4756–4768.

[70] J. Howlin, J. McBryan, S. Napoletano, T. Lambe, E. McArdle, T. Shioda, F. Martin, CITED1 homozygous null mice display aberrant pubertal mammary ductal morphogenesis, Oncogene 25 (2006) 1532–1542.

[71] K.B. Ewan, G. Shyamala, S.A. Ravani, Y. Tang, R. Akhurst, L. Wakefield, M. H. Barcellos-Hoff, Latent transforming growth factor-beta activation in mammary gland: regulation by ovarian hormones affects ductal and alveolar proliferation, Am. J. Pathol. 160 (2002) 2081–2093.

[72] E. Anderson, The role of oestrogen and progesterone receptors in human mammary development and tumorigenesis, Breast Cancer Res. 4 (2002) 197–201.

[73] G. Shyamala, X. Yang, G. Silberstein, M.H. Barcellos-Hoff, E. Dale, Transgenic mice carrying an imbalance in the native ratio of A to B forms of progesterone receptor exhibit developmental abnormalities in mammary glands, Proc. Natl. Acad. Sci. USA 95 (1998) 696–701.

[74] O.M. Conneely, B. Mulac-Jericevic, J.P. Lydon, F.J. De Mayo, Reproductive functions of the progesterone receptor isoforms: lessons from knock-out mice, Mol. Cell. Endocrinol. 179 (2001) 97–103.

[75] B. Mulac-Jericevic, Subgroup of reproductive functions of progesterone mediated by progesterone receptor-B isoform, Science 289 (2000) 1751–1754.

[76] C. Brisken, S. Park, T. Vass, J.P. Lydon, B.W. O'Malley, R.A. Weinberg, A paracrine role for the epithelial progesterone receptor in mammary gland development, Proc. Natl. Acad. Sci. USA 95 (1998) 5076–5081.

[77] R.C. Humphreys, J.P. Lydon, B.W. O'Malley, J.M. Rosen, Use of PRKO mice to study the role of progesterone in mammary gland development, J. Mammary Gland Biol. Neoplasia 2 (1997) 343–354.

[78] A.R. Lain, C.J. Creighton, O.M. Conneely, Research resource: progesterone receptor targetome underlying mammary gland branching morphogenesis, Mol. Endocrinol. 27 (2013) 1743–1761.

[79] B. Pal, T. Bouras, W. Shi, F. Vaillant, J.M. Sheridan, N. Fu, K. Breslin, K. Jiang, M. E. Ritchie, M. Young, G.J. Lindeman, G.K. Smyth, J.E. Visvader, Global changes in the mammary epigenome are induced by hormonal cues and coordinated by Ezh2, Cell Rep. 3 (2013) 411–426.

[80] M. Shehata, A. Teschendorff, G. Sharp, N. Novcic, I.A. Russell, S. Avril, M. Prater, P. Eirew, C. Caldas, C.J. Watson, J. Stingl, Phenotypic and functional characterisation of the luminal cell hierarchy of the mammary gland, Breast Cancer Res. 14 (2012) R134.

[81] G. Shyamala, Y.C. Chou, S.G. Louie, R.C. Guzman, G.H. Smith, S. Nandi, Cellular expression of estrogen and progesterone receptors in mammary glands: regulation by hormones, development and aging, J. Steroid Biochem. Mol. Biol. 80 (2002) 137–148.

[82] D. Schams, S. Kohlenberg, W. Amselgruber, B. Berisha, M. Pfaffl, F. Sinowatz, Expression and localisation of oestrogen and progesterone receptors in the bovine mammary gland during development, function and involution, J. Endocrinol. 177 (2003) 305–317.

[83] M. Beleut, R.D. Rajaram, M. Caikovski, A. Ayyanan, D. Germano, Y. Choi, P. Schneider, C. Brisken, Two distinct mechanisms underlie progesterone-induced proliferation in the mammary gland, Proc. Natl. Acad. Sci. USA 107 (2010) 2989–2994.

[84] R. Fernandez-Valdivia, A. Mukherjee, Y. Ying, J. Li, M. Paquet, F.J. DeMayo, J. P. Lydon, The RANKL signaling axis is sufficient to elicit ductal side-branching and alveologenesis in the mammary gland of the virgin mouse, Dev. Biol. 328 (2009) 127–139.

[85] P. Sicinski, J.L. Donaher, S.B. Parker, T. Li, A. Fazeli, H. Gardner, S.Z. Haslam, R. T. Bronson, S.J. Elledge, R.A. Weinberg, Cyclin D1 provides a link between development and oncogenesis in the retina and breast, Cell 82 (1995) 621–630.

[86] V. Fantl, G. Stamp, A. Andrews, I. Rosewell, C. Dickson, Mice lacking cyclin D1 are small and show defects in eye and mammary gland development, Genes Dev. 9 (1995) 2364–2372.

[87] R.D. Rajaram, D. Buric, M. Caikovski, A. Ayyanan, J. Rougemont, J. Shan, S. J. Vainio, O. Yalcin-Ozuysal, C. Brisken, Progesterone and Wnt4 control mammary stem cells via myoepithelial crosstalk, EMBO J. 34 (2015) 641–652.

[88] W. Ruan, M.E. Monaco, D.L. Kleinberg, Progesterone stimulates mammary gland ductal morphogenesis by synergizing with and enhancing insulin-like growth factor-I action, Endocrinology 146 (2005) 1170–1178.

[89] R.A. Jones, C.I. Campbell, E.J. Gunther, L.A. Chodosh, J.J. Petrik, R. Khokha, R. A. Moorehead, Transgenic overexpression of IGF-IR disrupts mammary ductal morphogenesis and induces tumor formation, Oncogene 26 (2007) 1636–1644.

[90] J.M. Carboni, A.V. Lee, D.L. Hadsell, B.R. Rowley, F.Y. Lee, D.K. Bol, A. E. Camuso, M. Gottardis, A.F. Greer, C.P. Ho, W. Hurlburt, A. Li, M. Saulnier, U. Velaparthi, C. Wang, M.L. Wen, R.A. Westhouse, M. Wittman, K. Zimmermann, B.A. Rupnow, T.W. Wong, Tumor development by transgenic expression of a constitutively active insulin-like growth factor I receptor, Cancer Res. 65 (2005) 3781–3787.

[91] M.M. Richert, T.L. Wood, The insulin-like growth factors (IGF) and IGF type I receptor during postnatal growth of the murine mammary gland: sites of messenger ribonucleic acid expression and potential functions, Endocrinology 140 (1999) 454–461.

[92] K.K. de Ostrovich, I. Lambertz, J.K.L. Colby, J. Tian, J.E. Rundhaug, D. Johnston, C.J. Conti, J. DiGiovanni, R. Fuchs-Young, Paracrine overexpression of insulin-like growth factor-1 enhances mammary tumorigenesis in vivo, Am. J. Pathol. 173 (2008) 824–834.

[93] S.G. Bonnette, D.L. Hadsell, Targeted disruption of the IGF-I receptor gene decreases cellular proliferation in mammary terminal end buds, Endocrinology 142 (2001) 4937–4945.

[94] W. Ruan, D.L. Kleinberg, Insulin-like growth factor I is essential for terminal end bud formation and ductal morphogenesis during mammary development, Endocrinology 140 (1999) 5075–5081.

[95] M.D. Aupperlee, J.R. Leipprandt, J.M. Bennett, R.C. Schwartz, S.Z. Haslam, Amphiregulin mediates progesterone-induced mammary ductal development during puberty, Breast Cancer Res. 15 (2013) R44.

[96] L.M. McCaffrey, J. Montalbano, C. Mihai, I.G. Macara, Loss of the Par3 polarity protein promotes breast tumorigenesis and metastasis, Cancer Cell 22 (2012) 601–614.

[97] R.A. Guyer, I.G. Macara, Loss of the polarity protein PAR3 activates STAT3 signaling via an atypical protein kinase C (aPKC)/NF-κB/interleukin-6 (IL-6) axis in mouse mammary cells, J. Biol. Chem. 290 (2015) 8457–8468.

[98] S. Kumar, A. Nandi, A. Mahesh, S. Sinha, E. Flores, R. Chakrabarti, Inducible knockout of ΔNp63 alters cell polarity and metabolism during pubertal mammary gland development, FEBS Lett. 594 (2020) 973–985.

[99] L.M. McCaffrey, I.G. Macara, The Par3/aPKC interaction is essential for end bud remodeling and progenitor differentiation during mammary gland morphogenesis, Genes Dev. 23 (2009) 1450–1460.

[100] Y. Huo, I.G. Macara, The Par3-like polarity protein Par3L is essential for mammary stem cell maintenance, Nat. Cell Biol. 16 (2014) 529–537.

[101] W. Xu, A.C. Gulvady, G.J. Goreczny, E.C. Olson, C.E. Turner, Paxillin-dependent regulation of apical-basal polarity in mammary gland morphogenesis, Development 146 (2019) 146.

[102] A. Santoro, T. Vlachou, M. Carminati, P.G. Pelicci, M. Mapelli, Molecular mechanisms of asymmetric divisions in mammary stem cells, EMBO Rep. 17 (2016) 1700–1720, https://doi.org/10.15252/embr.201643021.

[103] B. Xue, K. Krishnamurthy, D.C. Allred, S.K. Muthuswamy, Loss of Par3 promotes breast cancer metastasis by compromising cell-cell cohesion, Nat. Cell Biol. 15 (2013) 189–200.

[104] S. Chatterjee, L. Seifried, M.E. Feigin, D.L. Gibbons, C. Scuoppo, W. Lin, Z. H. Rizvi, E. Lind, D. Dissanayake, J. Kurie, P. Ohashi, S.K. Muthuswamy, Dysregulation of cell polarity proteins synergize with oncogenes or the microenvironment to induce invasive behavior in epithelial cells, PLoS One 7 (2012), e34343.

[105] M.E. Nolan, V. Aranda, S. Lee, B. Lakshmi, S. Basu, D.C. Allred, S.K. Muthuswamy, The polarity protein Par6 induces cell proliferation and is overexpressed in breast cancer, Cancer Res. 68 (2008) 8201–8209.

[106] M.E. Feigin, S.D. Akshinthala, K. Araki, A.Z. Rosenberg, L.B. Muthuswamy, B. Martin, B.D. Lehmann, H.K. Berman, J.A. Pietenpol, R.D. Cardiff, S. K. Muthuswamy, Mislocalization of the cell polarity protein scribble promotes mammary tumorigenesis and is associated with basal breast cancer, Cancer Res. 74 (2014) 3180–3194.

[107] I.H. Russo, J. Russo, Developmental stage of the rat mammary gland as determinant of its susceptibility to 7,12-dimethylbenz[a]anthracene, J. Natl. Cancer Inst. 61 (1978) 1439–1449.

[108] I. Segatto, M.D.M. Zompit, F. Citron, S. D'Andrea, G.L.R. Vinciguerra, T. Perin, S. Berton, G. Mungo, M. Schiappacassi, C. Marchini, A. Amici, A. Vecchione, G. Baldassarre, B. Belletti, Stathmin is required for normal mouse mammary gland development and Δ16HER2-driven tumorigenesis, Cancer Res. 79 (2019) 397–409.

[109] S. Elias, et al., Huntingtin is required for epithelial polarity through RAB11A-mediated apical trafficking of PAR3-aPKC, PLoS Biol. 13 (2015), e1002142, https://doi.org/10.1371/journal.pbio.1002142.

[110] N. Akhtar, C.H. Streuli, An integrin-ILK-microtubule network orients cell polarity and lumen formation in glandular epithelium, Nat. Cell Biol. 15 (2013) 17–27, https://doi.org/10.1038/ncb2646.

[111] S.J. Kurley, B. Bierie, R.H. Carnahan, N.A. Lobdell, M.A. Davis, I. Hofmann, H. L. Moses, W.J. Muller, A.B. Reynolds, p120-catenin is essential for terminal end bud function and mammary morphogenesis, Development 139 (2012) 1754–1764, https://doi.org/10.1242/dev.072769.

[112] M. Romagnoli, L. Bresson, A. Di-Cicco, M. Pérez-Lanzón, P. Legoix, S. Baulande, P. de la Grange, A. De Arcangelis, E. Georges-Labouesse, A. Sonnenberg, M. A. Deugnier, M.A. Glukhova, M.M. Faraldo, Laminin-binding integrins are essential for the maintenance of functional mammary secretory epithelium in lactation, Development 147 (2020), dev181552, https://doi.org/10.1242/dev.181552.
[113] W.P. Bocchinfuso, J.K. Lindzey, S.C. Hewitt, J.A. Clark, P.H. Myers, R. Cooper, K. S. Korach, Induction of mammary gland development in estrogen receptor-alpha knockout mice, Endocrinology 141 (2000) 2982–2994.
[114] J.P. Lydon, F.J. DeMayo, C.R. Funk, S.K. Mani, A.R. Hughes, C.A. Montgomery, G. Shyamala, O.M. Conneely, B.W. O'Malley, Mice lacking progesterone receptor exhibit pleiotropic reproductive abnormalities, Genes Dev. 9 (1995) 2266–2278.
[115] G.B. Silberstein, K. Van Horn, G. Shyamala, C.W. Daniel, Essential role of endogenous estrogen in directly stimulating mammary growth demonstrated by implants containing pure antiestrogens, Endocrinology 134 (1994) 84–90.
[116] V. Kumar, P. Chambon, The estrogen receptor binds tightly to its responsive element as a ligand-induced homodimer, Cell 55 (1988) 145–156.
[117] S.S. Skandalis, N. Afratis, G. Smirlaki, D. Nikitovic, A.D. Theocharis, G. N. Tzanakakis, N.K. Karamanos, Cross-talk between estradiol receptor and EGFR/IGF-IR signaling pathways in estrogen-responsive breast cancers: focus on the role and impact of proteoglycans, Matrix Biol. 35 (2014) 182–193.
[118] P.A. Joshi, P.D. Waterhouse, N. Kannan, S. Narala, H. Fang, M.A. Di Grappa, H. W. Jackson, J.M. Penninger, C. Eaves, R. Khokha, RANK signaling amplifies WNT-responsive mammary progenitors through R-SPONDIN1, Stem Cell Rep. 5 (2015) 31–44.
[119] C. Brisken, et al., Essential function of Wnt-4 in mammary gland development downstream of progesterone signaling, Genes Dev. 14 (2000) 650–654.
[120] B. Mulac-Jericevic, J.P. Lydon, F.J. DeMayo, O.M. Conneely, Defective mammary gland morphogenesis in mice lacking the progesterone receptor B isoform, Proc. Natl. Acad. Sci. USA 100 (2003) 9744–9749.
[121] J.E. Fata, Y.Y. Kong, J. Li, T. Sasaki, J. Irie-Sasaki, R.A. Moorehead, R. Elliott, S. Scully, E.B. Voura, D.L. Lacey, W.J. Boyle, R. Khokha, J.M. Penninger, The osteoclast differentiation factor osteoprotegerin-ligand is essential for mammary gland development, Cell 103 (2000) 41–50.
[122] E. Gonzalez-Suarez, D. Branstetter, A. Armstrong, H. Dinh, H. Blumberg, W. C. Dougall, RANK overexpression in transgenic mice with mouse mammary tumor virus promoter-controlled RANK increases proliferation and impairs alveolar differentiation in the mammary epithelia and disrupts lumen formation in cultured epithelial acini, Mol. Cell. Biol. 27 (2007) 1442–1454.
[123] Y. Cao, G. Bonizzi, T.N. Seagroves, F.R. Greten, R. Johnson, E.V. Schmidt, M. Karin, IKKalpha provides an essential link between RANK signaling and cyclin D1 expression during mammary gland development, Cell 107 (2001) 763–775.
[124] S. Rao, S.J.F. Cronin, V. Sigl, J.M. Penninger, RANKL and RANK: from mammalian physiology to cancer treatment, Trends Cell Biol. 28 (2018) 213–223.
[125] H.J. Lee, D. Gallego-Ortega, A. Ledger, D. Schramek, P. Joshi, M.M. Szwarc, C. Cho, J.P. Lydon, R. Khokha, J.M. Penninger, C.J. Ormandy, Progesterone drives mammary secretory differentiation via RankL-mediated induction of Elf5 in luminal progenitor cells, Development 140 (2013) 1397–1401.
[126] D.M. Moore, et al., Effect of calcium on oxytocin-induced contraction of mammary gland myoepithelium as visualized by NBD-phallacidin, J. Cell Sci. 88 (Pt 5) (1987) 563–569.
[127] W.S. Young III, E. Shepard, J. Amico, L. Hennighausen, K.U. Wagner, M. E. LaMarca, C. McKinney, E.I. Ginns, Deficiency in mouse oxytocin prevents milk ejection, but not fertility or parturition, J. Neuroendocr. 8 (1996) 847–853.
[128] F.M. Davis, A. Janoshazi, K.S. Janardhan, N. Steinckwich, D.M. D'Agostin, J. G. Petranka, P.N. Desai, S.J. Roberts-Thomson, G.S. Bird, D.K. Tucker, S. E. Fenton, S. Feske, G.R. Monteith, J.W. Putney, Essential role of Orai1 store-operated calcium channels in lactation, Proc. Natl. Acad. Sci. 112 (2015) 5827–5832.
[129] T.A. Stewart, K. Hughes, A.J. Stevenson, N. Marino, A.L. Ju, M. Morehead, F. M. Davis, Mammary mechanobiology: PIEZO1 mechanically-activated ion channels in lactation and involution, bioRxiv (2019), https://doi.org/10.1101/649038.
[130] A.C. Rios, N.Y. Fu, P.R. Jamieson, B. Pal, L. Whitehead, K.R. Nicholas, G. J. Lindeman, J.E. Visvader, Essential role for a novel population of binucleated mammary epithelial cells in lactation, Nat. Commun. 7 (2016) 11400.
[131] B.K. Vonderhaar, et al., Difference between mammary epithelial cells from mature virgin and primiparous mice, Cancer Res. 38 (1978) 4059–4065.
[132] B.K. Vonderhaar, G.H. Smith, Dissociation of cytological and functional differential in virgin mouse mammary gland during inhibition of DNA synthesis, J. Cell Sci. 53 (1982) 97–114.
[133] G.H. Smith, B.K. Vonderhaar, Functional differentiation in mouse mammary gland epithelium is attained through DNA synthesis, inconsequent of mitosis, Dev. Biol. 88 (1981) 167–179.
[134] G.H. Smith, D. Medina, A morphologically distinct candidate for an epithelial stem cell in mouse mammary gland, J. Cell Sci. 90 (Pt 1) (1988) 173–183.
[135] L. Hennighausen, G.W. Robinson, Signaling pathways in mammary gland development, Dev. Cell 1 (2001) 467–475.
[136] C.J. Ormandy, N. Binart, P.A. Kelly, Mammary gland development in prolactin receptor knockout mice, J. Mammary Gland Biol. Neoplasia 2 (1997) 355–364.
[137] C.J. Ormandy, A. Camus, J. Barra, D. Damotte, B. Lucas, H. Buteau, M. Edery, N. Brousse, C. Babinet, N. Binart, P.A. Kelly, Null mutation of the prolactin receptor gene produces multiple reproductive defects in the mouse, Genes Dev. 11 (1997) 167–178.
[138] A.J. Vomachka, S.L. Pratt, J.A. Lockefeer, N.D. Horseman, Prolactin gene-disruption arrests mammary gland development and retards T-antigen-induced tumor growth, Oncogene 19 (2000) 1077–1084.
[139] A. Cordero, P. Pellegrini, A. Sanz-Moreno, E.M. Trinidad, J. Serra-Musach, C. Deshpande, W.C. Dougall, M.A. Pujana, E. González-Suárez, Rankl impairs lactogenic differentiation through inhibition of the prolactin/Stat5 pathway at midgestation, Stem Cells 34 (2016) 1027–1039.
[140] H. Rui, et al., Activation of receptor-associated tyrosine kinase JAK2 by prolactin, J. Biol. Chem. 269 (1994) 5364–5368.
[141] H. Wakao, F. Gouilleux, B. Groner, Mammary gland factor (MGF) is a novel member of the cytokine regulated transcription factor gene family and confers the prolactin response, EMBO J. 13 (1994) 2182–2191.
[142] S. Ali, Prolactin receptor regulates Stat5 tyrosine phosphorylation and nuclear translocation by two separate pathways, J. Biol. Chem. 273 (1998) 7709–7716.
[143] G. Li, Z. Wang, Y. Zhang, Z. Kang, E. Haviernikova, Y. Cui, L. Hennighausen, R. Moriggl, D. Wang, W. Tse, K.D. Bunting, STAT5 requires the N-domain to maintain hematopoietic stem cell repopulating function and appropriate lymphoid-myeloid lineage output, Exp. Hematol. 35 (2007) 1684–1694.
[144] F. Liu, G. Kunter, M.M. Krem, W.C. Eades, J.A. Cain, M.H. Tomasson, L. Hennighausen, D.C. Link, Csf3r mutations in mice confer a strong clonal HSC advantage via activation of Stat5, J. Clin. Investig. 118 (2008) 946–955.
[145] S. Li, J.M. Rosen, Nuclear factor I and mammary gland factor (STAT5) play a critical role in regulating rat whey acidic protein gene expression in transgenic mice, Mol. Cell. Biol. 15 (1995) 2063–2070.
[146] M. Schmitt-Ney, W. Doppler, R.K. Ball, B. Groner, Beta-casein gene promoter activity is regulated by the hormone-mediated relief of transcriptional repression and a mammary-gland-specific nuclear factor, Mol. Cell. Biol. 11 (1991) 3745–3755.
[147] H.Y. Shin, M. Willi, K.H. Yoo, X. Zeng, C. Wang, G. Metser, L. Hennighausen, Hierarchy within the mammary STAT5-driven Wap super-enhancer, Nat. Genet. 48 (2016) 904–911.
[148] S.R. Oakes, M.J. Naylor, M.L. Asselin-Labat, K.D. Blazek, M. Gardiner-Garden, H. N. Hilton, M. Kazlauskas, M.A. Pritchard, L.A. Chodosh, P.L. Pfeffer, G. J. Lindeman, J.E. Visvader, C.J. Ormandy, The Ets transcription factor Elf5 specifies mammary alveolar cell fate, Genes Dev. 22 (2008) 581–586.
[149] J. Zhou, R. Chehab, J. Tkalcevic, M.J. Naylor, J. Harris, T.J. Wilson, S. Tsao, I. Tellis, S. Zavarsek, D. Xu, E.J. Lapinskas, J. Visvader, G.J. Lindeman, R. Thomas, C.J. Ormandy, P.J. Hertzog, I. Kola, M.A. Pritchard, Elf5 is essential for early embryogenesis and mammary gland development during pregnancy and lactation, EMBO J. 24 (2005) 635–644.
[150] Y.S. Choi, R. Chakrabarti, R. Escamilla-Hernandez, S. Sinha, Elf5 conditional knockout mice reveal its role as a master regulator in mammary alveolar development: Failure of Stat5 activation and functional differentiation in the absence of Elf5, Dev. Biol. 329 (2009) 227–241.
[151] G. Metser, H.Y. Shin, C. Wang, K.H. Yoo, S. Oh, A.V. Villarino, J.J. O'Shea, K. Kang, L. Hennighausen, An autoregulatory enhancer controls mammary-specific STAT5 functions, Nucleic Acids Res. 44 (2016) 1052–1063.
[152] T. Komurasaki, H. Toyoda, D. Uchida, S. Morimoto, Epiregulin binds to epidermal growth factor receptor and ErbB-4 and induces tyrosine phosphorylation of epidermal growth factor receptor, ErbB-2, ErbB-3 and ErbB-4, Oncogene 15 (1997) 2841–2848.
[153] X. Zeng, M. Willi, H.Y. Shin, L. Hennighausen, C. Wang, Lineage-specific and non-specific cytokine-sensing genes respond differentially to the master regulator STAT5, Cell Rep. 17 (2016) 3333–3346.
[154] J. Mapes, Q. Li, A. Kannan, L. Anandan, M. Laws, J.P. Lydon, I.C. Bagchi, M. K. Bagchi, CUZD1 is a critical mediator of the JAK/STAT5 signaling pathway that controls mammary gland development during pregnancy, PLOS Genet. 13 (2017), e1006654.
[155] B.-M. Zhu, K. Kang, J.H. Yu, W. Chen, H.E. Smith, D. Lee, H.W. Sun, L. Wei, L. Hennighausen, Genome-wide analyses reveal the extent of opportunistic STAT5 binding that does not yield transcriptional activation of neighboring genes, Nucleic Acids Res. 40 (2012) 4461–4472.
[156] P.V. Elizalde, R.I. Cordo Russo, M.F. Chervo, R. Schillaci, ErbB-2 nuclear function in breast cancer growth, metastasis and resistance to therapy, Endocr. Relat. Cancer 23 (2016) T243–T257.
[157] L. Baker, M. BeGora, F. Au Yeung, M.E. Feigin, A.Z. Rosenberg, S.W. Lowe, T. Kislinger, S.K. Muthuswamy, Scribble is required for pregnancy-induced alveologenesis in the adult mammary gland, J. Cell Sci. 129 (2016) 2307–2315.
[158] S.M. McDaniel, K.K. Rumer, S.L. Biroc, R.P. Metz, M. Singh, W. Porter, P. Schedin, Remodeling of the mammary microenvironment after lactation promotes breast tumor cell metastasis, Am. J. Pathol. 168 (2006) 608–620.
[159] E. Rodriguez-Boulan, I.G. Macara, Organization and execution of the epithelial polarity programme, Nat. Rev. Mol. Cell Biol. 15 (2014) 225–242.
[160] F. Liu, A. Pawliwec, Z. Feng, Z. Yasruel, J.J. Lebrun, S. Ali, Prolactin/Jak2 directs apical/basal polarization and luminal linage maturation of mammary epithelial cells through regulation of the Erk1/2 pathway, Stem Cell Res. 15 (2015) 376–383.
[161] S. Jindal, D. Gao, P. Bell, G. Albrektsen, S.M. Edgerton, C.B. Ambrosone, A. D. Thor, V.F. Borges, P. Schedin, Postpartum breast involution reveals regression of secretory lobules mediated by tissue-remodeling, Breast Cancer Res. 16 (2014) R31.
[162] J.A. Sharp, C. Lefevre, A.J. Brennan, K.R. Nicholas, The fur seal-a model lactation phenotype to explore molecular factors involved in the initiation of apoptosis at involution, J. Mammary Gland Biol. Neoplasia 12 (2007) 47–58.
[163] F.O. Baxter, K. Neoh, M.C. Tevendale, The beginning of the end: death signaling in early involution, J. Mammary Gland Biol. Neoplasia 12 (2007) 3–13.

[164] T.J. Sargeant, B. Lloyd-Lewis, H.K. Resemann, A. Ramos-Montoya, J. Skepper, C. J. Watson, Stat3 controls cell death during mammary gland involution by regulating uptake of milk fat globules and lysosomal membrane permeabilization, Nat. Cell Biol. 16 (2014) 1057–1068.
[165] S.R. Hennigar, Y.A. Seo, S. Sharma, D.I. Soybel, S.L. Kelleher, ZnT2 is a critical mediator of lysosomal-mediated cell death during early mammary gland involution, Sci. Rep. 5 (2015) 8033.
[166] S. Lee, O.C. Rivera, S.L. Kelleher, Zinc transporter 2 interacts with vacuolar ATPase and is required for polarization, vesicle acidification, and secretion in mammary epithelial cells, J. Biol. Chem. 292 (2017) 21598–21613.
[167] W. Chowanadisai, B. Lonnerdal, S.L. Kelleher, Identification of a mutation in SLC30A2 (ZnT-2) in women with low milk zinc concentration that results in transient neonatal zinc deficiency, J. Biol. Chem. 281 (2006) 39699–39707.
[168] N.I. Walker, R.E. Bennett, J.F.R. Kerr, Cell death by apoptosis during involution of the lactating breast in mice and rats, Am. J. Anat. 185 (1989) 19–32.
[169] M. Matsuda, T. Imaoka, A.J. Vomachka, G.A. Gudelsky, Z. Hou, M. Mistry, J. P. Bailey, K.M. Nieport, D.J. Walther, M. Bader, N.D. Horseman, Serotonin regulates mammary gland development via an autocrine-paracrine loop, Dev. Cell 6 (2004) 193–203.
[170] V.P. Pai, N.D. Horseman, Multiple cellular responses to serotonin contribute to epithelial homeostasis, PLoS One 6 (2011), e17028.
[171] E.A. Kritikou, A dual, non-redundant, role for LIF as a regulator of development and STAT3-mediated cell death in mammary gland, Development 130 (2003) 3459–3468.
[172] C. Schere-Levy, Leukemia inhibitory factor induces apoptosis of the mammary epithelial cells and participates in mouse mammary gland involution, Exp. Cell Res. 282 (2003) 35–47.
[173] P.G. Tiffen, N. Omidvar, N. Marquez-Almuina, D. Croston, C.J. Watson, R.W. E. Clarkson, A dual role for oncostatin M signaling in the differentiation and death of mammary epithelial cells in vivo, Mol. Endocrinol. 22 (2008) 2677–2688, https://doi.org/10.1210/me.2008-0097.
[174] A.V. Nguyen, J.W. Pollard, Transforming growth factor beta3 induces cell death during the first stage of mammary gland involution, Development 127 (2000) 3107–3118.
[175] R.C. Humphreys, B. Bierie, L. Zhao, R. Raz, D. Levy, L. Hennighausen, Deletion of Stat3 blocks mammary gland involution and extends functional competence of the secretory epithelium in the absence of lactogenic stimuli, Endocrinology 143 (2002) 3641–3650.
[176] B.A. Creamer, K. Sakamoto, J.W. Schmidt, A.A. Triplett, R. Moriggl, K.U. Wagner, Stat5 promotes survival of mammary epithelial cells through transcriptional activation of a distinct promoter in Akt1, Mol. Cell. Biol. 30 (2010) 2957–2970.
[177] J.W. Schmidt, B.L. Wehde, K. Sakamoto, A.A. Triplett, S.M. Anderson, P. N. Tsichlis, G. Leone, K.U. Wagner, Stat5 regulates the phosphatidylinositol 3-Kinase/Akt1 pathway during mammary gland development and tumorigenesis, Mol. Cell. Biol. 34 (2014) 1363–1377.
[178] E.C. Kordon, O.A. Coso, Postlactational involution: molecular mechanisms and relevance for breast cancer development, in: Current Topics in Lactation, InTech, 2017.
[179] K.A. Green, L.R. Lund, ECM degrading proteases and tissue remodelling in the mammary gland, Bioessays 27 (2005) 894–903.
[180] J. Fornetti, S. Jindal, K.A. Middleton, V.F. Borges, P. Schedin, Physiological COX-2 expression in breast epithelium associates with COX-2 levels in ductal carcinoma in situ and invasive breast cancer in young women, Am. J. Pathol. 184 (2014) 1219–1229.
[181] T.R. Lyons, J. O'Brien, V.F. Borges, M.W. Conklin, P.J. Keely, K.W. Eliceiri, A. Marusyk, A.C. Tan, P. Schedin, Postpartum mammary gland involution drives progression of ductal carcinoma in situ through collagen and COX-2, Nat. Med. 17 (2011) 1109–1115.
[182] N. Ben-Jonathan, E. Hugo, Prolactin (PRL) in adipose tissue: regulation and functions, Adv. Exp. Med. Biol. 846 (2015) 1–35.
[183] Y. Lin, Q. Li, Expression and function of leptin and its receptor in mouse mammary gland, Sci. China Ser. C Life Sci. 50 (2007) 669–675.
[184] T. Stein, J.S. Morris, C.R. Davies, S.J. Weber-Hall, M.A. Duffy, V.J. Heath, A. K. Bell, R.K. Ferrier, G.P. Sandilands, B.A. Gusterson, Involution of the mouse mammary gland is associated with an immune cascade and an acute-phase response, involving LBP, CD14 and STAT3, Breast Cancer Res. 6 (2004) R75–R91.
[185] J. Monks, D. Rosner, F. Jon Geske, L. Lehman, L. Hanson, M.C. Neville, V. A. Fadok, Epithelial cells as phagocytes: apoptotic epithelial cells are engulfed by mammary alveolar epithelial cells and repress inflammatory mediator release, Cell Death Differ. 12 (2005) 107–114.
[186] N. Akhtar, W. Li, A. Mironov, C.H. Streuli, Rac1 controls both the secretory function of the mammary gland and its remodeling for successive gestations, Dev. Cell 38 (2016) 522–535.
[187] F. Schuler, F. Baumgartner, V. Klepsch, M. Chamson, E. Müller-Holzner, C. J. Watson, S. Oh, L. Hennighausen, P. Tymoszuk, W. Doppler, A. Villunger, The BH3-only protein BIM contributes to late-stage involution in the mouse mammary gland, Cell Death Differ. 23 (2016) 41–51.
[188] M.K. Jena, S. Jaswal, S. Kumar, A.K. Mohanty, Molecular mechanism of mammary gland involution: an update, Dev. Biol. 445 (2019) 145–155.
[189] J. Xu, S. Lamouille, R. Derynck, TGF-β-induced epithelial to mesenchymal transition, Cell Res. 19 (2009) 156–172.
[190] M.-F. Pang, A.M. Georgoudaki, L. Lambut, J. Johansson, V. Tabor, K. Hagikura, Y. Jin, M. Jansson, J.S. Alexander, C.M. Nelson, L. Jakobsson, C. Betsholtz, M. Sund, M.C.I. Karlsson, J. Fuxe, TGF-β1-induced EMT promotes targeted migration of breast cancer cells through the lymphatic system by the activation of CCR7/CCL21-mediated chemotaxis, Oncogene 35 (2016) 748–760.
[191] C.B. Betts, N.D. Pennock, B.P. Caruso, B. Ruffell, V.F. Borges, P. Schedin, Mucosal immunity in the female murine mammary gland, J. Immunol. 201 (2018) 734–746.
[192] J. Fornetti, H.A. Martinson, C.B. Betts, T.R. Lyons, S. Jindal, Q. Guo, L. M. Coussens, V.F. Borges, P. Schedin, Mammary gland involution as an immunotherapeutic target for postpartum breast cancer, J. Mammary Gland Biol. Neoplasia 19 (2014) 213–228.
[193] A. Janssen, J. Villacorta Hidalgo, D.X. Beringer, S. van Dooremalen, F. Fernando, E. van Diest, A.R. Terrizi, P. Bronsert, S. Kock, A. Schmitt-Gräff, M. Werner, K. Heise, M. Follo, T. Straetemans, Z. Sebestyen, D.M. Chudakov, S.A. Kasatskaya, F.E. Frenkel, S. Ravens, E. Spierings, I. Prinz, R. Küppers, M. Malkovsky, P. Fisch, J. Kuball, γδ T-cell receptors derived from breast cancer-infiltrating T lymphocytes mediate antitumor reactivity, Cancer Immunol. Res. 8 (2020) 530–543.
[194] A.A. Zuppa, A. Tornesello, P. Papacci, G. Tortorolo, G. Segni, G. Lafuenti, E. Moneta, A. Diodato, M. Sorcini, S. Carta, Relationship between maternal parity, basal prolactin levels and neonatal breast milk intake, Biol. Neonate 53 (1988) 144–147.
[195] J. Ingram, M. Woolridge, R. Greenwood, Breastfeeding: it is worth trying with the second baby, Lancet (Lond., Engl. ) 358 (2001) 986–987.
[196] S.J. Huh, K. Clement, D. Jee, A. Merlini, S. Choudhury, R. Maruyama, R. Yoo, A. Chytil, P. Boyle, F.A. Ran, H.L. Moses, M.H. Barcellos-Hoff, L. Jackson-Grusby, A. Meissner, K. Polyak, Age- and pregnancy-associated DNA methylation changes in mammary epithelial cells, Stem Cell Rep. 4 (2015) 297–311.
[197] C.O. dos Santos, E. Dolzhenko, E. Hodges, A.D. Smith, G.J. Hannon, An epigenetic memory of pregnancy in the mouse mammary gland, Cell Rep. 11 (2015) 1102–1109.
[198] M.J. Feigman, M.A. Moss, C. Chen, S.L. Cyrill, M.F. Ciccone, M.C. Trousdell, S. T. Yang, W.D. Frey, J.E. Wilkinson, C.O. dos Santos, Pregnancy reprograms the epigenome of mammary epithelial cells and blocks the development of premalignant lesions, Nat. Commun. 11 (2020) 2649.
[199] T.R. Wallace, S.E. Tarullo, L.S. Crump, T.R. Lyons, Studies of postpartum mammary gland involution reveal novel pro-metastatic mechanisms, J. Cancer Metastas. Treat. 2019 (2019) 2019.
[200] N.Y. Fu, E. Nolan, G.J. Lindeman, J.E. Visvader, Stem cells and the differentiation hierarchy in mammary gland development, Physiol. Rev. 100 (2020) 489–523.
[201] V. Muncan, O.J. Sansom, L. Tertoolen, T.J. Phesse, H. Begthel, E. Sancho, A. M. Cole, A. Gregorieff, I.M. de Alboran, H. Clevers, A.R. Clarke, Rapid loss of intestinal crypts upon conditional deletion of the Wnt/Tcf-4 target gene c-Myc, Mol. Cell. Biol. 26 (2006) 8418–8426.
[202] V. Korinek, N. Barker, P. Moerer, E. van Donselaar, G. Huls, P.J. Peters, H. Clevers, Depletion of epithelial stem-cell compartments in the small intestine of mice lacking Tcf-4, Nat. Genet. 19 (1998) 379–383.
[203] R. van Amerongen, A.N. Bowman, R. Nusse, Developmental stage and time dictate the fate of Wnt/β-catenin-responsive stem cells in the mammary gland, Cell Stem Cell 11 (2012) 387–400.
[204] A. Van Keymeulen, A.S. Rocha, M. Ousset, B. Beck, G. Bouvencourt, J. Rock, N. Sharma, S. Dekoninck, C. Blanpain, Distinct stem cells contribute to mammary gland development and maintenance, Nature 479 (2011) 189–193.
[205] M.R. Zou, J. Cao, Z. Liu, S.J. Huh, K. Polyak, Q. Yan, Histone demethylase jumonji AT-rich interactive domain 1B (JARID1B) controls mammary gland development by regulating key developmental and lineage specification genes, J. Biol. Chem. 289 (2014) 17620–17633.
[206] K. Hinohara, H.J. Wu, S. Vigneau, T.O. McDonald, K.J. Igarashi, K.N. Yamamoto, T. Madsen, A. Fassl, S.B. Egri, M. Papanastasiou, L. Ding, G. Peluffo, O. Cohen, S. C. Kales, M. Lal-Nag, G. Rai, D.J. Maloney, A. Jadhav, A. Simeonov, N. Wagle, M. Brown, A. Meissner, P. Sicinski, J.D. Jaffe, R. Jeselsohn, A.A. Gimelbrant, F. Michor, K. Polyak, KDM5 histone demethylase activity links cellular transcriptomic heterogeneity to therapeutic resistance, Cancer Cell 34 (2018) 939–953.e9.
[207] S. Yamamoto, Z. Wu, H.G. Russnes, S. Takagi, G. Peluffo, C. Vaske, X. Zhao, H. K. Moen Vollan, R. Maruyama, M.B. Ekram, H. Sun, J.H. Kim, K. Carver, M. Zucca, J. Feng, V. Almendro, M. Bessarabova, O.M. Rueda, Y. Nikolsky, C. Caldas, X.S. Liu, K. Polyak, JARID1B is a luminal lineage-driving oncogene in breast cancer, Cancer Cell 25 (2014) 762–777.
[208] A. Roesch, A. Vultur, I. Bogeski, H. Wang, K.M. Zimmermann, D. Speicher, C. Körbel, M.W. Laschke, P.A. Gimotty, S.E. Philipp, E. Krause, S. Pätzold, J. Villanueva, C. Krepler, M. Fukunaga-Kalabis, M. Hoth, B.C. Bastian, T. Vogt, M. Herlyn, Overcoming intrinsic multidrug resistance in melanoma by blocking the mitochondrial respiratory chain of slow-cycling JARID1B(high) cells, Cancer Cell 23 (2013) 811–825.
[209] A. Roesch, M. Fukunaga-Kalabis, E.C. Schmidt, S.E. Zabierowski, P.A. Brafford, A. Vultur, D. Basu, P. Gimotty, T. Vogt, M. Herlyn, A temporarily distinct subpopulation of slow-cycling melanoma cells is required for continuous tumor growth, Cell 141 (2010) 583–594.
[210] S.V. Sharma, D.Y. Lee, B. Li, M.P. Quinlan, F. Takahashi, S. Maheswaran, U. McDermott, N. Azizian, L. Zou, M.A. Fischbach, K.K. Wong, K. Brandstetter, B. Wittner, S. Ramaswamy, M. Classon, J. Settleman, A chromatin-mediated reversible drug-tolerant state in cancer cell subpopulations, Cell 141 (2010) 69–80.
[211] J.R. Horton, A. Engstrom, E.L. Zoeller, X. Liu, J.R. Shanks, X. Zhang, M.A. Johns, P.M. Vertino, H. Fu, X. Cheng, Characterization of a linked jumonji domain of the KDM5/JARID1 family of histone H3 lysine 4 demethylases, J. Biol. Chem. 291 (2016) 2631–2646.
[212] C. Johansson, S. Velupillai, A. Tumber, A. Szykowska, E.S. Hookway, R.P. Nowak, C. Strain-Damerell, C. Gileadi, M. Philpott, N. Burgess-Brown, N. Wu, J. Kopec,

A. Nuzzi, H. Steuber, U. Egner, V. Badock, S. Munro, N.B. LaThangue, S. Westaway, J. Brown, N. Athanasou, R. Prinjha, P.E. Brennan, U. Oppermann, Structural analysis of human KDM5B guides histone demethylase inhibitor development, Nat. Chem. Biol. 12 (2016) 539–545.

[213] S. Pippa, C. Mannironi, V. Licursi, L. Bombardi, G. Colotti, E. Cundari, A. Mollica, A. Coluccia, V. Naccarato, G. La Regina, R. Silvestri, R. Negri, Small molecule inhibitors of KDM5 histone demethylases increase the radiosensitivity of breast cancer cells overexpressing JARID1B, Molecules 24 (2019) 24.

[214] E.M. Michalak, K. Nacerddine, A. Pietersen, V. Beuger, I. Pawlitzky, P. Cornelissen-Steijger, E. Wientjens, E. Tanger, J. Seibler, M. van Lohuizen, J. Jonkers, Polycomb group gene Ezh2 regulates mammary gland morphogenesis and maintains the luminal progenitor pool, Stem Cells 31 (2013) 1910–1920.

[215] R. Margueron, G. Li, K. Sarma, A. Blais, J. Zavadil, C.L. Woodcock, B.D. Dynlacht, D. Reinberg, Ezh1 and Ezh2 maintain repressive chromatin through different mechanisms, Mol. Cell 32 (2008) 503–518.

[216] X. Shen, Y. Liu, Y.J. Hsu, Y. Fujiwara, J. Kim, X. Mao, G.C. Yuan, S.H. Orkin, EZH1 mediates methylation on histone H3 lysine 27 and complements EZH2 in maintaining stem cell identity and executing pluripotency, Mol. Cell 32 (2008) 491–502.

[217] K.H. Yoo, S. Oh, K. Kang, T. Hensel, G.W. Robinson, L. Hennighausen, Loss of EZH2 results in precocious mammary gland development and activation of STAT5-dependent genes, Nucleic Acids Res. 43 (2015) 8774–8789.

[218] A.M. Pietersen, B. Evers, A.A. Prasad, E. Tanger, P. Cornelissen-Steijger, J. Jonkers, M. van Lohuizen, Bmi1 regulates stem cells and proliferation and differentiation of committed cells in mammary epithelium, Curr. Biol. 18 (2008) 1094–1099, https://doi.org/10.1016/j.cub.2008.06.070.

[219] T. Goller, F. Vauti, S. Ramasamy, H.H. Arnold, Transcriptional regulator BPTF/FAC1 is essential for trophoblast differentiation during early mouse development, Mol. Cell. Biol. 28 (2008) 6819–6827.

[220] J.W. Landry, S. Banerjee, B. Taylor, P.D. Aplan, A. Singer, C. Wu, Chromatin remodeling complex NURF regulates thymocyte maturation, Genes Dev. 25 (2011) 275–286.

[221] D. Koludrovic, P. Laurette, T. Strub, C. Keime, M. Le Coz, S. Coassolo, G. Mengus, L. Larue, I. Davidson, Chromatin-remodelling complex NURF is essential for differentiation of adult melanocyte stem cells, PLOS Genet. 11 (2015), e1005555.

[222] A.J. Ruthenburg, H. Li, T.A. Milne, S. Dewell, R.K. McGinty, M. Yuen, B. Ueberheide, Y. Dou, T.W. Muir, D.J. Patel, C.D. Allis, Recognition of a mononucleosomal histone modification pattern by BPTF via multivalent interactions, Cell 145 (2011) 692–706.

[223] B. Xu, L. Cai, J.M. Butler, D. Chen, X. Lu, D.F. Allison, R. Lu, S. Rafii, J.S. Parker, D. Zheng, G.G. Wang, The chromatin remodeler BPTF activates a stemness gene-expression program essential for the maintenance of adult hematopoietic stem cells, Stem Cell Rep. 10 (2018) 675–683.

[224] G. Domenici, I. Aurrekoetxea-Rodríguez, B.M. Simões, M. Rábano, S.Y. Lee, J. S. Millán, V. Comaills, E. Oliemuller, J.A. López-Ruiz, I. Zabalza, B.A. Howard, R. M. Kypta, M.M. Vivanco, A Sox2-Sox9 signalling axis maintains human breast luminal progenitor and breast cancer stem cells, Oncogene 38 (2019) 3151–3169.

[225] R. Jäger, S. Schäfer, M. Hau-Liersch, H. Schorle, Loss of transcription factor AP-2gamma/TFAP2C impairs branching morphogenesis of the murine mammary gland, Dev. Dyn. 239 (2010) 1027–1033.

[226] D. Hong, T.L. Messier, C.E. Tye, J.R. Dobson, A.J. Fritz, K.R. Sikora, G. Browne, J. L. Stein, J.B. Lian, G.S. Stein, Runx1 stabilizes the mammary epithelial cell phenotype and prevents epithelial to mesenchymal transition, Oncotarget 8 (2017) 17610–17627.

[227] H.K. Athwal, G. Murphy, E. Tibbs, A. Cornett, E. Hill, K. Yeoh, E. Berenstein, M. P. Hoffman, I.M.A. Lombaert, Sox10 regulates plasticity of epithelial progenitors toward secretory units of exocrine glands, Stem Cell Rep. 12 (2019) 366–380.

[228] H. Huh, D. Kim, H.S. Jeong, H. Park, Regulation of TEAD transcription factors in cancer biology, Cells 8 (2019) 8.

[229] H. Kendrick, J.L. Regan, F.A. Magnay, A. Grigoriadis, C. Mitsopoulos, M. Zvelebil, M.J. Smalley, Transcriptome analysis of mammary epithelial subpopulations identifies novel determinants of lineage commitment and cell fate, BMC Genom. 9 (2008) 591.

[230] S.S. Sikandar, A.H. Kuo, T. Kalisky, S. Cai, M. Zabala, R.W. Hsieh, N.A. Lobo, F. A. Scheeren, S. Sim, D. Qian, F.M. Dirbas, G. Somlo, S.R. Quake, M.F. Clarke, Role of epithelial to mesenchymal transition associated genes in mammary gland regeneration and breast tumorigenesis, Nat. Commun. 8 (2017) 1669.

[231] W.D. Frey, A. Chaudhry, P.F. Slepicka, A.M. Ouellette, S.E. Kirberger, W.C. K. Pomerantz, G.J. Hannon, C.O. dos Santos, BPTF maintains chromatin accessibility and the self-renewal capacity of mammary gland stem cells, Stem Cell Rep. 9 (2017) 9–31.

[232] B. Gu, P. Sun, Y. Yuan, R.C. Moraes, A. Li, A. Teng, A. Agrawal, C. Rhéaume, V. Bilanchone, J.M. Veltmaat, K.I. Takemaru, S. Millar, E.Y.H.P. Lee, M.T. Lewis, B. Li, X. Dai, Pygo2 expands mammary progenitor cells by facilitating histone H3 K4 methylation, J. Cell Biol. 185 (2009) 811–826, https://doi.org/10.1083/jcb.200810133.

[233] B. Gu, K. Watanabe, P. Sun, M. Fallahi, X. Dai, Chromatin effector Pygo2 mediates wnt-notch crosstalk to suppress luminal/alveolar potential of mammary stem and basal cells, Cell Stem Cell 13 (2013) 48–61, https://doi.org/10.1016/j.stem.2013.04.012.

[234] B.E. Bernstein, T.S. Mikkelsen, X. Xie, M. Kamal, D.J. Huebert, J. Cuff, B. Fry, A. Meissner, M. Wernig, K. Plath, R. Jaenisch, A. Wagschal, R. Feil, S.L. Schreiber, E.S. Lander, A bivalent chromatin structure marks key developmental genes in embryonic stem cells, Cell 125 (2006) 315–326, https://doi.org/10.1016/j.cell.2006.02.041.

[235] T.S. Mikkelsen, M. Ku, D.B. Jaffe, B. Issac, E. Lieberman, G. Giannoukos, P. Alvarez, W. Brockman, T.K. Kim, R.P. Koche, W. Lee, E. Mendenhall, A. O'Donovan, A. Presser, C. Russ, X. Xie, A. Meissner, M. Wernig, R. Jaenisch, C. Nusbaum, E.S. Lander, B.E. Bernstein, Genome-wide maps of chromatin state in pluripotent and lineage-committed cells, Nature 448 (2007) 553–560, https://doi.org/10.1038/nature06008.

[236] D. Yamaji, R. Na, Y. Feuermann, S. Pechhold, W. Chen, G.W. Robinson, L. Hennighausen, Development of mammary luminal progenitor cells is controlled by the transcription factor STAT5A, Genes Dev. 23 (2009) 2382–2387.

[237] V. Vafaizadeh, P. Klemmt, C. Brendel, K. Weber, C. Doebele, K. Britt, M. Grez, B. Fehse, S. Desrivières, B. Groner, Mammary epithelial reconstitution with gene-modified stem cells assigns roles to Stat5 in luminal alveolar cell fate decisions, differentiation, involution, and mammary tumor formation, Stem Cells 28 (2010) 928–938.

[238] C.M. McQueen, E.E. Schmitt, T.R. Sarkar, J. Elswood, R.P. Metz, D. Earnest, M. Rijnkels, W.W. Porter, PER2 regulation of mammary gland development, Development 145 (2018) 145.

[239] W.W. Hwang-Verslues, P.H. Chang, Y.M. Jeng, W.H. Kuo, P.H. Chiang, Y. C. Chang, T.H. Hsieh, F.Y. Su, L.C. Lin, S. Abbondante, C.Y. Yang, H.M. Hsu, J. C. Yu, K.J. Chang, J.Y. Shew, E.Y.H.P. Lee, W.H. Lee, Loss of corepressor PER2 under hypoxia up-regulates OCT1-mediated EMT gene expression and enhances tumor malignancy, Proc. Natl. Acad. Sci. USA 110 (2013) 12331–12336.

[240] W. Guo, Z. Keckesova, J.L. Donaher, T. Shibue, V. Tischler, F. Reinhardt, S. Itzkovitz, A. Noske, U. Zürrer-Härdi, G. Bell, W.L. Tam, S.A. Mani, A. van Oudenaarden, R.A. Weinberg, Slug and Sox9 cooperatively determine the mammary stem cell state, Cell 148 (2012) 1015–1028.

[241] Q. Shen, Y. Zhang, I.P. Uray, J.L. Hill, H.T. Kim, C. Lu, M.R. Young, E.J. Gunther, S.G. Hilsenbeck, L.A. Chodosh, N.H. Colburn, P.H. Brown, The AP-1 transcription factor regulates postnatal mammary gland development, Dev. Biol. 295 (2006) 589–603.

[242] B. To, E.R. Andrechek, Transcription factor compensation during mammary gland development in E2F knockout mice, PLoS One 13 (2018), e0194937.

[243] S. Liu, G. Dontu, I.D. Mantle, S. Patel, N. Ahn, K.W. Jackson, P. Suri, M.S. Wicha, Hedgehog signaling and Bmi-1 regulate self-renewal of normal and malignant human mammary stem cells, Cancer Res. 66 (2006) 6063–6071, https://doi.org/10.1158/0008-5472.CAN-06-0054.

[244] D. Pellacani, M. Bilenky, N. Kannan, A. Heravi-Moussavi, D.J.H.F. Knapp, S. Gakkhar, M. Moksa, A. Carles, R. Moore, A.J. Mungall, M.A. Marra, S.J. M. Jones, S. Aparicio, M. Hirst, C.J. Eaves, Analysis of normal human mammary epigenomes reveals cell-specific active enhancer states and associated transcription factor networks, Cell Rep. 17 (2016) 2060–2074, https://doi.org/10.1016/j.celrep.2016.10.058.

[245] S.J. Huh, K. Clement, D. Jee, A. Merlini, S. Choudhury, R. Maruyama, R. Yoo, A. Chytil, P. Boyle, F.A. Ran, H.L. Moses, M.H. Barcellos-Hoff, L. Jackson-Grusby, A. Meissner, K. Polyak, Age- and pregnancy-associated DNA methylation changes in mammary epithelial cells, Stem Cell Rep. 4 (2015) 297–311.

[246] K.G. Danielson, C.J. Oborn, E.M. Durban, J.S. Butel, D. Medina, Epithelial mouse mammary cell line exhibiting normal morphogenesis in vivo and functional differentiation in vitro, Proc. Natl. Acad. Sci. USA 81 (1984) 3756–3760.

[247] J.R. Johnson, C.A. Boulanger, T. Hudson, E. Savage, G.H. Smith, Microarray and pathway analysis of two COMMA-Dβ derived clones reveal important differences relevant to their developmental capacity in-vivo, Oncotarget 10 (2019) 2118–2135.

[248] I. Ibarra, Y. Erlich, S.K. Muthuswamy, R. Sachidanandam, G.J. Hannon, A role for microRNAs in maintenance of mouse mammary epithelial progenitor cells, Genes Dev. 21 (2007) 3238–3243.

[249] C.-H. Chao, C.C. Chang, M.J. Wu, H.W. Ko, D. Wang, M.C. Hung, J.Y. Yang, C. J. Chang, MicroRNA-205 signaling regulates mammary stem cell fate and tumorigenesis, J. Clin. Invest. 124 (2014) 3093–3106.

[250] K. Nagaoka, H. Zhang, G. Watanabe, K. Taya, Epithelial cell differentiation regulated by MicroRNA-200a in mammary glands, PLoS One 8 (2013), e65127.

[251] S.J. Song, L. Poliseno, M.S. Song, U. Ala, K. Webster, C. Ng, G. Beringer, N. J. Brikbak, X. Yuan, L.C. Cantley, A.L. Richardson, P.P. Pandolfi, MicroRNA-antagonism regulates breast cancer stemness and metastasis via TET-family-dependent chromatin remodeling, Cell 154 (2013) 311–324.

[252] C.-J. Chang, C.H. Chao, W. Xia, J.Y. Yang, Y. Xiong, C.W. Li, W.H. Yu, S. K. Rehman, J.L. Hsu, H.H. Lee, M. Liu, C.T. Chen, D. Yu, M.C. Hung, p53 regulates epithelial–mesenchymal transition and stem cell properties through modulating miRNAs, Nat. Cell Biol. 13 (2011) 317–323.

[253] Y. Shimono, M. Zabala, R.W. Cho, N. Lobo, P. Dalerba, D. Qian, M. Diehn, H. Liu, S.P. Panula, E. Chiao, F.M. Dirbas, G. Somlo, R.A.R. Pera, K. Lao, M.F. Clarke, Downregulation of miRNA-200c links breast cancer stem cells with normal stem cells, Cell 138 (2009) 592–603.

[254] K.H. Yoo, K. Kang, Y. Feuermann, S.J. Jang, G.W. Robinson, L. Hennighausen, The STAT5-regulated miR-193b locus restrains mammary stem and progenitor cell activity and alveolar differentiation, Dev. Biol. 395 (2014) 245–254.

[255] J. Wang, E. Aydoğdu, S. Mukhopadhyay, L.A. Helguero, C. Williams, A miR-206 regulated gene landscape enhances mammary epithelial differentiation, J. Cell. Physiol. 234 (2019) 22220–22233.

[256] M.-J. Lee, K.S. Yoon, K.W. Cho, K.S. Kim, H.S. Jung, Expression of miR-206 during the initiation of mammary gland development, Cell Tissue Res. 353 (2013) 425–433.

[257] R.E. Heinz, M.C. Rudolph, P. Ramanathan, N.S. Spoelstra, K.T. Butterfield, P. G. Webb, B.L. Babbs, H. Gao, S. Chen, M.A. Gordon, S.M. Anderson, M.C. Neville, H. Gu, J.K. Richer, Constitutive expression of microRNA-150 in mammary

epithelium suppresses secretory activation and impairs de novo lipogenesis, Development 143 (2016) 4236–4248.
[258] D. Llobet-Navas, R. Rodriguez-Barrueco, V. Castro, A.P. Ugalde, P. Sumazin, D. Jacob-Sendler, B. Demircan, M. Castillo-Martin, P. Putcha, N. Marshall, P. Villagrasa, J. Chan, F. Sanchez-Garcia, D. Pe'er, R. Rabadan, A. Iavarone, C. Cordon-Cardo, A. Califano, C. Lopez-Otin, E. Ezhkova, J.M. Silva, The miR-424 (322)/503 cluster orchestrates remodeling of the epithelium in the involuting mammary gland, Genes Dev. 28 (2014) 765–782.
[259] A.N. Shore, E.B. Kabotyanski, K. Roarty, M.A. Smith, Y. Zhang, C.J. Creighton, M. E. Dinger, J.M. Rosen, Pregnancy-induced noncoding RNA (PINC) associates with polycomb repressive complex 2 and regulates mammary epithelial differentiation, PLoS Genet. 8 (2012), e1002840.
[260] L. Standaert, C. Adriaens, E. Radaelli, A. Van Keymeulen, C. Blanpain, T. Hirose, S. Nakagawa, J.C. Marine, The long noncoding RNA Neat1 is required for mammary gland development and lactation, RNA 20 (2014) 1844–1849.
[261] M.E. Askarian-Amiri, J. Crawford, J.D. French, C.E. Smart, M.A. Smith, M. B. Clark, K. Ru, T.R. Mercer, E.R. Thompson, S.R. Lakhani, A.C. Vargas, I. G. Campbell, M.A. Brown, M.E. Dinger, J.S. Mattick, SNORD-host RNA Zfas1 is a regulator of mammary development and a potential marker for breast cancer, RNA 17 (2011) 878–891.
[262] M.R. Ginger, A.N. Shore, A. Contreras, M. Rijnkels, J. Miller, M.F. Gonzalez-Rimbau, J.M. Rosen, A noncoding RNA is a potential marker of cell fate during mammary gland development, Proc. Natl. Acad. Sci. USA 103 (2006) 5781–5786.
[263] R.A. Gupta, N. Shah, K.C. Wang, J. Kim, H.M. Horlings, D.J. Wong, M.C. Tsai, T. Hung, P. Argani, J.L. Rinn, Y. Wang, P. Brzoska, B. Kong, R. Li, R.B. West, M. J. van de Vijver, S. Sukumar, H.Y. Chang, Long non-coding RNA HOTAIR reprograms chromatin state to promote cancer metastasis, Nature 464 (2010) 1071–1076.
[264] A. Bhan, S.S. Mandal, LncRNA HOTAIR: a master regulator of chromatin dynamics and cancer, Biochim. Biophys. Acta 1856 (2015) 151–164.
[265] A.R. Amândio, A. Necsulea, E. Joye, B. Mascrez, D. Duboule, Hotair is dispensible for mouse development, PLoS Genet. 12 (2016), e1006232.
[266] S. Tao, H. He, Q. Chen, Estradiol induces HOTAIR levels via GPER-mediated miR-148a inhibition in breast cancer, J. Transl. Med. 13 (2015) 131.
[267] J. Russo, J. Santucci-Pereira, R.L. de Cicco, F. Sheriff, P.A. Russo, S. Peri, M. Slifker, E. Ross, M.L.S. Mello, B.C. Vidal, I. Belitskaya-Lévy, A. Arslan, A. Zeleniuch-Jacquotte, P. Bordas, P. Lenner, J. Ahman, Y. Afanasyeva, G. Hallmans, P. Toniolo, I.H. Russo, Pregnancy-induced chromatin remodeling in the breast of postmenopausal women, Int. J. Cancer 131 (2012) 1059–1070.
[268] J.L.C. Richard, P.J.A. Eichhorn, Deciphering the roles of lncRNAs in breast development and disease, Oncotarget 9 (2018) 20179–20212.
[269] S. Obad, C.O. dos Santos, A. Petri, M. Heidenblad, O. Broom, C. Ruse, C. Fu, M. Lindow, J. Stenvang, E.M. Straarup, H.F. Hansen, T. Koch, D. Pappin, G. J. Hannon, S. Kauppinen, Silencing of microRNA families by seed-targeting tiny LNAs, Nat. Genet. 43 (2011) 371–378.
[270] E.C. Kordon, G.H. Smith, An entire functional mammary gland may comprise the progeny from a single cell, Development 125 (1998) 1921–1930.
[271] **J. Stingl, P. Eirew, I. Ricketson, M. Shackleton, F. Vaillant, D. Choi, H.I. Li, C. J. Eaves, Purification and unique properties of mammary epithelial stem cells, Nature 439 (2006) 993–997,** https://doi.org/10.1038/nature04496.
[272] L.R. Rohrschneider, J.M. Custodio, T.A. Anderson, C.P. Miller, H. Gu, The intron 5/6 promoter region of the ship1 gene regulates expression in stem/progenitor cells of the mouse embryo, Dev. Biol. 283 (2005) 503–521.
[273] A.C. Rios, N.Y. Fu, G.J. Lindeman, J.E. Visvader, In situ identification of bipotent stem cells in the mammary gland, Nature 506 (2014) 322–327.
[274] C.L. Trejo, G. Luna, C. Dravis, B.T. Spike, G.M. Wahl, Lgr5 is a marker for fetal mammary stem cells, but is not essential for stem cell activity or tumorigenesis, npj Breast Cancer 3 (2017) 16.
[275] C.O. dos Santos, C. Rebbeck, E. Rozhkova, A. Valentine, A. Samuels, L.R. Kadiri, P. Osten, E.Y. Harris, P.J. Uren, A.D. Smith, G.J. Hannon, Molecular hierarchy of mammary differentiation yields refined markers of mammary stem cells, Proc. Natl. Acad. Sci. 110 (2013) 7123–7130.
[276] L. Bai, L.R. Rohrschneider, s-SHIP promoter expression marks activated stem cells in developing mouse mammary tissue, Genes Dev. 24 (2010) 1882–1892.
[277] **A. Centonze, S. Lin, E. Tika, A. Sifrim, M. Fioramonti, M. Malfait, Y. Song, A. Wuidart, J. Van Herck, A. Dannau, G. Bouvencourt, C. Dubois, N. Dedoncker, A. Sahay, V. de Maertelaer, C.W. Siebel, A. Van Keymeulen, T. Voet, C. Blanpain, Heterotypic cell–cell communication regulates glandular stem cell multipotency, Nature 584 (2020) 608–613,** https://doi.org/10.1038/s41586-020-2632-y.
[278] S. Cristea, K. Polyak, Dissecting the mammary gland one cell at a time, Nat. Commun. 9 (2018) 2473.
[279] A. Wuidart, A. Sifrim, M. Fioramonti, S. Matsumura, A. Brisebarre, D. Brown, A. Centonze, A. Dannau, C. Dubois, A. Van Keymeulen, T. Voet, C. Blanpain, Early lineage segregation of multipotent embryonic mammary gland progenitors, Nat. Cell Biol. 20 (2018) 666–676.
[280] R.R. Giraddi, C.Y. Chung, R.E. Heinz, O. Balcioglu, M. Novotny, C.L. Trejo, C. Dravis, B.M. Hagos, E.M. Mehrabad, L.W. Rodewald, J.Y. Hwang, C. Fan, R. Lasken, K.E. Varley, C.M. Perou, G.M. Wahl, B.T. Spike, Single-cell transcriptomes distinguish stem cell state changes and lineage specification programs in early mammary gland development, Cell Rep. 24 (2018) 1653–1666. e7.
[281] S. Elias, M.A. Morgan, E.K. Bikoff, E.J. Robertson, Long-lived unipotent Blimp1-positive luminal stem cells drive mammary gland organogenesis throughout adult life, Nat. Commun. 8 (2017) 1714.
[282] A.M. Lilja, V. Rodilla, M. Huyghe, E. Hannezo, C. Landragin, O. Renaud, O. Leroy, S. Rulands, B.D. Simons, S. Fre, Clonal analysis of Notch1-expressing cells reveals the existence of unipotent stem cells that retain long-term plasticity in the embryonic mammary gland, Nat. Cell Biol. 20 (2018) 677–687.
[283] C.-Y. Chung, Z. Ma, C. Dravis, S. Preissl, O. Poirion, G. Luna, X. Hou, R.R. Giraddi, B. Ren, G.M. Wahl, Single-cell chromatin analysis of mammary gland development reveals cell-state transcriptional regulators and lineage relationships, Cell Rep. 29 (2019) 495–510.e6.
[284] B. Pal, Y. Chen, F. Vaillant, P. Jamieson, L. Gordon, A.C. Rios, S. Wilcox, N. Fu, K. H. Liu, F.C. Jackling, M.J. Davis, G.J. Lindeman, G.K. Smyth, J.E. Visvader, Construction of developmental lineage relationships in the mouse mammary gland by single-cell RNA profiling, Nat. Commun. 8 (2017) 1627.
[285] C.L.G.J. Scheele, E. Hannezo, M.J. Muraro, A. Zomer, N.S.M. Langedijk, A. van Oudenaarden, B.D. Simons, J. van Rheenen, Identity and dynamics of mammary stem cells during branching morphogenesis, Nature 542 (2017) 313–317.
[286] H. Sun, Z. Miao, X. Zhang, U.I. Chan, S.M. Su, S. Guo, C.K.H. Wong, X. Xu, C. X. Deng, Single-cell RNA-Seq reveals cell heterogeneity and hierarchy within mouse mammary epithelia, J. Biol. Chem. 293 (2018) 8315–8329.
[287] S. Cai, T. Kalisky, D. Sahoo, P. Dalerba, W. Feng, Y. Lin, D. Qian, A. Kong, J. Yu, F. Wang, E.Y. Chen, F.A. Scheeren, A.H. Kuo, S.S. Sikandar, S. Hisamori, L.J. van Weele, D. Heiser, S. Sim, J. Lam, S. Quake, M.F. Clarke, A quiescent Bcl11b high stem cell population is required for maintenance of the mammary gland, Cell Stem Cell 20 (2017) 247–260.e5.
[288] K. Bach, S. Pensa, M. Grzelak, J. Hadfield, D.J. Adams, J.C. Marioni, W.T. Khaled, Differentiation dynamics of mammary epithelial cells revealed by single-cell RNA sequencing, Nat. Commun. 8 (2017) 2128.
[289] D. Wang, C. Cai, X. Dong, Q.C. Yu, X.O. Zhang, L. Yang, Y.A. Zeng, Identification of multipotent mammary stem cells by protein C receptor expression, Nature 517 (2015) 81–84.
[290] N. Kanaya, G. Chang, X. Wu, K. Saeki, L. Bernal, H.J. Shim, J. Wang, C. Warden, T. Yamamoto, J. Li, J.S. Park, T. Synold, S. Vonderfecht, M. Rakoff, S. L. Neuhausen, S. Chen, Single-cell RNA-sequencing analysis of estrogen- and endocrine-disrupting chemical-induced reorganization of mouse mammary gland, Commun. Biol. 2 (2019) 406.
[291] **C.M.-C. Li, H. Shapiro, C. Tsiobikas, L. Selfors, H. Chen, G.K. Gray, Y. Oren, L. Pinello, A. Regev, J.S. Brugge, Aging-associated alterations in the mammary gland revealed by single-cell RNA sequencing, bioRxiv (2019),** https://doi.org/10.1101/773408.
[292] Q.H. Nguyen, N. Pervolarakis, K. Blake, D. Ma, R.T. Davis, N. James, A.T. Phung, E. Willey, R. Kumar, E. Jabart, I. Driver, J. Rock, A. Goga, S.A. Khan, D.A. Lawson, Z. Werb, K. Kessenbrock, Profiling human breast epithelial cells using single cell RNA sequencing identifies cell diversity, Nat. Commun. 9 (2018) 2028.
[293] M.D. Luecken, F.J. Theis, Current best practices in single-cell RNA-seq analysis: a tutorial, Mol. Syst. Biol. 15 (2019), e8746.
[294] M. Simian, et al., The interplay of matrix metalloproteinases, morphogens and growth factors is necessary for branching of mammary epithelial cells, Development 128 (2001) 3117–3131.
[295] E.R. Shamir, A.J. Ewald, Three-dimensional organotypic culture: experimental models of mammalian biology and disease, Nat. Rev. Mol. Cell Biol. 15 (2014) 647–664.
[296] J.T. Emerman, S.J. Burwen, D.R. Pitelka, Substrate properties influencing ultrastructural differentiation of mammary epithelial cells in culture, Tissue Cell 11 (1979) 109–119.
[297] J.M. Shannon, D.R. Pitelka, The influence of cell shape on the induction of functional differentiation in mouse mammary cells in vitro, Vitro 17 (1981) 1016–1028.
[298] J.T. Emerman, D.R. Pitelka, Maintenance and induction of morphological differentiation in dissociated mammary epithelium on floating collagen membranes, Vitro 13 (1977) 316–328.
[299] J.T. Emerman, J. Enami, D.R. Pitelka, S. Nandi, Hormonal effects on intracellular and secreted casein in cultures of mouse mammary epithelial cells on floating collagen membranes, Proc. Natl. Acad. Sci. USA 74 (1977) 4466–4470.
[300] Q.J. Tonelli, S. Sorof, Induction of biochemical differentiation in three-dimensional collagen cultures of mammary epithelial cells from virgin mice, Differentiation 22 (1982) 195–200.
[301] M. Haeuptle, Y. Suard, E. Bogenmann, H. Reggio, L. Racine, J. Kraehenbuhl, Effect of cell shape change on the function and differentiation of rabbit mammary cells in culture, J. Cell Biol. 96 (1983) 1425–1434.
[302] E.M. Durban, D. Medina, J.S. Butel, Comparative analysis of casein synthesis during mammary cell differentiation in collagen and mammary gland development in vivo, Dev. Biol. 109 (1985) 288–298.
[303] D. Flynn, J. YANG, S. NANDI, Growth and differentiation of primary cultures of mouse mammary epithelium embedded in collagen gel, Differentiation 22 (1982) 191–194.
[304] E.Y. Lee, G. Parry, M.J. Bissell, Modulation of secreted proteins of mouse mammary epithelial cells by the collagenous substrata, J. Cell Biol. 98 (1984) 146–155.
[305] E.Y. Lee, W.H. Lee, C.S. Kaetzel, G. Parry, M.J. Bissell, Interaction of mouse mammary epithelial cells with collagen substrata: regulation of casein gene expression and secretion, Proc. Natl. Acad. Sci. USA 82 (1985) 1419–1423.
[306] J. Aggeler, et al., Cytodifferentiation of mouse mammary epithelial cells cultured on a reconstituted basement membrane reveals striking similarities to development in vivo, J. Cell Sci. 99 (Pt 2) (1991) 407–417.
[307] H.K. Kleinman, G.R. Martin, Matrigel: basement membrane matrix with biological activity, Semin. Cancer Biol. 15 (2005) 378–386.
[308] K. Wolf, S. Alexander, V. Schacht, L.M. Coussens, U.H. von Andrian, J. van Rheenen, E. Deryugina, P. Friedl, Collagen-based cell migration models in vitro and in vivo, Semin. Cell Dev. Biol. 20 (2009) 931–941.

[309] P.R. Jamieson, J.F. Dekkers, A.C. Rios, N.Y. Fu, G.J. Lindeman, J.E. Visvader, Derivation of a robust mouse mammary organoid system for studying tissue dynamics, Development 144 (2017) 1065–1071.
[310] S. Florian, Y. Iwamoto, M. Coughlin, R. Weissleder, T.J. Mitchison, A human organoid system that self-organizes to recapitulate growth and differentiation of a benign mammary tumor, Proc. Natl. Acad. Sci. USA 116 (2019) 11444–11453.
[311] J. Sumbal, A. Chiche, E. Charifou, Z. Koledova, H. Li, Primary mammary organoid model of lactation and involution, Front. Cell Dev. Biol. 8 (2020) 68.
[312] Z. Koledova, P. Lu, A 3D fibroblast-epithelium co-culture model for understanding microenvironmental role in branching morphogenesis of the mammary gland, Methods Mol. Biol. 1501 (2017) 217–231.
[313] S. Krause, M.V. Maffini, A.M. Soto, C. Sonnenschein, A novel 3D in vitro culture model to study stromal-epithelial interactions in the mammary gland, Tissue Eng. Part C Methods 14 (2008) 261–271.
[314] J.A. Reid, P.A. Mollica, R.D. Bruno, P.C. Sachs, Consistent and reproducible cultures of large-scale 3D mammary epithelial structures using an accessible bioprinting platform, Breast Cancer Res. 20 (2018) 122.
[315] M.H. Barcellos-Hoff, et al., Functional differentiation and alveolar morphogenesis of primary mammary cultures on reconstituted basement membrane, Development 105 (1989) 223–235.
[316] L.H. Chen, M.J. Bissell, A novel regulatory mechanism for whey acidic protein gene expression, Cell Regul. 1 (1989) 45–54.
[317] R. Mroue, M.J. Bissell, Three-dimensional cultures of mouse mammary epithelial cells, Methods Mol. Biol. 945 (2013) 221–250.
[318] C.Q. Lin, P.J. Dempsey, R.J. Coffey, M.J. Bissell, Extracellular matrix regulates whey acidic protein gene expression by suppression of TGF-alpha in mouse mammary epithelial cells: studies in culture and in transgenic mice, J. Cell Biol. 129 (1995) 1115–1126.
[319] C.H. Streuli, N. Bailey, M.J. Bissell, Control of mammary epithelial differentiation: basement membrane induces tissue-specific gene expression in the absence of cell-cell interaction and morphological polarity, J. Cell Biol. 115 (1991) 1383–1395.
[320] J. Alcaraz, R. Xu, H. Mori, C.M. Nelson, R. Mroue, V.A. Spencer, D. Brownfield, D. C. Radisky, C. Bustamante, M.J. Bissell, Laminin and biomimetic extracellular elasticity enhance functional differentiation in mammary epithelia, EMBO J. 27 (2008) 2829–2838.
[321] E.M. Michalak, M.J.G. Milevskiy, R.M. Joyce, J.F. Dekkers, P.R. Jamieson, B. Pal, C.A. Dawson, Y. Hu, S.H. Orkin, W.S. Alexander, G.J. Lindeman, G.K. Smyth, J. E. Visvader, Canonical PRC2 function is essential for mammary gland development and affects chromatin compaction in mammary organoids, PLoS Biol. 16 (2018), e2004986.
[322] T. Jardé, B. Lloyd-Lewis, M. Thomas, H. Kendrick, L. Melchor, L. Bougaret, P. D. Watson, K. Ewan, M.J. Smalley, T.C. Dale, Wnt and Neuregulin1/ErbB signalling extends 3D culture of hormone responsive mammary organoids, Nat. Commun. 7 (2016) 13207.
[323] B. Mohapatra, N. Zutshi, W. An, B. Goetz, P. Arya, T.A. Bielecki, I. Mustaq, M. D. Storck, J.L. Meza, V. Band, H. Band, An essential role of CBL and CBL-B ubiquitin ligases in mammary stem cell maintenance, Development 144 (2017) 1072–1086.
[324] S. Horibata, K.E. Rogers, D. Sadegh, L.J. Anguish, J.L. McElwee, P. Shah, P. R. Thompson, S.A. Coonrod, Role of peptidylarginine deiminase 2 (PAD2) in mammary carcinoma cell migration, BMC Cancer 17 (2017) 378.
[325] A.R. Lourenço, M.G. Roukens, D. Seinstra, C.L. Frederiks, C.E. Pals, S.J. Vervoort, A.S. Margarido, J. van Rheenen, P.J. Coffer, C/EBPα is crucial determinant of epithelial maintenance by preventing epithelial-to-mesenchymal transition, Nat. Commun. 11 (2020) 785.
[326] B.C. Hacker, J.D. Gomez, C.A.S. Batista, M. Rafat, Growth and characterization of irradiated organoids from mammary glands, J. Vis. Exp. (2019), https://doi.org/10.3791/59293.
[327] M.F. Ciccone, M.C. Trousdell, C.O. dos Santos, Characterization of 3D organoid culture to study the effects of pregnancy hormones on the epigenome and transcriptional output of mammary epithelial cells, J. Mammary Gland Neoplasia (2020).
[328] J.M. Rosenbluth, R.C.J. Schackmann, G.K. Gray, L.M. Selfors, C.M.C. Li, M. Boedicker, H.J. Kuiken, A. Richardson, J. Brock, J. Garber, D. Dillon, N. Sachs, H. Clevers, J.S. Brugge, Organoid cultures from normal and cancer-prone human breast tissues preserve complex epithelial lineages, Nat. Commun. 11 (2020) 1711.
[329] S.H. Moolgavkar, et al., Two-stage model for carcinogenesis: epidemiology of breast cancer in females, J. Natl. Cancer Inst. (1980).
[330] M.C. Pike, M.D. Krailo, B.E. Henderson, J.T. Casagrande, D.G. Hoel, "Hormonal" risk factors, "Breast tissue age" and the age-incidence of breast cancer, Nature 303 (1983) 767–770, https://doi.org/10.1038/303767a0.
[331] B. Rosner, G.A. Colditz, W.C. Willett, Reproductive risk factors in a prospective study of breast cancer: the nurses' health study, Am. J. Epidemiol. 139 (1994) 819–835, https://doi.org/10.1093/oxfordjournals.aje.a117079.
[332] H.J. Bowers, E.E. Fannin, A. Thomas, J.A. Weis, Characterization of multicellular breast tumor spheroids using image data-driven biophysical mathematical modeling, Sci. Rep. 10 (2020) 11583, https://doi.org/10.1038/s41598-020-68324-4.
[333] E. Koedoot, M. Fokkelman, V.M. Rogkoti, M. Smid, I. van de Sandt, H. de Bont, C. Pont, J.E. Klip, S. Wink, M.A. Timmermans, E.A.C. Wiemer, P. Stoilov, J. A. Foekens, S.E. Le Dévédec, J.W.M. Martens, B. van de Water, Uncovering the signaling landscape controlling breast cancer cell migration identifies novel metastasis driver genes, Nat. Commun. 10 (2019) 2983, https://doi.org/10.1038/s41467-019-11020-3.
[334] C. Wang, J.R. Christin, M.H. Oktay, W. Guo, Lineage-biased stem cells maintain estrogen-receptor-positive and -negative mouse mammary luminal lineages, Cell Rep. 18 (2017) 2825–2835.
[335] T. Bouras, B. Pal, F. Vaillant, G. Harburg, M.L. Asselin-Labat, S.R. Oakes, G. J. Lindeman, J.E. Visvader, Notch signaling regulates mammary stem cell function and luminal cell-fate commitment, Cell Stem Cell 3 (2008) 429–441.

Cell Reports

Article

# Parity-induced changes to mammary epithelial cells control NKT cell expansion and mammary oncogenesis

## Graphical abstract

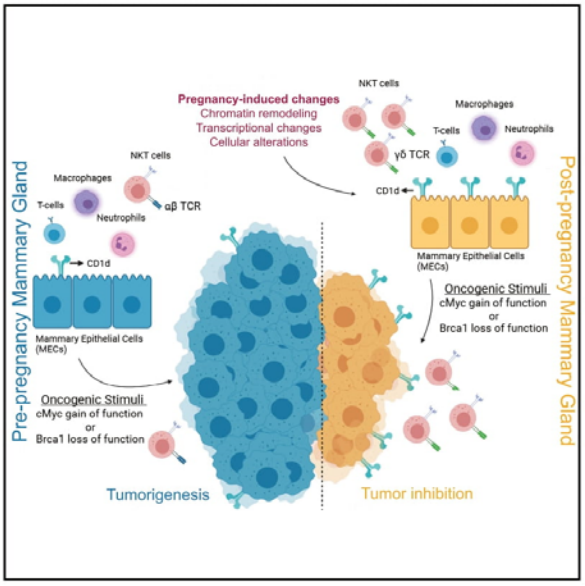


## Highlights

- Post-pregnancy MECs express higher levels of the antigen-presenting molecule CD1d
- γδTCR-expressing NKT cells are expanded in post-pregnancy mammary glands
- NKTs and CD1d expression associate with oncogenesis inhibition after pregnancy
- Loss of γδNKTs and CD1d expression supports mammary oncogenesis after pregnancy


## Authors

Amritha Varshini Hanasoge Somasundara, Matthew A. Moss, Mary J. Feigman, ..., Semir Beyaz, John E. Wilkinson, Camila O. dos Santos

## Correspondence

dossanto@cshl.edu



## In brief

Parity influences mammary cancer progression. Hanasoge Somasundara et al. demonstrate how pregnancy-induced changes modulate the communication between MECs and immune cells and establish a causal link between pregnancy, the immune microenvironment, and mammary oncogenesis in models of cMYC overexpression and Brca1 loss of function.


Hanasoge Somasundara et al., 2021, Cell Reports *37*, 110099
December 7, 2021 
https://doi.org/10.1016/j.celrep.2021.110099

CellPress

Cell Reports

CellPress
OPEN ACCESS

Article

# Parity-induced changes to mammary epithelial cells control NKT cell expansion and mammary oncogenesis

Amritha Varshini Hanasoge Somasundara,[1,2,6] Matthew A. Moss,[3,6] Mary J. Feigman,[1,6] Chen Chen,[1] Samantha L. Cyrill,[1] Michael F. Ciccone,[1] Marygrace C. Trousdell,[1] Macy Vollbrecht,[4] Siran Li,[1] Jude Kendall,[1] Semir Beyaz,[1] John E. Wilkinson,[5] and Camila O. dos Santos[1,7,*]

[1]Cold Spring Harbor Laboratory, Cold Spring Harbor, NY, USA
[2]CSHL School of Biological Sciences, Cold Spring Harbor, NY, USA
[3]Donald and Barbara Zucker School of Medicine at Hofstra/Northwell, Hempstead, NY, USA
[4]Department of Biology, Stanford University, Stanford, CA, USA
[5]Department of Comparative Medicine, University of Washington, Seattle, WA, USA
[6]These authors contributed equally
[7]Lead contact
*Correspondence: dossanto@cshl.edu
https://doi.org/10.1016/j.celrep.2021.110099

## SUMMARY

Pregnancy reprograms mammary epithelial cells (MECs) to control their responses to pregnancy hormone re-exposure and carcinoma progression. However, the influence of pregnancy on the mammary microenvironment is less clear. Here, we used single-cell RNA sequencing to profile the composition of epithelial and non-epithelial cells in mammary tissue from nulliparous and parous female mice. Our analysis indicates an expansion of γδ natural killer T-like immune cells (NKTs) following pregnancy and upregulation of immune signaling molecules in post-pregnancy MECs. We show that expansion of NKTs following pregnancy is due to elevated expression of the antigen-presenting molecule CD1d on MECs. Loss of CD1d expression on post-pregnancy MECs, or overall lack of activated NKTs, results in mammary oncogenesis. Collectively, our findings illustrate how pregnancy-induced changes modulate the communication between MECs and the immune microenvironment and establish a causal link between pregnancy, the immune microenvironment, and mammary oncogenesis.

## INTRODUCTION

Changes to the functions of immune cells modulate both the mammary immune microenvironment and mammary epithelial cell (MEC) lineages during all stages of mammary development, with $CD4^+$ T cells guiding lineage commitment and differentiation of MECs, while macrophages provide growth factors and assist in removal of cellular debris from apoptotic events (Dawson et al., 2020; Hitchcock et al., 2020; Plaks et al., 2015; Rahat et al., 2016; Stewart et al., 2019; Wang et al., 2020). Accordingly, changes that impact immune cell function and abundance can also influence the development and progression of mammary oncogenesis, particularly in tissue reconstruction during post-partum involution (Bach et al., 2021; Ibrahim et al., 2020; Lyons et al., 2011; Martinson et al., 2015; Freire-de-Lima et al., 2006; Guo et al., 2017; Fornetti et al., 2012; O'Brien et al., 2010).

Conversely, cell-autonomous processes in post-pregnancy MECs contribute to a lasting effect that decreases the risk of breast cancer by ~30% in rodents and humans (Medina et al., 2004; Britt et al., 2007; Terry et al., 2018). Epigenetic-mediated alterations of post-pregnant MECs have been shown to suppress mammary oncogenesis via oncogene-induced senescence (Feigman et al., 2020). Given that oncogene-induced senescence signals influence the immune system, a link between normal pregnancy-induced mammary development, the immune microenvironment, and oncogenesis needs to be addressed to fully understand the effects of pregnancy on breast cancer development.

In this study, we characterize the interactions between cell-autonomous (MECs) and non-cell-autonomous (immune cells) factors that are part of normal pregnancy-induced mammary development and are involved in inhibiting mammary oncogenesis. Our analysis identified that pregnancy induces the expansion of natural killer T-like cells (NKT) during the late stages of involution, which preferentially populates the fully involuted, post-pregnancy mammary tissue. Unlike typical NKTs that bear αβ T cell receptors (TCRs), pregnancy-induced NKTs express γδTCRs on their surface, indicating a role in specialized antigen recognition. NKT cell expansion was linked with increased expression of the antigen-presenting molecule, CD1d, on the surface of post-pregnancy MECs, which was associated with the stable gain of active transcription marks at the *Cd1d* locus and increased mRNA levels. Further analysis demonstrated that gain of CD1d expression on post-pregnancy

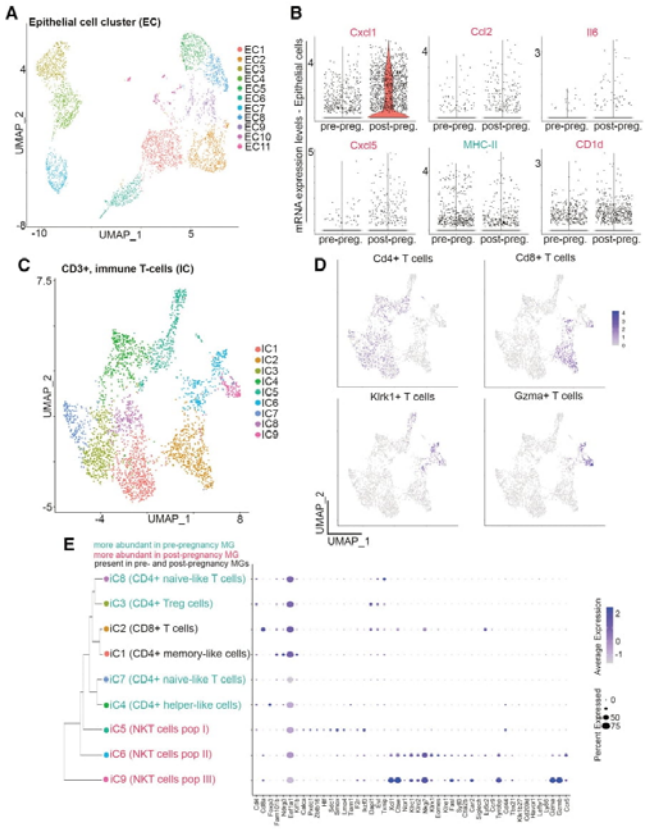


**Figure 1. Identification of transcriptional programs and immune cellular heterogeneity in mammary tissue from parous female mice**

(A) UMAP of mammary epithelial cells from pre- and post-pregnancy mammary glands.

(B) mRNA levels of senescence-associated, immune communication genes *Cxcl1*, *Ccl2*, *Il6*, *Cxcl5*, *Mhc-ii*, and *Cd1d* in pre- and post-pregnancy MECs.

(C) UMAP of T cells (CD3e$^+$ cells) from pre- and post-pregnancy mammary glands.

(D) Feature plots showing the expression of T cell markers *Cd4*, *Cd8*, *Klrk1*, and *Gzma*.

(E) Dendrogram clustering and dot plot showing the molecular signature and lineage identity of pre- and post-pregnancy mammary resident CD3$^+$ immune cells.

See also Figures S1–S4.

MECs, and expansion of γδNKTs was observed in tissues that failed to undergo mammary oncogenesis in response to oncogenic signals, such as cMyc overexpression or Brca1 loss of function. Altogether, our findings elucidate how signals brought to MECs during pregnancy-induced development regulate epigenomic changes, gene expression, and immune surveillance, which together control mammary oncogenesis.

## RESULTS

### Identification of transcriptional programs and immune cellular heterogeneity in mammary tissue from parous female mice

The use of single cell RNA sequencing (scRNA-seq) has elucidated the dynamics of epithelial cell-lineage specification and differentiation across major mammary developmental stages (Bach et al., 2017; Chung et al., 2019; Li et al., 2020a; Pal et al., 2017, 2021). Previous studies have indicated that post-pregnancy epithelial cells bear an altered transcriptome and epigenome, thus suggesting that pregnancy stably alters the molecular state of MECs (Blakely et al., 2006; Feigman et al., 2020; Huh et al., 2015; dos Santos et al., 2015). However, it is unclear whether pregnancy leads to disproportionate changes in the transcriptome of specific mammary cell populations.

In order to characterize the effects of parity on the cellular composition and heterogeneity of mammary glands, we used scRNA-seq to compare the abundance, identity, and gene expression of mammary epithelial and non-epithelial cells from nulliparous (virgin, never pregnant) and parous (20 days gestation, 21 days lactation, 40 days post-weaning) female mice. scRNA-seq clustering defined 20 clusters (TCs), which were further classified into five main cell types: epithelial cells (Krt8$^+$ and Krt5$^+$), B lymphocytes (CD20$^+$), and T lymphocytes (CD3e$^+$) and two smaller clusters, encompassing fibroblast-like cells (Rsg5$^+$) and myeloid-like cells (Itgax$^+$), with similar cell-cycle states (Figures S1A–S1C).

To characterize the cellular heterogeneity across pre- and post-pregnancy MECs, we used a re-clustering approach that resolved 11 clusters of mammary epithelial cells (ECs) (Henry et al., 2021) (Figure 1A). Analysis of cellular abundance and lineage identity revealed that clusters EC7 (mature myoepithelial MEC), EC9 (luminal common progenitor-like MEC), EC10, and EC11 (bi-potential-like MECs) were evenly represented in pre- and post-pregnancy mammary tissue, thus demonstrating populations of cells that are mostly unchanged by a pregnancy cycle. We also identified clusters predominantly represented in pre-pregnancy mammary tissue (EC2, EC4, and EC8), and those biased toward a post-pregnancy state (EC1, EC3, EC5, and EC6), classified as luminal alveolar-like clusters (EC1, EC2, and

EC6), myoepithelial progenitor-like clusters (EC3 and EC4), and luminal ductal-like clusters (EC5 and EC8) (Figures S1D–S1F). Comparative gene-expression analysis indicated that processes associated with immune cell communication were markedly enriched in luminal and myoepithelial cell clusters biased toward the post-pregnancy state (Figure 1B; Figures S1G and S1H; Table S1). This observation was supported by analysis of previously published pre- and post-pregnancy bulk RNA-seq data, which suggested an overall enrichment for immune communication signatures in epithelial cells after a full pregnancy cycle (Feigman et al., 2020) (Figure S1I; Table S2).

Changes in the immune microenvironment are known to contribute to pregnancy-induced mammary development and cancer (Coussens and Pollard, 2011; Bach et al., 2021; Dawson et al., 2020; Saeki et al., 2021). Therefore, and in light of the potentially altered epithelial-immune cell communication identified in post-pregnancy MECs suggested above, we set out to understand the effects of pregnancy on the mammary resident immune compartment using scRNA-seq. Transcriptional analysis of clusters representing B lymphocytes ($CD20^+$) did not identify major differences between cells from pre- and post-pregnancy mammary glands, suggesting that B cells may not be significantly altered in fully involuted mammary tissue (Figure S2A). Re-clustering of $CD3e^+$ T lymphocytes identified nine distinct immune cell clusters (IC) marked by the expression of immune lineage genes such as *Cd4*, *Cd8*, *Klrk1*, and *Gzma* (Figures 1C and 1D). Classification according to cell abundance and lineage identity of mammary resident lymphocytes revealed two cell clusters, IC1 ($CD4^+$ memory-like T cells) and IC2 ($CD8^+$ T cells), which were evenly represented across pre- and post-pregnancy mammary tissue (Figures S2B and S2C). Differential gene-expression analysis of clusters IC1 and IC2 identified minimal expression changes, suggesting that the transcriptional output of $CD8^+$ T cells (IC2), and certain populations of $CD4^+$ T cells (IC1) were not substantially altered by parity (Figures S2D and S2E).

Analysis of clusters biased toward a pre-pregnancy state identified several populations of $CD4^+$ T lymphocytes, with gene identifiers supporting their identity as $CD4^+$ Tregs (IC3), $CD4^+$ naive T cells (IC7 and IC8), and $CD4^+$ helper T cells (IC4), suggesting that pre-pregnancy mammary tissues are enriched for populations of $CD4^+$ T cells (Figure 1E). Conversely, clusters enriched with post-pregnancy mammary immune cells (IC5, IC6, and IC9) were classified as NKT cells, a specialized population of T cells involved in immune recruitment and cytotoxic activity (Godfrey et al., 2004) (Figure 1E). These clusters expressed master regulators of NKT cell fate, including transcription factors (TFs) *Tbx21* (*Tbet*) and *Zbtb16* (*Plzf*) (Townsend et al., 2004; Savage et al., 2008).

While natural killer (NK) cells are known to play a role in mammary gland involution and parity-associated mammary tumorigenesis (Fornetti et al., 2012; Martinson et al., 2015), the role of NKT cells in this process has yet to be determined. Therefore, we analyzed clusters of immune cells expressing the common NK/NKT marker *Nkg7* to further define the influence of pregnancy on the abundance and identity of NK and NKT cells. Deep-clustering analysis of $Nkg7^+$ immune cells revealed six distinct cell clusters (NC1–6). Cells classified under cluster NC5, which includes cells from both the pre- and post-pregnancy mammary tissue, lacked expression of *Cd3e* and therefore represents the only cluster with an NK cell identity in our dataset (Figures S2F–S2H). Further gene-expression analysis confirmed that post-pregnancy mammary glands are enriched with a variety of NKTs, including those expressing markers of cell activation (*Gzmb* and *Ccr5*) and of a resting state (*Bcl11b*) (Figure S2H). In agreement, each of the post-pregnancy-biased NKT cell clusters was enriched with an array of immune-activation signatures, suggesting an altered state for these cell populations after pregnancy (Figure S2I).

Collectively, our scRNA-seq analysis of fully involuted mammary tissue confirmed that pregnancy leads to a stable alteration of the transcriptional output of post-pregnancy MECs, including gene-expression signatures that suggest enhanced communication with the immune microenvironment. In addition, our study also indicates that mammary resident NKTs are present at higher levels in post-pregnancy glands, suggesting that pregnancy plays a role in inducing changes to the mammary immune microenvironment.

## Pregnancy induces the expansion of a specific population of NKTs

The post-partum mammary gland involution is marked by an influx of infiltrating mast cells, macrophages, neutrophils, dendritic cells, and natural killer cells, which remove apoptotic epithelial cells and support the remodeling of the gland (Guo et al., 2017; Kordon and Coso, 2017; O'Brien et al., 2010; Schwertfeger et al., 2001). Since our scRNA-seq analyses suggested that post-pregnancy mammary glands are enriched for populations of NKT cells, we next used a series of flow cytometry analyses to validate this observation.

Analysis using the markers NK1.1 and CD3, which defines NKTs ($NK1.1^+CD3^+$), identified a 12-fold increase in the abundance of NKTs in post-pregnancy mammary tissue, consistent with the results of our scRNA-seq data (Figure 2A). Further analysis indicated a 2.3-fold higher abundance of NKT cells in recently involuted mammary tissue (15 days post-offspring weaning), compared to mammary glands from nulliparous mice, or those exposed to pregnancy hormones for 12 days (mid-pregnancy), suggesting that the expansion of NKTs takes place at the final stages of post-pregnancy mammary involution (Figure S3A). The selective expansion of NKTs was further supported by the analysis of markers that define mammary resident neutrophils ($Ly6G^+$) and macrophages ($CD206^+$), which were largely unchanged between pre- and post-pregnancy mammary tissue (Figures S3B and S3C). Immunofluorescence analysis of Cxcr6-GFP-KI mammary tissue, previously described to label NKTs (Germanov et al., 2008), demonstrated several $GFP^+$ cells surrounding ductal structures, an observation that supports the presence of NKTs within the mammary tissue (Figure S3D). Moreover, analysis of bone marrow and spleen from nulliparous and parous mice showed no difference in the abundance of NKTs, suggesting that pregnancy-induced expansion of these cells is mammary specific (Figures S3E and S3F).

To further characterize the identity of the post-pregnancy, mammary resident NKTs, we combined cellsurface and intracellular staining to detect canonical NKT lineage markers, including

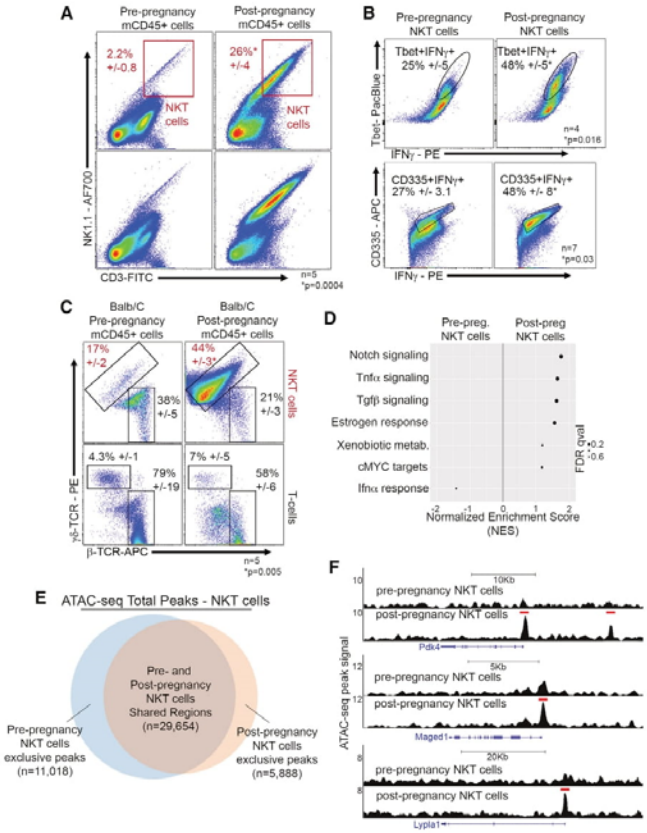


**Figure 2. Pregnancy induces the expansion of a specific population of NKTs**

(A) Flow cytometry analysis of resident CD45$^+$ NK1.1$^+$CD3$^+$ NKTs from pre- and post-pregnancy mammary tissue. n = 5 nulliparous and 5 parous female mice. *p = 0.0004.

(B) Flow cytometry analysis of the classic NKT cell markers T-bet, CD335, and IFN-γ in NKTs (CD45$^+$NK1.1$^+$CD3$^+$) from pre- and post-pregnancy mammary tissue. For Tbet analysis, n = 4 nulliparous and 4 parous female mice. *p = 0.016. For CD335 analysis, n = 7 nulliparous and 7 parous female mice. *p = 0.03.

(C) Flow cytometry analysis of β and γδ TCRs of pre- and post-pregnancy mammary NKTs. n = 5 nulliparous and 5 parous female mice. *p = 0.005.

(D) Gene set enrichment analysis of differentially expressed genes in FACS-isolated NKTs from pre- and post-pregnancy mammary tissue.

(E) Venn diagram demonstrating the number of shared and exclusive ATAC-seq peaks of FACS-isolated NKTs from pre- (blue circle) and post-pregnancy (orange circle) mammary tissue.

(F) Genome browser tracks showing distribution of MACS-called, ATAC-seq peaks at the *Pdk4*, *Maged1*, and *Lypla1* genomic loci from pre- and post-pregnancy NKTs. For all analyses, error bars indicate standard error of mean across samples of the same experimental group. Statistically significant differences were considered with Student's t test $p < 0.05$.

See also Figures S5 and S6 and Table S3.

the NKT master regulator Tbet, the NKT/T cell secreted factor interferon-γ (Ifn-γ), and the NKT lineage marker Nkp46 (CD335) (Yu et al., 2011). Pre- and post-pregnancy, mammary resident NK1.1$^+$CD3$^+$ cells expressed all three markers, supporting their NKT identity. However, we detected a 2-fold increase in the percentage of post-pregnancy cells expressing Tbet, Ifn-γ, and CD335, suggesting that specific populations of NKTs are expanded in post-involuted mammary tissue (Figure 2B).

We also investigated whether pregnancy-induced NKTs represented a specialized population of CD8$^+$ T cells, a cytotoxic cell type reported to reside in mammary tissue (Wu et al., 2019). We found that a fraction of NKTs present in both pre- and post-pregnancy mammary tissue expressed CD8 on their surface, accounting for 41% and 35% of the total NKTs, respectively (Figure S3G). To determine whether the triple-positive (CD3$^+$NK1.1$^+$CD8$^+$) cells contributed significantly to the expanded population of post-pregnancy NKTs, we analyzed the mammary tissue of nulliparous and parous RAG1 knockout (KO) mice, which lack mature CD8$^+$ T cells (Mombaerts et al., 1992). We observed a 10-fold expansion of NKTs in RAG1$^{KO}$ post-pregnancy mammary tissue, suggesting that CD8-expressing cells do not comprise a significant fraction of pregnancy-induced NKTs (Figure S3H). These results are consistent with our scRNA-seq data and further validate the existence of specific NKT subtypes in mammary glands after a full pregnancy cycle.

NKTs have multiple roles, including tissue homeostasis, host protection, microbial pathogen clearance, and anti-cancer activity, mediated through their ability to recognize both foreign- and self-antigens via TCRs (Balato et al., 2009). Therefore, we next investigated changes to the TCR repertoire of mammary resident, post-pregnancy NKTs. We found that 17% of pre-pregnancy NKTs expressed γδTCRs, in marked contrast to post-pregnancy NKTs, which mostly expressed γδTCRs (44%) (Figure 2C, top panels). A pregnancy cycle did not alter TCR composition across all immune cells, given that mammary resident, pre- and post-pregnancy CD8$^+$ T cells mostly express αβTCRs, suggesting that parity promotes expansion of subtypes of NKTs that bear a specific TCR repertoire (Figure 2C, bottom panels).

We next investigated the molecular signatures of fluorescence-activated cell sorting (FACS)-isolated, mammary resident, NKTs. Unbiased pathway analysis of bulk RNA-seq

datasets revealed the enrichment of post-pregnancy NKTs for processes controlling overall NKT development and activation, such as Notch signaling, tumor necrosis factor-α (TnfNF-α) signaling, transforming growth factor-β (Tgf-β) signaling, response to estrogen, and cMYC targets (Oh et al., 2015; Almishri et al., 2016; Doisne et al., 2009; Huber, 2015; Mycko et al., 2009). Conversely, pre-pregnancy NKTs were mainly enriched for processes previously associated with reduced immune activation, such as Ifn-α response (Bochtler et al., 2008) (Figure 2D; Table S3).

The activation of specific processes in post-pregnancy NKTs was also evident from analysis of their accessible chromatin landscape. ATAC sequencing (ATAC-seq) profiles showed similar genomic distributions of accessible regions across pre- and post-pregnancy NKTs, with a 93% overlap of their total accessible chromatin regions, suggesting that parity-induced changes did not substantially alter the chromatin accessibility associated with NKT lineage (Figure 2E; Figure S4A). General TF motif analysis identified chromatin accessible regions bearing classic NKT regulator DNA binding motifs such as *Tbet*, *Plzf*, and *Egr2*, further supporting their NKT lineage identity (Seiler et al., 2012) (Figure S4B). Analysis of accessible chromatin exclusive to post-pregnancy NKTs showed an enrichment for terms/genes associated with regulation of the adaptive immune response, killer cell activation, and antigen presentation, such as *Pdk4*, *Maged1*, and *Lypla1*, all involved in enhanced immune activation (Na et al., 2020; Connaughton et al., 2010; Lee et al., 2016; Jehmlich et al., 2013) (Figure 2F; Figure S4C). DNA motif analysis at accessible regions exclusive to post-pregnancy NKTs identified enrichment of specific TF motifs, including those recognized by Maf, a factor associated with an activated NKT state, and previously predicted by our scRNA-seq data to be expressed in cell clusters with an NKT identity (Figure S4D).

Overall, our analyses confirmed that post-pregnancy mammary tissue has an altered γδNKT cell composition, which bears molecular and cellular signatures of activated and mature adaptive immune cells.

### NKT expansion requires CD1d expression on post-pregnancy MECs

Classically, NKTs are subdivided based on their activating antigens, including the main antigen-presenting molecules MHC class I, MHC class II, and the non-classical class I molecule, CD1d, which can be expressed on the surface of macrophages and dendritic cells, as well on the surface of epithelial cells (Gapin et al., 2013; Rizvi et al., 2015; Thibeault et al., 2009). Therefore, we next analyzed whether the expression of antigen-presenting factors on the surface of mammary epithelial and non-epithelial cells could underlie NKT cell expansion after pregnancy.

Flow cytometry analysis detected a 5-fold increase in CD1d levels on the surface of post-pregnancy luminal and myoepithelial MECs, in marked contrast to the levels of MHC-I and MHC-II proteins, which were largely unchanged across pre- and post-pregnancy MECs (Figures 3A and 3B; Figures S5A and S5B). No difference in surface expression of CD1d on mammary CD45$^+$ immune cells was detected, suggesting that signals provided by CD1d$^+$ MECs could promote the post-pregnancy expansion of mammary NKT cells (Figure S5C).

Gene-expression analysis of scRNA-seq datasets and qPCR quantification of FACS-isolated epithelial cells confirmed that post-pregnancy MECs express higher levels of *Cd1d* mRNA, supporting that pregnancy-induced molecular alterations may represent the basis for the observed increase in percentage of CD1d$^+$ MECs (Figure 1D; Figure S5D). In agreement, we observed increased levels of the active transcription marker histone H3 lysine 27 acetylation (H3K27ac) at the *Cd1d* genomic locus in FACS-isolated post-pregnancy MECs, suggesting that increased mRNA levels could be associated with parity-induced epigenetic changes at the *Cd1d* locus (Figure 3C). These observations were confirmed in organoid systems that mimic the transcription and epigenetic alterations brought to MECs by pregnancy signals (Ciccone et al., 2020), where pregnancy hormones induced upregulation of *Cd1d* mRNA levels and increased H3K27ac levels at the *Cd1d* locus (Figures S5E and S5F). Thus, pregnancy-associated signals may induce epigenetic alterations that subsequently increase *Cd1d* mRNA and CD1d protein levels in post-pregnancy MECs.

To investigate whether CD1d expression is required for the expansion of NKTs after parity, we analyzed mammary glands from CD1d$^{KO}$ mice, which bear reduced levels of activated NKTs (Faunce et al., 2005; Macho-Fernandez and Brigl, 2015; Mantell et al., 2011). Mammary glands from nulliparous and parous CD1d$^{KO}$ mice displayed similar numbers of ductal structures as CD1d wild-type (WT) female mice, suggesting that loss of CD1d does not majorly alter mammary tissue homeostasis (Figure 3D). Further flow cytometry analysis indicated no statistically significant changes in the percentage of NKTs in mammary glands of nulliparous CD1d$^{KO}$ mice (2.2% ± 0.8), compared to nulliparous CD1d$^{WT}$ mice (3% ± 1.6) (Figures 2A, left panel, and 3E, left panel). Conversely, we found a 7-fold decrease in the percentage of NKTs in mammary tissue from fully involuted, parous CD1d$^{KO}$ female mice (3% ± 1.5) compared to parous CD1d$^{WT}$ mammary tissue (26% ± 4), supporting the role of CD1d in regulating NKT activation after pregnancy (Figures 2A, right panel, and 3E, right panel). Moreover, we found no difference in the abundance of NKTs in glands from pre- and post-pregnancy CD1d$^{KO}$ female mice, consistent with lack of CD1d expression reducing the activation of NKTs (Figure 3E). The analysis of an additional mouse strain that is deficient in mature/activated NKTs, due to the deletion of the histone-demethylase *Kdm6* (Utx$^{KO}$ mouse model), failed to detect an expansion of NKTs post-pregnancy, thus supporting that pregnancy induces the expansion of mature/active subtypes of NKTs (Beyaz et al., 2017) (Figure S5G). Moreover, NKTs observed in post-pregnancy CD1d$^{KO}$ mammary tissue mainly expressed αβTCR on their surface, in contrast to the γδNKTs observed in CD1d$^{WT}$ post-pregnancy glands, further confirming that loss of CD1d expression affects the expansion and activation of specific populations of NKTs in post-pregnancy mammary tissue (Figure 3F).

Collectively, our studies identified pregnancy-induced epigenetic changes that may control the increased expression of *Cd1d* mRNA in post-pregnancy MECs and elucidated a role for CD1d in mediating communication between MECs and the γδNKTs, unique to post-pregnancy mammary glands.

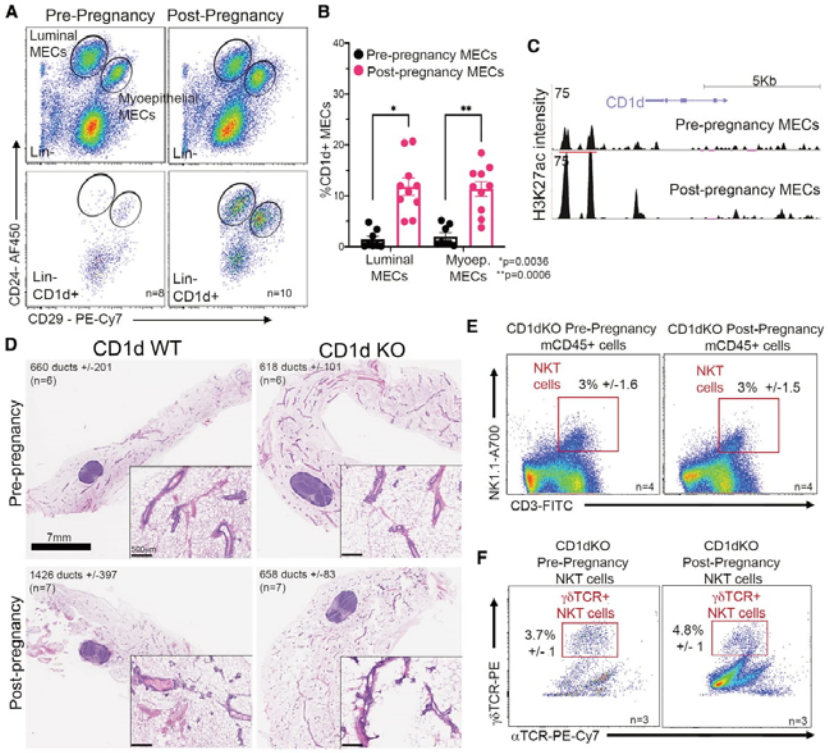


**Figure 3. NKT expansion depends on CD1d expression on post-pregnancy MECs**

(A and B) Flow cytometry analysis and quantification of CD1d$^+$ MECs harvested from pre-pregnancy (black bars, n = 8) and post-pregnancy (pink bars, n = 10) mammary tissue. *p = 0.0036 for luminal MECs and **p = 0.0006 for myoepithelial MECs.

(C) Genome browser tracks showing MACS-called, H3K27ac ChIP-seq peaks at the *Cd1d* genomic locus in FACS-isolated, pre- and post-pregnancy luminal MECs.

(D) H&E-stained histological images and duct quantification from mammary glands harvested from nulliparous (top left, n = 6) and parous (bottom left, n = 7) CD1d$^{WT}$ female mice and nulliparous (top right, n = 6) and parous (bottom right, n = 7) CD1d$^{KO}$ female mice. p = 0.86 for pre-pregnancy glands and p = 0.78 for post-pregnancy glands. Scale: 7 mm. Zoom-in panels, scale 500 µm.

(E) Flow cytometry analysis of mammary resident NKTs from pre- and post-pregnancy CD1d$^{KO}$ mammary tissue. n = 4 nulliparous and n = 4 parous female mice. *p = 0.3.

(F) Flow cytometry analysis of α and γδ TCRs of mammary resident NKTs from pre- (n = 3) and post-pregnancy (n = 3) CD1d$^{KO}$ mammary tissue. *p = 0.5.

For all analyses, error bars indicate standard error of mean across samples of the same experimental group. Statistically significant differences were considered with Student's t test p < 0.05. See also Figure S7.

## Lack of mammary oncogenesis is marked by NKT expansion and CD1d$^+$ MECs

Parity resulted in the expansion of γδNKTs in the mammary gland in response to the upregulation of CD1d on MECs, thus pointing to a mechanistic connection between pregnancy-induced changes to MECs and immune cell biology. Pregnancy-induced molecular modifications to MECs have also been associated with an oncogene-induced senescence response to cMyc overexpression, and suppression of mammary oncogenesis (Feigman et al., 2020). Therefore, we next investigated whether pregnancy-induced mammary cancer protection was associated with the expansion of NKTs.

Flow cytometry analysis of pre- and post-pregnancy mammary tissue from cMyc-overexpressing female mice (DOX-treated, CAGMYC model) demonstrated a 1.5-fold increase in the abundance of total CD3$^+$ T cells (Figure S6A). CD3$^+$ T cell expansion was also observed in mammary tissue transplanted with CAGMYC post-pregnancy MECs and in organoid cultures derived from post-pregnancy CAGMYC MECs; both conditions previously shown to lack mammary oncogenesis, thus further

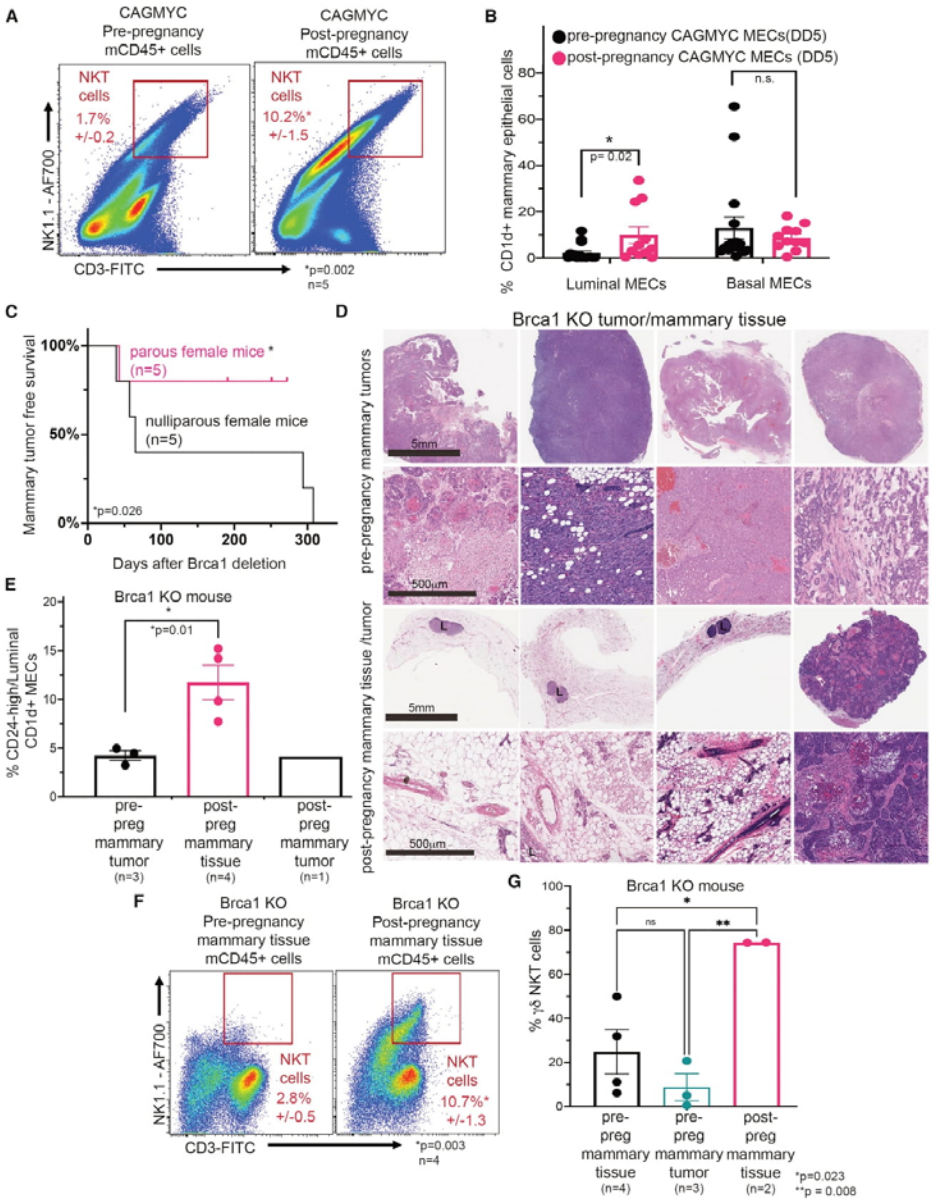


*(legend on next page)*

suggesting a link between pregnancy-induced tumorigenic inhibition and specific changes to the adaptive immune system (Figures S6B and S6C). This selective expansion of $CD3^+$ T cells was further supported by the analysis of markers that define mammary resident neutrophils ($Ly6G^+$) and macrophages ($CD206^+$), which were largely unchanged in mammary tissue transplanted with either pre- or post-pregnancy CAGMYC MECs (Figure S6B).

Further flow cytometry analysis identified a 6-fold increase in the percentage of NKTs in mammary tissue from parous CAGMYC female mice, which predominantly expressed γδTCRs (Figure 4A; Figure S6D). No changes in the abundance of $CD8^+$ T cells or $CD4^+$ T cells was observed between mammary tissue from nulliparous and parous CAGMYC female mice, supporting the parity-induced expansion of γδNKTs (Figures S6E and S6F) and suggesting that specific constituents of the mammary immune microenvironment may control tumorigenesis. In agreement, we also found a 5-fold higher percentage of $CD1d^+$ luminal MECs in post-pregnancy mammary tissue, thus linking gain of CD1d expression and the expansion of γδNKTs, which may collectively play a role in blocking tumorigenesis (Figure 4B).

cMYC overexpression is present in approximately 60% of basal-like breast cancers, with *cMYC* gain of function commonly found in *BRCA1*-mutated breast cancers (Chen and Olopade, 2008; Grushko et al., 2004). Interestingly, women harboring *BRCA1* mutations with a full-term pregnancy before the age of 25 benefit from pregnancy-induced breast cancer protection (Medina et al., 2004; Terry et al., 2018). Therefore, we developed an inducible mouse model of *Brca1* loss of function, for the purpose of investigating how pregnancy-induced changes influence *Brca1*-null mammary tumor development. In this model, tamoxifen (TAM) induces homozygous loss of Brca1 function in cells that express the cytokeratin 5 gene ($Krt5^+$ cells), which include MECs (dos Santos et al., 2013), cells from gastrointestinal tract (Sulahian et al., 2015), reproductive organs (Ricciardelli et al., 2017), and additional epithelial tissue (Castillo-Martin et al., 2010; Majumdar et al., 2012), in a p53 heterozygous background ($Krt5^{CRE\text{-}ERT2}Brca1^{fl/fl}p53^{-/+}$, hereafter referred as $Brca1^{KO}$ mouse).

Nulliparous $Brca1^{KO}$ mice exhibited signs of mammary hyperplasia approximately 12 weeks post-TAM treatment, which gradually progressed into mammary tumors at around 20 weeks after *Brca1* deletion (Figures S6G and S6H). $Brca1^{KO}$ mammary tumors display cellular and molecular features similar to those previously described in human breast tissue from *BRCA1* mutation carriers and animal models of Brca1 loss of function, including high EGFR and KRT17 protein levels and altered copy-number variation marked by gains and losses of genomic regions (Annunziato et al., 2019) (Figures S6I and S6J).

To investigate the effects of pregnancy on the mammary immune microenvironment and oncogenesis, age-matched, TAM-treated, $Brca1^{KO}$ nulliparous and parous female mice were monitored for tumor development (Figure S7A). Our study demonstrated that only 20% of the parous $Brca1^{KO}$ female mice developed mammary tumors (one out of five), compared to 100% of nulliparous $Brca1^{KO}$ female mice with mammary tumors (five out of five mice), thus indicating that a full pregnancy cycle decreases the frequency of $Brca1^{KO}$ mammary tumors by 80% (Figures 4C and 4D).

Histopathological analysis suggested that pre-pregnancy mammary tumors were quite diverse, as previously reported for tumors from $Brca1^{KO}$ mice (Brodie et al., 2001). These included poorly differentiated tumors, such as micro-lobular carcinomas with squamous trans-differentiation (Figure 4D, top rows, far-left panel), medullary-like carcinomas (Figure 4D, top rows, right panel), and solid carcinomas resembling high-grade invasive ductal carcinoma (IDC) (Figure 4D, top rows, left and far-right panels). Accordingly, the only tumor-bearing parous $Brca1^{KO}$ female mouse developed a poorly differentiated carcinoma with extensive squamous trans-differentiation and extensive necrosis, also previously reported for tumors from $Brca1^{KO}$ mice (Figure 4D, bottom rows, far-right panels). Additional histopathological analysis confirmed that mammary tissues from the remaining parous $Brca1^{KO}$ female mice (four out of five) were largely normal (Figure 4D, bottom rows, far-left, left and right panels; Figure S7B). Immunofluorescence analysis confirmed that both pre-pregnancy mammary tumors and post-pregnancy normal mammary tissue were indeed deficient for $Brca1^+$ epithelial cells, indicating that the lack of mammary tumors in parous female mice was not due to inefficient *Brca1* deletion (Figure S7C).

Flow cytometry analysis of $Brca1^{KO}$ MECs demonstrated a progressive loss of $CD24^{mid}CD29^{high}$ myoepithelial cells in tumor

**Figure 4. Lack of mammary oncogenesis is marked by NKT expansion and $CD1d^+$ MECs**

(A) Flow cytometry analysis of mammary resident NKTs ($CD45^+NK1.1^+CD3^+$) from DOX-treated, nulliparous (left panel, n = 5) and parous (right panel, n = 5) CAGMYC female mice. *p = 0.002.

(B) Flow cytometry quantification of $CD1d^+$ luminal and myoepithelial MECs from DOX-treated, nulliparous (left panel, n = 16) and parous (right panel, n = 11) CAGMYC female mice. *p = 0.02.

(C) Mammary tumor-free survival plot of nulliparous (black line, n = 5) and parous (pink line, n = 5) $Brca1^{KO}$ female mice.

(D) H&E-stained histological images from mammary tissue and tumors from nulliparous (top panels) and parous (bottom panels) $Brca1^{KO}$ female mice. Scale: 5 mm. Zoom-in panels, scale: 500 μm.

(E) Flow cytometry quantification of $CD1d^+CD24^{high}$ luminal MECs from $Brca1^{KO}$ pre-pregnancy mammary tumors (black bar, n = 3), $Brca1^{KO}$ post-pregnancy healthy mammary tissue (pink bar, n = 4), and $Brca1^{KO}$ post-pregnancy mammary tumor (blue bar, n = 1). *p = 0.02.

(F) Flow cytometry analysis of NKTs in normal mammary tissue from nulliparous, tumor-bearing, $Brca1^{KO}$ female mice (left panel, n = 4) and normal mammary tissue from healthy parous $Brca1^{KO}$ female mice (right panel, n = 4). *p = 0.003.

(G) Quantification of γδNKTs in normal mammary tissue from nulliparous, tumor-bearing, $Brca1^{KO}$ female mice (black bar panel, n = 4), in mammary tumor tissue from nulliparous $Brca1^{KO}$ female mice (blue bar, n = 3), and in normal mammary tissue from healthy parous $Brca1^{KO}$ female mice (black bar panel, n = 2). *p = 0.023 and **p = 0.008.

For all analyses, error bars indicate standard error of mean across samples of the same experimental group. Statistically significant differences were considered with Student's t test $p < 0.05$. See also Figures S8–S12.

tissue from nulliparous (2.5-fold) and parous (2-fold) Brca1$^{KO}$ female mice, and a marked increase in the percentage of CD24$^{high}$CD29$^{low}$ luminal-like MECs (Figure S7D). These results suggest that tumor progression in this model is accompanied by changes to the population of CD24$^{high}$ MECs, which has been associated with poor clinical outcomes in patients with triple-negative breast cancer (Chan et al., 2019). Further cellular analysis indicated a 2.7-fold increase in the percentage of CD24$^{high}$/luminal CD1d$^{+}$ cells in healthy, post-pregnancy Brca1$^{KO}$ mammary tissue compared to tissue from tumor-bearing nulliparous and parous Brca1$^{KO}$ mice, supporting that parity-induced expression of CD1d at the surface of MECs associates with inhibition of mammary oncogenesis (Figure 4E).

Given the increased levels of CD1d expression, we next investigated the presence of NKTs in mammary tissue from nulliparous and parous Brca1$^{KO}$ female mice. Flow cytometry analysis demonstrated a 3.8-fold increase in the percentage of NKTs in healthy, post-pregnancy Brca1$^{KO}$ mammary tissue compared to non-affected normal mammary tissue from tumor-bearing nulliparous Brca1$^{KO}$ mice, and mammary tumors from parous Brca1$^{KO}$ mice (Figure 4F; Figure S7E). Additional flow cytometry analysis demonstrated that approximately 70% of total NKTs from healthy, post-pregnancy Brca1$^{KO}$ mammary tissue expressed γδTCR, in marked contrast to NKTs from healthy (2.7%) and tumor-bearing (8.6%) mammary tissue from nulliparous Brca1$^{KO}$ mice (Figure 4G).

Collectively, our findings show that pregnancy-induced gain of CD1d expression at the surface of MECs and expansion of γδNKTs associates with lack of mammary oncogenesis in response to cMyc overexpression or Brca1 loss of function. These results support the link between pregnancy-induced molecular changes, mammary tissue immune alteration, and inhibition of mammary tumorigenesis in clinically relevant mouse models of breast cancer.

### Functionally active NKTs are required to block malignant progression of post-pregnancy MECs

Given that we demonstrated that pregnancy-induced changes block mammary oncogenesis in two distinct models (Figure 4), and that *cMyc* gain of function is commonly found in *Brca1*-mutated breast cancers, we utilized the cMyc overexpression mouse model to further characterize the effects of the immune microenvironment on the malignant development of post-pregnancy MECs. Analysis of fat-pad transplantations into severely immune-deficient NOD/SCID female mice, which lack T cells, B cells, NK, and NKTs, indicated that 100% of mammary tissue injected with pre-pregnancy (n = 5) or post-pregnancy (n = 5) CAGMYC MECs developed adeno-squamous-like carcinomas with acellular lamellar keratin, high levels of cell proliferation (Ki67 staining), and increased collagen deposition (Trichrome blue staining) (Figures S8A–S8C). Therefore, NKTs, or associated adaptive immune cells, are required for the parity-associated protection from oncogenesis in the CAGMYC model.

Bulk RNA-seq analysis demonstrated that post-pregnancy CAGMYC MECs transplanted into the fat pad of NOD/SCID female mice were less effective at activating the expression of canonical cMyc targets and estrogen response genes, compared to transplanted pre-pregnancy CAGMYC MECs, in agreement with the previously reported transcriptional state of post-pregnancy CAGMYC MECs (Feigman et al., 2020) (Figure S8D). We also found that organoid cultures derived from post-pregnancy CAGMYC MECs transplanted into NOD/SCID female mice retained a senescent-like state, characterized by reduced p300 protein levels and moderately increased p53 protein levels, in agreement with the previously reported senescent state of post-pregnancy CAGMYC MECs (Feigman et al., 2020) (Figure S8E). Together, these findings indicate that oncogenic progression of post-pregnancy CAGMYC MECs is associated with the immune-deficient mammary microenvironment of NOD/SCID mice.

While our investigation of post-pregnancy CAGMYC MECs that were transplanted into the mammary tissue of immunosuppressed animals alluded to the importance of a robust immune system in blocking mammary tumorigenesis, it did not uncouple whether functionally active NKTs, or CD1d expression at the surface of MECs, act to block oncogenesis in post-pregnancy mammary tissue. Therefore, to determine whether signaling between CD1d$^{+}$ MECs and NKTs is critical for the development of mammary oncogenesis after pregnancy, we developed a double-transgenic mouse model by crossing the DOX-inducible CAGMYC mice into a CD1d$^{KO}$ background (CAGMYC-CD1d$^{KO}$).

Histology analysis indicated that mammary tissue from DOX-treated, nulliparous, and parous CAGMYC-CD1d$^{KO}$ female mice showed signs of hyperplasia with atypia and abnormal ductal structures (Figure 5A, left and far-right panels; Figure S9A). Conversely, mammary tissue from DOX-treated, CAGMYC-CD1d$^{WT}$ parous female mice lacked malignant lesions in response to cMyc overexpression, thus suggesting that CD1d expression is required to inhibit the development of malignant lesions in post-pregnancy mammary gland (Figure 5A, right panels; Figure S9A). Flow cytometry analysis showed a lack of NKTs in mammary tissue from both nulliparous and parous CAGMYC-CD1d$^{KO}$ female mice, in marked contrast to the observed expansion of γδNKTs in healthy post-pregnancy CAGMYC-CD1d$^{WT}$ mammary glands that lacked tissue hyperplasia, supporting that CD1d expression may control pregnancy-induced expansion/activation of NKTs, and thus block mammary tumorigenesis (Figure S9B; Figure 4A). To further determine whether loss of CD1d expression underlies the malignant transformation of post-pregnancy MECs, we performed mammary transplantation assays of CAGMYC-CD1d$^{KO}$ MECs into the fat pad of syngeneic animals (CD1d$^{WT}$ female mice). We found that 100% of mammary tissue injected with pre-pregnancy CAGMYC-CD1d$^{KO}$ MECs and 70% of mammary glands injected with post-pregnancy CAGMYC-CD1d$^{KO}$ MECs developed signs of malignant lesions, supporting that loss of CD1d expression impacts with pregnancy-induced breast cancer protection (Figure 5B, black font; Figures S9C and S9D). This last observation was in marked contrast to the finding in glands transplanted with post-pregnancy CAGMYC-CD1d$^{WT}$ MECs, which, as previously reported, did not present signs of malignant transformation (Feigman et al., 2020) (Figure 5B, blue font; Figures S9E and S9F).

Altogether, these results suggest that loss of CD1d, with concomitant loss of pregnancy-induced expansion of NKTs,

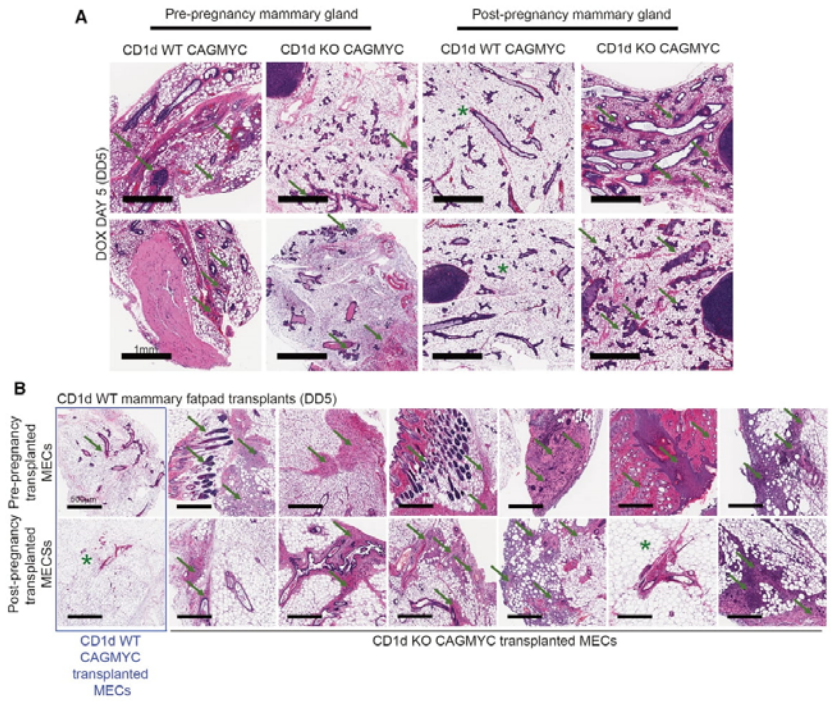


**Figure 5. Functionally active NKTs are required to block malignant progression of post-pregnancy MECs**

(A) H&E-stained images of mammary tissue harvested from DOX-treated (DD5), nulliparous CAGMYC-CD1d$^{WT}$ (far-left panels), nulliparous CAGMYC-CD1d$^{KO}$ (left panels), parous CAGMYC-CD1d$^{WT}$ (right panels), and parous CAGMYC-CD1d$^{KO}$ (far right panels) female mice. Green arrows indicate signs of malignant lesions/mammary hyperplasia. Green asterisks indicate normal-like ductal structures. Scale: 1 mm.

(B) H&E-stained images of DOX-treated, CD1d$^{WT}$ mammary tissue transplanted with pre-pregnancy CAGMYC-CD1d$^{WT}$ MECs (blue font, top far left panel), pre-pregnancy CAGMYC-CD1d$^{KO}$ MECs (black font, top panel), post-pregnancy CAGMYC-CD1d$^{WT}$ (blue font, bottom far left panel), or post-pregnancy CAGMYC-CD1d$^{KO}$ MECs (black font, bottom panel). Green arrows indicate signs of malignant lesions/mammary hyperplasia. Green asterisks indicate normal-like ductal structures. Scale: 500 μm. See also Figure S13.

supports the development of mammary malignant lesions, independently of parity. Moreover, our study elucidates that parity blocks the malignant transformation of MECs, both by inducing cell-autonomous, epigenetic alterations within the MECs, and non-autonomous communication between CD1d$^{+}$ MECs and NKTs in the mammary gland.

## DISCUSSION

In mammals, reprogramming of the immune system is initiated after birth and continues throughout the lifespan of an individual due to exposure to pathogens, hormonal fluctuations, and aging. This dynamic reprogramming is part of an immune surveillance system that detects abnormal cells across many tissues, helping to prevent cancer. Here, we characterized a population of NKT-like immune cells (NKTs) in post-pregnancy mammary tissue, and their role in inhibiting mammary oncogenesis.

Our findings suggest that post-pregnancy mammary homeostasis does not rely on the presence of γδNKTs, given the normal histology of mammary tissue in mice deficient for this cell type. It is possible that NKTs expand in response to the re-setting of whole-body immunity post-partum, with the child-bearing event providing signals that alter antigens across all maternal tissues as well as expanding specific immune cell populations. γδNKTs have been found in the pregnant uterus across many mammalian species, linking NKT specialization and the pregnancy cycle (Mincheva-Nilsson, 2003). Our results support that the expansion of NKTs was predominantly observed in post-involution tissue, thus suggesting that the immune reprogramming of mammary tissue takes place after lactation.

Several other immune subtypes have been described to be enriched in mammary tissue during gestation, lactation, and involution stages of mammary gland development. These studies identified alterations in leukocyte interaction with

mammary ductal structures, as well as specific transcriptional changes, suggesting that cell interaction and cellular identity of mammary resident cells are affected by pregnancy-induced development (Dawson et al., 2020; Hitchcock et al., 2020). Our analysis of leukocytes, specifically macrophages and neutrophils, did not show alterations to such cell populations in healthy parous murine mammary tissue or in post-pregnant CAGMYC mammary tissue lacking malignant lesions. However, given that leukocytes have been implicated in the activation of NKTs (Macho-Fernandez and Brigl, 2015; Rizvi et al., 2015), it is possible that molecular alterations, rather than changes to cellular abundance or antigen presentation of leukocytes, could play a role in inducing or sustaining the population of NKTs in post-pregnancy mammary tissue.

Our studies also provide evidence linking pregnancy-induced immune changes with the inhibition of mammary oncogenesis. Our previous research focused on how post-pregnancy MECs assume a senescence-like state in response to cMyc overexpression, an oncogene-induced response that activates the immune system via the expression of senescence-associated genes (Braig and Schmitt, 2006). Here, we found that CD1d expression at the surface of post-pregnancy MECs and the presence of NKTs were linked with the inhibition of mammary oncogenesis in two independent models of breast cancer, illustrating how epithelial and immune cells communicate to support pregnancy-induced mammary cancer prevention. Given that NKTs were previously shown to interact with senescent cells, it is possible that pregnancy-induced activation of CD1d expression and NKTs expansion represent additional responses to oncogene-induced cellular senescence (Kale et al., 2020).

Women completing a full-term pregnancy before the age of 25 have an approximate one-third reduction of the risk of breast cancer (Medina et al., 2004). This benefit applies to the risk of all breast cancer subtypes, including those from women harboring *BRCA1* mutations (Terry et al., 2018). Thus, our findings supporting a role for pregnancy in inhibiting the development of $Brca1^{KO}$ mammary tumors lends a clinical relevance to our studies. Interestingly, the mammary tumor from parous $Brca1^{KO}$ female mouse was associated with low abundance of γδNKTs and $CD1d^{+}$ MECs, suggesting that loss of the pregnancy-induced epithelial to immune microenvironment communication may be part of cellular changes that support mammary tumorigenesis. In fact, the genetically engineered loss of CD1d expression, with a consequent deficiency in activated NKTs, supported the malignant progression of cMYC-overexpressing MECs, further illustrating a link between epithelial and immune cells in supporting pregnancy-induced mammary cancer prevention.

Our findings are based on studies performed in mice that became pregnant at a young age (~8 weeks old), which reinforced pregnancy-induced changes to epithelial cells, and their effect on immune recruitment and oncogenesis inhibition. However, it remains unclear why such strong, pregnancy-induced changes do not fully prevent the development of breast cancer (Nichols et al., 2019). It has been suggested that specific mammary epithelial clones with oncogenic properties reside within the mammary tissue after pregnancy and may give rise to late-onset mammary oncogenesis in aged mice (Li et al., 2020b). It is possible that such populations of rare MECs lose some of their pregnancy-induced molecular signatures over time, thereby bypassing oncogene-induced senescence and immune recognition, and ultimately developing into mammary tumors. Moreover, given that pregnancy-induced breast cancer protection becomes apparent ~5–8 years after pregnancy, it is possible that additional immune reprogramming influenced by genetic makeup, age at pregnancy, and/or overall post-partum health may further modify breast tissue and erase pregnancy-induced changes that inhibit breast cancer development.

Nonetheless, the connection between pregnancy, immunity, and oncogenesis could be used to develop therapies to block cancer development. Indeed, a series of preclinical models have been developed to optimize the delivery of CD1d stimulatory factors, such as αGalcer and KRN7000, and induce expansion of NKTs (Zhang et al., 2019). Such strategies are mostly side-effect free and, if proven to support the expansion of pregnancy-induced NKT cells, could be used in cases of high breast cancer risk, including those with genetic alterations and/or family histories of breast cancer. Additionally, the characterization of specific, pregnancy-induced TCR rearrangements may be leveraged in CAR-NKT immunotherapy, for example, which could also efficiently target disease that has already developed. Collectively, such strategies could improve breast health and decrease cancer risk in women who experience their first pregnancy after 35 years of age, when they are at a greater risk to develop breast cancer.

### Limitations of the study

The majority of existing transgenic and knockout models of breast cancer utilize mammary gland-specific promoters to control oncogene activation, such as MMTV, BLG, and WAP, which are enhanced/activated by signals present during pregnancy and lactation, thus potentially confounding the analysis of the molecular basis of pregnancy and mammary cancer risk. Therefore, the development of new model systems of mammary tumorigenesis, that do not rely on pregnancy-induced promoters, will allow us to further understand the effect of pregnancy on oncogenesis across all breast cancer subtypes.

## STAR★METHODS

Detailed methods are provided in the online version of this paper and include the following:

- KEY RESOURCES TABLE
- RESOURCE AVAILABILITY
  - Lead contact
  - Materials availability
  - Data and code availability
- EXPERIMENTAL MODEL AND SUBJECT DETAILS
  - Animal studies
- METHOD DETAILS
  - Antibodies
  - Mammary gland isolation
  - Flow cytometry analysis
  - Mammary organoid culture
  - RT-qPCR
  - Mammary fat pad transplantation

- Histological analysis
- Immunofluorescence analysis
- Doxycycline treatment
- Tamoxifen treatment
- Monitoring tumor growth
- Western blot
- scRNA-seq data analysis
- RNA-seq library preparation and analysis
- ChIP-seq library analysis
- Cut&Run library analysis
- ATAC-seq library preparation and analysis
- DNA motif analysis
- Genomic library preparation and copy-number variation analysis

- QUANTIFICATION AND STATISTICAL ANALYSIS

## SUPPLEMENTAL INFORMATION

Supplemental information can be found online at https://doi.org/10.1016/j.celrep.2021.110099.

## ACKNOWLEDGMENTS

This work was performed with assistance from the following CSHL Shared Core Resources: Animal Facility, Tissue Histology, NextGen Sequencing, Single Cell, Flow Cytometry, and Microscopy, which are supported by the CSHL Cancer Center Support Grant 5P30CA045508. This work was financially supported by the CSHL and Northwell Health affiliation, the CSHL and Simons Foundation Award, the Rita Allen Scholar Award, the Pershing Square Sohn Prize for Cancer Research, the AACR-Breast Cancer Research Foundation, the NIH/NCI grant R01CA248158-01, and the NIH/NIA grant R01 AG069727-01 (C.O.d.S.). Whole-genome sequencing (CNV analysis) was performed with financial support provided to Dr. Michael Wigler by The Breast Cancer Research Foundation (BCRF-19-174) and the Simons Foundation, Life Sciences Founder Directed Giving-Research (519054). We would like to thank Mrs. Shih-Ting Yang for the mouse illustrations.

## AUTHOR CONTRIBUTIONS

C.O.d.S. designed and supervised the research; C.O.d.S., A.V.H.S., M.A.M., M.J.F., and S.L.C. wrote the manuscript. A.V.H.S., M.A.M., M.J.F., C.C., S.L.C., M.F.C., M.C.T., and M.V. performed experiments and analyzed the results. M.A.M. and M.C.T. performed bioinformatics analyses. S.L., and J.K. performed and analyzed whole-genome sequencing (CNV analysis). S.B. provided reagents and critical feedback. J.E.W. performed histopathological analysis.

## DECLARATION OF INTERESTS

The authors declare no competing interests.

Received: March 15, 2021
Revised: August 25, 2021
Accepted: November 15, 2021
Published: December 7, 2021

## REFERENCES

Almishri, W., Santodomingo-Garzon, T., Le, T., Stack, D., Mody, C.H., and Swain, M.G. (2016). TNFαNF6n omingo-Garzon competing interests to disclose.TNFR2. J. Innate Immun. *8*, 617–629.

Anders, S., and Huber, W. (2010). Differential expression analysis for sequence count data. Genome Biol. *11*, R106.

Andrews, S. (2015). FASTQC A Quality Control tool for High Throughput Sequence Data (Babraham Institute).

Angerer, P., Haghverdi, L., Büttner, M., Theis, F.J., Marr, C., and Buettner, F. (2016). destiny: diffusion maps for large-scale single-cell data in R. Bioinformatics *32*, 1241–1243.

Annunziato, S., de Ruiter, J.R., Henneman, L., Brambillasca, C.S., Lutz, C., Vaillant, F., Ferrante, F., Drenth, A.P., van der Burg, E., Siteur, B., et al. (2019). Comparative oncogenomics identifies combinations of driver genes and drug targets in BRCA1-mutated breast cancer. Nat. Commun. *10*, 397.

Bach, K., Pensa, S., Grzelak, M., Hadfield, J., Adams, D.J., Marioni, J.C., and Khaled, W.T. (2017). Differentiation dynamics of mammary epithelial cells revealed by single-cell RNA sequencing. Nat. Commun. *8*, 2128.

Bach, K., Pensa, S., Zarocsinceva, M., Kania, K., Stockis, J., Pinaud, S., Lazarus, K.A., Shehata, M., Simões, B.M., Greenhalgh, A.R., et al. (2021). Time-resolved single-cell analysis of Brca1 associated mammary tumourigenesis reveals aberrant differentiation of luminal progenitors. Nat. Commun. *12*, 1502.

Balato, A., Unutmaz, D., and Gaspari, A.A. (2009). Natural killer T cells: an unconventional T-cell subset with diverse effector and regulatory functions. J. Invest. Dermatol. *129*, 1628–1642.

Baslan, T., Kendall, J., Rodgers, L., Cox, H., Riggs, M., Stepansky, A., Troge, J., Ravi, K., Esposito, D., Lakshmi, B., et al. (2012). Genome-wide copy number analysis of single cells. Nat. Protoc. *7*, 1024–1041.

Benner, C., Heinz, S., and Glass, C.K. (2017). HOMER - Software for motif discovery and next generation sequencing analysis.

Beyaz, S., Kim, J.H., Pinello, L., Xifaras, M.E., Hu, Y., Huang, J., Kerenyi, M.A., Das, P.P., Barnitz, R.A., Herault, A., et al. (2017). The histone demethylase UTX regulates the lineage-specific epigenetic program of invariant natural killer T cells. Nat. Immunol. *18*, 184–195.

Blakely, C.M., Stoddard, A.J., Belka, G.K., Dugan, K.D., Notarfrancesco, K.L., Moody, S.E., D'Cruz, C.M., and Chodosh, L.A. (2006). Hormone-induced protection against mammary tumorigenesis is conserved in multiple rat strains and identifies a core gene expression signature induced by pregnancy. Cancer Res. *66*, 6421–6431.

Bochtler, P., Kröger, A., Schirmbeck, R., and Reimann, J. (2008). Type I IFN-induced, NKT cell-mediated negative control of CD8 T cell priming by dendritic cells. J. Immunol. *181*, 1633–1643.

Bolger, A.M., Lohse, M., and Usadel, B. (2014). Trimmomatic: a flexible trimmer for Illumina sequence data. Bioinformatics *30*, 2114–2120.

Braig, M., and Schmitt, C.A. (2006). Oncogene-induced senescence: putting the brakes on tumor development. Cancer Res. *66*, 2881–2884.

Britt, K., Ashworth, A., and Smalley, M. (2007). Pregnancy and the risk of breast cancer. Endocr. Relat. Cancer *14*, 907–933.

Brodie, S.G., Xu, X., Qiao, W., Li, W.M., Cao, L., and Deng, C.X. (2001). Multiple genetic changes are associated with mammary tumorigenesis in Brca1 conditional knockout mice. Oncogene *20*, 7514–7523.

Buenrostro, J.D., Giresi, P.G., Zaba, L.C., Chang, H.Y., and Greenleaf, W.J. (2013). Transposition of native chromatin for fast and sensitive epigenomic profiling of open chromatin, DNA-binding proteins and nucleosome position. Nat. Methods *10*, 1213–1218.

Castillo-Martin, M., Domingo-Domenech, J., Karni-Schmidt, O., Matos, T., and Cordon-Cardo, C. (2010). Molecular pathways of urothelial development and bladder tumorigenesis. Urol. Oncol. *28*, 401–408.

Chan, S.H., Tsai, K.W., Chiu, S.Y., Kuo, W.H., Chen, H.Y., Jiang, S.S., Chang, K.J., Hung, W.C., and Wang, L.H. (2019). Identification of the novel role of CD24 as an oncogenesis regulator and therapeutic target for triple-negative breast cancer. Mol. Cancer Ther. *18*, 147–161.

Chen, Y., and Olopade, O.I. (2008). MYC in breast tumor progression. Expert Rev. Anticancer Ther. *8*, 1689–1698.

Chung, C.Y., Ma, Z., Dravis, C., Preissl, S., Poirion, O., Luna, G., Hou, X., Giraddi, R.R., Ren, B., and Wahl, G.M. (2019). Single-Cell Chromatin Analysis of Mammary Gland Development Reveals Cell-State Transcriptional Regulators and Lineage Relationships. Cell Rep. *29*, 495–510.

Ciccone, M.F., Trousdell, M.C., and Dos Santos, C.O. (2020). Characterization of Organoid Cultures to Study the Effects of Pregnancy Hormones on the Epigenome and Transcriptional Output of Mammary Epithelial Cells. J. Mammary Gland Biol. Neoplasia *25*, 351–366.

Connaughton, S., Chowdhury, F., Attia, R.R., Song, S., Zhang, Y., Elam, M.B., Cook, G.A., and Park, E.A. (2010). Regulation of pyruvate dehydrogenase kinase isoform 4 (PDK4) gene expression by glucocorticoids and insulin. Mol. Cell. Endocrinol. *315*, 159–167.

Coussens, L.M., and Pollard, J.W. (2011). Leukocytes in mammary development and cancer. Cold Spring Harb. Perspect. Biol. *3*, a003285.

Dawson, C.A., Pal, B., Vaillant, F., Gandolfo, L.C., Liu, Z., Bleriot, C., Ginhoux, F., Smyth, G.K., Lindeman, G.J., Mueller, S.N., et al. (2020). Tissue-resident ductal macrophages survey the mammary epithelium and facilitate tissue remodelling. Nat. Cell Biol. *22*, 546–558.

Dobin, A., Davis, C.A., Schlesinger, F., Drenkow, J., Zaleski, C., Jha, S., Batut, P., Chaisson, M., and Gingeras, T.R. (2013). STAR: ultrafast universal RNA-seq aligner. Bioinformatics *29*, 15–21.

Doisne, J.M., Bartholin, L., Yan, K.P., Garcia, C.N., Duarte, N., Le Luduec, J.B., Vincent, D., Cyprian, F., Horvat, B., Martel, S., et al. (2009). iNKT cell development is orchestrated by different branches of TGF-β signaling. J. Exp. Med. *206*, 1365–1378.

dos Santos, C.O., Rebbeck, C., Rozhkova, E., Valentine, A., Samuels, A., Kadiri, L.R., Osten, P., Harris, E.Y., Uren, P.J., Smith, A.D., et al. (2013). Molecular hierarchy of mammary differentiation yields refined markers of mammary stem cells. Proc. Natl. Acad. Sci. USA *110*, 7123–7130.

dos Santos, C.O., Dolzhenko, E., Hodges, E., Smith, A.D., and Hannon, G.J. (2015). An epigenetic memory of pregnancy in the mouse mammary gland. Cell Rep. *11*, 1102–1109.

Dreszer, T.R., Karolchik, D., Zweig, A.S., Hinrichs, A.S., Raney, B.J., Kuhn, R.M., Meyer, L.R., Wong, M., Sloan, C.A., Rosenbloom, K.R., et al. (2013). The UCSC Genome Browser database: Extensions and updates 2011. Nucleic Acids Res. *41*, D64–D69.

Faunce, D.E., Palmer, J.L., Paskowicz, K.K., Witte, P.L., and Kovacs, E.J. (2005). CD1d-Restricted NKT Cells Contribute to the Age-Associated Decline of T Cell Immunity. J. Immunol. *175*, 3102–3109.

Feigman, M.J., Moss, M.A., Chen, C., Cyrill, S.L., Ciccone, M.F., Trousdell, M.C., Yang, S.T., Frey, W.D., Wilkinson, J.E., and Dos Santos, C.O. (2020). Pregnancy reprograms the epigenome of mammary epithelial cells and blocks the development of premalignant lesions. Nat. Commun. *11*, 2649.

Fornetti, J., Martinson, H., Borges, V., and Schedin, P. (2012). Emerging targets for the prevention of pregnancy-associated breast cancer. Cell Cycle *11*, 639–640.

Freire-de-Lima, C.G., Xiao, Y.Q., Gardai, S.J., Bratton, D.L., Schiemann, W.P., and Henson, P.M. (2006). Apoptotic cells, through transforming growth factor-β, coordinately induce anti-inflammatory and suppress pro-inflammatory eicosanoid and NO synthesis in murine macrophages. J. Biol. Chem. *281*, 38376–38384.

Gapin, L., Godfrey, D.I., and Rossjohn, J. (2013). Natural Killer T cell obsession with self-antigens. Curr. Opin. Immunol. *25*, 168–173.

Germanov, E., Veinotte, L., Cullen, R., Chamberlain, E., Butcher, E.C., and Johnston, B. (2008). Critical Role for the Chemokine Receptor CXCR6 in Homeostasis and Activation of CD1d-Restricted NKT Cells. J. Immunol. *181*, 81–91.

Godfrey, D.I., MacDonald, H.R., Kronenberg, M., Smyth, M.J., and Van Kaer, L. (2004). NKT cells: what's in a name? Nat. Rev. Immunol. *4*, 231–237.

Grant, C.E., Bailey, T.L., and Noble, W.S. (2011). FIMO: scanning for occurrences of a given motif. Bioinformatics *27*, 1017–1018.

Grushko, T.A., Dignam, J.J., Das, S., Blackwood, A.M., Perou, C.M., Ridderstråle, K.K., Anderson, K.N., Wei, M.J., Adams, A.J., Hagos, F.G., et al. (2004). MYC Is Amplified in BRCA1-Associated Breast Cancers. Clin. Cancer Res. *10*, 499–507.

Guo, Q., Betts, C., Pennock, N., Mitchell, E., and Schedin, P. (2017). Mammary Gland Involution Provides a Unique Model to Study the TGF-β Cancer Paradox. J. Clin. Med. *6*, E10.

Henry, S., Trousdell, M.C., Cyrill, S.L., Zhao, Y., Feigman, M.J., Bouhuis, J.M., Aylard, D.A., Siepel, A., and Dos Santos, C.O. (2021). Characterization of Gene Expression Signatures for the Identification of Cellular Heterogeneity in the Developing Mammary Gland. J. Mammary Gland Biol. Neoplasia *26*, 43–66.

Hitchcock, J.R., Hughes, K., Harris, O.B., and Watson, C.J. (2020). Dynamic architectural interplay between leucocytes and mammary epithelial cells. FEBS J. *287*, 250–266.

Huber, S. (2015). ERβ and ERα Differentially Regulate NKT and Vγ4+ T-cell Activation and T-regulatory Cell Response in Coxsackievirus B3 Infected Mice. J. Clin. Cell Immunol. *6*, 1–9.

Huh, S.J., Clement, K., Jee, D., Merlini, A., Choudhury, S., Maruyama, R., Yoo, R., Chytil, A., Boyle, P., Ran, F.A., et al. (2015). Age- and pregnancy-associated DNA methylation changes in mammary epithelial cells. Stem Cell Reports *4*, 297–311.

Ibrahim, A.M., Moss, M.A., Gray, Z., Rojo, M.D., Burke, C.M., Schwertfeger, K.L., Dos Santos, C.O., and Machado, H.L. (2020). Diverse Macrophage Populations Contribute to the Inflammatory Microenvironment in Premalignant Lesions During Localized Invasion. Front. Oncol. *10*, 569985.

Jehmlich, U., Alahmad, A., Biedenweg, D., and Hundt, M. (2013). The role of palmitoyl-protein thioesterases in T cell activation (P1398). J. Immunol. *190*, 204.2.

Kale, A., Sharma, A., Stolzing, A., Desprez, P.Y., Campisi, J., Desprez, P.Y., Campisi, J., and Campisi, J. (2020). Role of immune cells in the removal of deleterious senescent cells. Immun. Ageing *17*, 16.

Kim, D., Langmead, B., and Salzberg, S.L. (2015). HISAT: a fast spliced aligner with low memory requirements. Nat. Methods *12*, 357–360.

Kordon, E.C., and Coso, O.A. (2017). Postlactational Involution: Molecular Mechanisms and Relevance for Breast Cancer Development. Curr. Topics Lactation, Published: May 10, 2017. https://doi.org/10.5772/66526.

Langmead, B., Trapnell, C., Pop, M., and Salzberg, S.L. (2009). Ultrafast and memory-efficient alignment of short DNA sequences to the human genome. Genome Biol. *10*, R25.

Lee, Y.J., Starrett, G.J., Lee, S.T., Yang, R., Henzler, C.M., Jameson, S.C., and Hogquist, K.A. (2016). Lineage-Specific Effector Signatures of Invariant NKT Cells Are Shared amongst γδ T, Innate Lymphoid, and Th Cells. J. Immunol. *197*, 1460–1470.

Li, C.M.C., Shapiro, H., Tsiobikas, C., Selfors, L.M., Chen, H., Rosenbluth, J., Moore, K., Gupta, K.P., Gray, G.K., Oren, Y., et al. (2020a). Aging-Associated Alterations in Mammary Epithelia and Stroma Revealed by Single-Cell RNA Sequencing. Cell Rep. *33*, 108566.

Li, S., Gestl, S.A., and Gunther, E.J. (2020b). A multistage murine breast cancer model reveals long-lived premalignant clones refractory to parity-induced protection. Cancer Prev. Res. (Phila.) *13*, 173–184.

Liao, Y., Smyth, G.K., and Shi, W. (2014). featureCounts: an efficient general purpose program for assigning sequence reads to genomic features. Bioinformatics *30*, 923–930.

Lyons, T.R., O'Brien, J., Borges, V.F., Conklin, M.W., Keely, P.J., Eliceiri, K.W., Marusyk, A., Tan, A.C., and Schedin, P. (2011). Postpartum mammary gland involution drives progression of ductal carcinoma in situ through collagen and COX-2. Nat. Med. *17*, 1109–1115.

Macho-Fernandez, E., and Brigl, M. (2015). The extended family of CD1d-restricted NKT cells: Sifting through a mixed bag of TCRs, antigens, and functions. Front. Immunol. *6*, 362.

Majumdar, D., Tiernan, J.P., Lobo, A.J., Evans, C.A., and Corfe, B.M. (2012). Keratins in colorectal epithelial function and disease. Int. J. Exp. Pathol. *93*, 305–318.

Mantell, B.S., Stefanovic-Racic, M., Yang, X., Dedousis, N., Sipula, I.J., and O'Doherty, R.M. (2011). Mice lacking NKT cells but with a complete complement of CD8+ T-cells are not protected against the metabolic abnormalities of diet-induced obesity. PLoS ONE *6*, e19831.

Martinson, H.A., Jindal, S., Durand-Rougely, C., Borges, V.F., and Schedin, P. (2015). Wound healing-like immune program facilitates postpartum mammary gland involution and tumor progression. Int. J. Cancer *136*, 1803–1813.

McLean, C.Y., Bristor, D., Hiller, M., Clarke, S.L., Schaar, B.T., Lowe, C.B., Wenger, A.M., and Bejerano, G. (2010). GREAT improves functional interpretation of cis-regulatory regions. Nat. Biotechnol. *28*, 495–501.

McLeay, R.C., and Bailey, T.L. (2010). Motif Enrichment Analysis: a unified framework and an evaluation on ChIP data. BMC Bioinformatics *11*, 165.

Medina, D., Come, S., Santen, R., Ellis, M., Green, J., Nicholson, R., Brown, M., and Lee, A. (2004). Breast Cancer: The Protective Effect of Pregnancy. Clin. Cancer Res. *10*, 380S, 4S.

Meers, M.P., Tenenbaum, D., and Henikoff, S. (2019). Peak calling by Sparse Enrichment Analysis for CUT&RUN chromatin profiling. Epigenetics Chromatin *12*, 42.

Mincheva-Nilsson, L. (2003). Pregnancy and gamma/delta T cells: taking on the hard questions. Reprod. Biol. Endocrinol. *1*, 120.

Mombaerts, P., Iacomini, J., Johnson, R.S., Herrup, K., Tonegawa, S., and Papaioannou, V.E. (1992). RAG-1-deficient mice have no mature B and T lymphocytes. Cell *68*, 869–877.

Mycko, M.P., Ferrero, I., Wilson, A., Jiang, W., Bianchi, T., Trumpp, A., and MacDonald, H.R. (2009). Selective requirement for c-Myc at an early stage of V(α)14i NKT cell development. J. Immunol. *182*, 4641–4648.

Na, Y.R., Jung, D., Song, J., Park, J.W., Hong, J.J., and Seok, S.H. (2020). Pyruvate dehydrogenase kinase is a negative regulator of interleukin-10 production in macrophages. J. Mol. Cell Biol. *12*, 543–555.

Nichols, H.B., Schoemaker, M.J., Cai, J., Xu, J., Wright, L.B., Brook, M.N., Jones, M.E., Adami, H.O., Baglietto, L., Bertrand, K.A., et al. (2019). Breast cancer risk after recent childbirth: A pooled analysis of 15 prospective studies. Ann. Intern. Med. *170*, 22–30.

O'Brien, J., Lyons, T., Monks, J., Lucia, M.S., Wilson, R.S., Hines, L., Man, Y.G., Borges, V., and Schedin, P. (2010). Alternatively activated macrophages and collagen remodeling characterize the postpartum involuting mammary gland across species. Am. J. Pathol. *176*, 1241–1255.

Oh, S.J., Ahn, S., Jin, Y.-H., Ishifune, C., Kim, J.H., Yasutomo, K., and Chung, D.H. (2015). Notch 1 and Notch 2 synergistically regulate the differentiation and function of invariant NKT cells. J. Leukoc. Biol. *98*, 781–789.

Pal, B., Chen, Y., Vaillant, F., Jamieson, P., Gordon, L., Rios, A.C., Wilcox, S., Fu, N., Liu, K.H., Jackling, F.C., et al. (2017). Construction of developmental lineage relationships in the mouse mammary gland by single-cell RNA profiling. Nat. Commun. *8*, 1627.

Pal, B., Chen, Y., Milevskiy, M.J.G., Vaillant, F., Prokopuk, L., Dawson, C.A., Capaldo, B.D., Song, X., Jackling, F., Timpson, P., et al. (2021). Single cell transcriptome atlas of mouse mammary epithelial cells across development. Breast Cancer Res. *23*, 69.

Plaks, V., Boldajipour, B., Linnemann, J.R., Nguyen, N.H., Kersten, K., Wolf, Y., Casbon, A.J., Kong, N., van den Bijgaart, R.J.E., Sheppard, D., et al. (2015). Adaptive Immune Regulation of Mammary Postnatal Organogenesis. Dev. Cell *34*, 493–504.

Quinlan, A.R., and Hall, I.M. (2010). BEDTools: a flexible suite of utilities for comparing genomic features. Bioinformatics *26*, 841–842.

R Core Team (2019). R: A Language and Environment for Statistical Computing (R Foundation for Statistical Computing).

Rahat, M.A., Coffelt, S.B., Granot, Z., Muthana, M., and Amedei, A. (2016). Macrophages and Neutrophils: Regulation of the Inflammatory Microenvironment in Autoimmunity and Cancer. Mediators Inflamm. *2016*, 5894347.

Ricciardelli, C., Lokman, N.A., Pyragius, C.E., Ween, M.P., Macpherson, A.M., Ruszkiewicz, A., Hoffmann, P., and Oehler, M.K. (2017). Keratin 5 overexpression is associated with serous ovarian cancer recurrence and chemotherapy resistance. Oncotarget *8*, 17819–17832.

Rizvi, Z.A., Puri, N., and Saxena, R.K. (2015). Lipid antigen presentation through CD1d pathway in mouse lung epithelial cells, macrophages and dendritic cells and its suppression by poly-dispersed single-walled carbon nanotubes. Toxicol. In Vitro *29*, 1275–1282.

Saeki, K., Chang, G., Kanaya, N., Wu, X., Wang, J., Bernal, L., Ha, D., Neuhausen, S.L., and Chen, S. (2021). Mammary cell gene expression atlas links epithelial cell remodeling events to breast carcinogenesis. Commun. Biol *4*, 660.

Savage, A.K., Constantinides, M.G., Han, J., Picard, D., Martin, E., Li, B., Lantz, O., and Bendelac, A. (2008). The transcription factor PLZF directs the effector program of the NKT cell lineage. Immunity *29*, 391–403.

Schwertfeger, K.L., Richert, M.M., and Anderson, S.M. (2001). Mammary gland involution is delayed by activated Akt in transgenic mice. Mol. Endocrinol. *15*, 867–881.

Seiler, M.P., Mathew, R., Liszewski, M.K., Spooner, C.J., Barr, K., Meng, F., Singh, H., and Bendelac, A. (2012). Elevated and sustained expression of the transcription factors Egr1 and Egr2 controls NKT lineage differentiation in response to TCR signaling. Nat. Immunol. *13*, 264–271.

Seshan, V.E., and Olshen, A.B. (2014). DNAcopy: A Package for Analyzing DNA Copy Data (Bioconductor Vignette).

Stewart, T.A., Hughes, K., Hume, D.A., and Davis, F.M. (2019). Developmental Stage-Specific Distribution of Macrophages in Mouse Mammary Gland. Front. Cell Dev. Biol. *7*, 250.

Stuart, T., Butler, A., Hoffman, P., Hafemeister, C., Papalexi, E., Mauck, W.M., 3rd, Hao, Y., Stoeckius, M., Smibert, P., and Satija, R. (2019). Comprehensive Integration of Single-Cell Data. Cell *177*, 1888–1902.

Subramanian, A., Tamayo, P., Mootha, V.K., Mukherjee, S., Ebert, B.L., Gillette, M.A., Paulovich, A., Pomeroy, S.L., Golub, T.R., Lander, E.S., et al. (2005). Gene set enrichment analysis: A knowledge-based approach for interpreting genome-wide expression profiles. Proc. Natl. Acad. Sci. USA *102*, 15545–15550.

Sulahian, R., Chen, J., Arany, Z., Jadhav, U., Peng, S., Rustgi, A.K., Bass, A.J., Srivastava, A., Hornick, J.L., and Shivdasani, R.A. (2015). SOX15 Governs Transcription in Human Stratified Epithelia and a Subset of Esophageal Adenocarcinomas. Cell Mol. Gastroenterol. Hepatol. *1*, 598–609.

Terry, M.B., Liao, Y., Kast, K., Antoniou, A.C., McDonald, J.A., Mooij, T.M., Engel, C., Nogues, C., Buecher, B., Mari, V., et al. (2018). The Influence of Number and Timing of Pregnancies on Breast Cancer Risk for Women With BRCA1 or BRCA2 Mutations. JNCI Cancer Spectr. *2*, pky078.

Thibeault, S.L., Rees, L., Pazmany, L., and Birchall, M.A. (2009). At the crossroads: mucosal immunology of the larynx. Mucosal Immunol. *2*, 122–128.

Townsend, M.J., Weinmann, A.S., Matsuda, J.L., Salomon, R., Farnham, P.J., Biron, C.A., Gapin, L., and Glimcher, L.H. (2004). T-bet regulates the terminal maturation and homeostasis of NK and Valpha14i NKT cells. Immunity *20*, 477–494.

Wang, Y., Chaffee, T.S., LaRue, R.S., Huggins, D.N., Witschen, P.M., Ibrahim, A.M., Nelson, A.C., Machado, H.L., and Schwertfeger, K.L. (2020). Tissue-resident macrophages promote extracellular matrix homeostasis in the mammary gland stroma of nulliparous mice. eLife *9*, e57438.

Wu, Y., Kyle-Cezar, F., Woolf, R.T., Naceur-Lombardelli, C., Owen, J., Biswas, D., Lorenc, A., Vantourout, P., Gazinska, P., Grigoriadis, A., et al. (2019). An innate-like Vd1+ gd T cell compartment in the human breast is associated with remission in triple-negative breast cancer. Sci. Transl. Med. *11*, eaax9364.

Yu, J., Mitsui, T., Wei, M., Mao, H., Butchar, J.P., Shah, M.V., Zhang, J., Mishra, A., Alvarez-Breckenridge, C., Liu, X., et al. (2011). NKp46 identifies an NKT cell subset susceptible to leukemic transformation in mouse and human. J. Clin. Invest. *121*, 1456–1470.

Zhang, Y., Liu, T., Meyer, C.A., Eeckhoute, J., Johnson, D.S., Bernstein, B.E., Nusbaum, C., Myers, R.M., Brown, M., Li, W., and Liu, X.S. (2008). Model-based analysis of ChIP-Seq (MACS). Genome Biol. *9*, R137.

Zhang, Y., Springfield, R., Chen, S., Li, X., Feng, X., Moshirian, R., Yang, R., and Yuan, W. (2019). α-GalCer and iNKT cell-based cancer immunotherapy: Realizing the therapeutic potentials. Front. Immunol. *10*, 1126.

Zheng, G.X., Terry, J.M., Belgrader, P., Ryvkin, P., Bent, Z.W., Wilson, R., Ziraldo, S.B., Wheeler, T.D., McDermott, G.P., Zhu, J., et al. (2017). Massively parallel digital transcriptional profiling of single cells. Nat. Commun. *8*, 14049.

## STAR★METHODS

### KEY RESOURCES TABLE

| Reagent or resource | Source | Identifier |
|---|---|---|
| Antibodies | | |
| Biotinylated anti-CD45 | Thermo Fisher Scientific | Cat# 13-0451-85; RRID:AB_466447 |
| Biotinylated anti-CD31 | Thermo Fisher Scientific | Cat# 13-0311-85; RRID:AB_466421 |
| Biotinylated anti-Ter119 | Thermo Fisher Scientific | Cat# 13-5921-85; RRID:AB_466798 |
| Biotinylated anti-CD34 | Thermo Fisher Scientific | Cat# 13-0341-82; RRID:AB_466425 |
| eFluor 450 conjugated anti-CD24 | Thermo Fisher Scientific | Cat# 48-0242-82; RRID:AB_1311169 |
| PE-Cy7 conjugated anti-CD29 | BioLegend | Cat# 102222; RRID:AB_528790 |
| 7-AAD viability staining solution | BioLegend | Cat# 420404; RRID:SCR_020993 |
| PerCP-Cy5.5 conjugated anti-CD1d | BioLegend | Cat# 123514; RRID:AB_2073523 |
| PE conjugated anti-CD1d | BioLegend | Cat# 140805; RRID:AB_10643277 |
| APC conjugated anti-CD45 | BioLegend | Cat# 103112; RRID:AB_312977 |
| FITC conjugated anti-CD3 | BioLegend | Cat# 100204; RRID:AB_312661 |
| Alexa Fluor 700 conjugated. anti-NK1.1 | BioLegend | Cat# 108730; RRID:AB_2291262 |
| APC/Cy7 conjugated anti-CD8 | BioLegend | Cat# 100714; RRID:AB_312753 |
| PE conjugated anti-TCR g/d | BioLegend | Cat# 118108; RRID:AB_313832 |
| APC conjugated anti-TCR b | BioLegend | Cat# 109212; RRID:AB_313435 |
| APC conjugated anti-H-2Kb | BioLegend | Cat# 116517; RRID:AB_10568693 |
| Pacific Blue conjugated anti-I-Ab | BioLegend | Cat# 116421; RRID:AB_10613291 |
| Brilliant Violet 421 conjugated anti-CD206 | BioLegend | Cat# 141717; RRID:AB_2562232 |
| Alexa Fluor 700 conjugated anti-Ly6G | BioLegend | Cat# 127621; RRID:AB_10640452 |
| PE conjugated anti-IFNg | BioLegend | Cat# 505808; RRID:AB_315402 |
| Pacific Blue conjugated anti-T-bet | BioLegend | Cat# 644807; RRID:AB_1595586 |
| eFluor 450 conjugated mouse IgG | Thermo Fisher Scientific | Cat# 48-4015-82; RRID:AB_2574060 |
| FITC conjugated rat IgG | Thermo Fisher Scientific | Cat# 11-4811-85; RRID:AB_465229 |
| PE-Cy7 conjugated mouse IgG | BioLegend | Cat# 405315; RRID:AB_10662421 |
| biotinylated anti-CD1d | BioLegend | Cat# 123505; RRID:AB_1236543 |
| anti-p300 antibody | Santa Cruz Biotechnology | Cat# SC-585; RRID:AB_2231120 |
| anti-Vinculin antibody | Abcam | Cat# ab129002; RRID:AB_11144129 |
| anti-p53 antibody | Leica Biosystems | Cat# P53-CM5P; RRID:AB_2744683 |
| goat anti-rabbit IgG HRP | Abcam | Cat# ab6721; RRID:AB_955447 |
| goat anti-mouse IgG HRP | Abcam | Cat# ab97051; RRID:AB_10679369 |
| anti-Cytokeratin 5 (KRT5) | BioLegend | Cat# 905501; RRID:AB_2565050 |
| anti-Cytokeratin 7/17 (KRT7/17) | Santa Cruz Biotechnology | Cat# sc-8421; RRID:AB_627856 |
| anti-EGFR | Santa Cruz Biotechnology | Cat# sc-373746; RRID:AB_10920395 |
| anti-AR | Santa Cruz Biotechnology | Cat# sc-7305; RRID:AB_626671 |
| anti-Ki67 | Spring Bioscience | Cat# M3062; RRID:AB_11219741 |
| Alexa Fluor 647 conjugated anti-Cytokeratin 5 (KRT5) | Abcam | Cat# AB193895; RRID:AB_2728796 |
| unconjugated rabbit anti-BRCA1 | Bioss | Cat# bs-0803R; RRID:AB_10858843 |
| Alexa Fluor 568 conjugated goat anti-rabbit IgG | Thermo Fisher Scientific | Cat# A-11036; RRID:AB_10563566 |
| Alexa Fluor 488 conjugated anti-GFP | BioLegend | Cat# 338007; RRID:AB_2563287 |
| Alexa Fluor 405 conjugated anti-Cytokeratin 8 (KRT8) | Abcam | Cat# ab210139; RRID:AB_2890924 |
| Chemicals, peptides, and recombinant proteins | | |
| DNase I | Sigma | Cat #D4263 |
| Collagenase A, type IV solution | Sigma | Cat #C5138-1G |
| ITS (Insulin/Transferrin/Sodium selenite) | GIBCO | Cat #41400-045 |

(*Continued on next page*)

*Continued*

| Reagent or resource | Source | Identifier |
|---|---|---|
| FGF-2 | PeproTech | Cat #450-33 |
| Progesterone | Sigma | Cat #P8783 |
| 17-β-Estradiol | Sigma | Cat #E2758 |
| Prolactin | Sigma | Cat #L4021 |
| Doxycycline | Clontech | Cat# 631311 |
| Collagenase/Hyaluronidase 10x solution | Stem Cell Technology | Cat #07912 |
| Growth factor reduced matrigel solution | Corning | Cat #356230 |
| Trilogy | Cell Marque | Cat# 920P-10 |
| ProLong Glass Antifade Mountant | Invitrogen | Cat# P36980 |
| 17b-Estradiol (0.5 mg/pellet) + Progesterone (10 mg/pellet) | Innovative Research of America | Cat# HH-112 |
| Luminata Crescendo Western HRP substrate | Millipore | Cat# WBLUR0100 |
| TrypLE Express | Thermo Fisher Scientific | Cat #12604-013 |
| Dispase | Stem Cell Technology | Cat #07913 |
| **Critical commercial assays** | | |
| Ovation ultralow DR multiplex system | Nugen Technologies | Cat #0331-32 |
| Nextera DNA sample Preparation kit | Illumina | Cat #FC-121-1031 |
| Ovation RNA-seq system (V2) | Nugen Technologies | Cat #7102-32 |
| DNeasy Blood & Tissue Kit | QIAgen | Cat# 69504 |
| SuperScript III kit | Thermo Fisher Scientific | Cat #18080-051 |
| **Deposited data** | | |
| ATAC-seq data | This paper | PRJNA708263 |
| RNA-seq data | This paper | PRJNA708263 |
| WGS data | This paper | PRJNA708263 |
| scRNA-seq data, Figure 1 (pre-pregnancy) | Henry et al., 2021 | PRJNA677888 |
| RNA-seq (pre- and post-pregnancy) | dos Santos et al., 2013 | PRJNA192515 |
| H3K27ac ChIP-seq (pre- and post-pregnancy) | Feigman et al., 2020 | PRJNA544746 |
| H3K27ac Cut&Run, Figure S7F | Ciccone et al., 2020 | PRJNA656955 |
| **Experimental models: Organisms/strains** | | |
| Mouse: BALB/c | Charles River | https://www.criver.com/ |
| Mouse: NOD/SCID | Jackson Laboratory | https://www.jax.org/ |
| Mouse: CAGMYC | Feigman et al., 2020 | N/A |
| Mouse: Cxcr6-GFP KI | Jackson Laboratory | https://www.jax.org/strain/005693 |
| Mouse: RAG1 KO | Jackson Laboratory | https://www.jax.org/ |
| Mouse: UTX KO | Beyaz et al., 2017 | N/A |
| Mouse: CD1d KO | Jackson Laboratory | https://www.jax.org/ |
| Mouse: $Krt5^{CRE\text{-}ERT2}Brca1^{fl/fl}p53^{het}$ | This paper | N/A |
| **Oligonucleotides** | | |
| Cd1d qPCR FWD: 5′ TCC GGT GAC TCT TCC TTA CA 3′ | This paper | N/A |
| Cd1d qPCR REV: 5′ CTG GCT GCT CTT CAC TTC TT 3′ | This paper | N/A |
| b-actin qPCR FWD: 5′ TGT TAC CAA CTG GGA CGA CA 3′ | This paper | N/A |
| b-actin qPCR REV: 5′ GGG GTG TTG AAG GTC TCA AA 3′ | This paper | N/A |
| **Software and algorithms** | | |
| Fiji | ImageJ | Version 2.1.0 |
| Zen lite software, Blue edition | ZEN Digital Imaging for Light Microscopy | Version 2.0.0.0 |
| FlowJo | BD Biosciences | Version 10.0 |
| Prism | Graphpad | Version 9.0 |

(*Continued on next page*)

*Continued*

| Reagent or resource | Source | Identifier |
|---|---|---|
| CellRanger | Zheng et al., 2017 | Version 3.1.0 |
| Seurat | Stuart et al., 2019 | Version 3.1.1 |
| GSEA | Broad Institute | Version 3.0 |
| BD FACSDiva Software | BD Biosciences | Version 6.0 |
| STAR | Dobin et al., 2013 | Version 2.4.0 |
| Bowtie2 | Langmead et al., 2009 | Version 2.4.2 |
| MACS2 | Zhang et al., 2008 | Version 2.2.5 |
| GREAT | McLean et al., 2010 | Version 4.0.4 |
| HOMER | Benner et al., 2017 | Version 4.11 |
| Bedtools | Quinlan and Hall, 2010 | Version 2.28.0 |
| UCSC Genome Browser | Dreszer et al., 2013 | N/A |
| Hisat2 | Kim et al., 2015 | version 2.1.0 |
| DNAcopy | Seshan and Olshen, 2014 | version 1.50.1 |
| DESeq | Anders and Huber, 2010 | N/A |

## RESOURCE AVAILABILITY

### Lead contact

Further information for resources and reagents should be directed to and will be fulfilled by the lead contact, Camila dos Santos (dossanto@cshl.edu).

### Materials availability

All unique/stable reagents generated in this study are available from the lead contact upon request.

### Data and code availability

scRNA-seq, RNA-seq, ATAC-seq datasets were deposited into BioProject database under number PRJNA708263 [https://www.ncbi.nlm.nih.gov/bioproject/PRJNA708263], and are publicly available as of the date of publication. All accession numbers are listed in the key resources table. Results shown in Figure 1 (pre-pregnancy scRNA-seq) were previously deposited into BioProject database number PRJNA677888 [https://www.ncbi.nlm.nih.gov/bioproject/?term=PRJNA677888]. Results shown in Figure S2C (pre- and post-pregnancy RNA-seq), Figure 3C (pre- and post-pregnancy H3K27ac ChIP-seq) were previously deposited in the BioProject database under numbers PRJNA192515 [https://www.ncbi.nlm.nih.gov/bioproject/?term=PRJNA192515] and PRJNA544746 [https://www.ncbi.nlm.nih.gov/bioproject/PRJNA544746]. Results shown on Figure S7F (H3K27ac Cut&Run of organoid cultures) were previously deposited in the BioProject database under number PRJNA656955 [https://www.ncbi.nlm.nih.gov/sra/?term=PRJNA656955]. This manuscript does not report original code. Any additional information required to reanalyze the data reported in this paper is available from the lead contact upon request.

## EXPERIMENTAL MODEL AND SUBJECT DETAILS

### Animal studies

All experiments were performed in agreement with approved CSHL Institutional Animal Care and Use Committee (IACUC). All animals were housed at a 12 hour light/12 hour dark cycle, with a controlled temperature of 72°F and 40%–60% of humidity. Balb/C female mice were purchased from The Jackson Laboratory and Charles River. $RAG1^{KO}$ mice (B6.129S7-$Rag1^{tm1Mom}$/J, IMSR Cat# JAX:002216, RRID:IMSR_JAX:002216) were purchased from The Jackson Laboratory. VavCre $UTX^{KO}$ were generated as previously described (Beyaz et al., 2017). CXCR6-KO-EGFP-KI mice (B6.129P2-$Cxcr6^{tm1Litt}$/J, IMSR Cat# JAX:005693, RRID:IMSR_JAX:005693) were purchased from The Jackson Laboratory. CAGMYC transgenic mouse strain was generated as previously described (Feigman et al., 2020). $CD1d^{KO}$ CAGMYC transgenic mouse stain was generated by crossing $CD1d^{KO}$ (C.129S2-$Cd1^{tm1Gru}$/J, IMSR Cat# JAX:003814, RRID:IMSR_JAX:003814) mice with CAGMYC mice. $Krt5^{CRE\text{-}ERT2}Brca1^{fl/fl}p53^{het}$ ($Brca1^{KO}$) transgenic mouse strain was generated by crossing $Blg^{CRE}Brca1^{fl/fl}p53^{het}$ transgenic mouse strain ($Trp53^{tm1Brd}Brca1^{tmAash}$Tg(B-cre)74Acl/J, IMSR Cat# JAX:012620, RRID:IMSR_JAX:012620) with $Krt5^{CRE\text{-}ERT2}$ transgenic mouse strain (B6N.129S6(Cg)-$Krt5^{tm1.1(cre/ERT2)Blh}$/J, IMSR Cat# JAX:029155, RRID:IMSR_JAX:029155). Female mice ranging from 3 weeks old to 30 weeks old were utilized in the described research.

## METHOD DETAILS

### Antibodies

All antibodies were purchased from companies as indicated below and used without further purification. Antibodies for lineage depletion: biotinylated anti-CD45 (Thermo Fisher Scientific Cat# 13-0451-85, RRID:AB_466447), biotinylated anti-CD31 (Thermo Fisher Scientific Cat# 13-0311-85, RRID:AB_466421), biotinylated anti-Ter119 (Thermo Fisher Scientific Cat# 13-5921-85, RRID:AB_466798) and biotinylated anti-CD34 (Thermo Fisher Scientific Cat# 13-0341-82, RRID:AB_466425). Antibodies for cell surface flow cytometry: eFluor 450 conjugated anti-CD24 (Thermo Fisher Scientific Cat# 48-0242-82, RRID:AB_1311169), PE-Cy7 conjugated anti-CD29 (BioLegend Cat# 102222, RRID:AB_528790), 7-AAD viability staining solution (BioLegend Cat# 420404, RRID:SCR_020993), PerCP-Cy5.5 conjugated anti-CD1d (BioLegend Cat# 123514, RRID:AB_2073523), PE conjugated anti-CD1d (BioLegend Cat# 140805, RRID:AB_10643277), APC conjugated anti-CD45 (BioLegend Cat# 103112, RRID:AB_312977), FITC conjugated anti-CD3 (BioLegend Cat# 100204, RRID:AB_312661), Alexa Fluor 700 conjugated. anti-NK1.1 (BioLegend Cat# 108730, RRID:AB_2291262), APC/Cy7 conjugated anti-CD8 (BioLegend Cat# 100714, RRID:AB_312753), PE conjugated anti-TCR γ/δ (BioLegend Cat# 118108, RRID:AB_313832), APC conjugated anti-TCR β (BioLegend Cat# 109212, RRID:AB_313435), APC conjugated anti-H-2Kb (BioLegend Cat# 116517, RRID:AB_10568693), Pacific Blue conjugated anti-I-Ab (BioLegend Cat# 116421, RRID:AB_10613291), Brilliant Violet 421 conjugated anti-CD206 (BioLegend Cat# 141717, RRID:AB_2562232), Alexa Fluor 700 conjugated anti-Ly6G (BioLegend Cat# 127621, RRID:AB_10640452). Antibodies for intracellular flow cytometry: PE conjugated anti-IFNγ (BioLegend Cat# 505808, RRID:AB_315402), Pacific Blue conjugated anti-T-bet (BioLegend Cat# 644807, RRID:AB_1595586). Antibodies for negative controls: eFluor 450 conjugated mouse IgG (Thermo Fisher Scientific Cat# 48-4015-82, RRID:AB_2574060), FITC conjugated rat IgG (Thermo Fisher Scientific Cat# 11-4811-85, RRID:AB_465229), and PE-Cy7 conjugated mouse IgG (BioLegend Cat# 405315, RRID:AB_10662421). Antibody for MaSC enrichment: biotinylated anti-CD1d (BioLegend Cat# 123505, RRID:AB_1236543). Antibodies for Western Blot: anti-p300 antibody (Santa Cruz Biotechnology Cat# SC-585, RRID:AB_2231120), anti-Vinculin antibody (Abcam Cat# ab129002, RRID:AB_11144129), anti-p53 antibody (Leica Biosystems Cat# P53-CM5P, RRID:AB_2744683), goat anti-rabbit IgG HRP (Abcam Cat# ab6721, RRID:AB_955447) and goat anti-mouse IgG HRP (Abcam Cat# ab97051, RRID:AB_10679369). Antibodies for Immunohistochemistry (IHC) staining: anti-Cytokeratin 5 (KRT5) (BioLegend Cat# 905501, RRID:AB_2565050), anti-Cytokeratin 7/17 (KRT7/17) (Santa Cruz Biotechnology Cat# sc-8421, RRID:AB_627856), anti-EGFR (Santa Cruz Biotechnology Cat# sc-373746, RRID:AB_10920395), anti-AR (Santa Cruz Biotechnology Cat# sc-7305, RRID:AB_626671), and anti-Ki67 (Spring Bioscience Cat# M3062, RRID:AB_11219741). Antibodies for Immunofluorescence (IF) staining: Alexa Fluor 647 conjugated anti-Cytokeratin 5 (KRT5) (Abcam Cat# AB193895, RRID:AB_2728796), unconjugated rabbit anti-BRCA1 (Bioss Cat# bs-0803R, RRID:AB_10858843), Alexa Fluor 568 conjugated goat anti-rabbit IgG (Thermo Fisher Scientific Cat# A-11036, RRID:AB_10563566), Alexa Fluor 488 conjugated anti-GFP (BioLegend Cat# 338007, RRID:AB_2563287), Alexa Fluor 405 conjugated anti-Cytokeratin 8 (KRT8) (Abcam Cat# ab210139, RRID:AB_2890924).

### Mammary gland isolation

Female mice classified as Pre-pregnancy (nulliparous, never pregnant), Post-pregnancy (parous, 1 gestation cycle, 21 days of lactation and 40 days of involution post offspring weaning), were housed together for 1-2 weeks to allow for estrous cycle synchronization prior to mammary gland isolation. For the experiments utilizing exposure to pregnancy hormones (EPH), never pregnant female mice (~8 weeks old) were implanted with 21 days-slow-release estrogen and progesterone pellets (17β-Estradiol (0.5 mg/pellet) + Progesterone (10 mg/pellet) – Innovative Research of America Cat# HH-112) prior to mammary gland isolation (at D12 post pellet implantation). Females classified as involution D15 had 1 gestation cycle, 21 days of lactation and 15 days of involution post offspring weaning. In all cases, mammary gland isolation was performed as previously described (dos Santos et al., 2013). In short, mammary glands (one to four pairs per mouse) were harvested, minced, and incubated for 2 hours with 1x Collagenase/Hyaluronidase (10x solution, Stem Cell Technology Cat# 07912) in RPMI 1640 GlutaMAX supplemented with 5% FBS. Digested mammary gland fragments were washed with cold HBSS (Thermo Fisher Scientific Cat# 14175103) supplemented with 5% FBS, followed by incubation with TrypLE Express (Thermo Fisher Scientific Cat# 12604-013) and an additional HBSS wash. Cells were incubated with 2 mL of Dispase (Stem Cell Technology Cat# 07913) supplemented with 40 μL DNase I (Sigma Cat# D4263) for 2 minutes and then filtered through a 100 μm Cell Strainer (BD Falcon Cat# c352360). The single cell suspension was incubated with lineage depletion antibodies and loaded onto a MACS magnetic column (Miltenyi Biotec Cat# 130-042-401). Lineage negative, flow-through cells (epithelial cells) were utilized for flow cytometry, and transcriptomic analysis. Lineage positive cells (immune cells) were eluted from column with 3ml of MACS buffer and utilized for flow cytometry, transcriptomic and epigenomic analysis. For cell analysis, Dual Fortessa II cell analyzer (BD Biosciences) was used. Data analysis was performed using BD FACSDiva Software (RRID:SCR_001456) or FlowJo (FlowJo, RRID:SCR_008520). Statistically significant differences were considered with Student's t test *p-value* lower than 0.05 ($p < 0.05$).

### Flow cytometry analysis

Mammary resident cells (epithelial and non-epithelial) were harvested from both top and bottom mammary glands, and analyzed according to the bellow indicated strategy. For all flow cytometry analysis an average of 300,000 cells live cells (7-AAD negative) were recorded. Gating strategy for all flow cytometry analysis is available in Methods S1.

### Mammary organoid culture

Mammary tissue dissected was minced and digested for ~40 minutes in Collagenase A, type IV solution (Sigma, Cat# C5138-1G), following a series of centrifugations to enrich for mammary organoids. Freshly isolated mammary organoids were cultured with Essential medium (Advanced DMEM/F12, supplemented with ITS (Insulin/Transferrin/Sodium selenite, GIBCO Cat# 41400-045, and FGF-2 (PeproTech, Cat# 450-33)) prior to analysis. For experiments shown in Figures S5E and S5F, organoid cultures were derived from normal mammary tissue from pre- or post-pregnancy Balb/C female mice (RRID:IMSR_CRL:028), cultured in the presence of FGF-2 for 6 days, following FGF-2 withdrawal for 24 hr and then incubated with Complete medium (AdDF+++, supplemented with ITS (Final Concentration:1x, Insulin/Transferrin/Sodium Selenite, GIBCO Cat# 41400-045), 17-β-Estradiol (Final concentration: 40ng/mL, Sigma Cat# E2758), Progesterone (Final concentration: 120ng/mL, Sigma Cat# P8783), Prolactin (Final concentration: 120ng/mL, Sigma Cat# L4021), as previously described (Ciccone et al., 2020). For experiments shown in Figure S6C, organoids cultures were derived from pre- or post-pregnancy CAGMYC MECs, following treatment with doxycycline (DOX, 0.1mg/mL, Clontech Cat# 631311) for 2 days (DD2). For experiments shown in Figure S8E, organoid cultures were derived from NOD/SCID female mice, transplanted with either pre- or post-pregnancy CAGMYC MECs, following treatment with doxycycline (DOX, 0.1mg/mL) for 2 days (DD2).

### RT-qPCR

Lineage depleted MECs or organoid cultures were washed with 0.5mL 1x PBS, following RNA extraction with Trizol (0.5mL, Thermo Fisher Scientific, Cat# 15596018). Reverse transcription was carried out using SuperScript III kit (Thermo Fisher Scientific, Cat# 18080-051). RT-qPCR was performed using a Quantstudio 6 with SYBR Green Master mix (Applied Biosystems, Cat# 4368577). Relative mRNA expression of target gene was calculated via the ΔΔCt method and normalized to *β-actin* mRNA levels.

Cd1d qPCR primers: FWD: 5′ TCC GGT GAC TCT TCC TTA CA 3′ and REV: 5′ CTG GCT GCT CTT CAC TTC TT 3′.
β-actin qPCR primers: FWD: 5′ TGT TAC CAA CTG GGA CGA CA 3′ and, REV: 5′ GGG GTG TTG AAG GTC TCA AA 3′.

### Mammary fat pad transplantation

MaSCs-enrichment was performed as previously described (dos Santos et al., 2013). In short, lineage depleted MECs were incubated with biotinylated anti-CD1d antibody, to allow for MaSC enrichment. CD1d-enriched MEC fractions were resuspended with 50% growth factor reduced matrigel solution (Corning, Cat# 356230) and injected into the cleared fat-pad of the inguinal mammary gland (anterior part of the gland). For experiments presented on Figure S5B CD1d-enriched MECs fractions (~100K) were injected into the mammary fatpad of 12 weeks old CAG-only female mice, followed by DOX-treatment and histology analysis. For experiments presented on Figure S8 CD1d-enriched MECs fractions (~100K) were injected into the mammary fatpad of 12 weeks old NOD/SCID (RRID:IMSR_JAX:001303) female mice, followed by DOX-treatment and histology analysis. For experiments presented on Figure 5 and Figure S9, pre- or post-pregnancy CAGMYC-CD1d$^{WT}$ MECs (~10K) or CAGMYC-CD1d$^{KO}$ MECs (~10K) were injected into the mammary fatpad of 8-10 weeks old CD1d WT female mice, and allowed 3-days of tissue engraftment prior to DOX-treatment for 5 days.

### Histological analysis

For histological analysis, the left inguinal mammary gland was harvested and fixed in 4% Paraformaldehyde overnight prior to paraffin embedding. For conventional histological analysis, mammary gland tissue slides were stained with Hematoxylin and Eosin (H&E). For ductal quantification, mammary gland H&E histological images were uploaded into Fiji (Fiji, RRID:SCR_002285), and ducts present in the posterior part of the gland were manually counted. Immunohistochemistry staining (IHC) was performed on a Roche Discovery Ultra Automated IHC/ISH stainer. For Masson's trichrome staining, Leica Multistainer Stainer/Coverslipper Combo (ST5020-CV5030) was used to stain slides according to standard reagents and protocols. Images were acquired using Aperio ePathology (Leica Biosystems) slide scanner in 40X lenses.

### Immunofluorescence analysis

Paraffin-embedded mammary gland sections were deparaffinized in Xylene (Sigma Cat# 534056) and rehydrated, followed by antigen retrieval in Trilogy (Cell Marque Cat# 920P-10). Tissue was washed in 1x PBS (phosphate-buffered saline) for 1 min then blocked with blocking solution (10mM Tris-HCl pH 7.4, 100mM $MgCl_2$, 0.5% Tween 20, 10% FBS, 5% goat serum) for 4 hours in a humidified chamber. Sections were stained with the appropriate conjugated primary antibodies in blocking solution for 16 hours at 4°C. After subsequent washings with 1x PBS and blocking solution, tissues were incubated with DAPI (Sigma Cat# 10236276001) for 10 minutes to stain nuclei, and slides were mounted in ProLong Glass Antifade Mountant (Invitrogen Cat# P36980). Cell visualization and image collection was performed on a Zeiss LSM780 confocal laser-scanning microscope utilizing Zen lite software, Blue edition (ZEN Digital Imaging for Light Microscopy, RRID:SCR_013672) version 2.0.0.0.

### Doxycycline treatment

Doxycycline was purchased from Takara Bio USA, Inc. (Cat# 631311) and sucrose was purchased from Sigma (Cat# S7903). DOX drinking solution (1 mg/mL) was prepared using sterile 1% sucrose water.

### Tamoxifen treatment

Tamoxifen USP grade was purchased from Sigma-Aldrich (Cat# 1643306) and sunflower seed oil (European Pharmacopoeia grade) was purchased from Sigma-Aldrich (Cat# 88921). To prepare the working solution, the Tamoxifen powder was weighed and dissolved in ethanol by vortexing. Heat sterilized sunflower oil was added at a ratio of 19:1 oil:ethanol mixture to a final concentration of 5mg/100ul (one dose), heated to 55°C and shaken vigorously to homogenize the mixture. $Krt5^{CRE\text{-}ERT2}Brca1^{fl/fl}p53^{het}$ transgenic female mice received a total of three intraperitoneal doses of Tamoxifen warmed to 37°C on alternate days.

### Monitoring tumor growth

3 week old $Krt5^{CRE\text{-}ERT2}Brca1^{fl/fl}p53^{-/+}$ female mice were treated with TAM. Half of TAM-treated female mice were housed together (pre-pregnancy/nulliparous group), and the other half were paired with a male (1 female and 1 male per breeding cage). Breeding TAM-treated females were allowed to give birth, nurse the offspring (21 days), and were considered post-pregnant (parous) after 40 days from offspring weaning. Both pre- and post-pregnancy mice were monitored for signs of tumor growth, and added to the Kaplan-Meier curve as soon as there was a palpable tumor. Mice with a tumor burden exceeding the limit of the animal's well-being (> 2 cm), or mice showing signs of distress independently of tumor development were euthanized. At experimental end point, mammary tissue or mammary tumors were harvested for histological and flow cytometry analysis. Statistical analysis was performed with Logrank (Mantel-Cox) test.

### Western blot

DOX-treated and control organoid cultures were homogenized in 1x Laemmli sample buffer (Bio-Rad, Cat# 1610747). Samples were loaded into homemade 10% SDS-PAGE gel and transferred overnight to PVDF membrane (Bio-Rad, Cat# 162-0177) using wet-transfer apparatus. Membranes were blocked with 1% BSA solution and incubated overnight with a diluted solution of primary antibody, followed by incubation with HRP-conjugated antibody for 40 minutes. HRP signal was developed with Luminata Crescendo Western HRP substrate (Millipore, Cat# WBLUR0100) in autoradiography film (Lab Scientific, Cat# XARALF2025). Developed films were scanned on Epson Perfection 2450 photo scanner.

### scRNA-seq data analysis

Single cell RNA-seq data (pre-pregnancy mammary glands = 3,439 cells from n = 2 biological replicates; post-pregnancy mammary glands = 4,412 cells from n = 2 biological replicates) were aligned to mm10 using CellRanger v.3.1.0 (10x Genomics) (Cell Ranger, RRID:SCR_017344) (Zheng et al., 2017), and downstream processing was performed using Seurat v3.1.1 (SEURAT, RRID:SCR_007322) (Stuart et al., 2019). Cells with fewer than 250 features or higher than 10% mitochondrial gene content were removed prior to further analysis. Genes with fewer than 3 cells expressing them were removed, and the data were then log-normalized. Post-filtering analysis was performed on 3,075 cells (pre-pregnancy) and 4,029 cells (post-pregnancy). Principal component analysis was performed using the top 2,000 variable genes. This analysis was used to identify the number of significant components before clustering. Clustering was performed by calculating a shared nearest neighbor graph, using a resolution of 0.6. Subsetting into different cell types was performed using known markers for MECs, T cells, Myeloid cells, B cells and NK cells. Epithelial cells for both datasets were defined by the expression of Epcam, Krt8, Krt18, Krt5 and Krt14(cluster average expression > 2). Non-epithelial were cells considered having low expression of Epcam, Krt8, Krt18, Krt5 and Krt14. Epithelial lineage identification and T cell lineage identification was performed utilizing a previously validated gene signature (Henry et al., 2021). Genes used to define each immune cluster (differentially expressed genes, DEGs) were determined using known cell type markers and using the FindAllMarkers function, which uses a Wilcoxon Rank Sum test to identify differentially expressed genes between all clusters in the dataset. Cell cycle scoring was performed with the CellCycleScoring function, using the default gene lists provided by Seurat. Cell dendrograms were generated using the BuildClusterTree function in Seurat, using default arguments. Diffusion mapping was performed using the DiffusionMap function from the "destiny" R package (Angerer et al., 2016). Gene Set Enrichment Analysis (GSEA, RRID:SCR_003199) (Subramanian et al., 2005) was used for global analyses of differentially expressed genes.

### RNA-seq library preparation and analysis

FACS-isolated pre- and post-pregnancy NKTs were collected and homogenized in TRIzol LS (Thermo Fisher Scientific, Cat# 10296010) for RNA extraction. Double stranded cDNA synthesis and Illumina libraries were prepared utilizing the Ovation RNA-seq system (V2) (Nugen Technologies, Cat# 7102-32). RNA-seq libraries were prepared utilizing the Ovation ultralow DR multiplex system (Nugen Technologies, Cat# 0331-32). Each library (n = 2 biological replicates per experimental condition) was barcoded with Illumina TrueSeq adaptors to allow sample multiplexing, followed by sequencing on an Illumina NextSeq500, 76bp single-end run. Analyses were performed with command-line interfaced tools such as FastQC (FastQC, RRID:SCR_014583) (Andrews, 2015) for quality control and Trimmomatic (Trimmomatic, RRID:SCR_011848) (Bolger et al., 2014) for sequence trimming. We used STAR (STAR, RRID:SCR_004463) for mapping reads (Dobin et al., 2013), FeatureCounts (featureCounts, RRID:SCR_012919) for assigning reads to genomic features (Liao et al., 2014) and DESeq (DESeq, RRID:SCR_000154) to assess changes in expression levels simultaneously across multiple conditions and in multi-factor experimental designs, incorporating information from multiple replicates (Anders and Huber, 2010). Genes with a statistically significant pvalue of $p < 0.05$ were considered differentially expressed. Gene Set Enrichment Analysis (GSEA) (Gene Set Enrichment Analysis, RRID:SCR_003199) was used for global analyses

of differentially expressed genes (Subramanian et al., 2005). GSEA terms with statistically significant pvalue of $p < 0.05$ were selected for data plotting and data interpretation. For experiments presented on Figure 2D, FACS-isolated, pre- and post-pregnancy $CD45^+NK1.1^+CD3^+$ NKT cells (n = 2 females per experimental group, n = 4 pairs of mammary glands per female, n = 2 biological replicates per experimental group) were utilized. For experiments presented on Figure S8D, total mammary tissue isolated from DOX-treated, NOD/SCID female mice transplanted with either pre- or post-pregnancy CAGMYC MECs (n = 2 biological replicates per group) were utilized.

### ChIP-seq library analysis

Previously published H3K27ac ChIP-seq datasets (Feigman et al., 2020) were mapped to the indexed mm9 genome using bowtie2 short-read aligner tool (Langmead et al., 2009), using default settings. MACS2 peak-calling program (MACS, RRID:SCR_013291) (Zhang et al., 2008) was used to identify enriched genomic regions in this data by comparing the pulldown ChIP data to the control (Input) data using a q-value cutoff of $1.00^{-3}$ . Identification of genes closest to these differentially called peaks was performed using Genomic Regions Enrichment of Annotations Tool (UCSC Genome Browser, RRID:SCR_005780) (McLean et al., 2010). Peak visualizations were generated using the UCSC Genome Browser (UCSC Genome Browser, RRID:SCR_005780) (Dreszer et al., 2013).

### Cut&Run library analysis

Previously published H3K27ac Cut&Run datasets (Ciccone et al., 2020), were mapped to the indexed mm9 genome using bowtie2 short-read aligner tool (Langmead et al., 2009) using default settings. Sparse Enrichment Analysis for Cut&Run (SEACR) peak-calling program (Meers et al., 2019) was used to identify enriched genomic regions with an empirical threshold of n = 0.01, returning the top n fraction of peaks based on total signal within peaks. The stringent argument was implemented, which used the summit of each curve. Identification of genes closest to these differentially called peaks was performed using Genomic Regions Enrichment of Annotations Tool (UCSC Genome Browser, RRID:SCR_005780) (McLean et al., 2010). Peak visualizations were generated using the UCSC Genome Browser (UCSC Genome Browser, RRID:SCR_005780) (Dreszer et al., 2013).

### ATAC-seq library preparation and analysis

Nuclei of FACS-isolated, pre- and post-pregnancy NKTs were isolated utilizing hypotonic lysis buffer and incubated with Tn5 enzyme from Nextera DNA sample Preparation kit (Illumina, Cat# FC-121-1031) for the preparation of ATAC libraries. Each library (n = 2 per experimental condition) was amplified and barcoded as previously described (Buenrostro et al., 2013), then pooled for sequencing on an Illumina Nextseq500, 76bp single-end run. ATACseq library reads (n = 2 per cell condition) were mapped to the indexed mm9 genome using Bowtie2 short read-aligner (Bowtie 2, RRID:SCR_016368) (Langmead et al., 2009) and replicate alignment files were merged. MACS2 (MACS, RRID:SCR_013291) (Zhang et al., 2008) was used to identify enriched genomic regions in both conditions using a tag size of 25bp and a q-value cutoff of $1.00^{-2}$. Peaks were annotated using Homer (HOMER, RRID:SCR_010881) (Benner et al., 2017) with standard mm9 genome reference. Location of peaks was then grouped into intergenic, promoter and genic (containing 5′UTR, Exons, Introns, Transcription Termination Sites, 3′UTR, ncRNA, miRNA, snoRNA, and rRNA) regions. The UCSC genome browser (UCSC Genome Browser, RRID:SCR_005780) (Dreszer et al., 2013) was used to analyze genomic regions for overlap, using the Bedtools intersect function (BEDTools, RRID:SCR_006646) (Quinlan and Hall, 2010) . Any base pair overlap was enough to consider two regions "shared" and regions where no overlap existed defined the regions as exclusively being in one condition. The comparison was made into a Venn-diagram using tool available at https://www.meta-chart.com/venn.

### DNA motif analysis

Peaks from pre- and post-pregnancy NKTs ATAC-seq libraries were utilized as input for an unbiased transcription factor analyses using Analysis of Motif Enrichment (AME) (McLeay and Bailey, 2010) and Find Individual Motif Occurrences (FIMO) (MEME Suite - Motif-based sequence analysis tools, RRID:SCR_001783) (Grant et al., 2011) was used to computationally define DNA binding motif regions to identify sequences of known motifs, with a statistical threshold of 0.0001.

### Genomic library preparation and copy-number variation analysis

Mammary normal tissue and tumor from nulliparous $Brca1^{KO}$ female mice were dissociated as above described. Lineage depleted tumor cells were utilized for DNA extraction using DNeasy Blood & Tissue Kit (QIAGEN Cat# 69504). Genomic DNA was sonicated to an average of 300bp using Covaris E220 Focused-ultrasonicator. For library preparation, fragmented DNA went through standard end-repair (NEB Cat# E6050), dA-tailing (NEB Cat# E6053), and sequencing adaptor ligation (NEB Cat# M2200) steps. Following universal adaptor ligation, eight cycles of PCR was performed for each sample. During the PCR step, a unique pair of Illumina TrueSeq i7 index and i5 index was added to each sample. The PCR library was purified with AMPure XP beads (Beckman Coulter Cat# A63881), and quantified using NanoDrop spectrophotometer and Agilent Technologies 2100 Bioanalyzer. Whole-genome-sequencing libraries with different combination of Illumina indexes were pooled together for one lane of Illumina MiSeq. 150 base pairs from both ends were sequenced along with two 8-bp indexes. For CNV analysis, Read 1 of the sequence data was mapped to the mm9 reference genome using Hisat2 version 2.1.0 in single read alignment mode (Kim et al., 2015). The reference genome was divided into 5,000 variable-length bins with equal mappability as previously described (Baslan et al., 2012). The ratio of mapped reads in the tumor sample to mapped reads in the diploid sample (normal tissue) was used to compute a fitted piecewise constant function

(segmentation). This segmentation used DNAcopy version 1.50.1 implementation of the circular binary segmentation algorithm (Seshan and Olshen, 2014) and the copy number profiles were plotted using R version 3.4.4 (R Core Team, 2019).

## QUANTIFICATION AND STATISTICAL ANALYSIS

Data represent results from three or more independent biological replicates, unless otherwise specified. Sequencing data are from two biological replicates from each condition. All statistical analyses were performed using GraphPad Prism V9 software. For all analyses, error bars indicate standard error of mean across samples of the same experimental group. Statistically significant differences were considered with *p-value*s lower than 0.05 ($p < 0.05$) from unpaired Student's t tests, or otherwise indicated, as described in the figure legends.